Performance of Jointed Concrete Pavements

Volume VI Appendix C - Synthesis of Concrete Pavement Design Methods and Analysis Models

Volume VI Appendix D - Summary of Analysis Data for the Evaluation of Predictive Models

FHWA-RD-89-141

July 1990

NJ Route 130 10-in. JRCP 12-in. gravel base 36 Years 35 Million ESAL's PSR - 3.8

U.S. Department of Transportation
Federal Highway Administration

Research, Development, and Technology
Turner-Fairbank Highway Research Center
6300 Georgetown Pike
McLean, Virginia 22101-2296

FOREWORD

This report is one volume of a two-volume set of interim reports documenting a comprehensive evaluation of jointed concrete pavement design and analysis models. The capabilities and limitations and a sensitivity analysis of the various design and analysis models are given. New prediction models were developed for Present Serviceability Rating, longitudinal cracking, transverse joint faulting, transverse cracking (joint plain concrete pavement only) and transverse joint spalling.

Volumes I, IV and V document the performance of 95 experimental or other in-service pavements in United States or Canada. These volumes have been previously distributed. Volume III (Summary of Research Findings) and the Technical Summary will be given widespread distribution in the near future. This report will be of interest to those involved in the design, construction and maintenance of jointed concrete pavements.

Sufficient copies of this report are being distributed by FHWA memorandum to provide one copy to each FHWA Region and Division and two copies to each State highway agency. Direct distribution is being made to the Division offices. Additional copies for the public are available from the National Technical Information Service (NTIS), U. S. Department of Commerce, 5285 Port Royal Road, Springfield, Virginia 22161. A small charge will be imposed for each copy ordered from NTIS.

for Thomas J. Pasko, Jr., P.E.
Director, Office of Engineering and
Highway Operations Research and Development

NOTICE

This document is disseminated under the sponsorship of the Department of Transportation in the interest of information exchange. The United States Government assumes no liability for its contents or use thereof. The contents of this report reflect the views of the contractor, who is responsible for the accuracy of the data presented herein. The contents do not necessarily reflect the official policy of the Department of Transportation. This report does not constitute a standard, specification, or regulation.

The United States Government does not endorse products or manufacturers. Trade or manufacturers' names appear herein only because they are considered essential to the object of this document.

TECHNICAL REPORT STANDARD TITLE PAGE

1. Report No.	2. Government Accession No.	3. Recipient's Catalog No.
FHWA-RD-89-141		

4. Title and Subtitle	5. Report Date
PERFORMANCE OF JOINTED CONCRETE PAVEMENTS Volume VI - Appendix C Synthesis of Conc. Pvt. Design Methods & Analysis Models Appendix D Summary of Analysis Data for the Eval. of Predictive Models	July 1990
	6. Performing Organization Code
7. Author(s) A. L. Mueller, D. G. Peshkin, K. D. Smith, M. I. Darter	8. Performing Organization Report No.
9. Performing Organization Name and Address ERES Consultants, Inc. 1401 Regency Drive East Savoy, Illinois 61874	10. Work Unit No. 3C1A2012
	11. Contract or Grant No. DTFH61-86-C-00079
12. Sponsoring Agency Name and Address Office of Engrg. and Highway Operations R & D Federal Highway Administration 6300 Georgetown Pike McLean, VA 22101-2296	13. Type of Report and Period Covered Interim Report Oct. 1986 - Feb. 1990
	14. Sponsoring Agency Code

15. Supplementary Notes

FHWA Contract Manager (COTR):
Roger M. Larson, HNR-20

Dr. Mark B. Snyder assisted in the development of Appendix C.

16. Abstract

A major national field and analytical study has been conducted into the effect of various design features on the performance of jointed concrete pavements. Extensive design, construction, traffic, and performance data were obtained from numerous experimental and other concrete pavement sections throughout the country. Field data collected and analyzed included distress, drainage, roughness, present serviceability rating (PSR), deflections, destructive testing (coring and boring), and weigh-in-motion (WIM) on selected sites. This information was compiled into a comprehensive microcomputer database. Projects were evaluated on an individual basis and then compared at a national level to identify performance trends. The performance data was used to evaluate and modify several concrete pavement design procedures and analysis models.

This volume provides a general evaluation of several concrete pavement design and analysis models. This includes RISC, ILLISLAB, JSLAB, H-51, WESLIQUID, WESLAYER, JSC-1, JCP-1, AASHTO, RPS-3, PCA, PMARP, PEARDARP, PREDICT, BERM, CMS, Liu-Lytton, JRCP-4, and California Rigid Design. Sensitivity analyses are included for each section. This volume also provides supporting documentation for Volume II.

This volume is the sixth in a series. The other volumes are:

FHWA No.	Vol. No.	Short Title
FHWA-RD-89-136	I	Evaluation of Concrete Pavement Performance and Design Features
FHWA-RD-89-137	II	Evaluation and Modification of Concrete Pavement Design and Analysis Models
FHWA-RD-89-138	III	Summary of Research Findings
FHWA-RD-89-139	IV	Appendix A Project Summary Reports & Summary Tables
FHWA-RD-89-140	V	Appendix B Data Collection & Analysis Procedures

17. Key Words	18. Distribution Statement
Concrete, concrete pavement, pavement performance, pavement evaluation, pavement design models, pavements analysis models, pavement performance models.	No restrictions. This document is available to the public through the National Technical Information Service, Springfield, Virginia 22161.

19. Security Classif. (of this report)	20. Security Classif. (of this page)	21. No. of Pages	22. Price
Unclassified	Unclassified	389	

Form DOT F 1700.7 (8-69) Reproduction of form and completed page authorized.

SI* (MODERN METRIC) CONVERSION FACTORS

APPROXIMATE CONVERSIONS TO SI UNITS

Symbol	When You Know	Multiply By	To Find	Symbol
		LENGTH		
in	inches	25.4	millimetres	mm
ft	feet	0.305	metres	m
yd	yards	0.914	metres	m
mi	miles	1.61	kilometres	km
		AREA		
in^2	square inches	645.2	millimetres squared	mm^2
ft^2	square feet	0.093	metres squared	m^2
yd^2	square yards	0.836	metres squared	m^2
ac	acres	0.405	hectares	ha
mi^2	square miles	2.59	kilometres squared	km^2
		VOLUME		
fl oz	fluid ounces	29.57	millilitres	mL
gal	gallons	3.785	litres	L
ft^3	cubic feet	0.028	metres cubed	m^3
yd^3	cubic yards	0.765	metres cubed	m^3

NOTE: Volumes greater than 1000 L shall be shown in m^3.

		MASS		
oz	ounces	28.35	grams	g
lb	pounds	0.454	kilograms	kg
T	short tons (2000 lb)	0.907	megagrams	Mg
		TEMPERATURE (exact)		
°F	Fahrenheit temperature	5(F-32)/9	Celcius temperature	°C

APPROXIMATE CONVERSIONS FROM SI UNITS

Symbol	When You Know	Multiply By	To Find	Symbol
		LENGTH		
mm	millimetres	0.039	inches	in
m	metres	3.28	feet	ft
m	metres	1.09	yards	yd
km	kilometres	0.621	miles	mi
		AREA		
mm^2	millimetres squared	0.0016	square inches	in^2
m^2	metres squared	10.764	square feet	ft^2
ha	hectares	2.47	acres	ac
km^2	kilometres squared	0.386	square miles	mi^2
		VOLUME		
mL	millilitres	0.034	fluid ounces	fl oz
L	litres	0.264	gallons	gal
m^3	metres cubed	35.315	cubic feet	ft^3
m^3	metres cubed	1.308	cubic yards	yd^3
		MASS		
g	grams	0.035	ounces	oz
kg	kilograms	2.205	pounds	lb
Mg	megagrams	1.102	short tons (2000 lb)	T
		TEMPERATURE (exact)		
°C	Celcius temperature	1.8C + 32	Fahrenheit temperature	°F

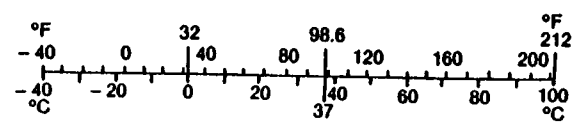

* SI is the symbol for the International System of Measurement

(Revised April 1989)

TABLE OF CONTENTS

VOLUME I EVALUATION OF CONCRETE PAVEMENT PERFORMANCE AND DESIGN FEATURES

Chapter		Page
1	INTRODUCTION	1
	1. OBJECTIVES	1
	2. BACKGROUND AND RESEARCH APPROACH	2
	3. SEQUENCE OF REPORT	3
2	DESCRIPTION OF PROJECTS IN STUDY	4
	1. INTRODUCTION	4
	2. DESCRIPTION OF EXPERIMENTAL AND SINGLE PAVEMENT SECTIONS	6
	Dry-Freeze Environmental Region	6
	Minnesota 1	6
	Minnesota 2	6
	Minnesota 3	6
	Minnesota 4	6
	Minnesota 6	8
	Dry-Nonfreeze Environmental Region	8
	Arizona 1	8
	Arizona 2	8
	California 1	8
	California 2	8
	California 6	11
	California 7	11
	California 8	11
	Wet-Freeze Environmental Region	11
	Michigan 1	11
	Michigan 3	13
	Michigan 4	13
	Michigan 5	13
	New York 1	13
	New York 2	13
	Ohio 1	15
	Ohio 2	15
	Ontario 1	15
	Ontario 2	15
	Pennsylvania 1	15
	New Jersey 2	18
	New Jersey 3	18
	Wet-Nonfreeze Environmental Region	18
	California 3	18
	North Carolina 1	21
	North Carolina 2	21
	Florida 2	21
	Florida 3	21
	3. GENERAL DATA COLLECTION EFFORTS	21

TABLE OF CONTENTS (continued)

VOLUME I EVALUATION OF CONCRETE PAVEMENT PERFORMANCE AND DESIGN FEATURES (continued)

Chapter		Page
3	PERFORMANCE EVALUATION OF PROJECTS	25
	1. INTRODUCTION	25
	2. DRY-FREEZE ENVIRONMENTAL REGION	25
	Minnesota 1	27
	Observations	27
	Conclusions	27
	Minnesota 2	31
	Observations	31
	Conclusions	34
	Minnesota 3	35
	Minnesota 4	35
	Minnesota 6	37
	3. DRY-NONFREEZE ENVIRONMENTAL REGION	37
	Arizona 1	37
	Observations	40
	Conclusions	40
	Arizona 2	41
	California 1	41
	Observations	44
	Conclusions	44
	California 2	45
	Observations	45
	Conclusions	48
	California 6	48
	California 7	50
	Observations	50
	Conclusions	50
	California 8	51
	4. WET-FREEZE ENVIRONMENTAL REGION	51
	Michigan 1	51
	Observations	54
	Conclusions	55
	Michigan 3	56
	Michigan 4	56
	Observations	56
	Conclusions	60
	Michigan 5	61
	Observations	61
	Conclusions	61
	New York 1	63
	Observations	63
	Conclusions	63
	New York 2	65
	Observations	65
	Conclusions	68
	Ohio 1	69

TABLE OF CONTENTS (continued)

VOLUME I EVALUATION OF CONCRETE PAVEMENT PERFORMANCE AND DESIGN FEATURES (continued)

Chapter		Page
	Observations	69
	Conclusions	72
	Ohio 2	72
	Observations	73
	Conclusions	75
	Ontario 1	75
	Observations	78
	Conclusions	79
	Ontario 2	79
	Observations	80
	Conclusions	80
	Pennsylvania 1	80
	Observations	80
	Conclusions	84
	New Jersey 2	85
	Observations	85
	Conclusions	85
	New Jersey 3	85
	Observations	88
	Conclusions	89
	5. WET-NONFREEZE ENVIRONMENTAL REGION	89
	California 3	89
	Observations	89
	Conclusions	92
	North Carolina 1	92
	Observations	93
	Conclusions	96
	North Carolina 2	96
	Observations	97
	Conclusions	97
	Florida 2	97
	Florida 3	97
	Observations	99
	Conclusions	101
4	EFFECT OF DESIGN FEATURES ON PAVEMENT PERFORMANCE	102
	1. INTRODUCTION	102
	2. SLAB THICKNESS	102
	Minnesota 1 and Minnesota 2	102
	Arizona 1	102
	California 1	104
	Ohio 2	104
	Ontario 1	104
	North Carolina 2	104
	Summary of the Effects of Slab Thickness	104
	3. BASE TYPE	106

TABLE OF CONTENTS (continued)

VOLUME I EVALUATION OF CONCRETE PAVEMENT PERFORMANCE AND DESIGN FEATURES (continued)

Chapter		Page
	Minnesota 1	106
	Minnesota 6	107
	Arizona 1	107
	California 1	107
	California 2	107
	California 6	109
	Michigan 1	109
	Michigan 3	109
	Michigan 5	109
	New York 1	111
	Ohio 1	111
	Ontario 1	111
	Pennsylvania 1	111
	New Jersey 3	113
	North Carolina 1	113
	North Carolina 2	113
	Florida 3	113
	Summary of the Effects of Base Type	115
4.	JOINT SPACING	117
	Minnesota 1	117
	Minnesota 2	121
	California 1	121
	Michigan 1	121
	New York 1	121
	New York 2	123
	Ohio 1	123
	New Jersey 2	123
	North Carolina 1	123
	Florida 3	123
	Summary of the Effects of Joint Spacing	123
5.	REINFORCEMENT DESIGN	133
	Minnesota 1	133
	Ohio 1	135
	New Jersey 2 and New Jersey 3	135
	Other Sections	135
	Summary of the Effects of Reinforcement	135
6.	JOINT ORIENTATION	135
	New York 1	137
	North Carolina 1	137
	Summary of the Effects of Joint Orientation	137
7.	TRANSVERSE JOINT LOAD TRANSFER	137
	Doweled and Nondoweled Comparisons	139
	Minnesota 1	139
	North Carolina 1	139
	Nondoweled Sections	141
	Other Doweled Sections	141
	Summary of the Effects of Load Transfer	144

TABLE OF CONTENTS (continued)

VOLUME I EVALUATION OF CONCRETE PAVEMENT PERFORMANCE AND DESIGN FEATURES (continued)

Chapter		Page
8.	DOWEL BAR COATINGS	144
	Michigan 1	144
	Michigan 5	144
	Ohio 1	145
	New York 2	145
	New Jersey 2	145
	Summary of the Effects of Dowel Coatings	145
9.	LONGITUDINAL JOINT DESIGN	145
	Summary of the Effects of Longitudinal Joint Design	148
10.	TRANSVERSE JOINT SEALANT	148
	Direct Sealant Comparisons	148
	California 3	148
	Minnesota 2	149
	Nonsealed Joints in California	149
	Preformed Compression Seals	149
	Other Sealant Types	150
	Summary of the Effects of Joint Sealing	150
11.	TIED PCC SHOULDERS/WIDENED LANES	150
	Minnesota 2	150
	Arizona 1	151
	Michigan 1	151
	Michigan 4	151
	New York 2	151
	Ohio 2	153
	Ontario 1	153
	California 3	153
	Widened Lanes	153
	Summary of the Effects of Tied PCC Shoulders/ Widened Lanes	153
12.	SUBDRAINAGE	154
	Michigan 1	154
	Michigan 5	156
	Arizona 1	156
	California 2	156
	Pennsylvania 1	156
	New Jersey 3	156
	Summary of the Effects of Subdrainage	156
5	SUMMARY AND CONCLUSIONS	159
	1. SUMMARY OF THE EFFECT OF DESIGN FEATURES	159
	2. FUTURE RESEARCH	164
	3. SUGGESTIONS FOR FUTURE DATA COLLECTION AND TESTING	165
6	BIBLIOGRAPHY	166

TABLE OF CONTENTS (continued)

VOLUME II EVALUATION AND MODIFICATION OF CONCRETE PAVEMENT DESIGN AND ANALYSIS MODELS

Chapter		Page
1	INTRODUCTION	1
	1. INTRODUCTION	1
	2. PROJECT BACKGROUND	2
	Selection of Models	2
	Research Approach	3
	3. SEQUENCE OF REPORT	4
2	DESCRIPTION OF PAVEMENT SECTIONS	5
	1. DRY-FREEZE ENVIRONMENTAL REGION	5
	2. DRY-NONFREEZE ENVIRONMENTAL REGION	6
	3. WET-FREEZE ENVIRONMENTAL REGION	6
	4. WET-NONFREEZE ENVIRONMENTAL REGION	9
	5. OVERALL DISTRIBUTION OF DESIGN FEATURES	9
	Base Type	9
	Slab Thickness	12
	Joint Spacing/Pavement Type	12
	Load Transfer	12
	Shoulder Type/Widened Lanes	17
3	ANALYSIS OF THE ACCURACY OF SELECTED PREDICTION MODELS	19
	1. INTRODUCTION	19
	2. DESCRIPTION OF PREDICTION MODELS	19
	AASHTO Design Model	20
	PEARDARP Prediction Models	25
	Spalling Model	26
	PSI Model	26
	Roughness Model	26
	Pumping Models	27
	Cracking Model	29
	Faulting Models	30
	COPES Prediction Models	31
	JPCP Pumping Model	31
	JRCP Pumping Model	32
	JPCP Joint Faulting Model	32
	JRCP Joint Faulting Model	33
	JPCP Joint Deterioration Model	33
	JRCP Joint Deterioration Model	34
	JPCP Slab Cracking Model	35
	JRCP Slab Cracking Model	35
	JPCP Present Serviceability Rating (PSR) Model	36
	JRCP Present Serviceability Rating (PSR) Model	36
	PFAULT Faulting Prediction Models	37
	Doweled Jointed Concrete Pavements	37

TABLE OF CONTENTS (continued)

VOLUME II EVALUATION AND MODIFICATION OF CONCRETE PAVEMENT DESIGN AND ANALYSIS MODELS (continued)

Chapter		Page
	Nondoweled Jointed Concrete Pavements	37
	3. STATISTICAL ANALYSIS OF PREDICTION MODELS	39
	4. ABILITY OF MODELS TO PREDICT THE PERFORMANCE OF INSERVICE PAVEMENTS	41
	AASHTO	43
	PEARDARP	46
	PSI Model	46
	Roughness Model	46
	Pumping Model	49
	Spalling Model	49
	Faulting Models	50
	Cracking Model	51
	COPES	52
	Pumping Models	52
	Faulting Models	56
	Joint Deterioration Models	57
	Cracking Models	59
	Present Serviceability Rating (PSR) Models	61
	PFAULT Faulting Models	62
	5. SUMMARY	65
4	CASE STUDIES	67
	1. INTRODUCTION	67
	Climatic Model	67
	Drainage Model	68
	Structural Analysis Models	68
	Design Method	69
	Shoulder Analysis and Design	69
	2. PRESENTATION OF SECTIONS FOR CASE STUDIES	69
	Minnesota 1	69
	California 1	71
	Michigan 1	71
	North Carolina 1	71
	3. EVALUATION OF THE CMS PROGRAM	75
	Introduction	75
	Brief Technical Description	75
	Analysis of Results	78
	Rothsay, Minnesota	78
	Tracy, California	85
	Clare, Michigan	89
	Rocky Mount, North Carolina	99
	Conclusions and Recommendations	101
	4. EVALUATION OF LIU-LYTTON DRAINAGE MODELS	104
	Introduction	104
	Brief Technical Description	104
	Analysis of Results	105

TABLE OF CONTENTS (continued)

VOLUME II EVALUATION AND MODIFICATION OF CONCRETE PAVEMENT DESIGN AND ANALYSIS MODELS (continued)

Chapter		Page
	Rothsay, Minnesota	107
	Tracy, California	114
	Clare, Michigan	119
	Rocky Mount, North Carolina	125
	Conclusions and Recommendations	128
5.	ANALYSIS OF JSLAB AND ILLISLAB	131
	Introduction	131
	Analysis of Results	132
	Analysis of the Edge Loading Condition	137
	Analysis of the Corner Loading Condition	137
	Analysis of a Temperature Gradient Through the Slab	138
	Conclusions	138
6.	EVALUATION OF THE ILLISLAB PROGRAM	139
	Introduction	139
	Brief Technical Description	140
	Analysis of Results	141
	Analysis of the Edge Loading Condition	141
	Analysis of the Corner Loading Condition	144
	Analysis of Voids Beneath the Slab	146
	Analysis of a Temperature Gradient Through a Slab	149
	Conclusions and Recommendations	153
7.	EVALUATION OF THE PMARP PROGRAM	153
	Introduction	153
	Brief Technical Description	154
	Analysis of Results	156
	Analysis of the Edge Loading Condition	158
	Analysis of the Corner Loading Condition	160
	Conclusions and Recommendations	161
8.	EVALUATION OF THE ZERO-MAINTENANCE DESIGN PROCEDURE	162
	Introduction	162
	Brief Technical Description	162
	Analysis of Results	165
	Conclusions and Recommendations	168
9.	EVALUATION OF JCS-1	168
	Brief Technical Description	168
	Analysis of Results	169
	Conclusions and Recommendations	170
10.	EVALUATION OF BERM	171
	Brief Technical Description	171
	Analysis of Results	172
	Conclusions and Recommendations	173
11.	SUMMARY AND CONCLUSIONS	173
5	DEVELOPMENT OF NEW PREDICTION MODELS	175
1.	INTRODUCTION	175

TABLE OF CONTENTS (continued)

VOLUME II EVALUATION AND MODIFICATION OF CONCRETE PAVEMENT DESIGN AND ANALYSIS MODELS (continued)

Chapter		Page
2.	NEW PREDICTION MODELS	175
	Present Serviceability Rating (PSR)	175
	Jointed Plain Concrete Pavements	175
	Jointed Reinforced Concrete Pavements	176
	Longitudinal Cracking	177
	Transverse Joint Faulting	178
	Doweled Concrete Pavements	181
	Nondoweled Concrete Pavements	183
	Transverse Cracking	191
	Applied n	191
	Allowable N	192
	JPCP Cracking Model	196
	Transverse Joint Spalling	200
	JPCP Joint Spalling Model	200
	JRCP Joint Spalling Model	202
6	EVALUATION OF THE COST-EFFECTIVENESS OF SELECTED PAVEMENT DESIGN FEATURES	207
1.	INTRODUCTION	207
2.	ANALYSIS PROCEDURE	207
	Cost Information	209
	Life Prediction	209
	Cost-Effectiveness	209
3.	RESULTS	210
	Arizona	210
	Comparative Design 1	210
	Comparative Design 2	210
	Comparative Design 3	212
	California	212
	Comparative Design 1	212
	Comparative Design 2	212
	Comparative Design 3	215
	Comparative Design 4	215
	Comparative Design 5	215
	Comparative Design 6	215
	Michigan	216
	Comparative Design 1	216
	Comparative Design 2	216
	Comparative Design 3	219
	Comparative Design 4	219
	Comparative Design 5	219
	Comparative Design 6	219
	Minnesota	220
	Comparative Design 1	220
	Comparative Design 2	220
	Comparative Design 3	220

TABLE OF CONTENTS (continued)

VOLUME II EVALUATION AND MODIFICATION OF CONCRETE PAVEMENT DESIGN AND ANALYSIS MODELS (continued)

Chapter		Page
	Comparative Design 4	223
	Comparative Design 5	223
	North Carolina	223
	Comparative Design 1	223
	Comparative Design 2	225
	Comparative Design 3	225
	4. SUMMARY	225
7	SUMMARY AND CONCLUSIONS	228
	APPENDIX A — PAVEMENT DESIGNS FOR COST-EFFECTIVENESS EVALUATION	230
	REFERENCES	239

VOLUME III SUMMARY OF RESEARCH FINDINGS

Chapter		Page
1	INTRODUCTION	1
	STUDY OBJECTIVES	1
	BACKGROUND AND RESEARCH SCOPE	2
	DESCRIPTION OF REPORTS	2
2	STUDY SECTIONS AND DATA COLLECTION	3
	STUDY SECTIONS	3
	DRY-FREEZE ENVIRONMENTAL REGION	3
	DRY-NONFREEZE ENVIRONMENTAL REGION	3
	WET-FREEZE ENVIRONMENTAL REGION	8
	WET-NONFREEZE ENVIRONMENTAL REGION	8
	OVERALL DISTRIBUTION OF DESIGN FEATURES	8
	BASE TYPE	8
	SLAB THICKNESS	8
	JOINT SPACING/PAVEMENT TYPE	12
	LOAD TRANSFER	12
	SHOULDER TYPE/WIDENED LANES	12
	SINGLE PAVEMENT SECTIONS	12
	FIELD DATA COLLECTION	12
	PAVEMENT CONDITION SURVEY	17
	DRAINAGE SURVEY	17
	PHOTO SURVEY	18
	FALLING WEIGHT DEFLECTOMETER (FWD)	18
	PAVEMENT ROUGHNESS	18

TABLE OF CONTENTS (continued)

VOLUME III SUMMARY OF RESEARCH FINDINGS (continued)

Chapter		Page
	WEIGH-IN-MOTION (WIM)	18
	CORING AND BORING	18
	DATA BASE DESCRIPTION	19
3	SUMMARY OF THE EFFECTS OF DESIGN FEATURES	21
	PROJECT SUMMARIES	21
	EFFECTS OF PAVEMENT DESIGN FEATURES	21
	SLAB THICKNESS	21
	BASE TYPE	21
	SLAB LENGTH	23
	SLAB REINFORCEMENT	24
	JOINT ORIENTATION	26
	JOINT LOAD TRANSFER	26
	DOWEL BAR COATINGS	27
	LONGITUDINAL JOINT DESIGN	27
	JOINT SEALING	27
	TIED SHOULDERS	28
	WIDENED TRAFFIC LANES	28
	SUBDRAINAGE	29
	SUMMARY	29
4	CONCRETE PAVEMENT DESIGN AND ANALYSIS MODELS	30
	SYNTHESIS AND SELECTION OF INITIAL MODELS	30
	ANALYSIS OF THE ACCURACY OF SELECTED PREDICTION MODELS	30
	STATISTICAL ANALYSIS OF PREDICTION MODELS	31
	AASHTO PAVEMENT DESIGN MODEL	31
	PEARDARP	32
	NCHRP 277 (COPES)	35
	PFAULT FAULTING MODELS	35
	OVERALL EVALUATION OF THE PREDICTION MODELS	40
	CASE STUDIES FOR SELECTED ANALYSIS MODELS	40
	EVALUATION OF THE CMS PROGRAM	41
	EVALUATION OF THE LIU-LYTTON DRAINAGE MODELS	42
	EVALUATION OF THE ILLISLAB PROGRAM	43
	ANALYSIS OF JSLAB AND ILLISLAB	44
	Analysis of the Edge Loading Condition	45
	Analysis of the Corner Loading Condition	45
	Analysis of a Temperature Gradient Through the Slab	46
	Conclusions	47
	EVALUATION OF THE PMARP PROGRAM	47
	EVALUATION OF THE ZERO-MAINTENANCE DESIGN PROCEDURE	49
	EVALUATION OF JCS-1	49
	EVALUATION OF BERM	50
	SUMMARY AND CONCLUSIONS	51

TABLE OF CONTENTS (continued)

VOLUME III SUMMARY OF RESEARCH FINDINGS (continued)

Chapter		Page
5	DEVELOPMENT OF NEW PREDICTION MODELS	53
	INTRODUCTION	53
	PRESENT SERVICEABILITY RATING (PSR)	54
	LONGITUDINAL CRACKING	54
	TRANSVERSE JOINT FAULTING	55
	DOWELED CONCRETE PAVEMENTS	57
	NONDOWELED CONCRETE PAVEMENTS	57
	TRANSVERSE CRACKING	60
	TRANSVERSE JOINT SPALLING	62
	JPCP JOINT SPALLING MODEL	65
	JRCP JOINT SPALLING MODEL	65
	USE OF MODELS IN DESIGN	65
	ACCURACY OF MODELS	68
	SUMMARY	71
6	COST EFFECTIVENESS EVALUATION OF SELECTED PAVEMENT DESIGN FEATURES	73
	INTRODUCTION	73
	ANALYSIS PROCEDURE	73
	RESULTS	75
	SUMMARY OF COST EVALUATION	75
APPENDIX A	PARTIAL LISTING OF CANDIDATE SECTIONS	78
APPENDIX B	NEW PREDICTION MODELS	82
	PRESENT SERVICEABILITY RATING	82
	JOINTED PLAIN CONCRETE PAVEMENTS	82
	JOINTED REINFORCED CONCRETE PAVEMENTS	83
	TRANSVERSE JOINT FAULTING	84
	DOWELED CONCRETE PAVEMENTS	84
	NONDOWELED CONCRETE PAVEMENTS	87
	TRANSVERSE CRACKING - JOINTED PLAIN CONCRETE PAVEMENTS	90
	TRANSVERSE JOINT SPALLING	91
	JPCP JOINT SPALLING MODEL	91
	JRCP JOINT SPALLING MODEL	92
REFERENCES		93

TABLE OF CONTENTS (continued)

VOLUME IV APPENDIX A - PROJECT SUMMARY REPORTS AND SUMMARY TABLES

Chapter		Page
1	INTERSTATE 94 -- ROTHSAY, MINNESOTA	1
	1. INTRODUCTION	1
	2. CLIMATE	1
	3. TRAFFIC	1
	4. MAINTENANCE AND REHABILITATION	2
	5. PHYSICAL TESTING RESULTS	2
	6. DRAINABILITY OF PAVEMENT SECTIONS	3
	7. DETERIORATION OF PAVEMENT SECTIONS	6
	Joint Spalling	6
	Best Performance	6
	Worst Performance	6
	Joint Faulting	6
	Best Performance	7
	Worst Performance	7
	Transverse Cracking	7
	Best Performance	8
	Worst Performance	8
	Longitudinal Cracking	8
	Best Performance	8
	Worst Performance	9
	Present Serviceability Rating (PSR) and Roughness	9
	Other Distress Types	9
	8. EFFECT OF DESIGN FEATURES ON PAVEMENT PERFORMANCE	9
	Base Type	9
	Joint Load Transfer	9
	Slab Thickness	10
	Joint Spacing	10
	9. COMPARISON OF OUTER LANE AND INNER LANE PERFORMANCE	10
	10. SUMMARY AND CONCLUSIONS	11
	11. ADDITIONAL READING	12
2	INTERSTATE 90 -- ALBERT LEA, MINNESOTA	13
	1. INTRODUCTION	13
	2. CLIMATE	13
	3. TRAFFIC	13
	4. MAINTENANCE AND REHABILITATION	13
	5. PHYSICAL TESTING RESULTS	14
	6. DRAINABILITY OF PAVEMENT SECTIONS	15
	7. DETERIORATION OF PAVEMENT SECTIONS	15
	Joint Spalling	15
	Joint Faulting	17
	Transverse Cracking	17
	Longitudinal Cracking	17
	Present Serviceability Rating (PSR) and Roughness	18
	Overall Shoulder Condition	18

TABLE OF CONTENTS (continued)

VOLUME IV APPENDIX A - PROJECT SUMMARY REPORTS AND SUMMARY TABLES (continued)

Chapter		Page
	8. EFFECT OF DESIGN FEATURES ON PAVEMENT PERFORMANCE	18
	Pavement Type	19
	Joint Spacing	19
	Slab Thickness	19
	Shoulder Type	19
	Widened Inside Lanes	20
	9. COMPARISON OF OUTER LANE AND INNER LANE PERFORMANCE	20
	10. SUMMARY AND CONCLUSIONS	20
	11. ADDITIONAL READING	22
3	INTERSTATE 90 -- AUSTIN, MINNESOTA	23
	1. INTRODUCTION	23
	2. DESIGN	23
	3. CLIMATE	23
	4. TRAFFIC	23
	5. DRAINABILITY AND OTHER PHYSICAL TESTING RESULTS	23
	6. MAINTENANCE AND REHABILITATION	24
	7. PAVEMENT PERFORMANCE	24
	8. CONCLUSIONS	24
4	TRUNK HIGHWAY 15 -- NEW ULM, MINNESOTA	25
	1. INTRODUCTION	25
	2. DESIGN	25
	3. CLIMATE	25
	4. TRAFFIC	25
	5. DRAINABILITY AND OTHER PHYSICAL TESTING RESULTS	25
	6. MAINTENANCE AND REHABILITATION	26
	7. PAVEMENT PERFORMANCE	26
	8. CONCLUSIONS	26
5	TRUNK HIGHWAY 15 -- TRUMAN, MINNESOTA	27
	1. INTRODUCTION	27
	2. DESIGN	27
	3. CLIMATE	27
	4. TRAFFIC	27
	5. DRAINABILITY AND OTHER PHYSICAL TESTING RESULTS	27
	6. MAINTENANCE AND REHABILITATION	28
	7. PAVEMENT PERFORMANCE	28
	8. CONCLUSIONS	28
6	STATE ROUTE 360 (SUPERSTITION FREEWAY) -- PHOENIX, ARIZONA	29
	1. INTRODUCTION	29

TABLE OF CONTENTS (continued)

VOLUME IV APPENDIX A - PROJECT SUMMARY REPORTS AND SUMMARY TABLES (continued)

Chapter		Page
	2. CLIMATE	29
	3. TRAFFIC	29
	4. MAINTENANCE AND REHABILITATION	30
	5. PHYSICAL TESTING RESULTS	30
	6. DRAINABILITY OF PAVEMENT SECTIONS	31
	7. DETERIORATION OF PAVEMENT SECTIONS	31
	Joint Spalling	34
	Joint Faulting	34
	Transverse Cracking	34
	Longitudinal Cracking	34
	Present Serviceability Rating (PSR) and Roughness	35
	8. EFFECT OF DESIGN FEATURES ON PAVEMENT PERFORMANCE	35
	Base Type	35
	Load Transfer Devices	35
	Slab Thickness	36
	Shoulder Type	36
	Subdrainage	36
	9. COMPARISON OF OUTER LANE AND MIDDLE LANE PERFORMANCE	36
	10. SUMMARY AND CONCLUSIONS	37
	11. ADDITIONAL READING	37
7	INTERSTATE 10 -- PHOENIX, ARIZONA	38
	1. INTRODUCTION	38
	2. DESIGN	38
	3. CLIMATE	38
	4. TRAFFIC	38
	5. DRAINABILITY AND OTHER PHYSICAL TESTING RESULTS	38
	6. MAINTENANCE AND REHABILITATION	39
	7. PAVEMENT PERFORMANCE	39
	8. CONCLUSIONS	39
8	INTERSTATE 5 -- TRACY, CALIFORNIA	41
	1. INTRODUCTION	41
	2. CLIMATE	41
	3. TRAFFIC	41
	4. MAINTENANCE AND REHABILITATION	42
	5. PHYSICAL TESTING RESULTS	42
	6. DRAINABILITY OF PAVEMENT SECTIONS	43
	7. DETERIORATION OF PAVEMENT SECTIONS	44
	Joint Spalling	44
	Joint Faulting	44
	Best Performance	47
	Worst Performance	47
	Transverse Cracking	47
	Best Performance	47

TABLE OF CONTENTS (continued)

VOLUME IV APPENDIX A - PROJECT SUMMARY REPORTS AND SUMMARY TABLES (continued)

Chapter		Page
	Worst Performance	48
	Longitudinal Cracking	48
	Present Serviceability Rating (PSR) and Roughness	48
	8. EFFECT OF DESIGN FEATURES ON PAVEMENT PERFORMANCE	49
	Base Type	49
	Joint Spacing	49
	High Strength Concrete	50
	Slab Thickness	50
	9. COMPARISON OF OUTER AND INNER LANE PERFORMANCE	50
	10. SUMMARY AND CONCLUSIONS	51
	11. ADDITIONAL READING	51
9	INTERSTATE 210 -- LOS ANGELES, CALIFORNIA	52
	1. INTRODUCTION	52
	2. CLIMATE	52
	3. TRAFFIC	52
	4. MAINTENANCE AND REHABILITATION	52
	5. PHYSICAL TESTING RESULTS	53
	6. DRAINABILITY OF PAVEMENT SECTIONS	53
	7. DETERIORATION OF PAVEMENT SECTIONS	54
	Joint Spalling	54
	Joint Faulting	54
	Transverse Cracking	56
	Longitudinal Cracking	56
	Present Serviceability Rating (PSR) and Roughness	56
	Other Pavement Distress	56
	8. EFFECT OF DESIGN FEATURES ON PAVEMENT PERFORMANCE	56
	9. COMPARISON OF OUTER AND MIDDLE LANE PERFORMANCE	57
	10. SUMMARY AND CONCLUSIONS	57
	11. ADDITIONAL READING	58
10	ROUTE 14 -- SOLEMINT, CALIFORNIA	59
	1. INTRODUCTION	59
	2. DESIGN	59
	3. CLIMATE	59
	4. TRAFFIC	59
	5. DRAINABILITY AND OTHER PHYSICAL TESTING RESULTS	59
	6. MAINTENANCE AND REHABILITATION	60
	7. PAVEMENT PERFORMANCE	60
	8. CONCLUSIONS	60
11	INTERSTATE 5 -- SACRAMENTO, CALIFORNIA	61
	1. INTRODUCTION	61
	2. DESIGN	61

TABLE OF CONTENTS (continued)

VOLUME IV APPENDIX A - PROJECT SUMMARY REPORTS AND SUMMARY TABLES (continued)

Chapter		Page
	3. CLIMATE	61
	4. TRAFFIC	61
	5. DRAINABILITY AND OTHER PHYSICAL TESTING RESULTS	62
	6. MAINTENANCE AND REHABILITATION	62
	7. PAVEMENT PERFORMANCE	62
	8. CONCLUSIONS	63
12	U.S. 101 -- THOUSAND OAKS, CALIFORNIA	64
	1. INTRODUCTION	64
	2. DESIGN	64
	3. CLIMATE	64
	4. TRAFFIC	64
	5. DRAINABILITY AND OTHER PHYSICAL TESTING RESULTS	64
	6. MAINTENANCE AND REHABILITATION	65
	7. PAVEMENT PERFORMANCE	65
	8. CONCLUSIONS	65
13	U.S. 10 -- CLARE, MICHIGAN	66
	1. INTRODUCTION	66
	2. CLIMATE	66
	3. TRAFFIC	66
	4. MAINTENANCE AND REHABILITATION	67
	5. PHYSICAL TESTING RESULTS	67
	6. DRAINABILITY OF PAVEMENT SECTIONS	68
	7. DETERIORATION OF PAVEMENT SECTIONS	69
	Joint Spalling	69
	Best Performance	72
	Worst Performance	72
	Joint Faulting	72
	Best Performance	73
	Worst Performance	73
	Transverse Cracking	73
	Best Performance	74
	Worst Performance	74
	Longitudinal Cracking	74
	Present Serviceability Rating (PSR) and Roughness	74
	8. EFFECT OF DESIGN FEATURES ON PAVEMENT PERFORMANCE	75
	Base Type	75
	Joint Load Transfer	75
	Subdrainage	75
	Joint Spacing	76
	Concrete Acceleration Ramp	76
	9. COMPARISON OF OUTER AND INNER LANE PERFORMANCE	76
	10. SUMMARY AND CONCLUSIONS	77
	11. ADDITIONAL READING	78

TABLE OF CONTENTS (continued)

VOLUME IV APPENDIX A - PROJECT SUMMARY REPORTS AND SUMMARY TABLES (continued)

Chapter		Page
14	INTERSTATE 94 -- MARSHALL, MICHIGAN	79
	1. INTRODUCTION	79
	2. DESIGN	79
	3. CLIMATE	79
	4. TRAFFIC	79
	5. DRAINABILITY AND OTHER PHYSICAL TESTING RESULTS	79
	6. MAINTENANCE AND REHABILITATION	80
	7. PAVEMENT PERFORMANCE	80
	8. CONCLUSIONS	80
15	INTERSTATE 69 -- CHARLOTTE, MICHIGAN	81
	1. INTRODUCTION	81
	2. CLIMATE	82
	3. TRAFFIC	82
	4. MAINTENANCE AND REHABILITATION	82
	5. PHYSICAL TESTING RESULTS	82
	6. DRAINABILITY OF PAVEMENT SECTIONS	83
	7. DETERIORATION OF PAVEMENT SECTIONS	84
	Joint Spalling	84
	Joint Faulting	84
	Transverse Cracking	84
	Transverse Crack Faulting	86
	Longitudinal Cracking	86
	Present Serviceability Rating and Roughness	86
	Shoulder Condition	87
	8. EFFECT OF DESIGN FEATURES ON PAVEMENT PERFORMANCE	87
	9. COMPARISON OF OUTER AND INNER LANE PERFORMANCE	88
	10. SUMMARY AND CONCLUSIONS	89
	11. ADDITIONAL READING	90
16	INTERSTATE 94 -- PAW PAW, MICHIGAN	91
	1. INTRODUCTION	91
	2. DESIGN	91
	3. CLIMATE	91
	4. TRAFFIC	91
	5. DRAINABILITY AND OTHER PHYSICAL TESTING RESULTS	91
	6. MAINTENANCE AND REHABILITATION	92
	7. PAVEMENT PERFORMANCE	92
	8. CONCLUSIONS	92
	9. ADDITIONAL READING	93
17	ROUTE 23 -- CATSKILL, NEW YORK	94
	1. INTRODUCTION	94
	2. CLIMATE	94

TABLE OF CONTENTS (continued)

VOLUME IV APPENDIX A - PROJECT SUMMARY REPORTS AND SUMMARY TABLES (continued)

Chapter		Page
	3. TRAFFIC	95
	4. MAINTENANCE AND REHABILITATION	95
	5. PHYSICAL TESTING RESULTS	95
	6. DRAINABILITY OF PAVEMENT SECTIONS	96
	7. DETERIORATION OF PAVEMENT SECTIONS	99
	Joint Spalling	99
	Best Performance	99
	Worst Performance	99
	Joint Faulting	99
	Best Performance	99
	Worst Performance	100
	Transverse Cracking	100
	Best Performance	100
	Worst Performance	100
	Longitudinal Cracking	100
	Present Serviceability Rating (PSR) and Roughness	101
	8. EFFECT OF DESIGN FEATURES ON PAVEMENT PERFORMANCE	101
	Base Type	101
	Load Transfer Devices	101
	Joint Spacing	102
	Joint Orientation	102
	9. COMPARISON OF OUTER LANE AND INNER LANE PERFORMANCE	102
	10. SUMMARY AND CONCLUSIONS	103
	11. ADDITIONAL READING	103
18	INTERSTATE 88 -- OTEGO, NEW YORK	104
	1. INTRODUCTION	104
	2. CLIMATE	105
	3. TRAFFIC	105
	4. MAINTENANCE AND REHABILITATION	105
	5. PHYSICAL TESTING RESULTS	105
	6. DRAINABILITY OF PAVEMENT SECTIONS	107
	7. DETERIORATION OF PAVEMENT SECTIONS	107
	Joint Spalling	107
	Joint Faulting	107
	Transverse Cracking	107
	Longitudinal Cracking	110
	Present Serviceability Rating (PSR) and Roughness	111
	Concrete Shoulder Distress Summary	111
	8. EFFECT OF DESIGN FEATURES ON PAVEMENT PERFORMANCE	111
	9. COMPARISON OF OUTER LANE AND INNER LANE PERFORMANCE	112
	10. SUMMARY AND CONCLUSIONS	112
19	U.S. 23 -- CHILLICOTHE, OHIO	114
	1. INTRODUCTION	114

TABLE OF CONTENTS (continued)

VOLUME IV APPENDIX A - PROJECT SUMMARY REPORTS AND SUMMARY TABLES (continued)

Chapter		Page
	2. CLIMATE	114
	3. TRAFFIC	114
	4. MAINTENANCE AND REHABILITATION	114
	5. PHYSICAL TESTING RESULTS	115
	6. DRAINABILITY OF PAVEMENT SECTIONS	116
	7. DETERIORATION OF PAVEMENT SECTIONS	116
	Joint Spalling	116
	Joint Faulting	119
	Best Performance	119
	Worst Performance	119
	Transverse Cracking	120
	Best Performance	120
	Worst Performance	120
	Longitudinal Cracking	120
	Present Serviceability Rating (PSR) and Roughness	120
	8. EFFECT OF DESIGN FEATURES ON PAVEMENT PERFORMANCE	121
	Base Type	121
	Joint Spacing	121
	Dowel Coating	121
	9. COMPARISON OF OUTER AND INNER LANE PERFORMANCE	122
	10. SUMMARY AND CONCLUSIONS	122
	11. ADDITIONAL READING	123
20	STATE ROUTE 2 -- VERMILION, OHIO	124
	1. INTRODUCTION	124
	2. CLIMATE	124
	3. TRAFFIC	124
	4. MAINTENANCE AND REHABILITATION	124
	5. PHYSICAL TESTING RESULTS	125
	6. DRAINABILITY OF PAVEMENT SECTIONS	125
	7. DETERIORATION OF PAVEMENT SECTIONS	125
	Joint Spalling	125
	Joint Faulting	127
	Transverse Cracking	127
	Longitudinal Cracking	127
	Present Serviceability Rating (PSR) and Roughness	127
	Other Pavement Distress	128
	"D" Cracking	128
	Pumping	128
	Longitudinal Joint Spalling	128
	8. EFFECT OF DESIGN FEATURES ON PAVEMENT PERFORMANCE	129
	9. COMPARISON OF OUTER AND INNER LANE PERFORMANCE	129
	10. SUMMARY AND CONCLUSIONS	130
	11. ADDITIONAL READING	131
21	HIGHWAY 3N -- RUTHVEN, ONTARIO	132

TABLE OF CONTENTS (continued)

VOLUME IV APPENDIX A - PROJECT SUMMARY REPORTS AND SUMMARY TABLES (continued)

Chapter		Page
	1. INTRODUCTION	132
	2. CLIMATE	132
	3. TRAFFIC	133
	4. MAINTENANCE AND REHABILITATION	133
	5. PHYSICAL TESTING RESULTS	133
	6. DRAINABILITY OF PAVEMENT SECTIONS	134
	7. DETERIORATION OF PAVEMENT SECTIONS	135
	Joint Spalling	135
	Joint Faulting	135
	Transverse Cracking	137
	Longitudinal Cracking	137
	Present Serviceability Rating (PSR) and Roughness	137
	Shoulder Condition	138
	Other Distresses	138
	8. EFFECT OF DESIGN FEATURES ON PAVEMENT PERFORMANCE	138
	Base Type	138
	Shoulder Type	139
	Slab Thickness	139
	Base Drainability	139
	9. COMPARISON OF LANE PERFORMANCE BY DIRECTION	140
	10. SUMMARY AND CONCLUSIONS	140
22	HIGHWAY 27 -- TORONTO, ONTARIO	142
	1. INTRODUCTION	142
	2. DESIGN	142
	3. CLIMATE	142
	4. TRAFFIC	142
	5. DRAINABILITY AND OTHER PHYSICAL TESTING RESULTS	142
	6. MAINTENANCE AND REHABILITATION	142
	7. PAVEMENT PERFORMANCE	143
	8. CONCLUSIONS	143
23	ROUTES 66 AND 422 -- KITTANNING, PENNSYLVANIA	144
	1. INTRODUCTION	144
	2. CLIMATE	145
	3. TRAFFIC	145
	4. MAINTENANCE AND REHABILITATION	145
	5. PHYSICAL TESTING RESULTS	145
	6. DRAINABILITY OF PAVEMENT SECTIONS	147
	7. DETERIORATION OF PAVEMENT SECTIONS	147
	Joint Spalling	150
	Joint Faulting	150
	Transverse Cracking	150
	Longitudinal Cracking	150
	Present Serviceability Rating (PSR) and Roughness	150

TABLE OF CONTENTS (continued)

VOLUME IV APPENDIX A - PROJECT SUMMARY REPORTS AND SUMMARY TABLES (continued)

Chapter		Page
	8. EFFECT OF DESIGN FEATURES ON PAVEMENT PERFORMANCE	150
	9. COMPARISON OF OUTER AND INNER LANE PERFORMANCE	151
	10. SUMMARY AND CONCLUSIONS	151
	11. ADDITIONAL READING	152
24	ROUTE 130 -- YARDVILLE, NEW JERSEY	153
	1. INTRODUCTION	153
	2. DESIGN	153
	3. CLIMATE	153
	4. TRAFFIC	153
	5. DRAINABILITY AND OTHER PHYSICAL TESTING RESULTS	153
	6. MAINTENANCE AND REHABILITATION	154
	7. PAVEMENT PERFORMANCE	154
	8. CONCLUSIONS	154
	9. ADDITIONAL READING	154
25	INTERSTATE 676 -- CAMDEN, NEW JERSEY	155
	1. INTRODUCTION	155
	2. CLIMATE	155
	3. TRAFFIC	155
	4. MAINTENANCE AND REHABILITATION	156
	5. PHYSICAL TESTING RESULTS	156
	6. DRAINABILITY OF PAVEMENT SECTIONS	157
	7. DETERIORATION OF PAVEMENT SECTIONS	157
	Joint Spalling	157
	Joint Faulting	159
	Transverse Cracking	159
	Longitudinal Cracking	159
	Present Serviceability Rating (PSR) and Roughness	159
	8. EFFECT OF DESIGN FEATURES ON PAVEMENT PERFORMANCE	159
	9. COMPARISON OF OUTER AND MIDDLE LANE PERFORMANCE	160
	10. SUMMARY AND CONCLUSIONS	160
	11. ADDITIONAL READING	161
26	U.S. 101 -- GEYSERVILLE, CALIFORNIA	162
	1. INTRODUCTION	162
	2. CLIMATE	162
	3. TRAFFIC	162
	4. MAINTENANCE AND REHABILITATION	163
	5. PHYSICAL TESTING RESULTS	163
	6. DRAINABILITY OF PAVEMENT SECTIONS	164
	7. DETERIORATION OF PAVEMENT SECTIONS	164
	Joint Spalling	164
	Joint Faulting	167

TABLE OF CONTENTS (continued)

VOLUME IV APPENDIX A - PROJECT SUMMARY REPORTS AND SUMMARY TABLES (continued)

Chapter		Page
	Transverse Cracking	167
	Longitudinal Cracking	168
	Present Serviceability Rating (PSR) and Roughness	168
	Other Pavement Distress	168
	8. EFFECT OF DESIGN FEATURES ON PAVEMENT PERFORMANCE	168
	Tied Concrete Shoulders	168
	Joint Sealant	169
	9. COMPARISON OF OUTER AND INNER LANE PERFORMANCE	169
	10. SUMMARY AND CONCLUSIONS	170
	11. ADDITIONAL READING	171
27	INTERSTATE 95 -- ROCKY MOUNT, NORTH CAROLINA	172
	1. INTRODUCTION	172
	2. CLIMATE	172
	3. TRAFFIC	172
	4. MAINTENANCE AND REHABILITATION	172
	5. PHYSICAL TESTING RESULTS	172
	6. DRAINABILITY OF PAVEMENT SECTIONS	174
	7. DETERIORATION OF PAVEMENT SECTIONS	174
	Joint Spalling	174
	Joint Faulting	174
	Best Performance	177
	Worst Performance	177
	Transverse Cracking	177
	Longitudinal Cracking	178
	Best Performance	178
	Worst Performance	178
	Present Serviceability Rating (PSR) and Roughness	178
	8. EFFECT OF DESIGN FEATURES ON PAVEMENT PERFORMANCE	179
	Base Type	179
	Joint Load Transfer	179
	Pavement Type/Joint Spacing	179
	Joint Orientation	180
	9. COMPARISON OF OUTER LANE AND INNER LANE PERFORMANCE	180
	10. SUMMARY AND CONCLUSIONS	181
	11. ADDITIONAL READING	182
28	INTERSTATE 85 -- GREENSBORO, NORTH CAROLINA	183
	1. INTRODUCTION	183
	2. DESIGN	183
	3. CLIMATE	183
	4. TRAFFIC	183
	5. DRAINABILITY AND OTHER PHYSICAL TESTING RESULTS	183
	6. MAINTENANCE AND REHABILITATION	184
	7. PAVEMENT PERFORMANCE	184

TABLE OF CONTENTS (continued)

VOLUME IV APPENDIX A - PROJECT SUMMARY REPORTS AND SUMMARY TABLES (continued)

Chapter		Page
	8. CONCLUSIONS	184
	9. ADDITIONAL READING	185
29	I-75 -- TAMPA, FLORIDA (HILLSBOROUGH COUNTY)	186
	1. INTRODUCTION	186
	2. DESIGN	186
	3. CLIMATE	186
	4. TRAFFIC	186
	5. DRAINABILITY AND OTHER PHYSICAL TESTING RESULTS	186
	6. MAINTENANCE AND REHABILITATION	187
	7. PAVEMENT PERFORMANCE	187
	8. CONCLUSIONS	187
30	INTERSTATE 75 -- TAMPA, FLORIDA (MANATEE COUNTY)	188
	1. INTRODUCTION	188
	2. DESIGN	188
	3. CLIMATE	188
	4. TRAFFIC	188
	5. DRAINABILITY AND OTHER PHYSICAL TESTING RESULTS	188
	6. MAINTENANCE AND REHABILITATION	189
	7. PAVEMENT PERFORMANCE	189
	8. CONCLUSIONS	191
	9. ADDITIONAL READING	191
31	KEY TO PROJECT SUMMARY TABLES	192
	1. GENERAL AND ENVIRONMENTAL DATA	192
	2. DESIGN DATA	193
	3. MONITORING DATA	199
	4. PERFORMANCE DATA	203
32	SUMMARY OF PROJECT DATA	205
33	REFERENCES	246

VOLUME V APPENDIX B - DATA COLLECTION AND ANALYSIS PROCEDURES

Chapter		Page
1	FIELD DATA COLLECTION PROCEDURES	1
	1. INTRODUCTION	1

TABLE OF CONTENTS (continued)

VOLUME V APPENDIX B - DATA COLLECTION AND ANALYSIS PROCEDURES (continued)

Chapter		Page
	2. CONDITION SURVEY	1
	Measurements	1
	Mapped Distresses	5
	Evaluated Conditions	6
	Noted Conditions	6
	3. PHOTO SURVEY	6
	4. DRAINAGE SURVEY	8
	5. FIELD TESTING	9
	Falling Weight Deflectometer (FWD)	9
	Coring and boring	9
	Roughness/PSR	14
	Traffic Control	14
	6. WEIGH-IN-MOTION DATA COLLECTION	14
	7. SUGGESTIONS FOR FUTURE DATA COLLECTION AND TESTING	16
2	WEIGH-IN-MOTION DATA COLLECTION PROCEDURES	17
	1. INTRODUCTION	17
	2. SITE SETUP AND CALIBRATION	17
	3. ACCURACY OF WIM DATA	19
3	TRAFFIC ANALYSIS	23
	1. INTRODUCTION	23
	2. INPUTS FOR PROCEDURE	23
	Average Daily Traffic, ADT	23
	Percentage of Heavy Trucks, TKS	23
	Directional Distribution, DD	24
	Lane Distribution, LD	24
	Average Truck Factor, TF	24
	3. CALCULATION PROCEDURE	25
	4. SUMMARY	25
4	DRAINAGE ANALYSIS AND DETERMINATION OF DRAINAGE COEFFICIENTS	26
	1. INTRODUCTION	26
	2. AASHTO DRAINAGE CRITERIA	27
	Roadbed Soils	27
	Cross Section	27
	3. MAD INDEX	28
	Base Drainability	29
	Climatic Moisture	29
	Subgrade	29
	MAD Index Categories	29
	Base Drainage	29
	Subgrade Drainage	30

TABLE OF CONTENTS (continued)

VOLUME V APPENDIX B - DATA COLLECTION AND ANALYSIS PROCEDURES (continued)

Chapter		Page
	Climatic Moisture Availability	30
4.	DEVELOPING A DRAINAGE COEFFICIENT	32
	Time of Saturation	32
	Base Drainability	35
	Subgrade Drainability	37
	Combining Base and Subgrade	37
	Cross Section	37
5.	DRAINAGE COEFFICIENTS FOR SECTIONS	39
	Arizona 1	40
	Arizona 2	40
	California 1	41
	California 2	41
	California 3	42
	California 6	43
	California 7	43
	California 8	44
	Florida 2	44
	Florida 3	44
	Michigan 1	44
	Michigan 3	45
	Michigan 4	46
	Michigan 5	46
	Minnesota 1	47
	Minnesota 2	48
	Minnesota 3	49
	Minnesota 4	49
	Minnesota 5	49
	Minnesota 6	50
	New Jersey 2	50
	New Jersey 3	51
	New York 1	51
	New York 2	52
	North Carolina 1	53
	North Carolina 2	54
	Ohio 1	54
	Ohio 2	55
	Ontario 1	55
	Ontario 2	56
	Pennsylvania 1	56
5	BACKCALCULATION METHODOLOGY	58
1.	INTRODUCTION	58
2.	FUNDAMENTAL CONCEPTS	58
3.	OUTLINE OF BACKCALCULATION PROCEDURE	63
4.	APPLICATION OF CLOSED-FORM BACKCALCULATION PROCEDURE	64
5.	VARIABILITY AND RELIABILITY OF TESTING AND	

TABLE OF CONTENTS (continued)

VOLUME V APPENDIX B - DATA COLLECTION AND ANALYSIS PROCEDURES (continued)

Chapter		Page
	BACKCALCULATED VALUES	65
	Plate Theory	66
	Deflection Measurement	69
	Finite Element Analysis	70
	6. ADVANTAGES OF CLOSED-FORM BACKCALCULATION PROCEDURE	75
6	DATABASE DESCRIPTION	77
7	REFERENCES	82
8	ANNOTATED BIBLIOGRAPHY	85
	1. EXPERIMENTAL PROJECTS AND PAVEMENT PERFORMANCE	85
	2. SUBDRAINAGE	102
	3. LOAD TRANSFER	109
	4. JOINTS AND JOINT SEALING	111
	5. CONCRETE SHOULDERS	116
	6. PAVEMENT DESIGN	119
	7. PAVEMENT ANALYSIS	123
	8. LIFE CYCLE COSTS	125
	9. WEIGH-IN-MOTION	126

VOLUME VI APPENDIX C AND APPENDIX D

APPENDIX C - SYNTHESIS OF CONCRETE PAVEMENT DESIGN METHODS AND ANALYSIS MODELS

Chapter		Page
PART I.	REVIEW OF SELECTED DESIGN AND ANALYSIS MODELS	1
	1. INTRODUCTION	1
	2. EVALUATION OF THE ANALYSIS AND DESIGN MODELS	1
	3. CAPABILITIES AND LIMITATIONS OF ANALYSIS MODELS	2
	ILLISLAB	2
	Capabilities	2
	Limitations	3
	JSLAB	4
	Capabilities	4
	Limitations	4
	WESLIQID	5
	Capabilities	5
	Limitations	5
	WESLAYER	6
	Capabilities	6
	Limitations	6

TABLE OF CONTENTS (continued)

VOLUME VI APPENDIX C AND APPENDIX D

APPENDIX C - SYNTHESIS OF CONCRETE PAVEMENT DESIGN METHODS AND ANALYSIS MODELS (continued)

Chapter		Page
	PMARP	7
	Capabilities	7
	Limitations	7
	RISC	9
	Capabilities	9
	Limitations	10
	H51	10
	Capabilities	10
	Limitations	11
	CMS	11
	Capabilities	11
	Limitations	12
	Liu-Lytton Drainage Models	12
	Capabilities	13
	Limitations	13
	JRCP4	14
	Capabilities	14
	Limitations	14
4.	CAPABILITIES AND LIMITATIONS OF DESIGN AND PREDICTION MODELS	15
	PREDICT	15
	Capabilities	15
	Limitations	16
	PEARDARP	16
	Capabilities	16
	Limitations	17
	JCP-1	17
	Capabilities	17
	Limitations	18
	DNPS86	19
	Capabilities	19
	Limitations	19
	RPS-3	20
	Capabilities	20
	Limitations	21
	PCA Design Procedure	22
	Capabilities	22
	Limitations	22
	California Rigid Pavement Design Procedure	23
	Capabilities	23
	Limitations	23
	BERM	24
	Capabilities	24
	Limitations	25
	JCS-1	25

TABLE OF CONTENTS (continued)

VOLUME VI APPENDIX C AND APPENDIX D

APPENDIX C - SYNTHESIS OF CONCRETE PAVEMENT DESIGN METHODS AND ANALYSIS MODELS (continued)

Chapter		Page
	Capabilities	25
	Limitations	26
5.	OVERALL PROGRAM EVALUATION	26
	Structural Analysis Models	27
	Drainage/Climatic Analysis Models	27
	Pavement Design Methods	28
6.	RECOMMENDATIONS	28
	Structural Analysis Model	28
	Prediction Models	30
	Drainage/Climatic Model	30
	Design Method	30
PART II.	STANDARD PAVEMENT SECTION AND VARIABLES UNDER CONSIDERATION	32
PART III.	SUMMARY OF INPUT AND OUTPUT VARIABLES	51
PART IV.	RESULTS OF SENSITIVITY ANALYSIS	79

APPENDIX D - SUMMARY OF ANALYSIS DATA FOR THE EVALUATION OF PREDICTIVE MODELS

Chapter		Page
1.	INTRODUCTION	115
2.	DESCRIPTION OF TABLES AND FIGURES	115
REFERENCES		329

LIST OF FIGURES

VOLUME I EVALUATION OF CONCRETE PAVEMENT PERFORMANCE AND DESIGN FEATURES

Figure	Title	Page
1.	States and Provinces participating in study	5
2.	Experimental design matrix for Minnesota 1	7
3.	Experimental design matrix for Minnesota 2	7
4.	Experimental design matrix for Arizona 1	9
5.	Experimental design matrix for California 1	10
6.	Experimental design matrix for California 2	10
7.	Experimental design matrix for Michigan 1	12
8.	Experimental design matrix for Michigan 4	12
9.	Experimental design matrix for New York 1	14
10.	Experimental design matrix for New York 2	14
11.	Experimental design matrix for Ohio 1	16
12.	Experimental design matrix for Ohio 2	16
13.	Experimental design matrix for Ontario 1	17
14.	Experimental design matrix for Pennsylvania 1	19
15.	Experimental design matrix for New Jersey 3	20
16.	Experimental design matrix for California 3	20
17.	Experimental design matrix for North Carolina 1	22
18.	Outer lane performance data for Minnesota 1 (Age = 17 years, ESAL's = 5.5 million)	29
19.	Outer lane performance data for Minnesota 2 (Age = 10 years, ESAL's = 2.8 million)	33
20.	Outer lane performance data for Arizona 1	39
21.	Outer lane performance data for California 1 (Age = 16 years, ESAL's = 7.6 million)	43
22.	Outer lane performance data for California 2 (Age = 7 years, ESAL's = 4.4 million)	47
23.	Outer lane performance data for Michigan 1 (Age = 12 years, ESAL's = 0.89 million)	53
24.	Outer lane performance data for Michigan 4 (Age = 17 years, ESAL's = 4.4 million)	58
25.	Outer lane performance data for New York 1 (Age = 19 years, ESAL's = 3.1 million)	64
26.	Outer lane performance data for New York 2 (Age = 12 years, ESAL's = 1.4 million)	67
27.	Outer lane performance data for Ohio 1 (Age = 14 years, ESAL's = 3.4 million)	71
28.	Outer lane performance data for Ohio 2 (Age = 13 years, ESAL's = 3.3 million)	74
29.	Performance data by direction for Ontario 1 (Age = 5 years, ESAL's = 1.0 million)	77
30.	Outer lane performance data for Pennsylvania 1	83
31.	Outer lane performance data for New Jersey 3 (Age = 8 years, ESAL's = 4.2 million)	87
32.	Outer lane performance data for California 3 (Age = 12 years, ESAL's = 3.6 million)	91
33.	Outer lane performance data for North Carolina 1 (Age = 20 years, ESAL's 9.1 million)	95

LIST OF FIGURES (continued)

VOLUME I EVALUATION OF CONCRETE PAVEMENT PERFORMANCE AND DESIGN FEATURES (continued)

Figure	Title	Page
34.	Percent cracked slabs vs. L/l for California 1 (Tracy) sections	131
35.	Percent cracked slabs vs. L/l for all sections with cement-treated and lean concrete bases	132
36.	Percent cracked slabs vs. L/l for all sections with aggregate bases	134

VOLUME II EVALUATION AND MODIFICATION OF CONCRETE PAVEMENT DESIGN AND ANALYSIS MODELS

Figure	Title	Page
1.	Distribution of base type by environmental region	13
2.	Distribution of slab thickness by environmental region	14
3.	Distribution of joint spacing and pavement type by environmental region (P=JPCP, R=JRCP)	15
4.	Distribution of load transfer method by environmental region	16
5.	Distribution of shoulder type by environmental region	18
6.	Scattergram of actual field-measured faulting versus faulting as predicted using the COPES faulting models for the dry-freeze region	42
7.	Experimental design matrix for Minnesota 1	70
8.	Experimental design matrix for California 1	72
9.	Experimental design matrix for Michigan 1	73
10.	Experimental design matrix for North Carolina 1	74
11.	Use of CMS in the design process	77
12.	Temperature profile versus depth through the slab on July 15, 1987, Rothsay, Minnesota	81
13.	Change in 6 a.m. thermal gradient in June 1987, Rothsay, Minnesota	82
14.	Change in 3 p.m. thermal gradient in June 1987, Rothsay, Minnesota	82
15.	Temperature profile versus depth through the slab on July 15, 1987, Tracy, California	86
16.	Change in 6 a.m. thermal gradient from January through June 1987, Tracy, California	88
17.	Change in 6 a.m. thermal gradient from July through December 1987, Tracy, California	88
18.	Change in 3 p.m. thermal gradient from January through June 1987, Tracy, California	90
19.	Change in 3 p.m. thermal gradient from July through December 1987, Tracy, California	90
20.	Temperature profile versus depth through the slab on July 15, 1987, Clare, Michigan	91
21.	Change in 6 a.m. thermal gradient in April 1987, Clare, Michigan	92
22.	Change in 3 p.m. thermal gradient in April 1987, Clare, Michigan	92
23.	Change in 6 a.m. thermal gradient in June 1987, Clare, Michigan	93
24.	Change in 3 p.m. thermal gradient in June 1987, Clare, Michigan	93

LIST OF FIGURES (continued)

VOLUME II EVALUATION AND MODIFICATION OF CONCRETE PAVEMENT DESIGN AND ANALYSIS MODELS (continued)

Figure	Title	Page
25.	Change in 6 a.m. thermal gradient in August 1987, Clare, Michigan	94
26.	Change in 3 p.m. thermal gradient in August 1987, Clare, Michigan	94
27.	Change in 6 a.m. thermal gradient in December 1987, Clare Michigan	95
28.	Change in 3 p.m. thermal gradient in December 1987, Clare Michigan	95
29.	Frostline versus depth in January, 1987, Clare, Michigan	96
30.	Temperature profile versus depth through the slab on July 15, 1987, Rocky Mount, North Carolina	100
31.	Change in 6 a.m. thermal gradient in July 1987, Rocky Mount, North Carolina	102
32.	Change in 3 p.m. thermal gradient in April 1987, Clare, Michigan	102
33.	Percent drainage versus time for MN 1-1, MN 1-5, and MN 1-9	108
34.	Percent saturation versus base course modulus for MN 1-1, MN 1-2, MN 1-3, and MN 1-4	111
35.	Percent saturation versus subgrade modulus for MN 1-1, MN 1-2, MN 1-3, and MN 1-4	113
36.	Percent drainage versus time for CA 1-1, CA 1-7, and CA 1-9	115
37.	Percent saturation versus subbase modulus for CA 1-1, CA 1-7, and CA 1-9	117
38.	Percent saturation versus subgrade modulus for CA 1-1, CA 1-7, and CA 1-9	118
39.	Percent drainage versus time for MI 1-1a, MI 1-4a, and MI 1-10b	120
40.	Percent saturation versus base or subbase modulus for MI 1-1a, MI 1-10a, and MI 1-10b	122
41.	Percent saturation versus subgrade modulus for MI 1-1a, MI 1-4a, and MI 1-10b	123
42.	Percent drainage versus time for NC 1-1, NC 1-2, and NC 1-7	126
43.	Percent saturation versus base modulus for NC 1-1, NC 1-7, and NC 1-8	127
44.	Percent saturation versus subgrade modulus for NC 1-1, NC 1-7, and NC 1-8	129
45.	Example finite element mesh for the edge loading condition	136
46.	FWD sensor location at the approach joint	148
47.	Measured deflection basin and calculated deflection basin from void analysis	150
48.	Finite element mesh for a 15-ft (4.6 m) slab used in the PMARP evaluation of the corner loading condition	157
49.	Original zero-maintenance fatigue damage curve supplemented with projects from current study	167
50.	Predicted versus actual faulting for doweled joint faulting model	184
51.	Sensitivity of doweled joint faulting model to dowel diameter	185
52.	Sensitivity of doweled joint faulting model to drainage and shoulder type	186
53.	Predicted versus actual faulting for nondoweled joint faulting model	189
54.	Sensitivity of doweled and nondoweled faulting models to drainage and shoulder type	190
55.	Relation between deflection load transfer efficiency and stress load transfer efficiency	195
56.	Percent slabs cracked versus accumulated fatigue damage	197
57.	Sensitivity of cracking model to shoulder type	198
58.	Sensitivity of cracking model to joint spacing	199
59.	Sensitivity of cracking model to slab thickness	201
60.	Sensitivity of JPCP joint spalling model to sealant type	203

LIST OF FIGURES (continued)

VOLUME II EVALUATION AND MODIFICATION OF CONCRETE PAVEMENT DESIGN AND ANALYSIS MODELS (continued)

Figure	Title	Page
61.	Sensitivity of JRCP joint spalling model to climate	204
62.	Sensitivity of JRCP joint spalling model to sealant type	206

VOLUME III SUMMARY OF RESEARCH FINDINGS

Figure	Title	Page
1.	States participating in study	4
2.	Distribution of base type by climatic region	11
3.	Distribution of slab thickness by climatic region	13
4.	Distribution of joint spacing/pavement type by climatic region	14
5.	Distribution of load transfer mechanism by climatic region	15
6.	Distribution of shoulder type (and widened lanes) by climatic region	16
7.	Percent slab cracking as a function of L/*l* for sections with aggregate bases	25
8.	Percent slab cracking as a function of L/*l* for sections with LCB and CTB bases	25
9.	Sensitivity of doweled faulting model to dowel diameter	58
10.	Sensitivity of doweled faulting model to drainage and shoulder type	58
11.	Sensitivity of faulting models to dowels, drainage, and shoulder type	59
12.	Percent slab cracking as a function of accumulated fatigue damage	59
13.	Sensitivity of JPCP cracking model to shoulder type	63
14.	Sensitivity of JPCP cracking model to joint spacing	63
15.	Sensitivity of JPCP cracking model to slab thickness	64
16.	Sensitivity of JPCP spalling model to joint sealant type	64
17.	Sensitivity of JPCP spalling model to climate	66
18.	Sensitivity of JRCP spalling model to joint sealant type	66

VOLUME IV APPENDIX A - PROJECT SUMMARY REPORTS AND SUMMARY TABLES

Figure	Title	Page
1.	Outer lane performance data for Minnesota 1	4
2.	Inner lane performance data for Minnesota 1	5
3.	Outer and inner lane performance data for Minnesota 2	16
4.	Outer lane performance data for Arizona 1	32
5.	Inner lane performance data for Arizona 1	33
6.	Outer lane performance data for California 1	45
7.	Inner lane performance data for California 1	46
8.	Outer and middle lane performance data for California 2	55
9.	Outer lane performance data for Michigan 1	70
10.	Inner lane performance data for Michigan 1	71
11.	Outer and inner lane performance data for Michigan 4	85
12.	Outer lane performance data for New York 1	97

LIST OF FIGURES (continued)

VOLUME IV APPENDIX A - PROJECT SUMMARY REPORTS AND SUMMARY TABLES (continued)

Figure	Title	Page
13.	Inner lane performance data for New York 1	98
14.	Outer lane performance data for New York 2	108
15.	Inner lane performance data for New York 2	109
16.	Outer lane performance data for Ohio 1	117
17.	Inner lane performance data for Ohio 1	118
18.	Outer and inner lane performance data for Ohio 2	126
19.	Performance data by direction for Ontario 1	136
20.	Outer lane performance data for Pennsylvania 1	148
21.	Inner lane performance data for Pennsylvania 1	149
22.	Outer and middle lane performance data for New Jersey 3	158
23.	Outer lane performance data for California 3	165
24.	Inner lane performance data for California 3	166
25.	Outer lane performance data for North Carolina 1	175
26.	Inner lane performance data for North Carolina 1	176

VOLUME V APPENDIX B - DATA COLLECTION AND ANALYSIS PROCEDURES

Figure	Title	Page
1.	General field survey sheet	2
2.	Drainage field survey sheet	3
3.	Field data collection form	4
4.	Project photographic record	7
5.	Layout for FWD testing of projects with AC shoulders	10
6.	Layout for FWD testing of projects with PCC shoulders	11
7.	Layout for FWD testing of projects with widened lanes	12
8.	Raw data file from the Dynatest model 8000	13
9.	Sample raw output from Mays Roughness Meter	15
10.	Climatic zones for AASHTO and FHWA procedures	31
11.	Plot of monthly rainfall and potential evapotranspiration for Clare, Michigan	34
12.	Procedure to combine drainabilities of base and subgrade	38
13.	Variation in deflection basin AREA with radius of relative stiffness	60
14.	Variation in dimensionless deflections with radius of relative stiffness for the dense liquid foundation	61
15.	Variation in dimensionless deflections with radius of relative stiffness for the elastic solid foundation	62
16.	Deflection basin as measured by the FWD and as calculated using the closed-form procedure	71
17.	Deflection basin as measured by the FWD and as calculated using the closed-form procedure	72
18.	Deflection basin as measured by the FWD and as calculated using the closed-form procedure	73
19.	Eh**3 versus kl**4 for all Phase I sections	74
20.	Main UNIFY database menu	79
21.	Inventory database menu	80
22.	Monitoring database menu	81

LIST OF FIGURES (continued)

VOLUME VI APPENDIX C AND APPENDIX D

APPENDIX C - SYNTHESIS OF CONCRETE PAVEMENT DESIGN METHODS AND ANALYSIS MODELS

Figure	Title	Page
1.	Assumed standard pavement section	33
2.	ILLISLAB and JSLAB finite element mesh for standard pavement section analysis	38
3.	ILLISLAB and JSLAB finite element mesh for 10-ft joint spacing analysis	39
4.	ILLISLAB and JSLAB finite element mesh for 20-ft joint spacing analysis	40
5.	ILLISLAB and JSLAB finite element mesh for widened lane analysis	41
6.	WESLIQID and WESLAYER finite element mesh for standard pavement analysis using a four-slab system	42
7.	WESLIQID and WESLAYER finite element mesh for standard pavement analysis using a two-slab system	43
8.	WESLIQID and WESLAYER finite element mesh for 10-ft joint spacing analysis	44
9.	WESLIQID and WESLAYER finite element mesh for 20-ft joint spacing analysis	45
10.	WESLIQID and WESLAYER finite element mesh for widened lane analysis	46
11.	PMARP finite element mesh for standard pavement section	47
12.	PMARP finite element mesh for widened lane analysis	48
13.	PMARP finite element mesh for 20-ft joint spacing analysis	49
14.	Wheel configuration used for H-51 analysis	50
15.	Temperature gradient as measured by CMS	93
16.	Climatic zones based on Thornthwaite potential evapotranspiration and moisture index and their interaction with performance, with similar performance expected in similar climatic regions (5)	98

APPENDIX D - SUMMARY OF ANALYSIS DATA FOR THE EVALUATION OF PREDICTIVE MODELS

Figure	Title	Page
17.	Actual ESAL's (based on ADT) versus ESAL's as predicted using the AASHTO design equation for all Phase I sections	119
18.	Actual ESAL's (based on ADT) versus ESAL's as predicted using the AASHTO design equation for the dry-freeze region	122
19.	Actual ESAL's (based on ADT) versus ESAL's as predicted using the AASHTO design equation for the dry-nonfreeze region	122
20.	Actual ESAL's (based on ADT) versus ESAL's as predicted using the AASHTO design equation for the wet-freeze region	126
21.	Actual ESAL's (based on ADT) versus ESAL's as predicted using the AASHTO design equation for the wet-nonfreeze region	126

LIST OF FIGURES (continued)

VOLUME VI APPENDIX C AND APPENDIX D

APPENDIX D - SUMMARY OF ANALYSIS DATA FOR THE EVALUATION OF PREDICTIVE MODELS (continued)

Figure	Title	Page
22.	Actual PSR as determined by a panel of users versus PSI as predicted by the PEARDARP PSI model for all Phase I sections	130
23.	Actual PSR as determined by a panel of users versus PSI as predicted by the PEARDARP PSI model for the dry-freeze region	133
24.	Actual PSR as determined by a panel of users versus PSI as predicted by the PEARDARP PSI model for the dry-nonfreeze region	133
25.	Actual PSR as determined by a panel of users versus PSI as predicted by the PEARDARP PSI model for the wet-freeze region	137
26.	Actual PSR as determined by a panel of users versus PSI as predicted by the PEARDARP PSI model for the wet-nonfreeze region	137
27.	Actual field measured roughness versus roughness as predicted using the PEARDARP roughness model for all Phase I sections	141
28.	Actual field measured roughness versus roughness as predicted using the PEARDARP roughness model for the dry-freeze region	144
29.	Actual field measured roughness versus roughness as predicted using the PEARDARP roughness model for the dry-nonfreeze region	144
30.	Actual field measured roughness versus roughness as predicted using the PEARDARP roughness model for the wet-freeze region	148
31.	Actual field measured roughness versus roughness as predicted using the PEARDARP roughness model for the wet-nonfreeze region	148
32.	Actual field measured spalling versus spalling as predicted using the PEARDARP spalling model for all Phase I sections	155
33.	Actual field measured spalling versus spalling as predicted using the PEARDARP spalling model for the dry-freeze region	158
34.	Actual field measured spalling versus spalling as predicted using the PEARDARP spalling model for the dry-nonfreeze region	158
35.	Actual field measured spalling versus spalling as predicted using the PEARDARP spalling model for the wet-freeze region	162
36.	Actual field measured spalling versus spalling as predicted using the PEARDARP spalling model for the wet-nonfreeze region	162
37.	Actual field measured faulting versus faulting as predicted using the PEARDARP faulting models for all Phase I sections	166
38.	Actual field measured faulting versus faulting as predicted using the PEARDARP faulting models for the dry-freeze region	168
39.	Actual field measured faulting versus faulting as predicted using the PEARDARP faulting models for doweled pavements for the dry-freeze region	171
40.	Actual field measured faulting versus faulting as predicted using the PEARDARP faulting models for nondoweled pavements for the dry-freeze region	171
41.	Actual field measured faulting versus faulting as predicted using the PEARDARP faulting models for the dry-nonfreeze region	173

LIST OF FIGURES (continued)

VOLUME VI APPENDIX C AND APPENDIX D

APPENDIX D - SUMMARY OF ANALYSIS DATA FOR THE EVALUATION OF PREDICTIVE MODELS (continued)

Figure	Title	Page
42.	Actual field measured faulting versus faulting as predicted using the PEARDARP faulting models for the wet-freeze region	176
43.	Actual field measured faulting versus faulting as predicted using the PEARDARP faulting models for doweled pavements for the wet-freeze region	179
44.	Actual field measured faulting versus faulting as predicted using the PEARDARP faulting models for nondoweled pavements for the wet-freeze region	179
45.	Actual field measured faulting versus faulting as predicted using the PEARDARP faulting models for the wet-nonfreeze region	181
46.	Actual field measured faulting versus faulting as predicted using the PEARDARP faulting models for doweled pavements for the wet-nonfreeze region	184
47.	Actual field measured faulting versus faulting as predicted using the PEARDARP faulting models for nondoweled pavements for the wet-nonfreeze region	184
48.	Actual field measured cracking versus cracking as predicted using the PEARDARP cracking models for all Phase I sections	188
49.	Actual field measured cracking versus cracking as predicted using the PEARDARP cracking model for the dry-freeze region	191
50.	Actual field measured cracking versus cracking as predicted using the PEARDARP cracking model for the dry-nonfreeze region	191
51.	Actual field measured cracking versus cracking as predicted using the PEARDARP cracking model for the wet-freeze region	195
52.	Actual field measured cracking versus cracking as predicted using the PEARDARP cracking model for the wet-nonfreeze region	195
53.	Actual field observed pumping versus pumping as predicted using COPES pumping models for all Phase I sections	199
54.	Actual field observed pumping versus pumping as predicted using COPES pumping models for the dry-freeze region	201
55.	Actual field observed pumping versus pumping as predicted using COPES JPCP pumping model for the dry-freeze region	204
56.	Actual field observed pumping versus pumping as predicted using COPES JRCP pumping model for the dry-freeze region	204
57.	Actual field observed pumping versus pumping as predicted using COPES pumping model for the dry-nonfreeze region	206
58.	Actual field observed pumping versus pumping as predicted using COPES pumping model for the wet-freeze region	209
59.	Actual field observed pumping versus pumping as predicted using COPES JPCP pumping model for the wet-freeze region	212
60.	Actual field observed pumping versus pumping as predicted using COPES JRCP pumping model for the wet-freeze region	212
61.	Actual field observed pumping versus pumping as predicted using COPES pumping model for the wet-nonfreeze region	214

LIST OF FIGURES (continued)

VOLUME VI APPENDIX C AND APPENDIX D

APPENDIX D - SUMMARY OF ANALYSIS DATA FOR THE EVALUATION OF PREDICTIVE MODELS (continued)

Figure	Title	Page
62.	Actual field measured faulting versus faulting as predicted using the COPES faulting models for all Phase I sections	218
63.	Actual field measured faulting versus faulting as predicted using the COPES faulting models for the dry-freeze region	220
64.	Actual field measured faulting versus faulting as predicted using the COPES JPCP faulting model for the dry-freeze region	223
65.	Actual field measured faulting versus faulting as predicted using the COPES JRCP faulting model for the dry-freeze region	223
66.	Actual field measured faulting versus faulting as predicted using the COPES faulting models for the dry-nonfreeze region	225
67.	Actual field measured faulting versus faulting as predicted using the COPES faulting models for the wet-freeze region	228
68.	Actual field measured faulting versus faulting as predicted using the COPES JPCP faulting model for the wet-freeze region	231
69.	Actual field measured faulting versus faulting as predicted using the COPES JRCP faulting model for the wet-freeze region	231
70.	Actual field measured faulting versus faulting as predicted using the COPES faulting models for the wet-nonfreeze region	233
71.	Actual field measured spalling versus joint deterioration (spalling) as predicted using the COPES spalling models for all Phase I sections	237
72.	Actual field measured spalling versus joint deterioration (spalling) as predicted using the COPES spalling models for the dry-freeze region	239
73.	Actual field measured spalling versus joint deterioration (spalling) as predicted using the COPES JPCP joint deterioration model for the dry-freeze region	242
74.	Actual field measured spalling versus joint deterioration (spalling) as predicted using the COPES JRCP joint deterioration model for the dry-freeze region	242
75.	Actual field measured spalling versus joint deterioration (spalling) as predicted using the COPES spalling models for the dry-nonfreeze region	244
76.	Actual field measured spalling versus joint deterioration (spalling) as predicted using the COPES spalling models for the wet-freeze region	247
77.	Actual field measured spalling versus joint deterioration (spalling) as predicted using the COPES JPCP joint deterioration model for the wet-freeze region	250
78.	Actual field measured spalling versus joint deterioration (spalling) as predicted using the COPES JRCP joint deterioration model for the wet-freeze region	250

LIST OF FIGURES (continued)

VOLUME VI APPENDIX C AND APPENDIX D

APPENDIX D - SUMMARY OF ANALYSIS DATA FOR THE EVALUATION OF PREDICTIVE MODELS (continued)

Figure	Title	Page
79.	Actual field measured spalling versus joint deterioration (spalling) as predicted using the COPES spalling models for the wet-nonfreeze region	252
80.	Actual field measured cracking versus cracking as predicted by the COPES cracking models for all Phase I sections	256
81.	Actual field measured cracking versus cracking as predicted by the COPES cracking models for the dry-freeze region	258
82.	Actual field measured cracking versus cracking as predicted by the COPES JPCP cracking model for the dry-freeze region	261
83.	Actual field measured cracking versus cracking as predicted by the COPES JRCP cracking model for the dry-freeze region	261
84.	Actual field measured cracking versus cracking as predicted by the COPES cracking models for the dry-nonfreeze region	263
85.	Actual field measured cracking versus cracking as predicted by the COPES cracking models for the wet-freeze region	266
86.	Actual field measured cracking versus cracking as predicted by the COPES JPCP cracking models for the wet-freeze region	269
87.	Actual field measured cracking versus cracking as predicted by the COPES JRCP cracking models for the wet-freeze region	269
88.	Actual field measured cracking versus cracking as predicted by the COPES cracking models for the wet-nonfreeze region	271
89.	Actual PSR as determined by a panel of users versus PSR as predicted by the COPES PSR models for all Phase I sections	275
90.	Actual PSR as determined by a panel of users versus PSR as predicted by the COPES PSR models for the dry-freeze region	277
91.	Actual PSR as determined by a panel of users versus PSR as predicted by the COPES JPCP PSR model for the dry-freeze region	280
92.	Actual PSR as determined by a panel of users versus PSR as predicted by the COPES JRCP PSR model for the dry-freeze region	280
93.	Actual PSR as determined by a panel of users versus PSR as predicted by the COPES PSR models for the dry-nonfreeze region	282
94.	Actual PSR as determined by a panel of users versus PSR as predicted by the COPES PSR models for the wet-freeze region	285
95.	Actual PSR as determined by a panel of users versus PSR as predicted by the COPES JPCP PSR model for the wet-freeze region	288
96.	Actual PSR as determined by a panel of users versus PSR as predicted by the COPES JRCP PSR model for the wet-freeze region	288
97.	Actual PSR as determined by a panel of users versus PSR as predicted by the COPES PSR models for the wet-nonfreeze region	290
98.	Actual field measured faulting versus faulting as predicted using the PFAULT models for all Phase I sections	294
99.	Actual field measured faulting versus faulting as predicted using the PFAULT models for the dry-freeze region	296

LIST OF FIGURES (continued)

VOLUME VI APPENDIX C AND APPENDIX D

APPENDIX D - SUMMARY OF ANALYSIS DATA FOR THE EVALUATION OF PREDICTIVE MODELS (continued)

Figure	Title	Page
100.	Actual field measured faulting versus faulting as predicted using the PFAULT models for doweled pavements for the dry-freeze region	299
101.	Actual field measured faulting versus faulting as predicted using the PFAULT models for nondoweled pavements for the dry-freeze region	299
102.	Actual field measured faulting versus faulting as predicted using the PFAULT models for the dry-nonfreeze region	301
103.	Actual field measured faulting versus faulting as predicted using the PFAULT models for the wet-freeze region	304
104.	Actual field measured faulting versus faulting as predicted using the PFAULT models for doweled pavements for the wet-freeze region	307
105.	Actual field measured faulting versus faulting as predicted using the PFAULT models for nondoweled pavements for the wet-freeze region	307
106.	Actual field measured faulting versus faulting as predicted using the PFAULT models for the wet-nonfreeze region	309
107.	Actual field measured faulting versus faulting as predicted using the PFAULT models for doweled pavements for the wet-nonfreeze region	312
108.	Actual field measured faulting versus faulting as predicted using the PFAULT models for nondoweled pavements for the wet-nonfreeze region	312

LIST OF TABLES

VOLUME I EVALUATION OF CONCRETE PAVEMENT PERFORMANCE AND DESIGN FEATURES

Table	Title	Page
1.	Listing of critical distress values by pavement type	26
2.	Slab modulus and composite k-values for Minnesota 1	28
3.	Deflection testing results and drainage coefficients for Minnesota 1	28
4.	Slab modulus and composite k-values for Minnesota 2	32
5.	Deflection testing results and drainage coefficients for Minnesota 2	32
6.	Longitudinal lane-shoulder joint load transfer efficiency for Minnesota 2	32
7.	Design and performance data for the outer lane of Minnesota 3 (Age = 1 year, ESAL's = 1.5 million)	36
8.	Design and performance data for the outer lane of Minnesota 4 (Age = 1 year, ESAL's = 0.22 million)	36
9.	Design and performance data for the outer lane of Minnesota 6 (Age = 4 years, ESAL's = 0.85 million)	36
10.	Traffic information for Arizona 1	38
11.	Slab modulus and composite k-values for Arizona 1	38
12.	Deflection testing results and drainage coefficients for Arizona 1	38
13.	Longitudinal lane-shoulder joint load transfer efficiency for Arizona 1	38
14.	Design and performance data for the outer lane of Arizona 2 (Age = 4 years, ESAL's = 1.6 million)	42
15.	Slab modulus and composite k-values for California 1	42
16.	Deflection testing results and drainage coefficients for California 1	42
17.	Slab modulus and composite k-values for California 2	46
18.	Deflection testing results and drainage coefficients for California 2	46
19.	Design and performance data for the outer lane of California 6 (Age = 7 years, ESAL's = 4.4 million)	49
20.	Design and performance data for the outer lane of California 7 (Age = 8 years, ESAL's = 10.5 million)	49
21.	Design and performance data for the outer lane of California 8 (Age = 4 years, ESAL's = 5.3 million)	49
22.	Slab modulus and composite k-values for Michigan 1	52
23.	Deflection testing results and drainage coefficients for Michigan 1	52
24.	Design and performance data for the outer lane of Michigan 3 (Age = 1 year, ESAL's = 2.8 million)	57
25.	Slab modulus and composite k-values for Michigan 4	57
26.	Deflection testing results and drainage coefficients for Michigan 4	57
27.	Longitudinal lane-shoulder joint load transfer efficiency for Michigan 4	57
28.	Design and performance data for the outer lane of Michigan 5 (Age = 3 years, ESAL's = 3.1 million)	62
29.	Slab modulus and composite k-values for New York 1	62
30.	Deflection testing results and drainage coefficients for New York 1	62
31.	Slab modulus and composite k-values for New York 2	66
32.	Deflection testing results and drainage coefficients for New York 2	66
33.	Longitudinal lane-shoulder joint load transfer efficiency for New York 2	66
34.	Slab modulus and composite k-values for Ohio 1	67
35.	Deflection testing results and drainage coefficients for Ohio 1	75
36.	Deflection testing results and drainage coefficients for Ontario 1	76
37.	Design and performance data for the outer lane of Ontario 2 (Age = 16 years, ESAL's = 36 million)	81

LIST OF TABLES (continued)

VOLUME I EVALUATION OF CONCRETE PAVEMENT PERFORMANCE AND DESIGN FEATURES (continued)

Table	Title	Page
38.	Traffic information for Pennsylvania 1	82
39.	Slab modulus and composite k-values for Pennsylvania 1	82
40.	Deflection testing results and drainage coefficients for Pennsylvania 1	82
41.	Design and performance data for the outer lane of New Jersey 2 (Age = 36 years, ESAL's = 35 million)	86
42.	Slab modulus and composite k-values for New Jersey 3	86
43.	Deflection testing results and drainage coefficients for New Jersey 3	86
44.	Slab modulus and composite k-values for California 3	90
45.	Deflection testing results and drainage coefficients for California 3	90
46.	Longitudinal lane-shoulder joint load transfer efficiency for California 3	90
47.	Slab modulus and composite k-values for North Carolina 1	94
48.	Deflection testing results and drainage coefficients for North Carolina 1	94
49.	Design and performance data for the outer lane of North Carolina 2 (Age = 5 years, ESAL's = 5.8 million)	98
50.	Design and performance data for the outer lane of Florida 2 (Age = 1 year, ESAL's = 2.0 million)	98
51.	Design and performance data for the outer lane of Florida 3 (Age = 5 years, ESAL's = 4.1 million)	100
52.	Transverse cracking by lane for Florida 3	100
53.	Effect of slab length on cracking for Florida 3	100
54.	Outer lane performance data relative to slab thickness for Minnesota 1 (Age = 17 years, ESAL's = 5.5 million)	103
55.	Outer lane performance data relative to slab thickness for Minnesota 2 (Age = 10 years, ESAL's = 2.8 million)	103
56.	Outer lane performance data relative to slab thickness for Arizona 1	103
57.	Outer lane performance data relative to slab thickness for California 1 (Age = 16 years, ESAL's = 7.6 million)	105
58.	Outer lane performance data relative to slab thickness for Ontario 1 (Age = 5 years, ESAL's = 0.84 million)	105
59.	Outer lane performance data relative to base type for Minnesota 1 (Age = 17 years, ESAL's = 5.5 million)	108
60.	Outer lane performance data relative to base type for Arizona 1	108
61.	Outer lane performance data relative to base type for California 1 (Age = 16 years, ESAL's = 7.6 million)	108
62.	Outer lane performance data relative to base type for California 2 (Age = 7 years, ESAL's = 4.4 million)	108
63.	Outer lane performance data relative to base type for Michigan 1 (Age = 12 years, ESAL's = 0.9 million)	110
64.	Outer lane performance data relative to base type for New York 1 (Age = 22 years, ESAL's = 2.0 million)	112
65.	Outer lane performance data relative to base type for Ohio 1 (Age = 14 years, ESAL's = 3.4 million)	112
66.	Average performance data relative to base type for Ontario 1 (Age = 5 years, ESAL's = 0.84 million)	112
67.	Outer lane performance data relative to base type for North Carolina 1 (Age = 20 years, ESAL's = 9.1 million)	114
68.	Overall relative summary of the performance of base types	116

LIST OF TABLES (continued)

VOLUME I EVALUATION OF CONCRETE PAVEMENT PERFORMANCE AND DESIGN FEATURES (continued)

Table	Title	Page
69.	Gradation information for permeable bases required for filter criteria evaluation	118
70.	Evaluation of filter criteria	119
71.	Outer lane performance data relative to joint spacing for Minnesota 1 (Age = 17 years, ESAL's = 5.5 million)	120
72.	Outer lane performance data relative to joint spacing for Minnesota 2 (Age = 10 years, ESAL's = 2.8 million)	120
73.	Outer lane performance data relative to joint spacing for California 1 (Age = 16 years, ESAL's = 7.6 million)	122
74.	Outer lane performance data relative to joint spacing for Michigan 1 (Age = 12 years, ESAL's = 0.9 million)	122
75.	Outer lane performance data relative to joint spacing for New York 1 (Age = 22 years, ESAL's = 2.0 million)	122
76.	Outer lane performance data relative to joint spacing for New York 2 (Age = 12 years, ESAL's = 1.43 million)	122
77.	Outer lane performance data relative to joint spacing for Ohio 1 (Age = 14 years, ESAL's = 3.4 million)	124
78.	Summary of cracking by slab length for sections with random joint spacing	126
79.	Ratio of slab length to the radius of relative stiffness (L/l)	127
80.	Effect of joint spacing, slab thickness, and base type on transverse cracking for California 1	130
81.	Summary of performance data related to reinforcement design	136
82.	Outer lane performance data relative to joint orientation for New York 1 (Age = 22 years, ESAL's = 2.0 million)	138
83.	Outer lane performance data relative to joint orientation for North Carolina 1 (Age = 20 years, ESAL's = 9.1 million)	138
84.	Outer lane performance data relative to joint load transfer for Minnesota 1 (Age = 17 years, ESAL's = 5.5 million)	140
85.	Outer lane performance data relative to joint load transfer for North Carolina 1 (Age = 20 years, ESAL's = 9.1 million)	140
86.	Load transfer performance data for nondoweled pavement sections	142
87.	Load transfer performance data for doweled sections	143
88.	Outer lane performance data relative to dowel coating for Ohio 1 (Age = 14 years, ESAL's = 3.4 million)	146
89.	Summary of longitudinal cracking and related design data	147
90.	Influence of shoulder on performance of mainline pavement for Michigan 4 (Age = 15 years, ESAL's = 4.4 million)	152
91.	Performance data relative to drainage for Michigan 1 (Age = 12 years, ESAL's = 0.9 million)	155
92.	Summary of selected performance data related to C_d	158

LIST OF TABLES (continued)

VOLUME II EVALUATION AND MODIFICATION OF CONCRETE PAVEMENT DESIGN AND ANALYSIS MODELS

Table	Title	Page
1.	Listing of pavement sections in dry-freeze environmental region	7
2.	Listing of pavement sections in dry-nonfreeze environmental region	8
3.	Listing of pavement sections in wet-freeze environmental region	10
4.	Listing of pavement sections in wet-nonfreeze environmental region	11
5.	Recommended levels of reliability for various functional classifications (1)	22
6.	Values of the drainage coefficient for the design of rigid pavements as presented in the AASHTO Guide (1)	24
7.	Load transfer coefficients for various pavement types and design conditions as presented in the AASHTO Guide (1)	24
8.	Actual field-measured faulting versus faulting as predicted using the COPES faulting models for the dry-freeze region	40
9.	Summary of the statistical analysis of the AASHTO design model	44
10.	Summary of the statistical analyses of the PEARDARP prediction models	47
11.	Summary of the statistical analyses of the COPES prediction models	53
12.	Summary of the statistical analyses of the PFAULT faulting prediction models	63
13.	CMS inputs for use with concrete pavements	76
14.	Specific sections and analyses performed using the CMS program	79
15.	Summary of thermal gradients at specified times for MN 1-1 for July 15 through July 21, 1987	80
16.	Analysis of stiffness of the paving layers in the deep frost, thaw-recovery, and nonfrost periods for MN 1-1	84
17.	Summary of thermal gradients at specified times for CA 1-1 for July 15 through July 21, 1987	87
18.	Summary of thermal gradients at specified times for MI 1-10a for July 15 through July 21, 1987	97
19.	Summary of thermal gradients at specified times for NC 1-1 for July 15 through July 21, 1987	101
20.	Summary of the results of the Liu-Lytton percent drainage versus time analyses for MN 1	107
21.	Relationships used in the Liu-Lytton drainage program to determine the base strength based on the level of saturation	112
22.	Summary of the results of the Liu-Lytton percent drainage versus time analysis for CA 1	114
23.	Permeabilities and porosities of subbase and subgrade for CA 1	114
24.	Time required to reach an 85 percent saturation level for CA 1 sections	116
25.	Probability of a wet subbase course for the CA 1 sections	119
26.	Summary of the results of the Liu-Lytton percent drainage versus time analyses for MI 1	119
27.	Permeabilities and porosities of subbase and subgrade for MI 1	121
28.	Time required to reach an 85 percent saturation level for MI 1 sections	124
29.	Probability of a wet subbase course for the MI 1 sections	124
30.	Summary of the results of the Liu-Lytton percent drainage versus time analyses for NC 1	125
31.	Time required to reach an 85 percent saturation level for NC 1 sections	128
32.	Summary of maximum surface deflection as calculated by ILLISLAB and JSLAB for a 14.4 kip (64 kN) dual wheel load with a tire pressure of 120 psi (83 kPa) placed at the slab's edge	133

LIST OF TABLES (continued)

VOLUME II EVALUATION AND MODIFICATION OF CONCRETE PAVEMENT DESIGN AND ANALYSIS MODELS (continued)

Table	Title	Page
33.	Summary of maximum tensile stress as calculated by ILLISLAB and JSLAB for a 14.4 kip (64 kN) dual wheel load with a tire pressure of 120 psi (83 kPa) placed at the slab's edge	133
34.	Summary of maximum surface deflection as calculated by ILLISLAB and JSLAB for a 14.4 kip (64 kN) dual wheel load with a tire pressure of 120 psi (83 kPa) placed at the slab's corner	134
35.	Summary of maximum tensile stress as calculated by ILLISLAB and JSLAB for a 14.4 kip (64 kN) dual wheel load with a tire pressure of 120 psi (83 kPa) placed at the slab's corner	134
36.	Summary of maximum thermal stresses as calculated by ILLISLAB and JSLAB	135
37.	Summary of maximum surface deflection, maximum edge stress, and maximum subgrade distress as calculated by ILLISLAB for a 14.4 kip (64 kN) dual wheel load with a tire pressure of 120 psi (83 kPa) placed at the slab's edge	142
38.	Summary of deflection and stress load transfer efficiencies as calculated by ILLISLAB for a 14.4 kip (64 kN) dual wheel load with a tire pressure of 120 psi (83 kPa) placed at the slab corner	145
39.	Measured deflection basin under 13,000 lb (58 kN) load at STA 3+73 approach joint, MI 1-10a	147
40.	Finite element analysis for the void analysis performed for STA 3+73, MI 1-10a	147
41.	Maximum positive and minimum negative thermal gradient calculated by the CMS program for MN 1, CA 1, MI 1, and NC 1	151
42.	Stresses developing due to thermal gradients through the slab	152
43.	Summary of PMARP results for the edge loading condition employing a 9 kip (40 kN) dual wheel load with a tire pressure of 80 psi (55 kPa)	159
44.	Summary of PMARP results for the corner loading condition employing a 9 kip (40 kN) dual wheel load with a tire pressure of 80 psi (55 kPa)	160
45.	Summary of Miner's fatigue damage and transverse cracking for MN 2, CA 2, MI 1, and NC 1	166
46.	Shoulder fatigue damage analysis for AZ 1 and MI 4-1 using the JCS-1 program	170
47.	Shoulder fatigue analysis for NC 1 using the BERM program	172
48.	Mean longitudinal cracking for all sections included in COPES and RIPPER databases	179
49.	Distribution of pavement sections and designs used in development of faulting models	180
50.	Yearly average daytime thermal gradients used in curling computations(2)	193
51.	Critical distress levels, by pavement type (46)	208
52.	Cost-effectiveness evaluation for Arizona	211
53.	Cost-effectiveness evaluation for California	213
54.	Cost-effectiveness evaluation for Michigan	217
55.	Cost-effectiveness evaluation for Minnesota	221
56.	Cost-effectiveness evaluation for North Carolina	224
57.	Arizona designs for cost-effectiveness evaluation	231
58.	California designs for cost-effectiveness evaluation	232
59.	Michigan designs for cost-effectiveness evaluation	234
60.	Minnesota designs for cost-effectiveness evaluation	236
61.	North Carolina designs for cost-effectiveness evaluation	238

LIST OF TABLES (continued)

VOLUME III SUMMARY OF RESEARCH FINDINGS

Table	Title	Page
1.	General information for pavements included in study	5
2.	Listing of pavement sections in dry-freeze environmental region	6
3.	Listing of pavement sections in dry-nonfreeze environmental regions	7
4.	Listing of pavement sections in wet-freeze environmental region	9
5.	Listing of pavement sections in wet-nonfreeze environmental region	10
6.	Listing of major data items contained in the data base	20
7.	Analysis and design models evaluated in this study	30
8.	Summary of the statistical analysis of the AASHTO design model	32
9.	Summary of the statistical analyses of the PEARDARP prediction models	33
10.	Summary of the statistical analyses of the COPES prediction models	36
11.	Summary of the statistical analyses of the PFAULT faulting prediction models	39
12.	Summary of maximum edge deflection as calculated by ILLISLAB and JSLAB	45
13.	Summary of maximum thermal stress as calculated by ILLISLAB and JSLAB	46
14.	Mean longitudinal cracking for all sections included in COPES and RIPPER data bases	56
15.	Suggested design limits for use with prediction models	67
16.	Performance results for 12 "replicate" inservice pavement sections in Illinois[41]	69
17.	Computed coefficients of variation for replicate pavement sections[41]	70
18.	Critical distress levels by pavement type[39]	74
19.	Example of the cost-effectiveness evaluation for Arizona projects	76

VOLUME IV APPENDIX A - PROJECT SUMMARY REPORTS AND SUMMARY TABLES

Table	Title	Page
1.	Corner voids on MN 1 sections at Rothsay	3
2.	Drainage summary for MN 1 and MN 5 sections	3
3.	Transverse joint spalling, by design variable	6
4.	Transverse joint faulting, by design variable	7
5.	Transverse cracking, by design variable	7
6.	Longitudinal cracking, by design variable	8
7.	Comparison of performance by lane	10
8.	Composite k-values	14
9.	Load transfer efficiency and corners with voids	14
10.	Drainage summary for MN 2 sections	15
11.	Transverse joint spalling on MN 2 sections	15
12.	Longitudinal cracking at MN 2, by design variable	17
13.	Shoulder performance at MN 2 sections	18
14.	Comparison of performance by lane at MN 2	21
15.	Traffic summary of AZ 1 sections	30
16.	Summary of k-value by base type	30
17.	Drainage summary for AZ 1 sections	31
18.	Comparison of performance by lane at AZ 1	36

LIST OF TABLES (continued)

VOLUME IV APPENDIX A - PROJECT SUMMARY REPORTS AND SUMMARY TABLES (continued)

Table	Title	Page
19.	Comparison of performance by lane at AZ 2	39
20.	Backcalculated E-value by concrete type	42
21.	Composite k-value by base type	43
22.	Corners with voids and pumping severity by base type	43
23.	Drainage summary for CA 1 sections	43
24.	Transverse joint faulting	44
25.	Transverse cracking on CA 1 sections	47
26.	Longitudinal cracking on CA 1 sections	48
27.	Roughness and present serviceability on CA 1 sections	48
28.	Performance summarized by base type	49
29.	Performance summarized by joint spacing	49
30.	Performance summarized by slab thickness	50
31.	Comparison of performance by lane at CA 1	50
32.	Summary of composite k-values of CA 2	53
33.	Load transfer efficiencies and corners with voids at CA 2	53
34.	Drainage summary for CA 2 sections	54
35.	Transverse joint faulting at CA 2	54
36.	Roughness and present serviceability at CA 2	56
37.	Comparison of performance by lane at CA 2	57
38.	Comparison of performance by lane at CA 6	60
39.	Summary of performance by lane at CA 7	62
40.	Comparison of performance by lane at CA 8	65
41.	Summary of composite k-value by base type	67
42.	Corners with voids at MI 1	68
43.	Drainage summary for MI 1 sections	69
44.	Transverse joint spalling on MI 1 sections	69
45.	Transverse joint faulting on MI 1 sections	72
46.	Transverse joint faulting summarized by subdrainage	73
47.	Roughness and present serviceability at MI 1	74
48.	Faulting as a function of load transfer and drainage	75
49.	Comparison of performance by transverse joint spacing	76
50.	Comparison of performance by lane at MI 1	77
51.	Corner void detection on MI 4 sections	83
52.	Drainage summary for MI 4 sections	83
53.	Composite k-value by base type	95
54.	Load transfer efficiencies and corners with voids at NY 1	96
55.	Drainage summary for NY 1 sections	96
56.	Roughness and present serviceability on NY 1 sections	101
57.	Comparison of performance by lane at NY 1	102
58.	Composite k-values and average mid-slab deflections at NY 2	106
59.	Load transfer efficiencies and corners with voids at NY 2	106
60.	Drainage summary for NY 2 sections	107
61.	Transverse cracking summarized by lane and transverse joint spacing	110
62.	Longitudinal cracking summarized by lane and transverse joint spacing	110
63.	Roughness and present serviceability at NY 2	111
64.	Summary of slab cracking on sections with concrete shoulders	111
65.	Performance comparison of sections with 20-ft transverse joint spacing	112

LIST OF TABLES (continued)

VOLUME IV APPENDIX A - PROJECT SUMMARY REPORTS AND SUMMARY TABLES (continued)

Table	Title	Page
66.	Comparison of performance by lane and pavement type at NY 2	112
67.	Composite k-values at OH 1	115
68.	Load transfer efficiencies and corners with voids at OH 1	115
69.	Drainage summary for OH 1 sections	116
70.	Transverse joint faulting at OH 1	119
71.	Roughness and present serviceability at OH 1	120
72.	Comparison of performance by lane and base type of OH 1	122
73.	Drainage summary for OH 2 Sections	125
74.	Transverse joint spalling at OH 2	125
75.	Transverse joint performance at OH 2	127
76.	Roughness and present serviceability on OH 2 sections	128
77.	Summary of longitudinal joint spalling at OH 2	129
78.	Outer shoulder performance at OH 2	129
79.	Comparison of performance by lane at OH 2	130
80.	Load transfer efficiency and corners with voids at ONT 1	134
81.	Summary of drainage characteristics at ONT 1	134
82.	Summary of transverse joint faulting by direction of traffic	135
83.	Roughness and present serviceability at ONT 1	137
84.	Shoulder performance at ONT 1	138
85.	Comparison of performance by lane at ONT 1	140
86.	Summary of performance variables at ONT 2	143
87.	Traffic summary of PA 1 sections	145
88.	Summary of composite k-value by base type	146
89.	FWD deflection testing results at PA 1	146
90.	Drainage summary for PA 1 sections	147
91.	Roughness and present serviceability at PA 1	150
92.	Comparison of performance by lane at PA 1	151
93.	Comparison of performance by lane at NJ 2	154
94.	Summary of composite k-values at NJ 3	156
95.	Drainage summary for NJ 3	157
96.	Transverse joint faulting at NJ 3	159
97.	Roughness and present serviceability at NJ 3	159
98.	Comparison of performance by lane at NJ 3	160
99.	Composite k-values at CA 3	163
100.	FWD deflection testing results at CA 3	164
101.	Drainage summary for CA 3	164
102.	Transverse joint spalling at CA 3	167
103.	Transverse joint faulting at CA 3	167
104.	Transverse cracking at CA 3	167
105.	Roughness and present serviceability at CA 3	168
106.	Outer shoulder performance at CA 3	169
107.	Comparison of performance by lane at CA 3	169
108.	Composite k-values and load transfer efficiency at NC 1	173
109.	Percent corners with voids at NC 1	173
110.	Drainage summary for NC 1 sections	174
111.	Transverse joint faulting by load transfer type	177
112.	Longitudinal cracking at NC 1	178

LIST OF TABLES (continued)

VOLUME IV APPENDIX A - PROJECT SUMMARY REPORTS AND SUMMARY TABLES (continued)

Table	Title	Page
113.	Comparison of performance by transverse joint orientation	180
114.	Comparison of performance by lane and base type at NC 1	180
115.	Comparison of performance by lane for NC 2	184
116.	Pavement performance at FL 2	187
117.	Comparison of performance by lane for FL 3	189
118.	Transverse cracking at FL 3	189
119.	Slab cracking as a function of slab length at FL 3	190
120.	General information and design data for projects included in study	205
121.	Slab design data for projects in dry-freeze environmental zone	206
122.	Base, subbase, subgrade, and outer shoulder design data for projects in dry-freeze environmental zone	207
123.	Pavement joint data for projects in dry-freeze environmental zone	208
124.	Outer lane deflection data of projects in dry-freeze environmental zone	209
125.	Outer shoulder and drainage information for projects in dry-freeze environmental zone	210
126.	Traffic information for projects in dry-freeze environmental zone	211
127.	Outer lane performance data for projects in dry-freeze environmental zone	212
128.	Lane 2 performance data for projects in dry-freeze environmental zone	213
129.	Slab design for projects in dry-nonfreeze environmental zone	214
130.	Base, subbase, subgrade, and outer shoulder design data for projects in dry-nonfreeze environmental zone	215
131.	Pavement joint data for projects in dry-nonfreeze environmental zone	216
132.	Outer lane deflection data of projects in dry-nonfreeze environmental zone	217
133.	Outer shoulder and drainage information for projects in dry-nonfreeze environmental zone	218
134.	Traffic information for projects in dry-nonfreeze environmental zone	219
135.	Outer lane performance data for projects in dry-nonfreeze environmental zone	220
136.	Lane 2 performance data for projects in dry-nonfreeze environmental zone	221
137.	Slab design for projects in wet-freeze environmental zone	222
138.	Base, subbase, subgrade, and outer shoulder design data for projects in wet-freeze environmental zone	224
139.	Pavement joint data for projects in wet-freeze environmental zone	226
140.	Outer lane deflection data of projects in wet-freeze environmental zone	228
141.	Outer shoulder and drainage information for projects in wet-freeze environmental zone	230
142.	Traffic information for projects in wet-freeze environmental zone	232
143.	Outer lane performance data for projects in wet-freeze environmental zone	234
144.	Lane 2 performance data for projects in wet-freeze environmental zone	236
145.	Slab design for projects in wet-nonfreeze environmental zone	238
146.	Base, subbase, subgrade, and outer shoulder design data for projects in wet-nonfreeze environmental zone	239
147.	Pavement joint data for projects in wet-nonfreeze environmental zone	240
148.	Outer lane deflection data of projects in wet-nonfreeze environmental zone	241
149.	Outer shoulder and drainage information for projects in wet-nonfreeze environmental zone	242
150.	Traffic information for projects in wet-nonfreeze environmental zone	243

LIST OF TABLES (continued)

VOLUME IV APPENDIX A - PROJECT SUMMARY REPORTS AND SUMMARY TABLES (continued)

Table	Title	Page
151.	Outer lane performance data for projects in wet-nonfreeze environmental zone	244
152.	Lane 2 performance data for projects in wet-nonfreeze environmental zone	245

VOLUME V APPENDIX B - DATA COLLECTION AND ANALYSIS PROCEDURES

Table	Title	Page
1.	WIM project locations	18
2.	FHWA vehicle classification types (5)	18
3.	Field procedures for collection of WIM data	20
4.	Chart to calculate saturation time curve	36
5.	Eh^3 values for all Phase I sections	67
6.	Effect of deflection error on backcalculated E and k	69
7.	Listing of major data items contained in the database	78

VOLUME VI APPENDIX C AND APPENDIX D

APPENDIX C - SYNTHESIS OF CONCRETE PAVEMENT DESIGN METHODS AND ANALYSIS MODELS

Table	Title	Page
1.	Evaluation of analysis models and design methods	29
2.	Levels of design variables	34
3.	Parameters assumed for use in the analysis models and design methods (5)	35
4.	Traffic data assumed in design models (5)	36
5.	Loadometer data assumed in design models (5)	37
6.	ILLISLAB input and output variables	52
7.	JSLAB input and output variables	53
8.	WESLIQID input and output variables	54
9.	WESLAYER input and output variables	55
10.	RISC input and output variables	56
11.	PMARP input and output variables	57

LIST OF TABLES (continued)

VOLUME VI APPENDIX C AND APPENDIX D

APPENDIX C - SYNTHESIS OF CONCRETE PAVEMENT DESIGN METHODS AND ANALYSIS MODELS (continued)

Table	Title	Page
12.	H-51 input and output variables	58
13.	CMS input and output variables	59
14.	Liu-Lytton drainage models input and output variables	60
15.	PREDICT input and output variables	61
16.	PEARDARP input and output variables	62
17.	JCP-1 input and output variables	63
18.	DNPS86 input and output variables	64
19.	RPS-3 input and output variables	65
20.	PCA and California Rigid Pavement Design Procedure input and output variables	67
21.	JCS-1 and BERM input and output variables	68
22.	Method of obtaining input variables for ILLISLAB	69
23.	Methods of obtaining input variables for JSLAB	70
24.	Methods of obtaining input variables for CMS	71
25.	Methods of obtaining input variables for Liu-Lytton Drainage Models	72
26.	Method of obtaining input variables for PMARP	73
27.	Method of obtaining input variables for PEARDARP	74
28.	Method of obtaining input variables for PREDICT	75
29.	Method of obtaining input variables for BERM	76
30.	Method of obtaining input variables for JCS-1	77
31.	Method of obtaining input variables for JCP-1	78
32.	Effect of slab thickness on pavement responses as measured by ILLISLAB, JSLAB, WESLIQID, and WESLAYER	80
33.	Effect of shoulder parameters on pavement responses as measured by ILLISLAB, JSLAB, WESLIQID, and WESLAYER	81
34.	Effect of subgrade strength on pavement responses as measured by ILLISLAB, JSLAB, WESLIQID, and WESLAYER	82
35.	Effect of joint width and slab length on pavement responses as measured by ILLISLAB, JSLAB, WESLIQID, and WESLAYER	83
36.	Effect of load transfer on pavement responses as measured by ILLISLAB and JSLAB	84
37.	Effect of base type on pavement responses as measured by ILLISLAB and JSLAB	85
38.	Effect of slab length/joint width, slab thickness, and shoulder parameters on pavement responses as measured by PMARP	86
39.	Effect of void depth, drainage factor, rainfall factor, and subbase treatment factor on pavement responses as measured by PMARP	87
40.	ILLISLAB and JSLAB curling analysis	88
41.	WESLIQID and WESLAYER curling analysis	89
42.	Analysis of RISC	90
43.	Effect of subgrade strength and pavement thickness on pavement response as measured by H-51	91
44.	CMS capabilities	92
45.	Effect of subgrade strength and slab thickness on cracking and PSR of JPCP as measured by PREDICT	94

LIST OF TABLES (continued)

VOLUME VI APPENDIX C AND APPENDIX D

APPENDIX C - SYNTHESIS OF CONCRETE PAVEMENT DESIGN METHODS AND ANALYSIS MODELS (continued)

Table	Title	Page
46.	Effect of subgrade strength and slab thickness on pumping of JPCP as measured by PREDICT	95
47.	Effect of climatic region on distresses of JPCP as measured by PREDICT	96
48.	Specific variables for the nine climatic zones (5)	97
49.	Effect of climatic region on distresses of JRCP as measured by PREDICT	99
50.	Effect of climatic region on distress of JRCP as measured by PREDICT	100
51.	Effect of subdrainage on JRCP distress as measured by PREDICT	101
52.	Effect of subgrade strength on JPCP distress as measured by PEARDARP	102
53.	Effect of pavement thickness on JPCP distress as measured by PEARDARP	103
54.	Effect of various inputs on fatigue damage as measured by JCP-1	104
55.	Effect of various inputs on serviceability as measured by JCP-1	105
56.	Effect of various inputs on DNPS86 design outputs	106
57.	Effect of loss of support, drainage factor, and ESAL's on design using DNPS86	107
58.	Effect of various inputs on RPS-3 outputs	108
59.	Effect of subgrade strength and load transfer on PCA design outputs	109
60.	Effect of subgrade strength on California rigid pavement design outputs	110
61.	Effect of shoulder type and thickness on BERM shoulder design outputs	111
62.	Effect of various inputs on JCS-1 design outputs	112
63.	Effect of various inputs on the Liu-Lytton drainage models outputs	113
64.	Effect of various inputs on JRCP4 outputs	114

VOLUME VI APPENDIX C AND APPENDIX D

APPENDIX D - SUMMARY OF ANALYSIS DATA FOR THE EVALUATION OF PREDICTIVE MODELS

Table	Title	Page
65.	Actual ESAL's (based on ADT) versus ESAL's as predicted using the AASHTO design equation for all Phase I sections	116
66.	Actual ESAL's (based on ADT) versus ESAL's as predicted using the AASHTO design equation for the dry-freeze region	120
67.	Actual ESAL's (based on ADT) versus ESAL's as predicted using the AASHTO design equation for the dry-nonfreeze region	121
68.	Actual ESAL's (based on ADT) versus ESAL's as predicted using the AASHTO design equation for the wet-freeze region	123
69.	Actual ESAL's (based on ADT) versus ESAL's as predicted using the AASHTO design equation for the wet-nonfreeze region	125
70.	Actual PSR as determined by a panel of users versus PSI as predicted by the PEARDARP PSI model for all Phase I sections	127
71.	Actual PSR as determined by a panel of users versus PSI as predicted by the PEARDARP PSI model for the dry-freeze region	131
72.	Actual PSR as determined by a panel of users versus PSI as predicted by the PEARDARP PSI model for the dry-nonfreeze region	132

LIST OF TABLES (continued)

VOLUME VI APPENDIX C AND APPENDIX D

APPENDIX D - SUMMARY OF ANALYSIS DATA FOR THE EVALUATION OF PREDICTIVE MODELS (continued)

Table	Title	Page
73.	Actual PSR as determined by a panel of users versus PSI as predicted by the PEARDARP PSI model for the wet-freeze region	134
74.	Actual PSR as determined by a panel of users versus PSI as predicted by the PEARDARP PSI model for the wet-nonfreeze region	136
75.	Actual field measured roughness versus roughness as predicted using the PEARDARP roughness model for all Phase I sections	138
76.	Actual field measured roughness versus roughness as predicted using the PEARDARP roughness model for the dry-freeze region	142
77.	Actual field measured roughness versus roughness as predicted using the PEARDARP roughness model for the dry-nonfreeze region	143
78.	Actual field measured roughness versus roughness as predicted using the PEARDARP roughness model for the wet-freeze region	145
79.	Actual field measured roughness versus roughness as predicted using the PEARDARP roughness model for the wet-nonfreeze region	147
80.	Comparison of actual field observed pumping with the normalized pumping index, volume of pumping, number of joints pumping, and volume of undersealing material required as predicted by the PEARDARP pumping model for all Phase I sections	149
81.	Actual field measured spalling versus spalling as predicted using the PEARDARP spalling model for all Phase I sections	152
82.	Actual field measured spalling versus spalling as predicted using the PEARDARP spalling model for the dry-freeze region	156
83.	Actual field measured spalling versus spalling as predicted using the PEARDARP spalling model for the dry-nonfreeze region	157
84.	Actual field measured spalling versus spalling as predicted using the PEARDARP spalling model for the wet-freeze region	159
85.	Actual field measured spalling versus spalling as predicted using the PEARDARP spalling model for the wet-nonfreeze region	161
86.	Actual field measured faulting versus faulting as predicted using the PEARDARP faulting models for all Phase I sections	163
87.	Actual field measured faulting versus faulting as predicted using the PEARDARP faulting models for the dry-freeze region	167
88.	Actual field measured faulting versus faulting as predicted using the PEARDARP faulting models for doweled pavements for the dry-freeze region	169
89.	Actual field measured faulting versus faulting as predicted using the PEARDARP faulting models for nondoweled pavements for the dry-freeze region	170
90.	Actual field measured faulting versus faulting as predicted using the PEARDARP faulting models for the dry-nonfreeze region	172
91.	Actual field measured faulting versus faulting as predicted using the PEARDARP faulting models for the wet-freeze region	174
92.	Actual field measured faulting versus faulting as predicted using the PEARDARP faulting models for doweled pavements for the wet-freeze region	177

LIST OF TABLES (continued)

VOLUME VI APPENDIX C AND APPENDIX D

APPENDIX D - SUMMARY OF ANALYSIS DATA FOR THE EVALUATION OF PREDICTIVE MODELS (continued)

Table	Title	Page
93.	Actual field measured faulting versus faulting as predicted using the PEARDARP faulting models for nondoweled pavements for the wet-freeze region	178
94.	Actual field measured faulting versus faulting as predicted using the PEARDARP faulting models for the wet-nonfreeze region	180
95.	Actual field measured faulting versus faulting as predicted using the PEARDARP faulting models for doweled pavements for the wet-nonfreeze region	182
96.	Actual field measured faulting versus faulting as predicted using the PEARDARP faulting models for nondoweled pavements for the wet-nonfreeze region	183
97.	Actual field measured cracking versus cracking as predicted using the PEARDARP cracking models for all Phase I sections	185
98.	Actual field measured cracking versus cracking as predicted using the PEARDARP cracking model for the dry-freeze region	189
99.	Actual field measured cracking versus cracking as predicted using the PEARDARP cracking model for the dry-nonfreeze region	190
100.	Actual field measured cracking versus cracking as predicted using the PEARDARP cracking model for the wet-freeze region	192
101.	Actual field measured cracking versus cracking as predicted using the PEARDARP cracking model for the wet-nonfreeze region	194
102.	Actual field observed pumping versus pumping as predicted using COPES pumping models for all Phase I sections	196
103.	Actual field observed pumping versus pumping as predicted using COPES pumping models for the dry-freeze region	200
104.	Actual field observed pumping versus pumping as predicted using COPES JPCP pumping model for the dry-freeze region	202
105.	Actual field observed pumping versus pumping as predicted using COPES JRCP pumping model for the dry-freeze region	203
106.	Actual field observed pumping versus pumping as predicted using COPES pumping model for the dry-nonfreeze region	205
107.	Actual field observed pumping versus pumping as predicted using COPES pumping model for the wet-freeze region	207
108.	Actual field observed pumping versus pumping as predicted using COPES JPCP pumping model for the wet-freeze region	210
109.	Actual field observed pumping versus pumping as predicted using COPES JRCP pumping model for the wet-freeze region	211
110.	Actual field observed pumping versus pumping as predicted using COPES pumping model for the wet-nonfreeze region	213
111.	Actual field measured faulting versus faulting as predicted using the COPES faulting models for all Phase I sections	215
112.	Actual field measured faulting versus faulting as predicted using the COPES faulting models for the dry-freeze region	219
113.	Actual field measured faulting versus faulting as predicted using the COPES JPCP faulting model for the dry-freeze region	221

LIST OF TABLES (continued)

VOLUME VI APPENDIX C AND APPENDIX D

APPENDIX D - SUMMARY OF ANALYSIS DATA FOR THE EVALUATION OF PREDICTIVE MODELS (continued)

Table	Title	Page
114.	Actual field measured faulting versus faulting as predicted using the COPES JRCP faulting model for the dry-freeze region	222
115.	Actual field measured faulting versus faulting as predicted using the COPES faulting models for the dry-nonfreeze region	224
116.	Actual field measured faulting versus faulting as predicted using the COPES faulting models for the wet-freeze region	226
117.	Actual field measured faulting versus faulting as predicted using the COPES JPCP faulting model for the wet-freeze region	229
118.	Actual field measured faulting versus faulting as predicted using the COPES JRCP faulting model for the wet-freeze region	230
119.	Actual field measured faulting versus faulting as predicted using the COPES faulting models for the wet-nonfreeze region	232
120.	Actual field measured spalling versus joint deterioration (spalling) as predicted using the COPES spalling models for all Phase I sections	234
121.	Actual field measured spalling versus joint deterioration (spalling) as predicted using the COPES spalling models for the dry-freeze region	238
122.	Actual field measured spalling versus joint deterioration (spalling) as predicted using the COPES JPCP joint deterioration model for the dry-freeze region	240
123.	Actual field measured spalling versus joint deterioration (spalling) as predicted using the COPES JRCP joint deterioration model for the dry-freeze region	241
124.	Actual field measured spalling versus joint deterioration (spalling) as predicted using the COPES spalling models for the dry-nonfreeze region	243
125.	Actual field measured spalling versus joint deterioration (spalling) as predicted using the COPES spalling models for the wet-freeze region	245
126.	Actual field measured spalling versus joint deterioration (spalling) as predicted using the COPES JPCP joint deterioration model for the wet-freeze region	248
127.	Actual field measured spalling versus joint deterioration (spalling) as predicted using the COPES JRCP joint deterioration model for the wet-freeze region	249
128.	Actual field measured spalling versus joint deterioration (spalling) as predicted using the COPES spalling models for the wet-nonfreeze region	251
129.	Actual field measured cracking versus cracking as predicted by the COPES cracking models for all Phase I sections	253
130.	Actual field measured cracking versus cracking as predicted by the COPES cracking models for the dry-freeze region	257
131.	Actual field measured cracking versus cracking as predicted by the COPES JPCP cracking model for the dry-freeze region	259

LIST OF TABLES (continued)

VOLUME VI APPENDIX C AND APPENDIX D

APPENDIX D - SUMMARY OF ANALYSIS DATA FOR THE EVALUATION OF PREDICTIVE MODELS (continued)

Table	Title	Page
132.	Actual field measured cracking versus cracking as predicted by the COPES JRCP cracking model for the dry-freeze region	260
133.	Actual field measured cracking versus cracking as predicted by the COPES cracking models for the dry-nonfreeze region	262
134.	Actual field measured cracking versus cracking as predicted by the COPES cracking models for the wet-freeze region	264
135.	Actual field measured cracking versus cracking as predicted by the COPES JPCP cracking models for the wet-freeze region	267
136.	Actual field measured cracking versus cracking as predicted by the COPES JRCP cracking model for the wet-freeze region	268
137.	Actual field measured cracking versus cracking as predicted by the COPES cracking models for the wet-nonfreeze region	270
138.	Actual PSR as determined by a panel of users versus PSR as predicted by the COPES PSR models for all Phase I sections	272
139.	Actual PSR as determined by a panel of users versus PSR as predicted by the COPES PSR models for the dry-freeze region	276
140.	Actual PSR as determined by a panel of users versus PSR as predicted by the COPES JPCP PSR model for the dry-freeze region	278
141.	Actual PSR as determined by a panel of users versus PSR as predicted by the COPES JRCP PSR model for the dry-freeze region	279
142.	Actual PSR as determined by a panel of users versus PSR as predicted by the COPES PSR models for the dry-nonfreeze region	281
143.	Actual PSR as determined by a panel of users versus PSR as predicted by the COPES PSR models for the wet-freeze region	283
144.	Actual PSR as determined by a panel of users versus PSR as predicted by the COPES JPCP PSR model for the wet-freeze region	286
145.	Actual PSR as determined by a panel of users versus PSR as predicted by the COPES JRCP PSR model for the wet-freeze region	287
146.	Actual PSR as determined by a panel of users versus PSR as predicted by the COPES PSR models for the wet-nonfreeze region	289
147.	Actual field measured faulting versus faulting as predicted using the PFAULT models for all Phase I sections	291
148.	Actual field measured faulting versus faulting as predicted using the PFAULT models for the dry-freeze region	295
149.	Actual field measured faulting versus faulting as predicted using the PFAULT models for doweled pavements for the dry-freeze region	297
150.	Actual field measured faulting versus faulting as predicted using the PFAULT models for nondoweled pavements for the dry-freeze region	298
151.	Actual field measured faulting versus faulting as predicted using the PFAULT models for the dry-nonfreeze region	300
152.	Actual field measured faulting versus faulting as predicted using the PFAULT models for the wet-freeze region	302
153.	Actual field measured faulting versus faulting as predicted using the PFAULT models for doweled pavements for the wet-freeze region	305

LIST OF TABLES (continued)

VOLUME VI APPENDIX C AND APPENDIX D

APPENDIX D - SUMMARY OF ANALYSIS DATA FOR THE EVALUATION OF PREDICTIVE MODELS (continued)

Table	Title	Page
154.	Actual field measured faulting versus faulting as predicted using the PFAULT models for nondoweled pavements for the wet-freeze region	306
155.	Actual field measured faulting versus faulting as predicted using the PFAULT models for the wet-nonfreeze region	308
156.	Actual field measured faulting versus faulting as predicted using the PFAULT models for doweled pavements for the wet-nonfreeze region	310
157.	Actual field measured faulting versus faulting as predicted using the PFAULT models for nondoweled pavements for the wet-nonfreeze region	311
158.	Data used for the analysis of the PEARDARP, COPES, AND PFAULT predictive models	313

APPENDIX C

SYNTHESIS OF CONCRETE PAVEMENT DESIGN METHODS AND ANALYSIS MODELS

PART I. REVIEW OF SELECTED DESIGN AND ANALYSIS MODELS

1. INTRODUCTION

The proper analysis and design of rigid pavements is critical to their performance. A number of design methods and analysis procedures for rigid pavements have been developed over the past several years. Each of the models and methods were developed to account for a variety of different effects such as environmental conditions, response to traffic loading, drainage, and various design parameters (e.g., dowel bars, shoulders, joint spacing, slab thickness, subgrade support, and many others).

This document provides an evaluation of 19 rigid pavement design methods and analysis procedures which was performed to assess their adequacy and sensitivity to key variables. The evaluations were based on the results of sensitivity analyses, program documentation, suitability of the procedure for meeting contract objectives, and other criteria. Recommendations are presented regarding the models which are to be used in future analysis.

2. EVALUATION OF THE ANALYSIS AND DESIGN MODELS

The following analysis models and design procedures were reviewed under this contract:

- RISC
- ILLISLAB
- WESLIQID
- JSC-1
- AASHTO (DNPS-86)
- PCA
- PMARP
- PREDICT
- CMS
- JRCP4
- JSLAB
- H-51
- WESLAYER
- JCP-1
- RPS-3
- California Rigid Design
- PEARDARP
- BERM
- Liu-Lytton Drainage

The documentation was obtained for each of these procedures and models and extensive sensitivity analyses were conducted to determine their suitability to fulfill the project objectives. The capabilities and limitations of each of the programs are listed in sections 3 and 4.

The details of the sensitivity analysis are contained in the subsequent parts of the report and the results are summarized herein.

Part II includes details pertinent to the construction of the finite element meshes that were used in the testing of the finite element programs. A cross-section of the standard pavement section used in the analyses is illustrated in figure 1. A 9-in (229 mm) PCC slab over a 5-in (129 mm) unbonded lean concrete base was chosen. The section has dowels across the transverse joints and tied concrete shoulders. Table 2 provides the range of variables used to evaluate the pertinent design features. Tables 3 through 5 provide the inputs used for the standard section. The finite element meshes required to run each program are shown in figures 2 through 13. The load configuration for the H51 program is illustrated in figure 14.

Part III presents summaries of the inputs and outputs required for all of the programs and procedures under consideration. Tables 6 through 21 are detailed lists of the inputs required to use each program or procedure and the outputs produced. Tables 22 through 31 contains lists of the methods of obtaining each input for the recommended programs.

Part IV summarizes the results of hundreds of computer runs and design procedure calculations in the form of tabular sensitivity analyses. The results of these analyses are shown in tables 32 through 64 and figures 15 and 16.

3. CAPABILITIES AND LIMITATIONS OF ANALYSIS MODELS

ILLISLAB

ILLISLAB is a finite element program, based on medium-thick plate theory, developed at the University of Illinois for the Federal Aviation Administration (FAA) for the structural evaluation of one- or two-layer concrete pavements.[1,2,3]

Capabilities

ILLISLAB has the following capabilities:

- Various types of load transfer systems, such as keyways, dowel bars, aggregate interlock, or a combination of dowels and aggregate interlock can be considered at joints and cracks. Nonuniformly-spaced dowel configurations may be considered.

- A second pavement layer such as an overlay (bonded and unbonded) or a base course layer may be modeled.

- Multiple wheel loads in any configuration located anywhere on the slab may be modeled.

- A combination of slabs such as multiple traffic lanes, traffic lanes and shoulders, or a series of transverse cracks may be modeled.

- Variable subgrade support conditions including complete loss of support at any location or combination of locations beneath the slab may be considered.

- Concrete shoulders with or without tie bars may be considered.

- Concrete slabs of varying thicknesses and strength properties and subgrade soil of varying strength may be modeled.

- A choice of four distinct subgrade models may be specified. These include Winkler (dense liquid), Vlasov (two-parameter system), Boussinesq (elastic solid), and the resilient subgrade formulation.

- A linear thermal gradient may be modeled to examine slab curling stresses. The ability to model a nonlinear thermal gradient through the slab is currently being investigated at the University of Illinois.

Limitations

The significant limitations of ILLISLAB are listed below:

- Jointed reinforced concrete pavements (JRCP) and continuously reinforced concrete pavements (CRCP) may be modeled only indirectly.

- A maximum of only two pavement layers in addition to the subgrade may be modeled.

- Moisture effects are not considered, although the moisture gradient can be modeled as an effective thermal gradient.

- Climatic variables, with the exception of the thermal gradient, are not considered.

- The drainability of the pavement section is not considered.

- The cumulative effects of traffic are not considered.

- Only circular dowels may be modeled.

- All transverse joints and/or cracks must have identical load transfer mechanisms.

- All longitudinal joints and/or cracks must have identical load transfer mechanisms.

- Only a center-loaded, single-slab system may be considered with the Vlasov and Boussinesq subgrade options.

JSLAB

JSLAB is a finite element program developed by the Portland Cement Association (PCA) to model jointed concrete pavements.[4,5]

Capabilities

The basic assumptions of JSLAB are very similar to those of ILLISLAB. JSLAB has identical capabilities to ILLISLAB with the exception of the choice of subgrade formulations. JSLAB uses the Winkler subgrade formulation exclusively. JSLAB has these added capabilities:

- Nonuniformly spaced and noncircular dowels may be modeled.

- Slab warping due to a linear top-to-bottom variation in slab moisture content for one-layer pavement systems may be considered as converted to an equivalent thermal gradient.

Limitations

The significant limitations of JSLAB include those listed in the ILLISLAB discussion excluding those concerning moisture effects, noncircular dowels, and the various subgrade formulations. Other significant limitations to the program are listed below:

- The principal bending stresses are not calculated.

- The vertical stress on the subgrade is not calculated.

- Only a one-layer pavement system with a uniform thickness can be analyzed when a thermal or moisture gradient through the slab is considered.

- Calculation of thermal curling stress typically requires three or more separate runs of the program and manual subtraction of the results.

- The combination of a weighted slab with thermal gradient and an applied load will does not execute and results cannot be obtained.

- The effects of a thermal gradient applied to two or more slabs with any degree of load transfer requires considerable knowledge of the development and theory behind the program.

- When vertical slab displacements are specified, applied loads cannot be located at that particular node or over any element adjacent to that node.

- The JSLAB program is based on an early version of the ILLISLAB program. This version of the program was shown to have errors in the stiffness matrix which, in term, cause errors in the deflection and stress calculations.[2]

- Only a Winkler subgrade option is available.

WESLIQID

WESLIQID is a finite element program, based on thin plate theory, developed by the U. S. Army Corps of Engineers Waterways Experiment Station Geotechnical Laboratory for the analysis of concrete pavement systems subject to multiple wheel loads and/or thermal gradients.[5,6]

Capabilities

WESLIQID has identical capabilities to ILLISLAB with the exception of the choice of subgrade formulations. WESLIQID uses the Winkler subgrade formulation. WESLIQID has these added capabilities:

- Partial contact of the slab with the subgrade may be modeled with or without initial gaps (voids).

- Longitudinal and transverse joints and cracks need not have the same load transfer efficiencies. For example, the user may specify different characteristics for the traffic lane transverse joints and the shoulder transverse joints.

- Load transfer may be modeled through use of dowel bar data, shear and moment efficiencies, or spring constants for each joint or crack.

- Subgrade stresses and strains may be modeled through use of the Boussinesq or Burmister equations.

Limitations

The significant limitations of WESLIQID include the following:

- The input data must be carefully chosen to ensure a converging solution.
- JRCP and CRCP may not be modeled directly.
- Computer memory requirements are limiting. The accuracy of the finite element mesh is limited by the inability of the program to efficiently store the program data.
- The effect of temperature gradients may be considered only for uniformly thick slabs.
- Moisture effects are not considered.
- The cumulative effects of traffic are not considered.
- The drainability of the pavement section is not considered.
- Climatic variables, with the exception of thermal gradient, are not considered.
- A maximum of only two layers in addition to the subgrade may be modeled.

WESLAYER

WESLAYER is a finite element program developed by the U. S. Army Corps of Engineers Waterways Experiment Station to compute the state of stress in rigid pavement systems based on an elastic solid subgrade formulation.[5,6]

Capabilities

WESLAYER has capabilities identical to those of the WESLIQID program with one exception: up to five subgrade layers may be modeled.

Limitations

WESLAYER has the identical limitations as the WESLIQID program with the exception that only two uniformly thick slabs may be modeled with one joint between them. This is due to the large computer storage capacity required for the elastic representation of the subgrade. Also, the program considers only transfer of shear stresses and assumes the moment transfer is zero at the joints.

PMARP

PMARP (Purdue Model for Analysis of Rigid Pavements) is an iterative, nonlinear finite element program used to analyze reinforced or unreinforced jointed concrete pavements. The procedure, developed at Purdue University, is based on modification of the ILLISLAB program to include a fatigue damage model.[7,8]

Capabilities

Results were obtained from the microcomputer version of PMARP dated June 1987. The capabilities of the program are as follows:

- Various types of load transfer systems, such as keyed joints, dowel bars, aggregate interlock, or a combination of dowels and aggregate interlock may be considered at joints and cracks.
- A combination of six slabs such as multiple traffic lanes, traffic lanes and shoulders, or a series of transverse cracks may be modeled.
- Voids beneath the slab may be modeled in terms of average void depth.
- Concrete shoulders with or without tie bars may be considered.
- JRCP may be modeled directly, including the reinforcement ratios in the x- and y-directions.
- The effect of cumulative traffic is considered as it effects stiffness of the concrete slab, amount of cracking, decay of the load transfer system, and amount of damage due to pumping.
- Stress dependency of the granular layers is considered.

Limitations

The significant limitations of PMARP are listed below:

- The memory requirements of the microcomputer version limit the accuracy of the finite element mesh. The equation presented below shows the limitations of the mesh size:

$$26xy^2 < 26{,}500$$

where:

x = number of node lines in the x-direction,
y = number of node lines in the y-direction.

This allows for a significantly smaller number of elements than the mainframe version.

- A second layer in addition to the subgrade may only be modeled indirectly though the *k*-value.

- The effect of thermal and moisture gradients are not considered.

- The effects of climate, with the exception of several correction factors developed for the pumping model, are not considered.

- Only circular uniformly spaced dowels may be modeled.

- All transverse joints and/or cracks must have identical load transfer mechanisms.

- All longitudinal joints and/or cracks must have identical load transfer mechanisms.

- CRCP may be modeled only indirectly.

- The program is based on an early version of the ILLISLAB program. Research at the University of Illinois has revealed that the errors in the stiffness matrix cause errors in the deflection and stress calculations.[2]

- If the microcomputer input processor is used, several of the input variables are misassigned, ignored, or changed.

  - The reinforcement ratio in the x-direction is assigned to the reinforcement ratio in the y-direction. The same is true for the dowel diameter inputs.

  - The largest aggregate interlock factor that the input processor allows the user to input is $10*10^8$; however, the input screen indicates values of $10*10^{10}$ are to be used for keyed joints.

  - The input processor changes the users values for the plate deflection versus the resilient modulus inputs. The first two entries are accepted while the third entry for both the deflection and modulus is changed to 0.0.

- Several of the inputs are difficult to obtain or estimate. For example, the user is required to supply the plate deflection versus resilient modulus for the given soil type. Also, the user is required to estimate the average void depth beneath the slab corner.

- The approach for the deterioration of load transfer based on the number of load repetitions has not been validated.

- The use of the resilient modulus of subgrade reaction for the characterization of the subgrade soil has not been validated.

- The fatigue damage effects are based on the use of several correlations and relationships which have not been validated.

RISC

RISC is a computer program developed by Resource International.[5,9] The program couples a finite element slab model, employing the theory of a flat thin elastic shell, with an elastic solid foundation of up to three discrete layers.

Capabilities

RISC has the following capabilities:

- Transverse joints may be doweled or nondoweled.

- Traffic loadings may be modeled through specification of the magnitude of the standard dual wheel truck axle for edge, corner, or midslab locations.

- A combination of slabs such as multiple traffic lanes, traffic lanes and shoulders, or a series of transverse cracks may be modeled (up to three slabs with shoulders).

- Concrete slabs of uniform thickness and strength properties may be modeled.

- The subgrade may be modeled as a one-, two-, or three-layer system.

- Environmental effects are incorporated into the model through use of the AASHTO regional factor. The regional factor is used to modify the traffic data.

- The cumulative effects of traffic may be examined through the use of fatigue damage equations.

- Faulting of joints and cracks may be examined.

- A linear thermal gradient may be modeled to examine the slab curling stresses.

Limitations

The significant limitations of RISC are listed below:

- Jointed reinforced concrete pavements (JRCP) and continuously reinforced concrete pavements (CRCP) may be modeled only indirectly.
- The dual wheels may be placed at the edge, corner, or midslab locations only.
- Moisture effects are not considered.
- Drainability of the pavement section is input as good or poor. Due to lack of published information, the actual method of consideration of this parameter cannot be evaluated.
- Only circular, uniformly-spaced dowels may be modeled.
- All transverse joints and/or cracks must have identical load transfer mechanisms.
- All longitudinal joints and/or cracks must have identical load transfer mechanisms.
- Only the maximum displacements and stresses are output.
- Large computer run times are required due to the very large work files that are generated internally.
- The fatigue and faulting models have not been tested and verified.

H-51

H-51 is a computerized solution to the Pickett and Ray influence charts for calculating the bending stress at the free edge of a loaded semi-infinite slab resting on a dense-liquid or elastic-solid foundation. The program was developed by Kreger.[5,10,11]

Capabilities

H-51 has the following capabilities:

- Multiple wheel loads in any configuration consisting of a double centerline of symmetry may be modeled.

- Orientation of the wheel configuration in any position with respect to the slab edge.

- The user may input the slab thickness and the edge stress will be calculated or the user may input the maximum allowable edge stress and the required thickness will be generated.

Limitations

The Pickett and Ray influence charts employed in H-51 were developed for determining stresses in a semi-infinite slab. The more significant limitations of the program are listed below:

- Jointing, slab size, and load transfer systems are not considered.

- The effects of thermal and moisture gradients are not considered.

- No climatic variables are considered.

- Base and subbase layers are not directly considered.

- Only edge stresses can be calculated.

- Loss of support beneath the slab is not considered.

- The cumulative effects of traffic are not considered.

- Drainability of the pavement system is not considered.

- Slab reinforcement cannot be modeled.

CMS

The CMS (Climatic-Material-Structural) model is a finite difference program developed by the University of Illinois.[12,13] The program uses climatic and material inputs to calculate temperature and moisture profiles and their variation with time. The information is then used in the material model to calculate the surface, base, subbase, and subgrade stiffness characteristics. This output can then be used in the structural analysis and performance models.

Capabilities

CMS has the following capabilities:

- The effects of climate and moisture are considered comprehensively.

- The temperature profile for the pavement system at time and depth intervals specified by the user is calculated.

- The locations of frost lines in the pavement system at the specified time are calculated.

- The moisture content for all granular layers is calculated at the specified time.

- The resilient modulus for each node is calculated for each specified time.

- The outputs from the CMS program may be used in any appropriate structural model to obtain the required design parameters.

Limitations

CMS has the following limitations:

- Many of the input parameters, which are listed in Part III, are obscure and difficult to obtain.

- The program is relatively difficult to use, in that numerous inputs are required, three separate executions are required, and the microcomputer version of the program is not interactive.

- The various output parameters must be used as input variables to an appropriate structural model in order to obtain pavement responses and/or design parameters.

- The output summary of input data is scattered throughout the output file which does not allow for a quick check of input variables.

- Loss of support beneath the slab is not considered.

- The moisture model only accounts for isothermal moisture movements from the water table into the pavement system. The subgrade cannot receive moisture by infiltration through the surface or from adjacent soil masses with higher pore water pressure.

- The interaction of the moisture, thermal, and materials model has not undergone extensive testing.

Liu-Lytton Drainage Models

The Liu-Lytton Drainage program is a computerized version of the drainage and infiltration models developed by the Texas A & M University and Texas

Transportation Institute (TTI).[14] The program examines the effects of water saturation of a pavement system.

Capabilities

The Liu-Lytton models have the following capabilities:

- The effect of soil type on drainage time is considered in the model.
- The effects of climatic variables such as rainfall and evaporation are considered in the model.
- The infiltration of moisture through the joints and cracks in the pavement surface is considered.
- The adequacy of the subdrainage system is evaluated.
- The drainage/infiltration through granular bases layers and subgrade soil is considered in the model.
- The effects of various points of water infiltration, such as surface cracking, are considered in the model.
- The loss in strength due to various moisture conditions is calculated for the granular layers and the subgrade.
- Results of the infiltration and drainage programs may be used as inputs to various structural models for use in design.

Limitations

The Liu-Lytton Models have the following limitations:

- The effect of temperature is not considered in the model.
- The output summary of the input data is scattered throughout the output file which does not allow for a quick check of input variables. Also, only select input variable are echoed in the output file.
- The "input processor" allows the user to input values that are out of bounds.
- Some of the input variables are somewhat obscure and difficult to obtain.

- Rigid pavements with a *single* granular layer may be evaluated. This is limiting in the evaluation of stabilized base materials and pavement sections with more than one granular subbase layer.

- The material properties are fixed based on testing performed at TTI for the types of material which are allowed in the program. The user cannot input material properties for a specific design material.

- The program only allows the analysis of fine-grained subgrade material (A-4 through A-7-6).

- The sign convention for the transverse slope is not defined within the program documentation, user's guide, or input processor.

JRCP4

JRCP4 is an updated computer program developed at the University of Texas.[27] The program models the stresses, strains, and movements occurring during the early life of a jointed reinforced concrete pavement slab, resulting from the combined effects of thermal and shrinkage movements, and frictional restraint exerted on the slab by a supporting base.

Capabilities

The JRCP4 program has the following capabilities:

- The program considers the effects of slab shortening caused by a drop in temperature after curing.

- The program considers the effect of drying shrinkage after curing.

- The program predicts the stresses generated from the interaction between the reinforcing steel and the concrete.

- The stresses and strains which develop due to the movements of the slabs as a function of time after casting.

- The program considers the strength gain with time relationship of portland cement concrete.

Limitations

JRCP4 has the following limitations:

- The analysis period is the first 28 days of concrete life.

- The stresses due to wheel loading are not considered.

- Fatigue cracking from cyclic loading is not considered.
- Stresses caused by daily temperature differentials and moisture differentials are not included in the model.
- Shrinkage rates between the top and bottom of the slab are not included.

4. CAPABILITIES AND LIMITATIONS OF DESIGN AND PREDICTION MODELS

PREDICT

The PREDICT program is a computerized version of the prediction equations developed under the NCHRP 1-19 Concrete Pavement Evaluation System (COPES) research study. The equations were developed at the University of Illinois.[15,16,17]

Capabilities

The COPES equations which are employed by the PREDICT program are empirical models developed from a nationwide database of inservice pavements. Models were developed for serviceability and the following distresses: pumping, joint deterioration, joint faulting, and slab cracking. The program has the following capabilities:

- The models consider the effects of climate.
- Drainability of the pavement section is considered in the JRCP models.
- The effects of tied concrete shoulders and transverse joint load transfer is considered in the models.
- The effect of joint spacing is considered in the JRCP models.
- The effects of reactive aggregate and various soil conditions are considered in the models.
- The effect of steel reinforcement is considered in the models.
- The cumulative effects of traffic (ESAL) are considered in the models.

Limitations

PREDICT has the following limitations:

- Models are empirical and usage is limited to the types of pavements from which they were developed, primarily conventional nondrained pavements.
- Variable subgrade support conditions are not considered in the model.
- The effects of joint sealant are evaluated indirectly through the presence or absence of incompressibles in the joints.
- The type and shape of the joint are not considered in the models.
- The models are based on a limited number of sample projects. They were developed for demonstration purposes and require further refinement to be used in concrete pavement design and analysis.

PEARDARP

PEARDARP (Purdue Economic Analysis of Rehabilitation and Design Alternatives for Rigid Pavements) is a computer program developed by Purdue University used to analyze rigid pavement performance.[8,18]

Capabilities

PEARDARP has the following capabilities:

- The pavement sections analyzed with the PMARP program can be further analyzed with the PEARDARP program.
- A comprehensive cost analysis based on EAROMAR2 is performed for every year of the analysis program, including maintenance, user, and rehabilitation costs.
- Pavement distress predictive models for pumping, faulting, cracking, joint spalling, roughness, and PSI for both JPCP and JRCP are calculated yearly by the analysis program.
- The effects of drainage, subbase type, sealant type, dowel bars, and reinforcement may be evaluated in terms of the pavement performance distress models.
- The cumulative effects of traffic are considered in the model.
- Several maintenance and rehabilitation strategies may be evaluated.

- The effect of climate is directly considered in the model.
- The effect of loss of subgrade support is considered.

Limitations

The major limitations of the PEARDARP program are listed below:

- Multiple runs of the program are required to find the most timely rehabilitation schedule.
- Several of the predictive models have not been verified.
- Dowel presence or absence is a variable, but dowel bar diameter and dowel spacing are not variables.
- The effect of shoulders is not considered.
- CRCP cannot be modeled.
- The program does not accept specific data values, for example, a joint spacing of 10 ft (3.0 m) or a thickness of 6 in (152 mm).

JCP-1

JCP-1 (Jointed Concrete Pavements-1) is a computerized version of the Zero Maintenance Design Procedure which was developed at the University of Illinois.[19,20] The design procedure is based on both theoretical studies and field surveys.

Capabilities

The JCP-1 computer program calculates the fatigue damage and serviceability index the input pavement sections. The Zero Maintenance design procedure recommends required design parameters for heavily trafficked pavement design. The procedure/program has the following capabilities:

- Serviceability/performance relationships are modeled in the procedure. These relationships were developed based on field performance data from the AASHO Road Test data and 10 other projects nationwide.
- The procedure considers the effect of various climatic variables, including, precipitation, potential evapotranspiration, frost heave, and freeze-thaw damage, through use of a regional/climatic factor.

- The procedure considers the effect of slab movement with respect to daily temperature cycles.

- The procedure considers the effect of cumulative traffic through a comprehensive fatigue damage analysis.

- Future traffic predictive equations were developed for use in the procedure.

- The effect of seasonal variation in subgrade soil is considered in the model.

- The effect of loss of support beneath the slab is modeled in the procedure as an erodibility factor.

- The procedure provides recommendations for the design of joints, such as type, spacing, shape, sealant type, load transfer device, and stabilized subbase. The joint spacing, load transfer efficiency, and subbase type are input directly into the JCP-1 computer program.

- The procedure recommends the use of tied concrete shoulders.

Limitations

The Zero Maintenance Procedure has the following limitations:

- The procedure does not consider the effect of moisture gradient through the slab but states that it may be considered through a -0.5 °F/in temperature gradient. (A negative thermal gradient occurs when the top of the slab is cooler that the bottom which corresponds a moisture condition where the top of the slab is dryer than the bottom. These conditions contribute to the development of a tensile stress at the bottom of the longitudinal edge of the slab midway between the joints.)

- No validation exists for the recommendations concerning the loss of support/erodibility factor.

- The climatic/regional factor was developed empirically and it has not been sufficiently verified.

- The joint design procedures, with the exception of joint spacing, are based on previous experience, not analytical procedures.

- Variation in construction procedures and material quality are not considered.

- The serviceability/performance model is based on limited field data.
- The procedure may only be used for plain jointed concrete pavements.

DNPS86

The DNPS86 (Design of New Pavement Systems - 1986) program is a computerized version of the AASHTO design procedure which was developed in 1985 by the subcommittee on Pavement Design for the "AASHTO Guide for Design of Pavement Structures."[5,21]

Capabilities

The AASHTO design procedure/DNPS86 program has the following capabilities:

- The procedure can be used for the design of JPCP or JRCP with or without an overlay.
- Reliability concepts are incorporated into the design procedure.
- Drainability of the pavement section is considered in the procedure through use of a drainage quality coefficient.
- Seasonal variation of the subgrade soil strength is considered in the procedure.
- The effects of swelling subgrade soil and frost heave are considered in the rate of serviceability loss.
- A loss of support factor is included in the design to account for potential loss of support due to subbase erosion and/or differential vertical soil movement.
- Stage construction may be modeled through use of the procedure.
- Traffic at the end of the design period is calculated based on the initial traffic and a growth factor.
- A life-cycle cost analysis is performed for the newly designed pavement.

Limitations

The AASHTO design procedure/DNPS86 program has the following limitations:

- The equation developed for use in the procedure was based in data from very short experimental AASHO Road Test sections where construction and material quality was very high. Considerably more variability will exist in a typical highway design project.

- The design equation was developed from a limited data base in terms of joint design, load transfer devices, subgrade variability, and climatic variability.

- The design equation does not reflect the impact of environmental conditions.

- The mathematical expression used for longitudinal reinforcement design is an oversimplification of the forces actually encountered.

- Loss of load transfer due to corrosion of steel reinforcement and dowel bars is not considered.

- Load equivalency factors, which relate all loads to an equivalent single-axle load, were developed for the conditions at the AASHO Road Test. The accuracy of extrapolating them to other regions is not known.

- Adequate guidance is not given for all the input variables, especially those concerning loss of support and drainage.

RPS-3

RPS-3 (Rigid Pavement System - 3) is a computer program developed by the University of Texas at Austin and the Texas Highway Department, for the design of JRCP and CRCP with or without an overlay.[5,22,23]

Capabilities

The RPS-3 program has the following capabilities:

- The procedure can be used to design JRCP and CRCP.

- The user inputs a lower and upper limit on joint spacing and layer thicknesses. The program outputs the optimum joint spacing and layer thicknesses, taking in to account cost and structural capacity.

- Longitudinal steel is designed based on cost variables and structural requirements.

- Stage construction design may be modeled.

- Alternative designs are output which are compared and optimized within the program by the single decision criterion of overall cost of the various designs.

- Design reliability is considered in the model.

- Erodibility of granular layers is considered in the model.

- Maintenance costs are analyzed in the cost analysis model.

- The cumulative effects of traffic are considered.

Limitations

The RPS-3 program has the following limitations:

- The equations developed for use in the procedure were based on data from very short experimental AASHO Road Test sections where construction and material quality was very high. Considerably more variability will exist in a typical highway design project.

- The design equations were developed from a limited data base in terms of joint design, load transfer devices, subgrade variability, and climatic variability.

- The design equations do not reflect the effects of various environmental conditions.

- Loss of load transfer through corrosion of steel reinforcement and dowel bars is not considered.

- The procedure optimizes the joint spacing and the area of steel in order to decrease the cost of transverse joints and reinforcement. Long joint spacings may decrease the total cost; however, lengthening the joint spacing may produce more joint deterioration. This is not considered in the model.

- No recommendations are provided for load transfer design. A dowel diameter of 1.25 in (32 mm) is assumed in the calculations.

- The equations used for reinforcement design are greatly simplified in comparison with the actual forces encountered.

- No recommendations are made concerning drainage design or shoulder design.

- Climatic variables are considered in the procedure.

- The effects of slab expansion and contraction are not considered in the design procedure.

PCA Design Procedure

The design procedure developed by the Portland Cement Association (PCA) is based on theoretical studies, research experience, and observations of inservice pavement performance.[5,24] It was developed in 1984.

Capabilities

The PCA procedure has the following capabilities:

- The procedure may be used for the design of JRCP or JPCP.
- The procedure considers the cumulative effects of traffic through use of a mechanistic-empirical fatigue equation. A criterion is set up for control of fatigue cracking.
- A load safety factor is provided in the procedure to compensate for the possibility of unprotected heavy truck overloads and normal construction variation in material properties and layer thicknesses.
- Erodibility of support is considered in the model. A criterion is set up for control of excessive pumping and joint faulting.
- Variation in concrete strength is considered by reducing the modulus of rupture by one standard deviation.
- Several joint design recommendations are provided in the procedure. Included in the procedure are recommendations for joint type, spacing, shape, load transfer devices, randomized and skewed transverse joints.
- The recommendations for the design of longitudinal steel in JRCP are similar to those provided by the AASHTO Guide.

Limitations

Limitations of the PCA procedure are listed below:

- The effects of moisture and thermal gradients are not considered in the model.

- Tensile stresses caused by friction between the slab and subbase and tensile stresses caused by full or partial seizure of the load transfer devices are not considered.

- The effect of the type of subbase is only considered through its effect on the k-value. Erodibility of the subbase is not considered.

- The effect of nonuniform support resulting from nonuniform subbase and subgrade materials is not considered.

- The procedure does not consider the effects of climate or drainage.

- Nonhomogeneity of pavement materials, with the exception of the concrete strength, is not considered.

California Rigid Pavement Design Procedure

The California Rigid Pavement Design Procedure was developed by the California Department of Transportation (Caltrans) for the design of JPCP.[5,25]

Capabilities

Using the California Rigid Pavement Design procedure, the designer uses subgrade soil and traffic information and a nomograph to chose a design from a series of standard cross-sections. The procedure has the following capabilities:

- Given the R-value, Traffic Index, subgrade Plasticity Index, and subgrade permeability, a design cross section may be chosen.

- A variety of subbase types are recommended for each of the design cross sections, including lean concrete base, asphalt concrete base, asphalt-treated permeable base, and cement-treated permeable base.

- The procedure emphasizes minimizing drainage related problems through good drainage design and the use of asphalt-treated and cement-treated *permeable* bases. In fact, permeable bases are to be given first consideration in design.

- Guidelines are provided for the design of the drainage system.

- Recommendations concerning the type and spacing of joints are given in the procedure.

Limitations

Specific limitations of the CALTRANS procedure are listed below:

- The slab thickness appears to be based on experience only. The maximum design slab thickness is 10.2 in (259 mm) for traffic levels of greater than 13.5 million ESAL over the design period. The structural design may not be adequate for pavements carrying very high truck volumes.

- The effect of slab warping and curling are considered indirectly through the recommendations for short joint spacings.

- The longitudinal and transverse joint design recommendations are based on previous experience. No analytical procedure is available for the project-specific design. No recommendations are provided for design of the joint sealant reservoir, joint sealant type, or type of load transfer.

- No climatic variables are considered in the design procedure.

- No provisions are made in the procedure for nonhomogeneity and variability in material properties or other design variables.

- JRCP and CRCP cannot be designed using the procedure.

- The procedure was developed for a specific set of climatic and material variable. Use of the procedure in other areas of the country has not been tested.

BERM

BERM is a program developed by Resource International, based on analysis of RISC output, for use in the design of portland cement concrete and asphalt cement concrete shoulders.

Capabilities

The program calculates the life of the shoulder in terms of number of cumulative 18-kip (80 kN) ESAL's for parked and encroaching traffic loadings. BERM has the following capabilities:

- Tied, keyed, or separate concrete shoulders as well as asphalt concrete shoulders may be modeled.

- For the design of flexible shoulders, the user may input the viscoelastic properties of the asphalt concrete or use the program default values.

- If an unreasonable value is input, the program prompts the user with a range of acceptable values.

- The cumulative effect traffic is considered (output of the program).
- The effects of inner and outer edge loading are considered for rigid shoulder design and the effects of parked and encroaching traffic are considered for asphalt concrete shoulder design.

Limitations

BERM has the following limitations:

- The mainline pavement type and thickness are not considered in the model.
- The effect of climate and moisture is not considered in the model.
- Only granular base courses may be modeled.
- The exact degree of load transfer may not be specified for the design of concrete shoulders.
- The effect of loss of subgrade support is not considered in the model.
- Drainability of the pavement section is not considered in the model.
- Design is based on only two locations on the shoulder.

JCS-1

JCS-1 (Jointed Concrete Shoulder-1) is a computer program developed by the University of Illinois to compute the accumulated fatigue damage over the design life of concrete shoulders.[5,26] The program was based on finite element methods employing classical thin plate theory and field data.

Capabilities

JCS-1 has the following capabilities:

- The cumulative effect of traffic is considered comprehensively.
- The effect of loss of subgrade support is directly considered.
- The lane/shoulder joint load transfer efficiency is directly considered; therefore, tied or untied concrete shoulders can be modeled.

- A number of shoulder and mainline pavement thicknesses, load transfer efficiencies, and shoulder widths may be examined in a single computer run.

- Fatigue damage is calculated at the lane/shoulder joint and at the outer edge of the shoulder.

Limitations

The significant limitations are listed below:

- Since the program was developed for the design of plain jointed concrete shoulders, the mainline pavement is not considered except for the thickness and load transfer.

- No climatic variables are considered.

- Drainability of the pavement section is not considered.

- Reinforcement is not considered.

- Design is based on only two locations on the shoulder.

- The design procedure has not been thoroughly tested.

- The program was developed based on a finite element analysis over a limited range of variables, i.e., subgrade modulus, concrete strength and Poisson's ratio, and slab thickness.

- The effects of thermal and moisture gradients are not considered.

5. OVERALL PROGRAM EVALUATION

An analytical scheme was developed to evaluate each of the models and methods based on the variables important to rigid pavement analysis and design. The important variables were assigned relative weights. In turn, each program was given a rating from 0.0 to 5.0 for each of the important variables. The rating was then multiplied by the weights and a weighted average was calculated for each program.

Each program considered could be placed in one of the following three categories:

1. Structural Analysis/Distress Models.

2. Drainage/Climatic Models.

3. Pavement Design Methods.

The variables that were assumed to be most important in each of these categories are described herein.

Structural Analysis Models

Each of the structural analysis models has been evaluated in terms of:

- Memory requirements.
- Run time.
- Reasonableness of results.
- Theory verified.
- Ease of use.
- Ability to consider:
  - PCC slab characteristics (thickness, fatigue, durability, stiffness, etc.).
  - Base/subbase characteristics (thickness, fatigue, erodibility, drainage, stiffness, etc.).
  - Subgrade characteristics (stiffness, moisture sensitivity, volume change potential, etc.).
  - Shoulder characteristics (thickness, width, fatigue, durability, tied, etc.).
  - Joint design (load transfer, aggregate interlock, dowels, sealant, etc.).
  - Moisture gradient.
  - Thermal gradient.
  - Drainage (permeability, type of drain, erosion potential, etc.).
  - Climatic variables (temperature, moisture, freeze, etc.).
  - Traffic (truck, axle type, truck distribution, etc.).
  - Special design factors (widened lanes, thickened edge, etc.).

Drainage/Climatic Analysis Models

Each of the drainage analysis models has been evaluated in terms of:

- Memory requirements.
- Run time.
- Reasonableness of results.
- Theory verified.
- Ease of use.
- Ability to consider:
  - Climate (temperature, moisture, freeze, etc.).
  - Material properties of lower pavement layers (stress dependency, moisture dependency, temperature dependency, etc.).
  - Ability to model pavement cross section.

Pavement Design Methods

Each of the design methods has been evaluated in terms of:

- Memory requirements.
- Run time.
- Reasonableness of results.
- Theory verified.
- Ease of use.
- Ability to consider:
  - PCC slab characteristics (thickness, fatigue, durability, stiffness, etc.).
  - Base/subbase characteristics (thickness, fatigue, erodibility, drainage, stiffness, etc.).
  - Subgrade characteristics (stiffness, moisture sensitivity, volume change potential, etc.).
  - Shoulder characteristics (thickness, width, fatigue, durability, tied, etc.).
  - Joint design (load transfer, aggregate interlock, dowels, sealant, etc.).
  - Moisture gradient.
  - Thermal gradient.
  - Drainage (permeability, type of drain, erosion potential, etc.).
  - Climatic variables (temperature, moisture, freeze, etc.).
  - Traffic (truck, axle type, truck distribution, etc.).
  - Reliability of design.

6. RECOMMENDATIONS

Table 1 shows the assigned variable weights and the resulting ratings for each program. The ratings were based on the results of the sensitivity analysis, review of the program documentation and experience in the use of the programs.

Based on the results of these ratings and work accomplished in deriving them, the following programs are recommended for further use in the Tasks E and F of this contract:

Structural Analysis Model

The ILLISLAB finite element model is efficient to use and can structurally model many key design factors. The main deficiencies of ILLISLAB (such as incomplete consideration of drainage and climate factors) can be addressed by using other models, such as CMS and Liu-Lytton, in conjunction with the ILLISLAB model.

Table 1. Evaluation of analysis models and design methods.

EVALUATION OF STRUCTURAL/DISTRESS MODELS

ALTERNATIVE	WEIGHT	RENDAY	RUN TIME	RESULTS	THEORY	EASE USE	SLAB	BASE	SUBGRADE	SHOULDER	JOINT	MOISTURE	THERMAL	DRAINAGE	CLIMATE	TRAFFIC	SPECIAL	AVERAGE
		4.0	4.0	7.0	8.0	4.0	8.0	8.0	8.0	6.0	6.0	4.0	6.0	7.0	7.0	8.0	8.0	
ICCI-SLAB		5.0	4.0	4.0	5.0	5.0	3.2	3.8	3.5	3.5	3.8	0.0	3.5	0.0	0.0	3.5	4.0	3.0
JSLAB		5.0	4.0	2.5	3.0	2.5	4.0	3.5	3.0	3.3	3.4	2.0	2.2	0.0	0.0	3.2	4.0	2.7
WESLIGID		1.0	2.8	1.5	3.8	1.0	3.0	4.0	2.8	2.8	3.4	0.0	2.6	0.0	0.0	3.2	3.8	2.3
WESLAYER		1.0	2.4	3.0	3.4	1.0	3.0	4.0	2.8	2.8	3.4	0.0	2.6	0.0	0.0	3.2	3.8	2.3
RISC		4.0	1.0	3.5	3.0	1.0	4.4	3.6	2.5	3.5	3.0	0.0	1.1	0.0	0.0	4.0	2.3	2.4
H-51		5.0	5.0	2.8	2.0	2.8	2.5	1.2	1.8	0.0	0.0	0.0	0.0	0.0	0.0	2.9	0.0	1.6
PREDICT		5.0	5.0	3.0	2.1	5.0	3.3	3.3	2.9	3.5	3.9	0.0	0.0	2.9	3.0	3.7	2.5	3.0
PEARDARP		5.0	4.5	3.0	2.2	4.0	3.3	3.5	2.9	3.5	4.0	0.0	0.0	2.8	2.5	4.0	3.2	2.9
PMARP		1.0	2.2	3.0	3.0	2.9	4.4	0.7	3.0	3.3	3.0	1.7	0.0	1.0	1.0	5.0	3.0	2.4

EVALUATION OF DRAINAGE/CLIMATIC MODELS

ALTERNATIVE	WEIGHT	RUN TIME	RESULTS	THEORY	EASE USE	CLIMATE	MATERIAL	MODEL	AVERAGE
		10.0	10.0	20.0	8.0	10.0	10.0	10.0	100.0
CRS		2.8	5.0	4.6	1.8	3.0	4.9	3.7	4.3
LUT-LYTTON		5.0	4.0	4.2	3.5	3.6	3.4	3.7	3.9

EVALUATION OF DESIGN MODELS

ALTERNATIVE	WEIGHT	RUN TIME	RESULTS	THEORY	EASE USE	SLAB	BASE	SUBGRADE	SHOULDER	JOINT	MOISTURE	THERMAL	DRAINAGE	CLIMATE	TRAFFIC	RELIABILITY	AVERAGE
		8.0	7.0	6.0	5.0	6.0	6.0	8.0	7.0	7.0	8.0	6.0	7.0	6.0	8.0	5.0	
JEP-1		4.3	4.0	3.8	1.3	4.5	3.4	3.5	2.4	3.3	1.7	3.0	2.1	2.4	4.5	2.4	3.2
DMPS86		4.3	3.9	2.0	4.5	3.5	3.2	4.3	2.0	2.5	2.2	0.0	2.7	2.5	3.5	3.7	3.0
RPS-3		3.4	4.0	2.0	2.6	3.5	3.2	3.0	2.3	2.4	0.0	0.0	0.0	0.0	4.6	3.8	2.4
PCA		4.5	4.2	3.9	3.5	4.4	2.9	4.1	3.3	3.1	0.8	1.2	0.0	0.0	4.6	3.7	3.0
CAL RIGID		2.0	3.8	2.2	2.8	1.2	2.6	2.8	2.0	3.0	0.0	0.0	0.0	0.0	2.2	0.0	1.7
BEAM		4.7	3.0	2.4	3.7	1.2	2.8	2.2	3.6	2.0	0.0	0.0	0.0	0.8	3.0	0.0	2.0
JCS-1		4.5	3.6	3.5	2.3	1.2	3.1	2.2	3.2	2.0	0.0	0.0	0.0	0.0	3.9	0.0	2.0

For the evaluation described herein, ILLISLAB has been shown to have several advantages over the JSLAB finite element model. For example, the analysis of curling requires several executions of JSLAB and then manually subtracting the results. Also, numerous attempts were made to execute JSLAB while specifying curling and load which resulted in aborted executions for no apparent reason. Analysis of warping stresses caused similar problems. ILLISLAB handles these same types of problems flawlessly and is recommended for general use. The ILLISLAB code is constantly being updated at the University of Illinois. Currently, the use of a nonlinear thermal gradient is being incorporated into the ILLISLAB model, thus fully emulating the thermal gradient capabilities of the CMS model.

Several problems were also noted with the PMARP finite element program. These include its limited mesh size capabilities, its neglect of thermal and moisture gradients, the errors associated with the input processor, and the errors in the stiffness matrix.

Prediction Models

The PEARDARP (using the appropriate PMARP output) program may be used as a prediction model for distress as well as a comprehensive cost analysis model. However, since several of the PEARDARP distress models have not been verified, it is recommended that the PREDICT program be used in conjunction with the PEARDARP program for comparative purposes.

Drainage/Climatic Model

The CMS program is a very comprehensive climatic and material analysis model. The program outputs, such as thermal gradient, moisture profiles, and soil strength properties, may be used as inputs to the analysis and predictive models and the design methods.

The Liu-Lytton drainage models also model many drainage variables which are considered key to the design of concrete pavements. The program is fairly adaptable to various soil and moisture conditions and may be used to evaluate or design a pavement drainage system.

Design Method

The Zero Maintenance Design Procedure incorporates many of the important rigid pavement design factors. If used in conjunction with both the CMS model and the Liu-Lytton models, the weaknesses of the Zero Maintenance Design Procedure described in section 4 can be rectified.

For rigid shoulder design, the JCS-1 program is recommended and for flexible shoulder design the BERM program is recommended. The JCS-1 procedure is recommended over the BERM rigid shoulder design procedure because JCS-1 incorporates more of the important shoulder design parameters.

PART II. STANDARD PAVEMENT SECTION AND VARIABLES UNDER CONSIDERATION

This section illustrates the standard section for the sensitivity analysis and the range of variables tested. A cross section of the standard pavement section used in the analyses is illustrated in figure 1. A 9-in (229 mm) PCC slab over a 5-in (129 mm) unbonded lean concrete base was chosen. The section has dowels across the transverse joints and tied concrete shoulders. Table 2 provides the range of variables tested for each of the design features evaluated. Tables 3 through 5 provide the inputs used for the standard section. The finite element meshes required to run ILLISLAB and JSLAB are shown in figures 2 through 5. A four-slab system loaded at the edge of the slab was chosen as the standard loading configuration. The maximum-density four-slab configuration mesh for WESLIQID and WESLAYER is shown in figure 6. The mesh is very coarse due to the considerable memory requirements of these programs. The accuracy of the results was greatly affected by the use of this mesh; thus a two-slab system was adopted for these programs. The two-slab meshes are shown in figures 7 through 10. The same problem of memory requirements was encountered in executing the PMARP program, therefore, a two-slab configuration was also developed for the PMARP program. These meshes are presented in figures 11 through 13. The use of a two-slab system does not greatly affect the stress calculation results for the longitudinal edge loading condition; however, in examining the corner loading condition a large affect can be seen. Figure 14 illustrates the load configuration employed by the H-51 program.

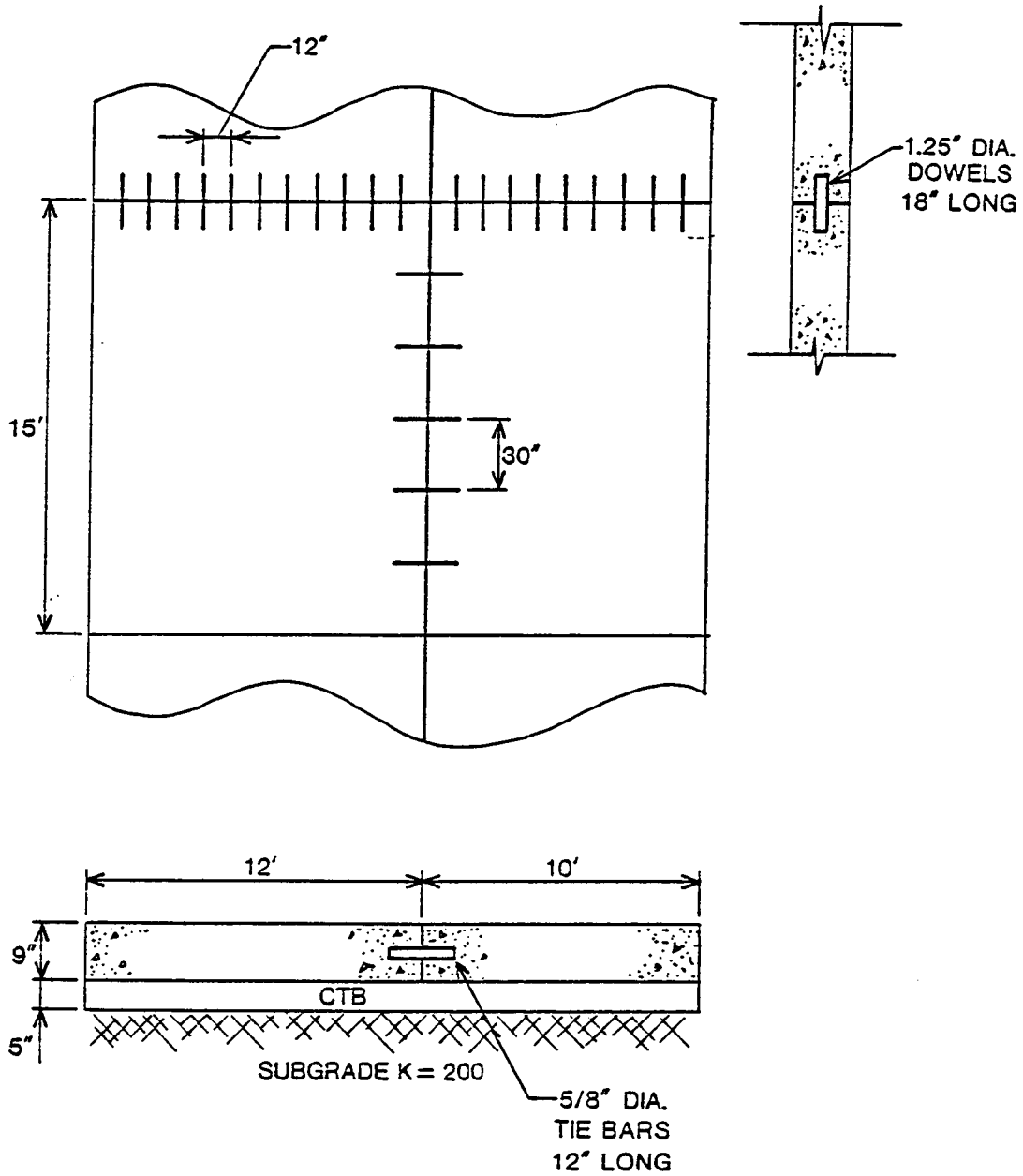

(1 in = 25.4 mm, 1 lb = 2.205 kg)

Figure 1. Assumed standard pavement section.

Table 2. Levels of design variables.

DESIGN VARIABLES	STANDARD LEVELS	VARIATION OF LEVELS
THICKNESS (in)	9	6, 12, 15
DOWELS (in)	Y, 1.25	NO / 0.0; YES / 1.0, 1.5
BASE TYPE	UNBONDED STAB.	GRANULAR, BONDED STAB.
REINFORCEMENT	NO	YES
SLAB LENGTH (ft)	15	10, 20 (JPCP)
JOINT WIDTH (in)	0.25	0.15, 0.24, 0.30, 0.48
TIED SHOULDERS	YES	NO
WIDENED LANES (ft)	NO	YES / 15
SOIL STRENGTH (k-value) (pci)	200	50, 100, 500

NOTE: Only main effects were examined. Each factor was varied from the standard in a separate computer run.

(1 in = 25.4 mm, 1 lb = 2.205 kg)

Table 3. Parameters assumed for use in the analysis models and design methods.[5]

SURFACE LAYER	
PCC Slab Thickness	9 in
Poisson's Ratio	0.20
Modulus of Rupture	5,000,000 psi
BASE LAYER	
Bonding Condition	Bonded/Unbonded
Thickness	5 in
Poisson's Ratio	0.20
Modulus of Elasticity	200,000 psi
SUBGRADE LAYER	
Subgrade Model	Winkler
Subgrade Modulus	200 pci
DOWEL AND JOINT PARAMETERS	
Transverse Joint	
Joint Width	0.25 in
Modulus of Dowel Support	1,500,000 pci
Modulus of Elasticity of Dowel Bars	29,000,000 psi
Poisson's Ratio of Dowel Bars	0.30
Dowel Bar Diameter	1.25 in
Dowel Bar Spacing	12.0 in
Dowel Concrete Interaction Factor By Friberg's Analysis[1]	1,514,419
Longitudinal Joint	
Tie Bar Diameter	0.625 in
Tie Bar Spacing	30.0 in
Interaction Factor (Friberg)	444,279
LOADING CONDITIONS	
Type of Axle	Dual Wheel
Gross Weight of Axle	18 kip
Tire Pressure	100 psi
Thermal Gradient (for curling analyses only)	1.5, -3.0 °F/in

[1] In calculating Friberg's dowel-concrete interaction factor, a coefficient of 1.0 instead of 1.8 was used. This corrects the problem of the analysis resulting in dowels which are too small.

Table 4. Traffic data assumed in design models.[5]

TRAFFIC DATA	
ADT at Beginning of Design Period	17,100
ADT at End of Design Period	39,100
Percent Trucks of ADT	21%
Percent Trucks in Design Traveled Lane	85.15%
Mean Axles Per Truck	2.60
Length of Surveyed Stretch	10 Miles
Average Total Length of Encroachments per Truck in the Shoulder Stretch	0.24 Miles
Percent Trucks that Park on Shoulder	0.016%

Table 5. Loadometer data assumed in design models.[5]

LOADOMETER DATA

Single Axle Load Distribution

Weight Distribution (Pounds)	Percent in Range
0 - 3000	5.75
3001 - 7000	10.33
7001 - 8000	7.76
8001 - 12000	29.54
12001 - 16000	4.37
16001 - 18000	1.77
18001 - 20000	1.02
20001 - 22000	0.54
20001 - 24000	0.34
24001 - 26000	0.14
26001 - 30000	0.04
30001 - 32000	0.01
32001 - 34000	0.01

Tandem Axle Load Distribution

Weight Distribution (Pounds)	Percent in Range
0 - 6000	0.27
6001 - 12000	13.34
12001 - 18000	7.05
18001 - 24000	5.51
24001 - 30000	14.92
30001 - 32000	3.61
32001 - 34000	1.40
34001 - 36000	0.50
36001 - 38000	0.25
38001 - 40000	0.16
40001 - 42000	0.11
42001 - 44000	0.08
44001 - 46000	0.07
46001 - 50000	0.07
50001 - 52000	0.02
52001 - 54000	0.01
54001 - 56000	0.01

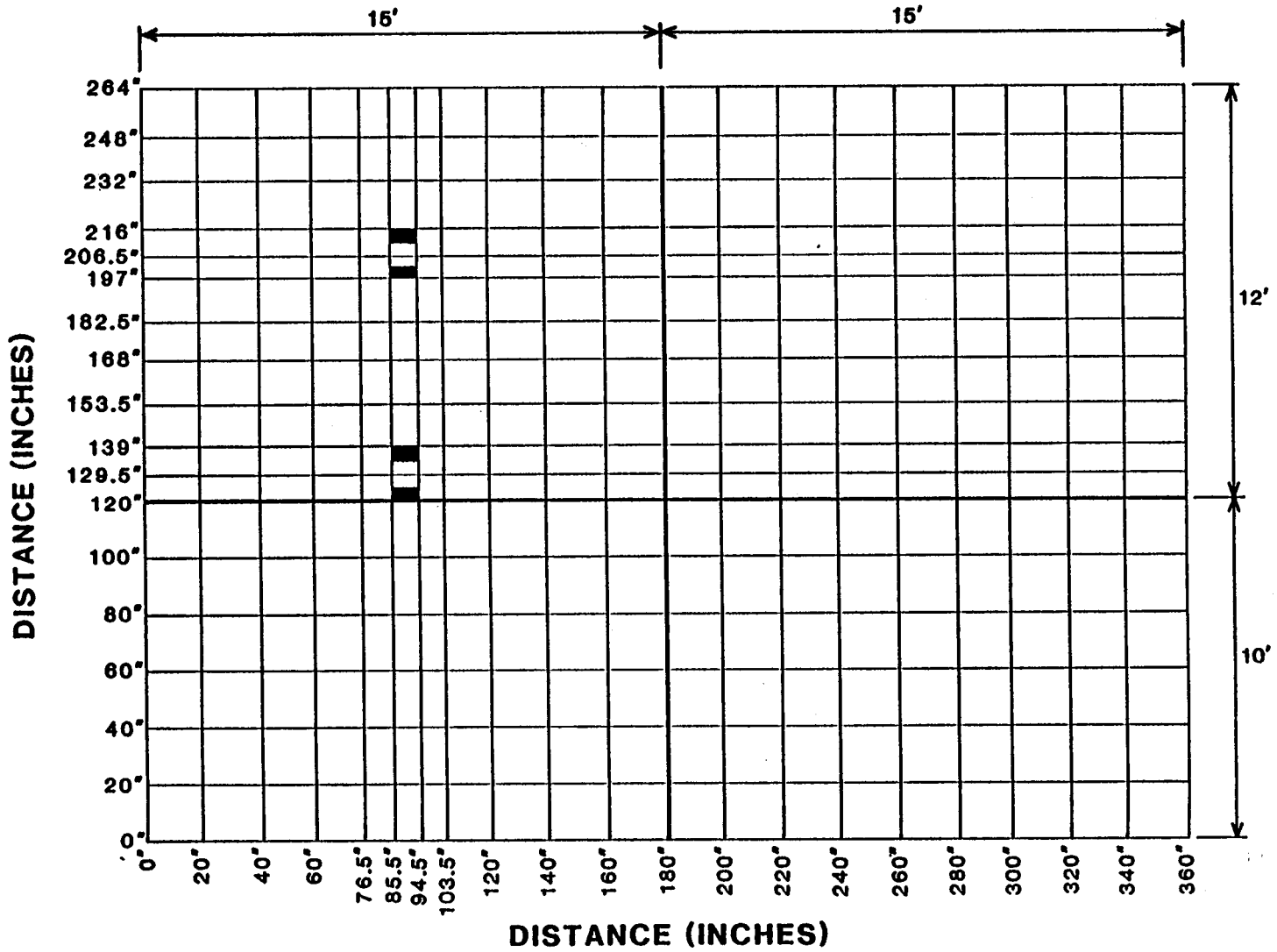

(1 in = 25.4 mm)

Figure 2. ILLISLAB and JSLAB finite element mesh for standard pavement section analysis.

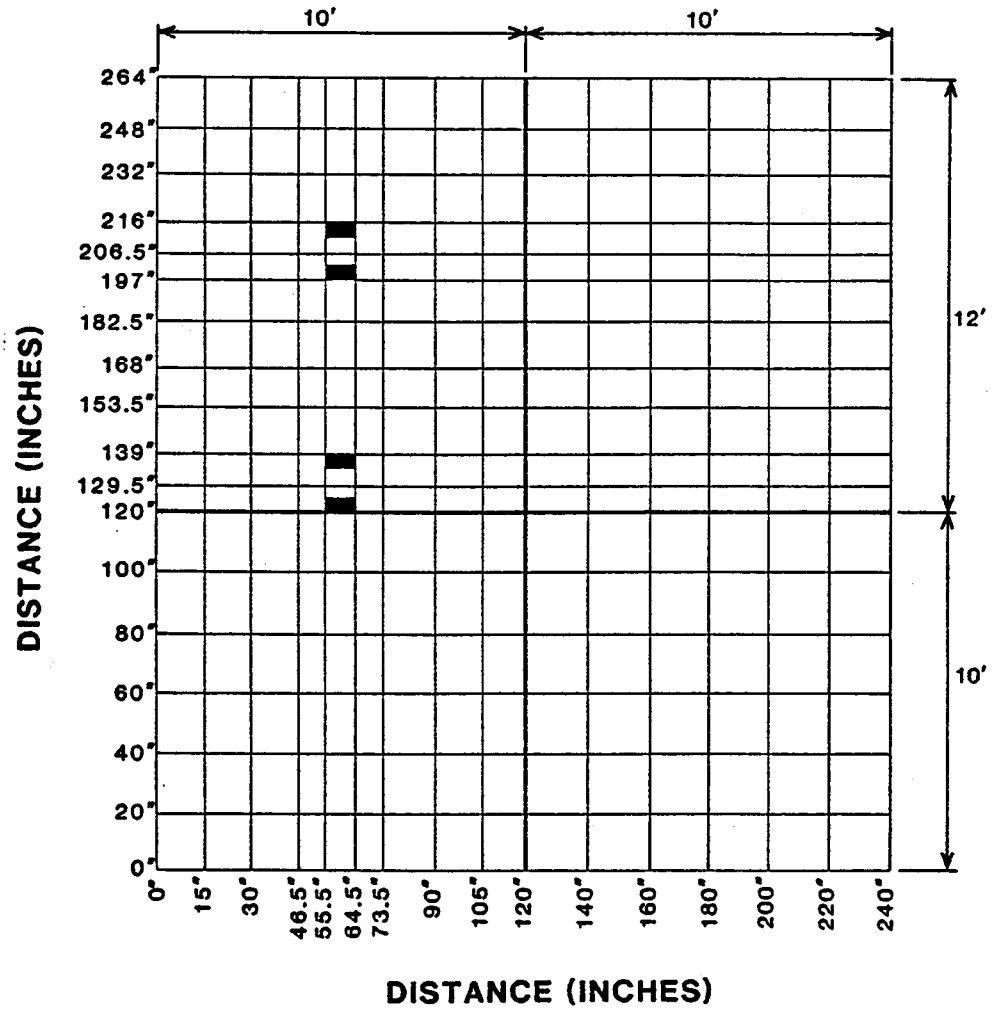

(1 in = 25.4 mm)

Figure 3. ILLISLAB and JSLAB finite element mesh for 10-ft joint spacing analysis.

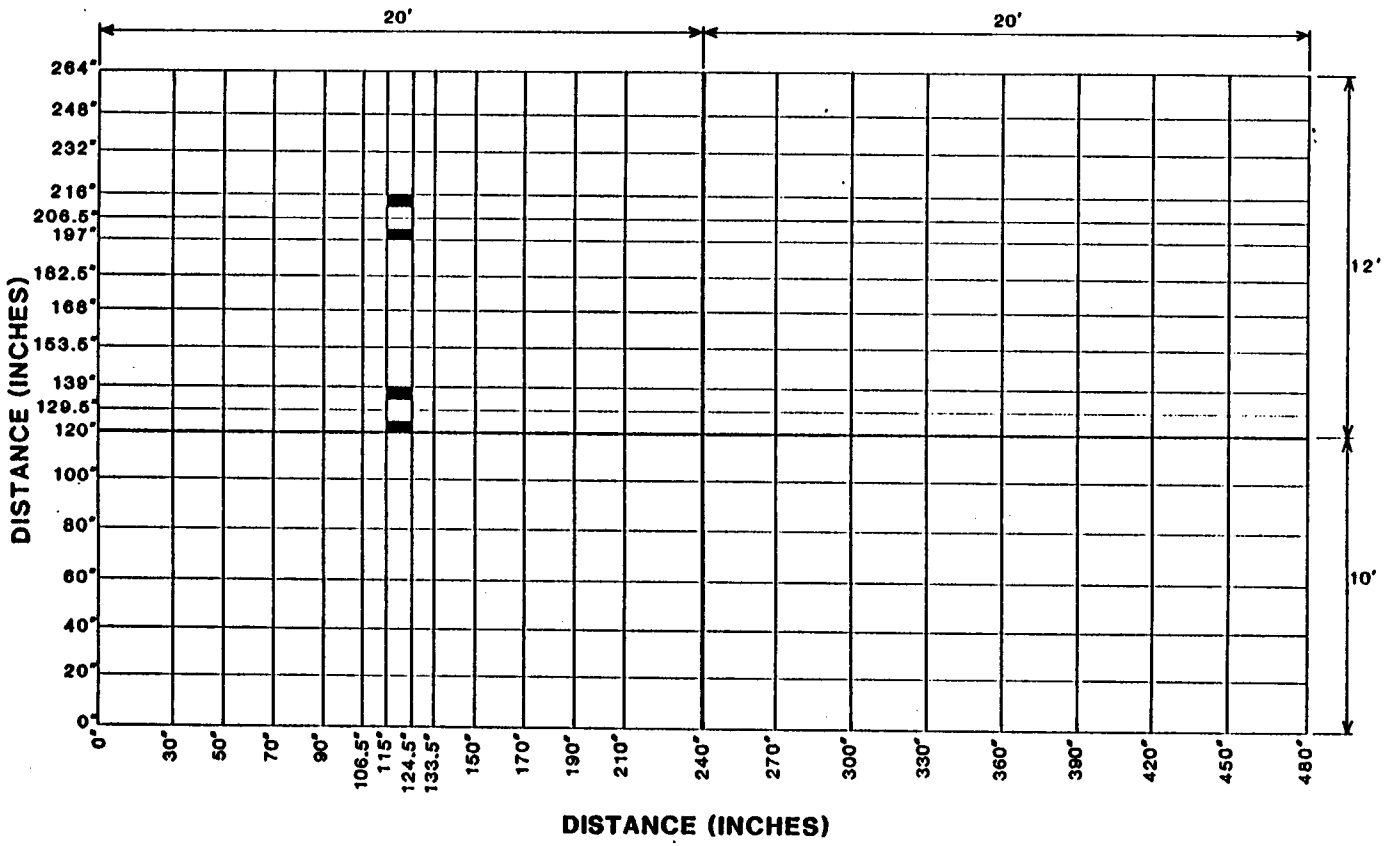

(1 in. = 25.4 mm)

Figure 4. ILLISLAB and JSLAB finite element mesh for 20-ft joint spacing analysis.

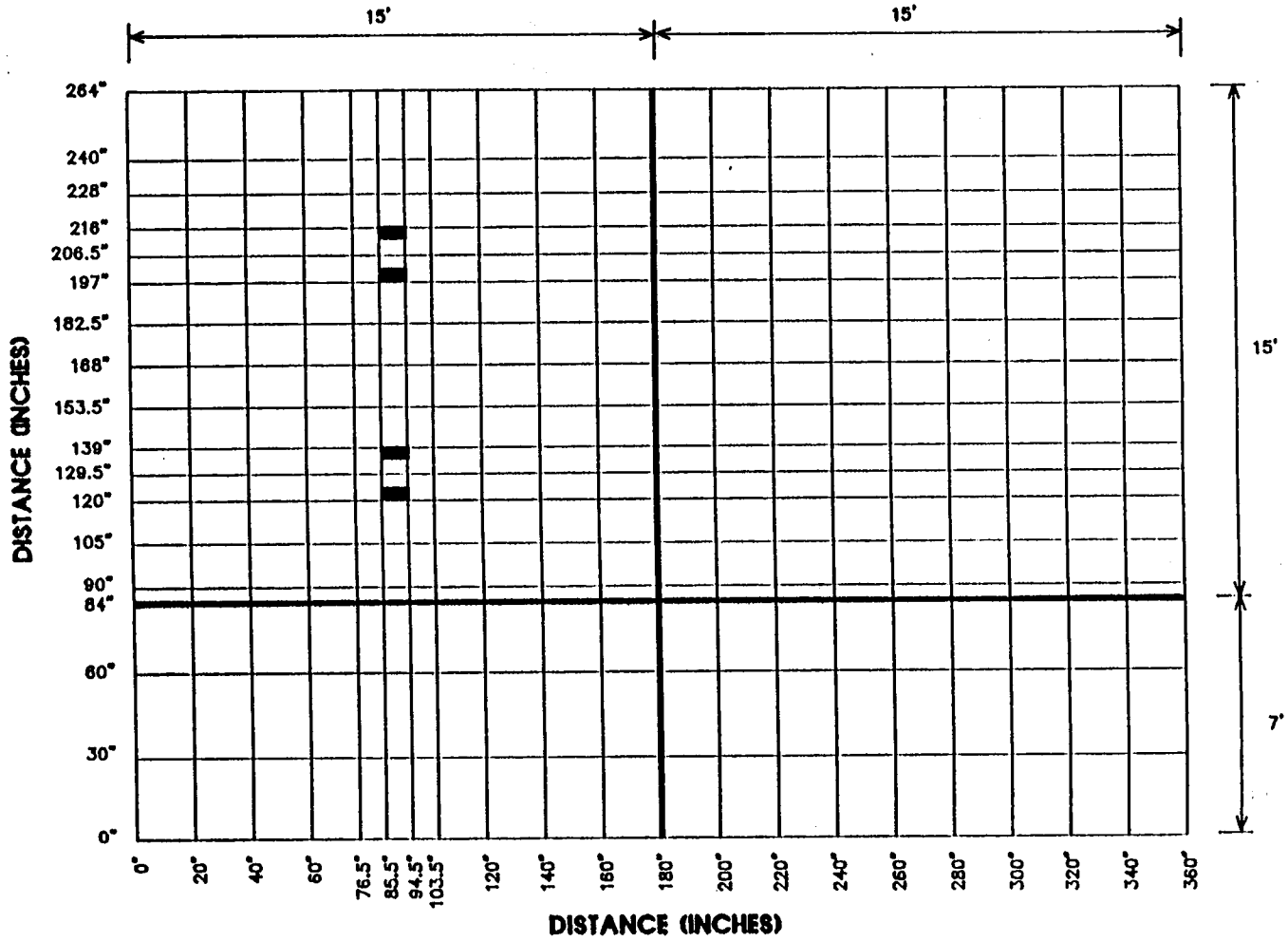

(1 in = 25.4 mm)

Figure 5. ILLISLAB and JSLAB finite element mesh for widened lane analysis.

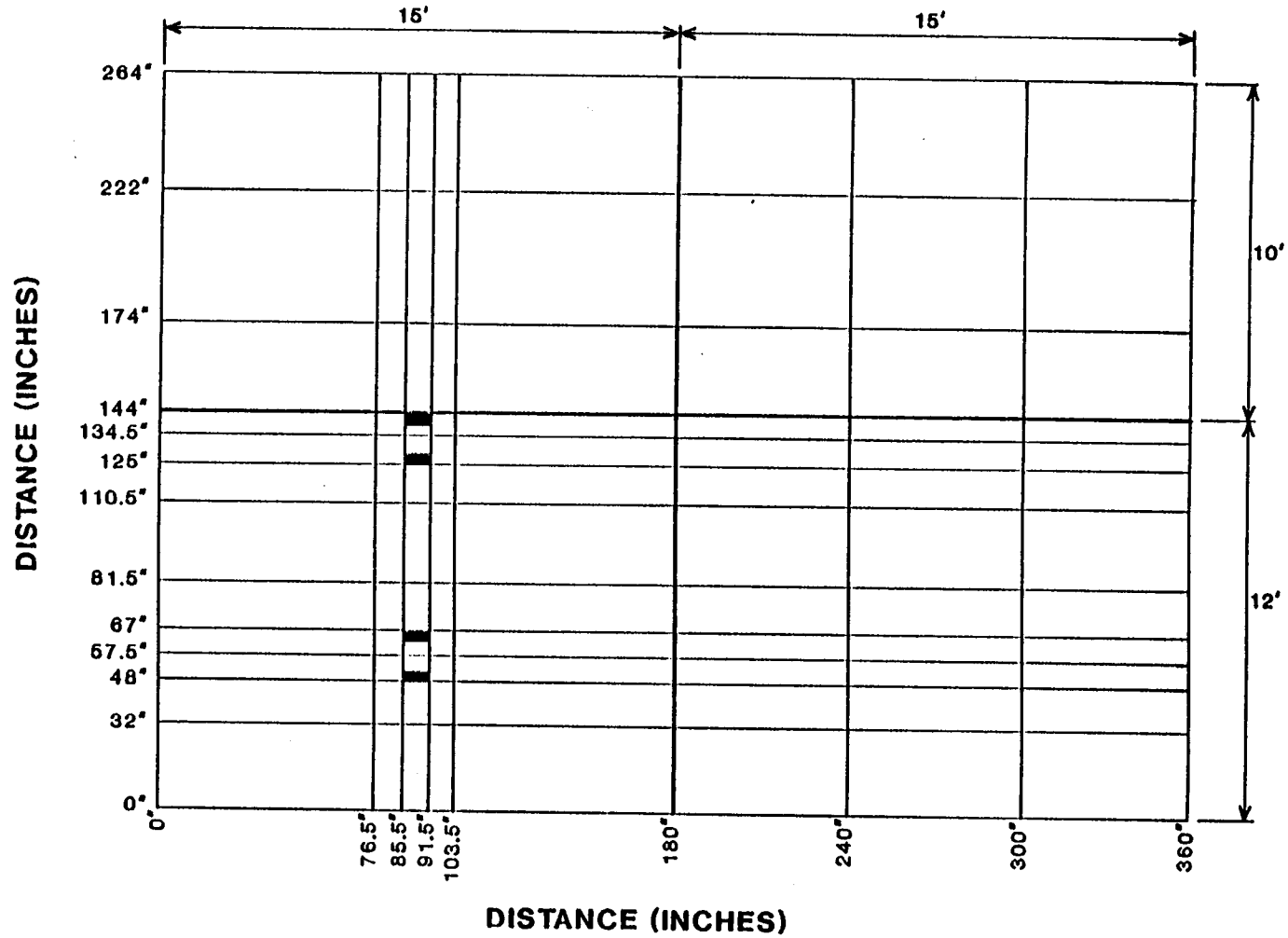

(1 in = 25.4 mm)

Figure 6. WESLIQID and WESLAYER finite element mesh for standard pavement analysis using four-slab system.

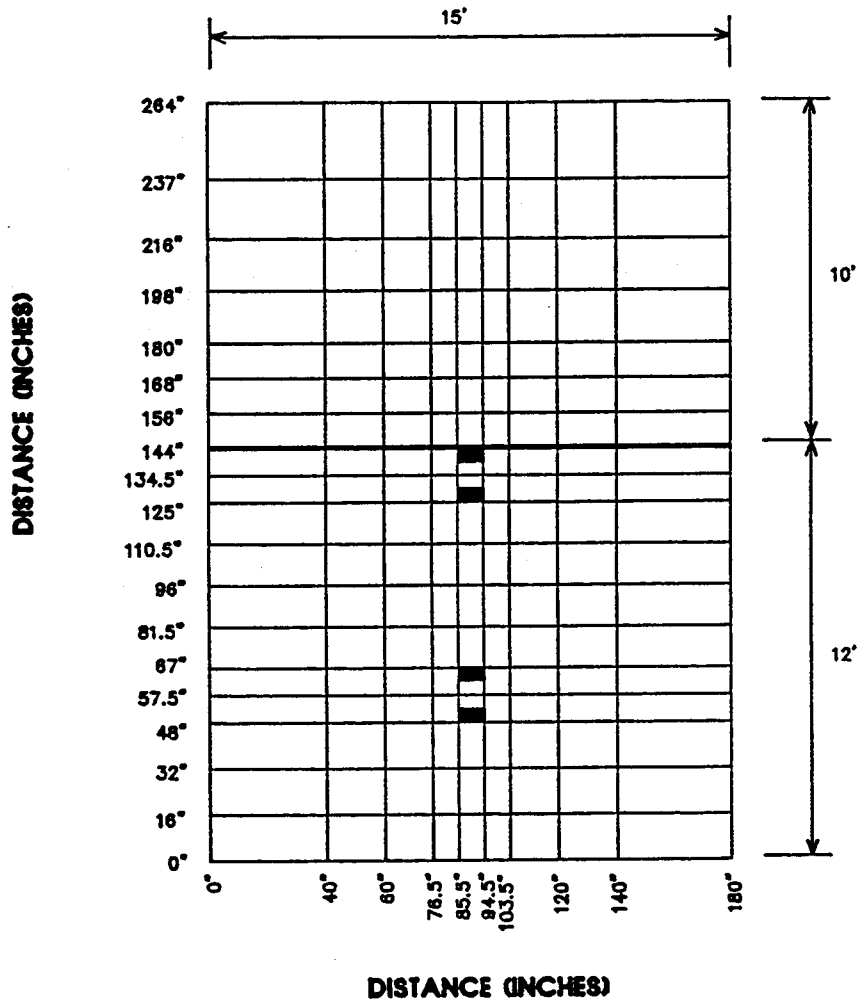

(1 in = 25.4 mm)

Figure 7. WESLIQID and WESLAYER finite element mesh for standard pavement analysis using a two-slab system.

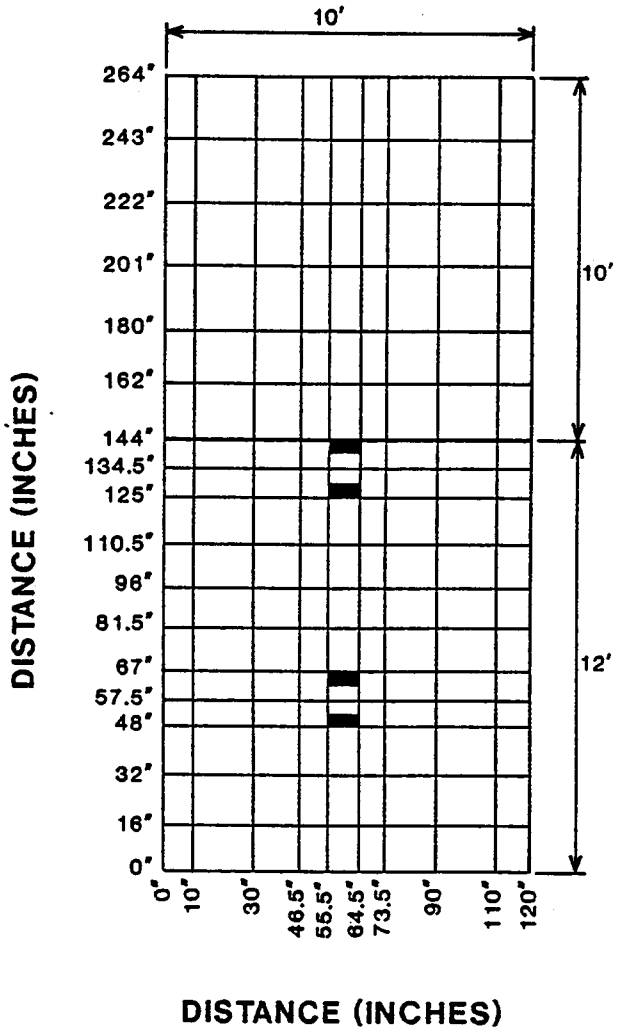

(1 in = 25.4 mm)

Figure 8. WESLIQID and WESLAYER finite element mesh for 10-ft joint spacing analysis.

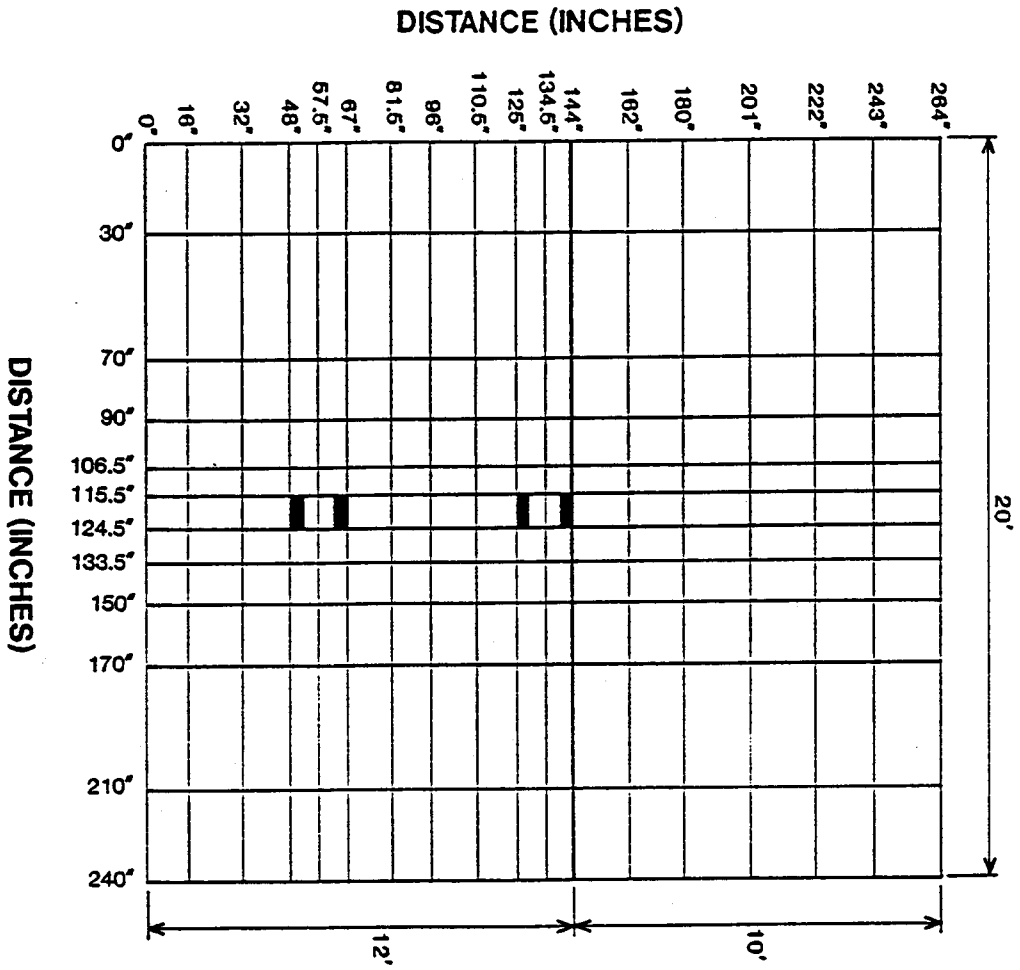

(1 in = 25.4 mm)

Figure 9. WESLIQID and WESLAYER finite element mesh for 20-ft joint spacing analysis.

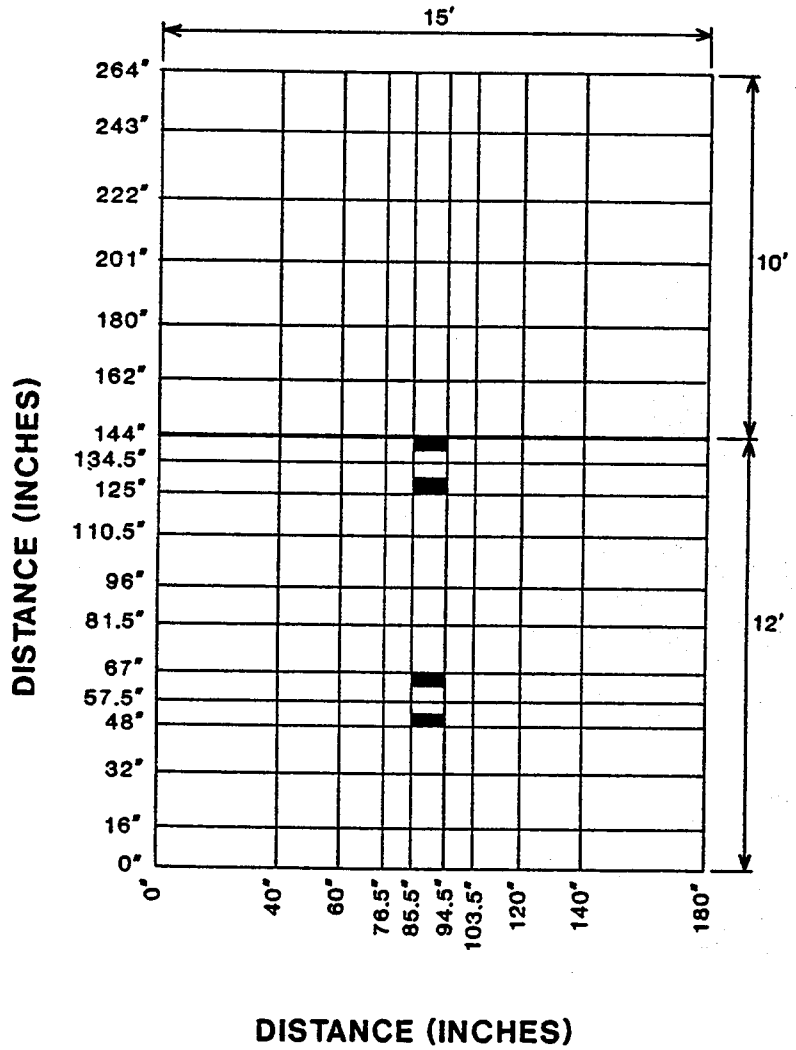

(1 in = 25.4 mm)

Figure 10. WESLIQID and WESLAYER finite element mesh for widened lane analysis.

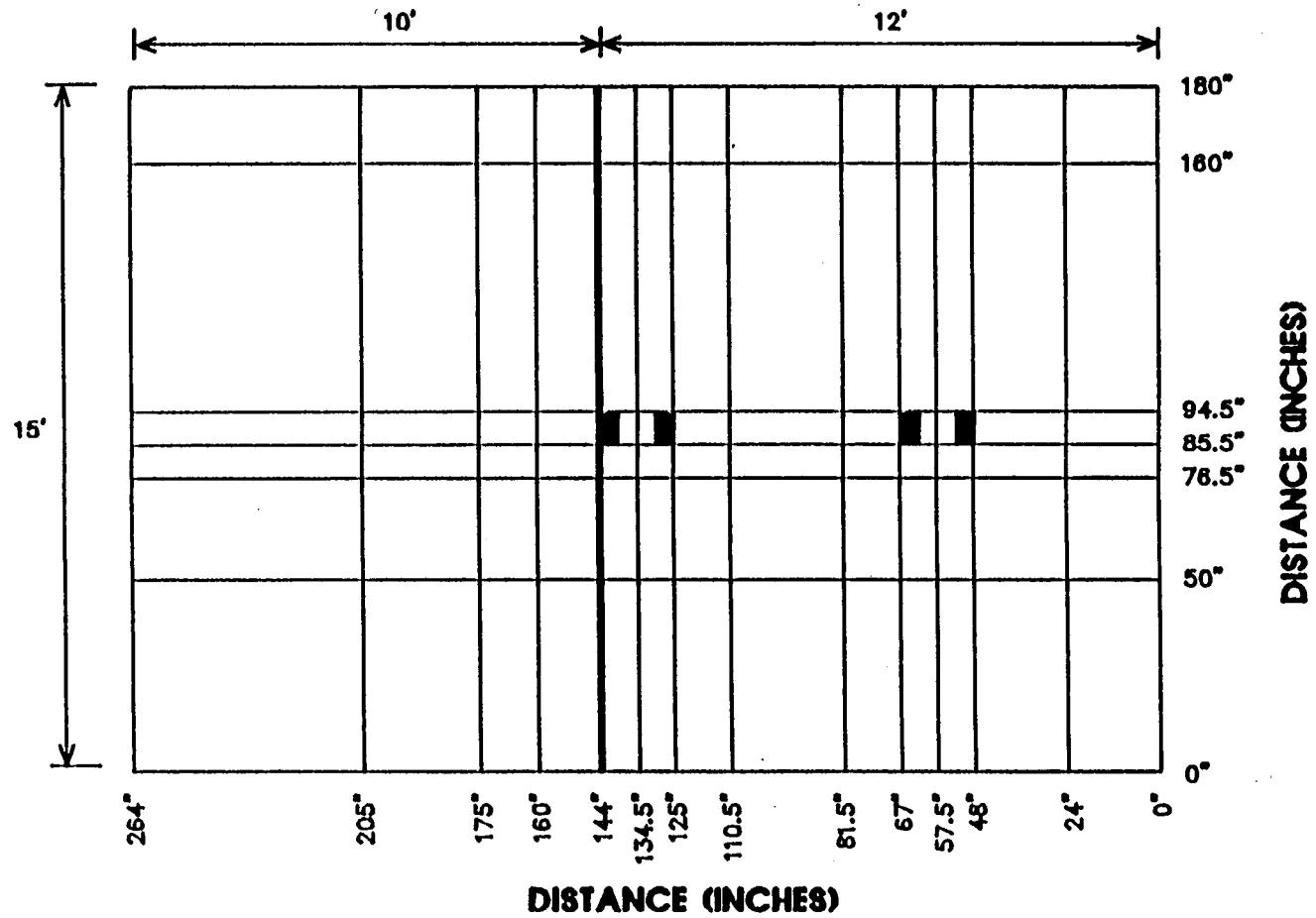

(1 in = 25.4 mm)

Figure 11. PMARP finite element mesh for standard pavement section.

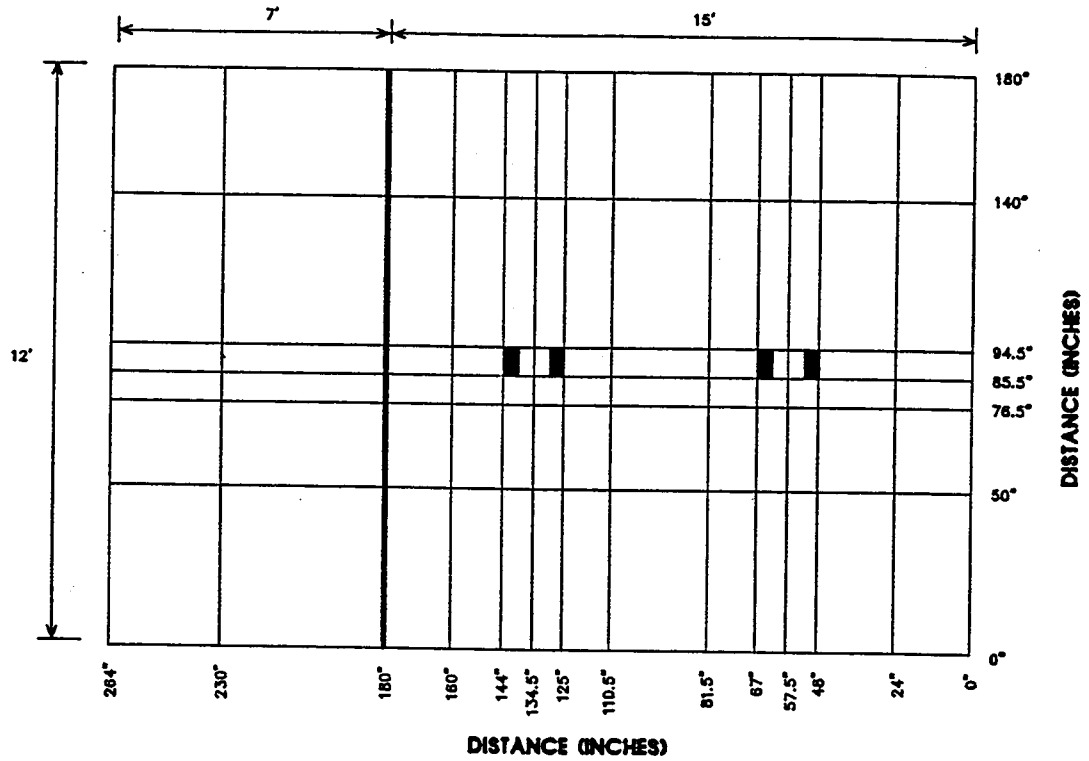

(1 in = 25.4 mm)

Figure 12. PMARP finite element mesh for widened lane analysis.

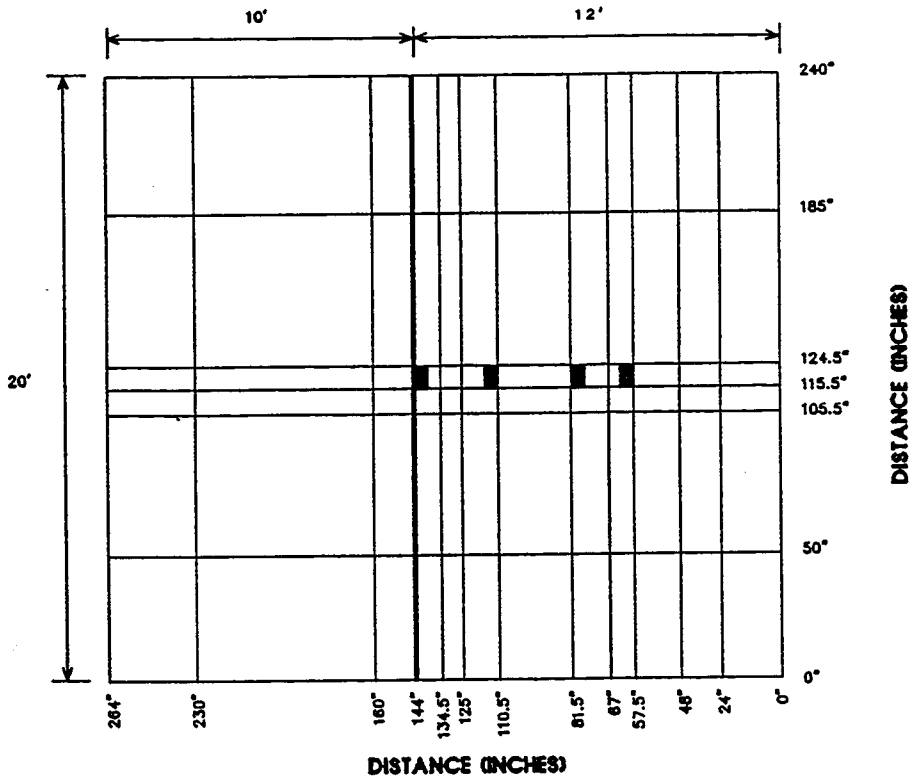

(1 in = 25.4 mm)

Figure 13. PMARP finite element mesh for 20-ft joint spacing analysis.

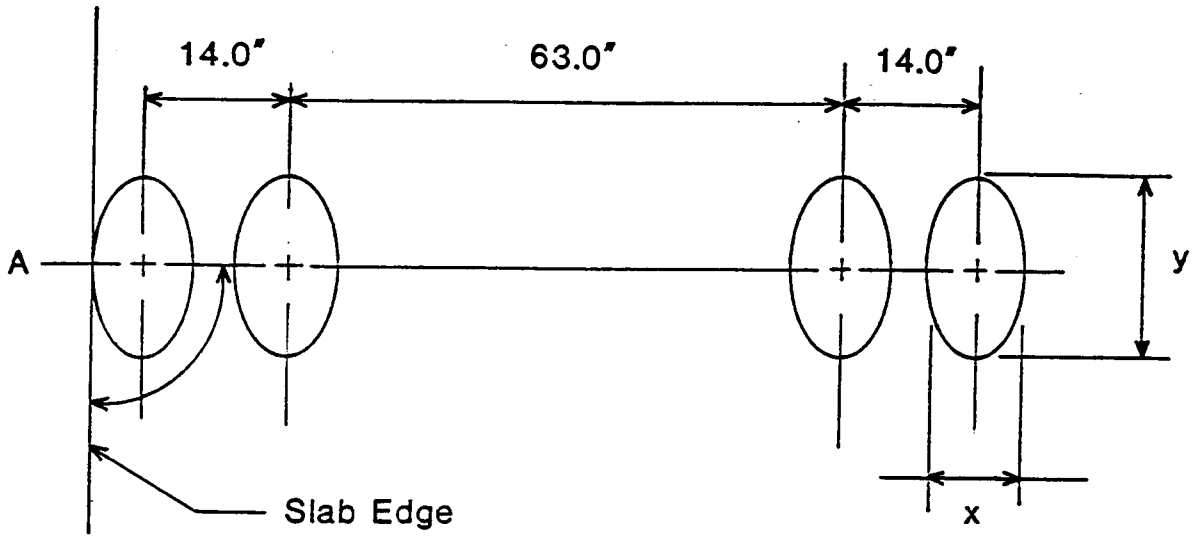

LONGITUDINAL EDGE

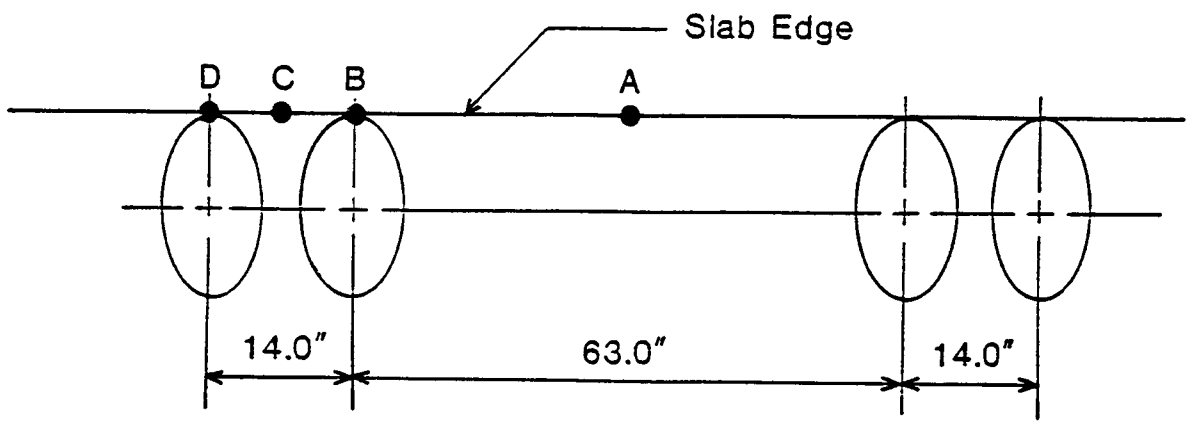

TRANSVERSE EDGE

(1 in = 25.4 mm)

Figure 14. Wheel configuration used for H-51 analysis.

PART III. SUMMARY OF INPUT AND OUTPUT VARIABLES

This section presents summaries of the inputs and outputs required for all of the programs and procedures under consideration. Tables 6 through 21 are detailed lists of the inputs required to use each program or procedure and the outputs produced. Tables 22 through 31 contains lists of the method of obtaining each input for the recommended programs.

Table 6. ILLISLAB input and output variables.

PROGRAM	INPUT	OUTPUT	COMMENTS
ILLISLAB	P.C.C. SLAB THICKNESS LENGTH (MESH DIMENSIONS) WIDTH (MESH DIMENSIONS) POISSON'S RATIO MODULUS OF ELASTICITY BASE COURSE INFORMATION BONDING CONDITION POISSON'S RATIO MODULUS OF ELASTICITY BASE THICKNESS SUBGRADE MODEL TYPE (WINKLER/SPRINGS, RESILIENT, ELASTIC SOLID, VLASOV) IF WINKLER/SPRINGS, INPUT: SUBGRADE MODULUS IF ELASTIC SOLID, INPUT: POISSON'S RATIO MODULUS OF ELASTICITY IF VLASOV, INPUT: VLASOV SHEAR PARAMETER LOAD TRANSFER AT JOINTS TYPE (AGG INT. OR DOWELS OR COMBO.) IF DOWELS SPECIFIED, INPUT: JOINT WIDTH MODULUS OF ELASTICITY OF DOWEL BARS DOWEL BAR INSIDE DIAMETER DOWEL BAR OUTSIDE DIAMETER DOWEL SPACING (TRANS. AND LONG.) DOWEL CONCRETE INTERACTION CALCULATED BY 3-DIMENSIONAL OR FRIBERG'S ANALYSIS IF FRIBERG'S USED, INPUT: MODULUS OF DOWEL SUPPORT IF AGG INT,WITH OR WITHOUT DOWEL, INPUT: AGGREGATE INTERLOCK FACTOR LOADING INFORMATION POSITION USING MESH COORDINATES TIRE PRESSURE CURLING STRESS ANALYSIS THERMAL GRADIENT WEIGHT OF SLAB	AT EACH NODE DEFLECTION X-ROTATION Y-ROTATION SUBGRADE STRESS X-STRESS Y-STRESS XY-STRESS MAJOR PRINCIPLE STRESS MINOR PRINCIPLE STRESS MAXIMUM VALUES OF: DEFLECTION SUBGRADE STRESS MAJ. PRINCIPLE STRESS AT BOTTOM OF LAYER MIN. PRINCIPLE STRESS AT BOTTOM OF LAYER X-STRESS AT BOTTOM OF EACH LAYER Y-STRESS AT BOTTOM OF EACH LAYER LOAD TRANSFER IN X & Y DIRECTION THERMAL CURLING STRESS	COMPUTER SYSTEM: MINICOMPUTER ** DATA INPUT METHOD: INPUT FILE BATCH FILE CAPABILITY: NO ** - A VERSION HAS RECENTLY BEEN CONVERTED FOR USE ON A MICROCOMPUTER.

Table 7. JSLAB input and output variables.

PROGRAM	INPUT	OUTPUT	COMMENTS
JSLAB	P.C.C. SLAB INFORMATION THICKNESS LENGTH (MESH DIMENSIONS) WIDTH (MESH DIMENSIONS) POISSON'S RATIO MODULUS OF ELASTICITY BASE COURSE INFORMATION BONDING CONDITION POISSON'S RATIO MODULUS OF ELASTICITY THICKNESS SUBGRADE MODULUS OF SUBGRADE REACTION LOAD TRANSFER AT JOINTS TYPE (AGG. INT. OR DOWELS OR COMBO) IF DOWELS SPECIFIED, INPUT: JOINT WIDTH MODULUS OF ELASTICITY OF DOWEL BARS DOWEL BAR INSIDE DIAMETER DOWEL BAR OUTSIDE DIAMETER DOWEL SPACING (TRANS. AND LONG.) DOWEL CONCRETE INTERACTION CALCULATED BY 3-DIMENSIONAL OR FRIBERG'S ANALYSIS IF FRIBERG'S USED, INPUT: MODULUS OF DOWEL SUPPORT IF AGG INT,WITH OR WITHOUT DOWEL, INPUT: AGGREGATE INTERLOCK FACTOR LOADING NUMBER OF LOADS POSITION OF LOADS USING MESH COORDINATES TIRE PRESSURE CURLING STRESS ANALYSIS THERMAL GRADIENT WEIGHT OF SLAB COEFFICIENT OF THERMAL EXPANSION WARPING STRESS ANALYSIS MOISTURE GRADIENT	AT EACH NODE DEFLECTION X-ROTATION Y-ROTATION X-STRESS Y-STRESS XY-STRESS MAJOR PRINCIPLE STRESS MINOR PRINCIPLE STRESS X-MOMENT Y-MOMENT THERMAL CURLING STRESS WARPING STRESS (MOISTURE)	COMPUTER SYSTEM: MINICOMPUTER DATA INPUT METHOD: INPUT FILE BATCH FILE CAPABILITY: NO SEVERAL PROBLEMS WERE ENCOUTERED IN TRYING TO EXECUTE THE FOLLOWING: THERMAL GRADIANT WITH LOAD MOISTURE GRADIANT SYMMETRY

Table 8. WESLIQID input and output variables.

PROGRAM	INPUT	OUTPUT	COMMENTS
WESLIQID	P.C.C. SLAB INFORMATION THICKNESS LENGTH (MESH DIMENSIONS) WIDTH (MESH DIMENSIONS) POISSON'S RATIO MODULUS OF ELASTICITY NUMBER OF NODES NOT IN CONTACT NUMBER OF GAPS BASE COURSE INFORMATION BONDING CONDITION POISSON'S RATIO MODULUS OF ELASTICITY BASE THICKNESS SUBGRADE INFORMATION MODULUS OF SUBGRADE REACTION LOAD TRANSFER AT JOINTS TYPE (AGG. INT. OR DOWELS) IF DOWELS SPECIFIED, INPUT: MODULUS OF ELASTICITY OF DOWEL BARS DOWEL BAR INSIDE DIAMETER DOWEL BAR OUTSIDE DIAMETER DOWEL SPACING (TRANS. AND LONG.) GAP BETWEEN DOWEL AND CONCRETE IF AGG. INT. USED, INPUT: AGGREGATE INTERLOCK FACTOR DOWEL CONCRETE INTERACTION CALCULATED BY 3-DIMENSIONAL OR FRIBERG'S ANALYSIS IF FRIBERG'S USED, INPUT: MODULUS OF DOWEL SUPPORT IF 3-DIM. USED, INPUT: DOWEL AND SLAB PARAMETERS JOINT DESIGN JOINT WIDTH SPRING SHEAR CONSTANT SPRING MOMENT CONSTANT LOADING POSITION USING MESH COORDINATES TIRE PRESSURE CURLING STRESS ANALYSIS THERMAL GRADIENT UNIT WEIGHT OF SLAB AND BASE	AT EACH NODE: SLAB DEFLECTION SUBGRADE DEFLECTION SUM OF REACTION FORCE & PRECOMPRESSION REACTIVE FORCE REACTIVE PRESSURE ROTATIONS MAJOR AND MINOR PRINCIPLE STRESS SHEAR STRESS X, Y, XY STRESSES AT EACH JOINT: SHEAR AND MOMENT SHEAR IN DOWEL BAR CONCRETE BEARING STRESS DOWEL SHEAR STRESS	COMPUTER SYSTEM: MINICOMPUTER DATA INPUT METHOD: INPUT FILE BATCH FILE CAPABILITY: NO THE MEMORY REQUIREMENTS OF THE PROGRAM ARE VERY LARGE. THE FINITE ELEMENT MESH IS RESTRICTED TO PROGRAM STORAGE CAPACITY.

Table 9. WESLAYER input and output variables.

PROGRAM	INPUT	OUTPUT	COMMENTS
WESLAYER	P.C.C. SLAB INFORMATION THICKNESS LENGTH (MESH DIMENSIONS) WIDTH (MESH DIMENSIONS) POISSON'S RATIO MODULUS OF ELASTICITY NUMBER OF NODES NOT IN CONTACT NUMBER OF GAPS BASE COURSE INFORMATION BONDING CONDITION POISSON'S RATIO MODULUS OF ELASTICITY BASE THICKNESS SUBGRADE INFORMATION YOUNG'S MODULUS POISSON'S RATIO LOAD TRANSFER AT JOINTS TYPE (AGG. INT. OR DOWELS) IF DOWELS SPECIFIED, INPUT: MODULUS OF ELASTICITY OF DOWEL BARS DOWEL BAR INSIDE DIAMETER DOWEL BAR OUTSIDE DIAMETER DOWEL SPACING (TRANS. AND LONG.) GAP BETWEEN DOWEL AND CONCRETE IF AGG. INT. USED, INPUT: AGGREGATE INTERLOCK FACTOR DOWEL CONCRETE INTERACTION CALCULATED BY 3-DIMENSIONAL OR FRIBERG'S ANALYSIS IF FRIBERG'S USED, INPUT: MODULUS OF DOWEL SUPPORT IF 3-DIM. USED, INPUT: DOWEL AND SLAB PARAMETERS JOINT DESIGN JOINT WIDTH SPRING SHEAR CONSTANT SPRING MOMENT CONSTANT LOADING POSITION USING MESH COORDINATES TIRE PRESSURE CURLING STRESS ANALYSIS THERMAL GRADIENT UNIT WEIGHT OF SLAB AND BASE	AT EACH NODE: SLAB DEFLECTION SUBGRADE DEFLECTION SUM OF REACTION FORCE & PRECOMPRESSION REACTIVE FORCE REACTIVE PRESSURE ROTATIONS MAJOR AND MINOR PRINCIPLE STRESS SHEAR STRESS X, Y, XY STRESSES AT EACH JOINT: SHEAR AND MOMENT SHEAR IN DOWEL BAR CONCRETE BEARING STRESS DOWEL SHEAR STRESS	COMPUTER SYSTEM: MINICOMPUTER DATA INPUT METHOD: INPUT FILE BATCH FILE CAPABILITY: NO THE MEMORY REQUIREMENTS OF THE PROGRAM ARE VERY LARGE. THE FINITE ELEMENT MESH IS RESTRICTED TO PROGRAM STORAGE CAPACITY.

Table 10. RISC input and output variables.

PROGRAM	INPUT	OUTPUT	COMMENTS
RISC	P.C.C. SLAB NUMBER OF SLABS THICKNESS LENGTH WIDTH POISSON'S RATIO MODULUS OF ELASTICITY TEMPERATURE LOAD INDICATOR MECHANICAL LOAD INDICATOR 28 DAY FLEXURAL STRENGTH BASE/SUBBASE/SUBGRADE INFORMATION NUMBER OF SUPPORT LAYERS POISSON'S RATIO OF EACH LAYER MODULUS OF ELASTICITY OF EACH LAYER THICKNESS OF EACH LAYER (EXCEPT SUB.) VOIDS PRESENT AT EDGE OR CORNER DRAINABILITY (POOR OR GOOD) SHOULDERS THICKNESS WIDTH LOAD TRANSFER AT JOINTS TRANSVERSE JOINTS (PLAIN OR DOWELED) IF DOWELED, INPUT: NUMBER OF DOWELS/TRANSVERSE JOINT BAR DIAMETER BAR LOOSENESS LONGITUDINAL JOINT (PLAIN OR TIED) IF TIED, INPUT: NUMBER OF BARS PER LINEAR FOOT BAR DIAMETER TRAFFIC INFORMATION DAILY DESIGN TRAFFIC NUMBER LOAD MAGNITUDE LOAD POSITION (EDGE, CORNER, MIDSLAB) CURLING STRESS ANALYSIS TEMPERATURE GRADIENT UNIT WEIGHT OF SLAB	MAXIMUM SLAB DEFLECTION MAXIMUM MAJOR PRINCIPLE STRESS MAXIMUM MINOR PRINCIPLE STRESS MAXIMUM SUBBASE REACTION FATIGUE LIFE PREDICTED FAULTING DURING LIFE	COMPUTER SYSTEM: MINICOMPUTER DATA INPUT METHOD: INPUT FILE BATCH FILE CAPABILITY: NO THE PROGRAM REQUIRES EXCEPTIONALLY LONG RUN-TIMES. FOR A TWO SLAB SYSTEM, 45 MINUTES OF CPU TIME RESULTING IN 120 MINUTES CONNECT TIME ON THE HARRIS COMPUTER AT THE UNIVERSITY OF ILLINOIS.

Table 11. PMARP input and output variables.

PROGRAM	INPUT	OUTPUT	COMMENTS
PMARP	MESH INFORMATION NUMBER OF SLABS NUMBER OF NODES PER SLAB NODAL COORDINATES P.C.C. SLAB INFORMATION THICKNESS TENSILE STRENGTH POISSON'S RATIO MODULUS OF ELASTICITY REINFORCEMENT INFORMATION REINFORCEMENT RATIO DIAMETER OF REINFORCING BARS SUBGRADE INFORMATION MODULUS OF ELASTICITY PRESENCE OF VOIDS AT EDGE OR CORNER DRAINABILITY (POOR OR GOOD) LOAD TRANSFER AT JOINTS TYPE OF LOAD TRANSFER AGGREGATE INTERLOCK ONLY DOWELS ONLY COMBINATION OF ABOVE KEYED ONLY FOR TRANSVERSE AND LONG. JOINTS IF DOWELS: INSIDE DOWEL DIAMETER OUTSIDE DOWEL DIAMETER DOWEL MODULUS OF ELASTICITY DOWEL SPACING DOWEL LENGTH DOWEL POISSON'S RATIO IF AGG. INT. OR KEYED: AGGREGATE INTERLOCK FACTOR JOINT WIDTH CONCRETE FATIGUE INFORMATION RESILIENT MODULUS VS. PLATE DEFLECTION CURVE PUMPING ADJUSTMENT FACTORS FACTOR DUE TO RAINFALL FACTOR DUE TO TYPE OF SUBBASE TREATMENT FACTOR DUE TO TYPE OF DRAINAGE ASSUMED AVERAGE VOID DEPTH	PUMPING INDEX FATIGUE DAMAGE AT EACH NODE: DEFLECTION X ROTATION Y ROTATION SUBGRADE STRESS MAJOR PRINCIPLE STRESS MINOR PRINCIPLE STRESS TRANSFERRED LOAD AT PROPER NODES	COMPUTER SYSTEM: MICROCOMPUTER DATA INPUT METHOD: INTERACTIVE BATCH FILE CAPABILITY: NO

Table 12. H-51 input and output variables.

PROGRAM	INPUT	OUTPUT	COMMENTS
H-51	P.C.C. SLAB INFORMATION SLAB THICKNESS SLAB YOUNG'S MODULUS SLAB POISSON'S RATIO SUBGRADE INFORMATION MODULUS OF SUBGRADE REACTION MAY USE ELASTIC SOLID MODEL. IF SO, SPECIFY: ELASTIC MODULUS POISSON'S RATIO LOADING INFORMATION TOTAL LOAD PER WHEEL TIRE CONTACT AREA WHEEL POSITION W.R.T. SLAB EDGE WHEEL POSITION W.R.T. POINT OF STRESS CALCULATION	STRESS AT BOTTOM OF SLAB AT SPECIFIED LOCATION BLOCK COUNT	COMPUTER SYSTEM: MAINFRAME DATA INPUT METHOD: INPUT FILE BATCH FILE CAPABILITY: YES

Table 13. CMS input and output variables.

PROGRAM	INPUT	OUTPUT	COMMENTS
CMS	SURFACE/ STABILIZED LAYER INFORMATION FREEZING/FROZEN/UNFROZEN THERMAL CONDUCT. FREEZING/FROZEN/UNFROZEN HEAT CAPACITIES FREEZING/FROZEN/UNFROZEN UNIT WEIGHT STIFFNESS GRAVIMETRIC WATER CONTENT RING AND BALL VALUE POISSON'S RATIO TEMPERATURE-STIFFNESS RELATIONSHIP PENETRATION VALUE SHORT-WAVE ABSORPTIVITY AIR CONTENT COARSE AGGRAGATE CONTENT NUMBER OF LAYERS MATERIAL CODE BASE COURSE/SUBBASE LAYER INFORMATION UNFROZEN RESILIENT MODULUS UNFROZEN POISSON'S RATIO FROZEN POISSON'S RATIO FROZEN RESILIENT MODULUS LENGTH OF RECOVERY PERIOD DRY DENSITY PERCENT PASSING NUMBER 200 SIEVE MATERIAL CODE SUBGRADE LAYER INFORMATION SPECIFIC SURFACE AREA CLAY LATTICE EXPANSION CONSTANT INITIAL SOIL TEMPERATURE PROFILE DRY HEAT CAPACITY SATURATED WATER CONTENT ACTIVITY RATIO SOIL FREEZING TEMPERATURE PLASTIC LIMIT LIQUID LIMIT UNFROZEN RESILIENT MODULUS UNFROZEN POISSON'S RATIO FROZEN POISSON'S RATIO FROZEN RESILIENT MODULUS LENGTH OF RECOVERY PERIOD DRY DENSITY PERCENT PASSING NUMBER 200 SIEVE MATERIAL CODE CLIMATIC INFORMATION EMISSIVITY FACTOR (SURFACE) DAILY EXTRATERRESTRIAL RADIATION GEIGER LONG-WAVE BACK RADIATION FACTOR AVERAGE DAILY WIND VELOCITY MAXIMUM GUST WIND VELOCITY CLOUD BASE FACTOR GROUND SURFACE VAPOR PRESSURE AIR TEMP OF FIRST OF DAY ANALYSIS AIR TEMP OF LAST OF DAY ANALYSIS TIME OF MAXIMUM AIR TEMPERATURE TIME OF MINIMUM AIR TEMPERATURE UPPER TEMP LIMIT OF FREEZING RANGE LOWER TEMP IN FREEZING RANGE CONSTANT DEEP GROUND TEMPERATURE MAXIMUM AND MINIMUM DAILY AIR TEMPERAURES AVERAGE DAILY SUNSHINE EACH DAY TIME SUN SET EACH DAY OF ANALYSIS PERIOD TIME SUN RISE EACH DAY OF ANALYSIS PERIOD INVENTORY/LOCATION INFORMATION NODAL THICKNESS NUMBER OF TERMINAL NODES # DAYS IN ANALYSIS PERIOD LOCATION OF ANALYSIS # TIMES A DAY THAT TEMP. PROFILE RECORD MAXIMUM ALLOWABLE CONVECTION COEFFICIENT TIME INCREMENT FOR TEMP CALCULATION ANALYSIS DATE DEPTH TO WATER TABLE FROM SURFACE THICKNESS INFORMATION TOTAL NUMBER OF LAYERS TOTAL PAVEMENT THICKNESS THICKNESS OF EACH LAYER	TEMPERATURE PROFILE AT TIME/DEPTH INTERVALS FROST LINES AT SPECIFIED INTERVALS MOISTURE PROFILE AT SPECIFIED INTERVALS BASE AND SUBBASE STRENGTH PARAMETERS SUBGRADE STRENGTH PARAMETERS	COMPUTER SYSTEM: MICROCOMPUTER DATA INPUT METHOD: INPUT FILE BATCH FILE CAPABILITY: NO THE CMS PROGRAM WAS WRITTEN FOR ANALYSIS OF ASPHALT CONCRETE. THE PROGRAM MUST BE "TRICKED" INTO ANALYZING CONCRETE BY GIVING IT THE APPROPRIATE INPUT VALUES.

Table 14. Liu-Lytton drainage models input and output variables.

PROGRAM	INPUT	OUTPUT	COMMENTS
LUI-LYTTON DRAINAGE MODELS	DRAINAGE MODEL	DRAINAGE MODEL	COMPUTER SYSTEM: MICROCOMPUTER DATA INPUT METHOD: INTERACTIVE BATCH FILE CAPABILITY: NO
	CHARACTERISTICS OF BASE & SUBGRADE WIDTH OF BASE DEPTH OF BASE BASE SLOPE RATIO BASE PERMEABILITY SUBGRADE PERMEABILITY BASE POROSITY SUBGRADE POROSITY	HEAD ON X COORDINATE HEIGHT WATER LEVEL-SUBDRAIN ONLY AVERAGE HEIGHT OF WATER LEVEL TIME (STAGE 1) DRAINAGE DEGREE	
	MATERIAL PROPERTIES BASE & SUBGRADE BASE COURSE INDEX PAVEMENT TYPE SOIL CLASSIFICATION SUBGRADE SOIL HORIZON	HEAD ON Y COORDINATE HEIGHT WATER LEVEL-SUBDRAIN ONLY AVERAGE HEIGHT OF WATER LEVEL TIME (STAGE 2) DRAINAGE DEGREE	
	CRACK AND JOINT SURVEY INFORMATION LENGTH OF JOINTS AND CRACKS LENGTH OF SURVEY	PERCENT DRAINAGE VS. TIME	
	INTENSITY-DURATION-RECURRENCE EVALUATED PERIOD K CONSTANT POWER OF RECURRENCE INTERVAL POWER OF RAINFALL DURATION RAINFALL CURVE SHAPE FACTOR	% WATER DRAINED DUE TO GRAVEL % GRAVEL IN SAMPLE % WATER DRAINDED DUE TO SAND % SAND IN SAMPLE % WATER THAT WILL BE DRAINED	
	RAINFALL QUANTITY & FREQUENCY DATA NUMBER OF EVALUATION PERIODS AMOUNT OF RAINFALL PER DAY NUMBER OF CONSECUTIVE WET DAYS NUMBER OF CONSECUTIVE DRY DAYS	CRITICAL DRAINAGE DEGREE (85% SAT.) DRAINING TIME FOR 85% SAT.	
		ACCEPTABILITY OF DRAINAGE DESIGN	
		PARAMETERS OF GAMMA DISTRBUTION PARAMETERS OF MARKOV CHAIN MODEL TRANSITION PROBABILITY MATRIX	
		TIME-% DRAINAGE-PROB(CON. DRY DAYS)	
		WATER CARRYING CAPACITY OF BASE AVERAGE DEGREE OF DRAINAGE OVERALL PROB(SATURATED BASE)	
		PROB(DRY BASE) PROB(WET BASE)	
		PROB DISTRIBUTION OF BASE COURSE	
		AVERAGE FREE WATER IN BASE DURATION OF AVERAGE RAINFALL AVERAGE RAINFALL AMOUNT AVERAGE BASE COURSE MODULUS (WET) AVERAGE BASE COURSE MODULUS AVERAGE SUBGRADE MODULUS	
	INFILTRATION MODEL	INFILTRATION MODEL	
	BASE COURSE CRACKS/JOINTS WIDTH OF JOINT/CRACK DEPTH OF JOINT/CRACK HORIZONTAL PERMEABILITY POROSITY CAPILLARY HEAD	WATER DISTRIBUTION OF BASE COURSE TIME-HORIZ/VERT DIST-CRK WATER DEPTH	
		DEPTH OF WATER PENETRATION	
		TIME-SOIL DEPTH-SUCTION DISTRIBUTION	
	WATER EVAPORATION CHARACTERISTICS SUCTION OF ATMOSPHERE INITIAL SUCTION OF BASE COURSE DIFFUSION COEFFICIENT SLOPE OF WATER CONTENT-SUCTION EVAPORATION COEFFICIENT	EVAPORATION TIME - AMOUNT EVAPORATED	

Table 15. PREDICT input and output variables.

PROGRAM	INPUT	OUTPUT	COMMENTS
PREDICT	TYPE OF PAVEMENT (PLAIN OR REINFORCED) SLAB AND SHOULDER DESIGN SLAB THICKNESS TRANSVERSE JOINT SPACING DIAMETER OF DOWEL BAR MODULUS OF RUPTURE IF PLAIN: UNITUBE INSERT USED TIED CONCRETE SHOULDERS IF REINFORCED: AREA OF REINFORCEMENT FOUNDATION AND DRAINAGE INPUTS TYPE OF BASE COURSE SUBGRADE SOIL TYPE MODULUS OF SUBGRADE REACTION IF REINFORCED: LONGITUDINAL SUBDRAINS AGE AND TRAFFIC LOADING INPUTS IS ESAL/YEAR CONSTANT OVER AGE (Y/N) IF NO: SPECIFY AGE/ESAL COMBINATIONS POTENTIAL PAVEMENT CONDITION INPUTS "D" CRACKING AGGREGATE IN SLAB INCOMPRESSIBLES IN TRANSVERSE JOINTS IF REINFORCED: REACTIVE AGGREGATE IN SLAB CLIMATIC INPUTS MEAN ANNUAL PRECIPITATION CORPS OF ENGINEERS FREEZING INDEX MEAN ANNUAL TEMPERATURE TEMPERATURE RANGE	PAVEMENT DISTRESSES PUMPING FAULTING CRACKING JOINT DETERIORATION PSR	COMPUTER SYSTEM: MICROCOMPUTER DATA INPUT METHOD: INTERACTIVE BATCH FILE CAPABILITY: NO

Table 16. PEARDARP input and output variables.

PROGRAM	INPUT	OUTPUT	COMMENTS
PEARDARP	P.C.C SLAB INFORMATION THICKNESS LENGTH ELASTIC MODULUS MODULUS OF RUPTURE SUBGRADE INFORMATION SUBGRADE TYPE MODULUS OF SUBGRADE REACTION THICKNESS EFFICIENCY OF DRAINAGE DISTRESS INFORMATION CRITICAL FAULT 1 CRITICAL FAULT 2 STANDARD DEV. OF FAULTING AVERAGE VOID VOLUME SUBDRAINAGE EXCELLENT/GOOD/FAIR/POOR SUBBASE TYPE STABILIZED/UNSTABILIZED SEALANT TYPE LIQUID ASPHALT/LOW MODULUS CLIMATIC REGION DRY-WARM OR COLD/WET-WARM OR COLD LOAD TRANSFER DEVICE UNDOWELED/DOWELED REINFORCEMENT UNREINFORCED/REINFORCED TRAFFIC INFORMATION ANNUAL AVERAGE DAILY TRAFFIC TRUCK FACTOR PROPORTION IN DESIGN LANE TRAFFIC GROWTH RATE PASSENGER CAR EQUIVALENT MAXIMUM SERVICE FLOW NUMBER OF TRAFFIC LANES WIDTH FACTOR DESIGN SPEED SPEED LIMIT SPEED FACTOR TRAFFIC VOLUME DISTRIBUTION TRAFFIC AND ACCIDENT COST INFORMATION PROPORTION OF PASS. CARS PROPORTION OF P.U. TRUCKS PROPORTION OF S-U TRUCKS PROPORTION OF COMBINATION TRUCKS PROPORTION OF DIESEL TRUCKS SECTION LENGTH COST PER ACCIDENT ACCIDENT RATE USER COSTS (FOR EACH OF THE ABOVE GROUPS) GASOLINE OIL TIRES TIME COST ANALYSIS INFORMATION ANALYSIS PERIOD LAST YEAR FOR ANALYSIS INITIAL CONSTRUCTION COST MAINTENANCE AND REHABILITATION ACTIVITIES	PAVEMENT DISTRESSES SPALLS PUMPING (VOL. AND JOINTS) CRACKING (AREA AND LENGTH) CONDITION OF SEAL.S PATCHING ROUGHNESS PSI VEHICLE CONSUMPTION RATES OIL TIRES ROAD USERS COSTS VEHICLE TIME CONSTRUCTION AND MAINTENANCE COSTS ANNUAL COSTS PRESENT VALUE	COMPUTER SYSTEM: MICROCOMPUTER DATA INPUT METHOD: INTERACTIVE BATCH FILE CAPABILITY: NO

Table 17. JCP-1 input and output variables.

PROGRAM	INPUT	OUTPUT	COMMENTS
JCP1 (ZERO MAINTENANCE DESIGN)	DESIGN CRITERIA DESIGN LIFE CONSTRUCTION SERVICEABILITY INDEX TERMINAL SERVICEABILITY INDEX TIME SLABS OPEN TO TRAFFIC MONTH PAVEMENT WILL BE OPENED P.C.C SLAB INFORMATION THICKNESS LENGTH MEAN MODULUS OF RUPTURE (MR) COEFFICIENT OF VARIATION FOR MR COEFFICIENT OF THERMAL EXPANSION MODULUS OF ELASTICITY MONTHLY THERMAL GRADIENTS (DAY/NIGHT) TRAFFIC INFORMATION ADT AT BEGINNING OF DESIGN PERIOD ADT AT END OF DESIGN PERIOD PERCENT TRUCKS OF ADT PERCENT OF TRUCKS IN DESIGN LANE PERCENT DIRECTIONAL DISTRIBUTION MEAN AXLES PER TRUCK PERCENT TRUCKS DURING DAYLIGHT MEAN DISTANCE SLAB EDGE TO DUAL SINGLE AXLE LOAD DISTRIBUTION TANDEM AXLE LOAD DISTRIBUTION MONTHLY TRUCK PERCENTAGE SUBGRADE INFORMATION MONTHLY MODULUS OF SUBGRADE REACTION ERODABILITY OF FOUNDATION SUPPORT AT BEGINNING OF DESIGN PERIOD AT END OF DESIGN PERIOD CLIMATIC REGIONAL FACTOR	FATIGUE INFORMATION FATIGUE DAMAGE AT SLAB EDGE FATIGUE DAMAGE FOR DAY LOADING FATIGUE DAMAGE FOR NIGHT LOADING SERVICEABILITY INDEX AT SPECIFIED YEAR NUMBER OF 18-KIP ESAL AT SPECIFIED YEAR	COMPUTER SYSTEM: MICROCOMPUTER DATA INPUT METHOD: INTERACTIVE BATCH FILE CAPABILITY: YES

Table 18. DNPS86 input and output variables.

PROGRAM	INPUT	OUTPUT	COMMENTS
DNPS86 (AASHTO)	GENERAL DESIGN INPUT ANALYSIS PERIOD DISCOUNT RATE NUMBER OF TRAFFIC LANES (ONE DIR) LANE WIDTH COMBINED WIDTH OF SHOULDERS (ONE DIR) ROADBED SOIL SEASONAL RESILIENT MODULUS IF SWELLING SOIL: POTENTIAL VERTICAL RISE SWELLING PROBABILITY SWELL RATE CONSTANT IF FROST HEAVE: MAXIMUM POTENTIAL SERVICEABILITY LOSS FROST HEAVE PROBABILITY FROST HEAVE RATE DESIRED LEVEL OF RELIABILITY PERFORMANCE PERIOD FOR INITIAL PAVEMENT SERVICEABILITY INFORMATION TERMINAL SERVICEABILITY SERVICEABILITY AFTER CONSTRUCTION TRAFFIC GROWTH RATE TYPE OF GROWTH INIT YEARLY 18-KIP ESAL (BOTH DIR) DIRECTIONAL DISTRIBUTION FACTOR LANE DISTRIBUTION FACTOR SUBBASE SUBBASE TYPE THICKNESS ELASTIC MODULUS UNIT COST SALVAGE VALUE PORTLAND CEMENT CONCRETE SLAB CONSTRUCTION TYPE PCC ELASTIC MODULUS AVERAGE PCC MODULUS OF RUPTURE UNIT COST OF PCC SALVAGE VALUE STRUCTURAL CHARACTERISTICS LOAD TRANSFER COEFFICIENT DRAINAGE COEFFICIENT LOSS OF SUPPORT FACTOR OTHER CONSTRUCTION RELATED COSTS SHOULDERS DRAINAGE MOBILIZATION AND OTHER FIXED COSTS MAINTENANCE COST YEAR COSTS BEGIN TO ACCRUE YEARLY INCREASE	RIGID PAVEMENT STRUCTURAL DESIGN EFFECTIVE MODULUS OF SUBGRADE REACTION REQUIRED SLAB THICKNESS ALLOWABLE 18-KIP ESAL REPETITIONS LIFE-CYCLE COSTS INIT CONSTRUCTION MAINTENANCE SALVAGE VALUE FIRST OVERLAY CONSTRUCTION FIRST OVERLAY MAINTENANCE FIRST OVERLAY SALVAGE VALUE SECOND OVERLAY CONSTRUCTION SECOND OVERLAY MAINTENANCE SECOND OVERLAY SALVAGE VALUE TOTAL NET PRESENT VALUE	COMPUTER SYSTEM: MICROCOMPUTER DATA INPUT METHOD: INTERACTIVE BATCH FILE CAPABILITY: NO CAN BE USED FOR THE DESIGN OF FLEXIBLE OR RIGID PAVEMENT SYSTEMS.

Table 19. RPS-3 input and output variables.

PROGRAM	INPUT	OUTPUT	COMMENTS
RPS-3	TRAFFIC INFORMATION AXLE GROWTH FACTOR ADT GROWTH RATE DIRECTIONAL DISTRIBUTION FACTOR DESIGN LANE DISTRIBUTION FACTOR INITIAL ADT TOTAL 18-KIP ESAL FOR ANALYSIS PERIOD RESTRAINTS MAXIMUM INTIAL FUNDS/SQ YD MAX INITIAL THICKNESS MIN TIME TO FIRST OVERLAYS MIN TIME BETWEEN OVERLAYS MAX TOTAL AC OVERLAY THICKNESS MIN AC OL THICK @ ONE TIME MAX TOTAL CONC OL THICK MIN TOTAL CONC OL THICK AVERAGE LEVEL UP THICKNESS LENGTH OF ANALYSIS PERIOD CONFIDENCE LEVEL PERFORMANCE VARIABLES INITIAL SERVICABILITY TERMINAL SERVICABILITY SERVICABILITY AFTER OVERLAY PROBABILITY OF BAD SOIL SWELLING RATE CONSTANT SWELLING ACTIVITY TRAFFIC DELAY COST DIST OF SLOW TRAFFIC (OV/NON) @ OF OPEN LANES RESTRICT ZONE % STOPPED BY ROAD EQUIPMENT AVG DELAY BY ROAD EQUIPMENT AVG SPEED THROUGH OL ZONE AVG APPROACH SPEED TO OL ZONE DETOUR DISTANCE @ HOURS/DAY OL CONSTRUCT TRAFFIC MODEL ROAD LOCATION CONCRETE INFORMATION AGE OF TESTING MEASURING POINT FLEXTURAL STRENGTH TENSILE STRENGTH ELASTIC MODULUS UNIT WEIGHT CONSTRUCTION EQUIPMENT COST COST/CU YD OF CONCRETE COST OF SURFACING CONCRETE SALVAGE VALUE OF CONCRETE STEEL INFORMATION BARS (LONGITUDINAL/TRANSVERSE) BAR STEEL ASTM DESIG TENSILE STRENGTH COST/LB BAR NUMBERS TO BE TRIED WIRE MESHES WIRE MESH ASTM DESIG TENSILE STRENGTH COST/LB MESH SIZES TO BE TRIED LONG. WIRE SPACING TRAN. WIRE SPACING TIE BARS USED WITH MESH TIE BAR ASTM DESIG TENSILE STRENGTH COST/LB TIE BAR NUMBERS TO BE TRIED SUBBASE INFORMATION TYPE ERODABILITY FACTOR FRICTION FACTOR ELASTIC MODULUS CONSTRUCTION EQUIPEMENT COST COST/COMPACTED CU YD SALVAGE VALUE MIN ALLOWED THICKNESS MAX ALLOWED THICKNESS	DESIGN REQUIREMENTS SLAB THICKNESS SUBBASE THICKNESS TOTAL PERFORMANCE LIFE SPACING TRANVERSE JOINTS SPACING LONGITUDINAL JOINTS COST ANALYSIS	COMPUTER SYSTEM: MICROCOMPUTER DATA INPUT METHOD: INPUT FILE BATCH FILE CAPABILITY: YES

Table 19. RPS-3 input and output variables (continued).

PROGRAM	INPUT	OUTPUT	COMMENTS
	INCREMENT FOR SUBBASE		
	SUBGRADE INFORMATION		
	MODULUS OF SUBGRADE REACTION		
	SUBGRADE FRICTION FACTOR		
	ERODABILITY FACTOR		
	COST/LANE MILE PREPARATION		
	OVERLAY INFORMATION		
	INITIAL COST/LANE MILE		
	COST/CU YD COMPACTED ASPHALT		
	SALVAGE VALUE		
	ASPHALT MODULUS		
	PRODUCTION RATE OF ASPHALT		
	PRODUCTION RATE OF CONCRETE		
	CONCRETE COEFFICIENT		
	ADDTIONAL COSTS		
	JOINT DESIGN		
	COST/FT TRANSVERSE JOINT		
	COST/FT LONGITUDINAL JOINT		
	RANGE OF SPACING TRANSVERSE		
	LOWER VALUE		
	UPPER VALUE		
	INCREMENT OF SPACING		
	MAINTENANCE		
	FREEZING TEMPERATURE/YEAR		
	COMPOSITE LABOR WAGE		
	COMPOSITE EQUIPMENT RENTAL RATE		
	COST OF MATERIALS		
	WIDTH OF EACH LANE		
	# LANES IN BOTH DIRECTIONS		
	RATE OF INTEREST		
	CONFIDENCE LEVEL VARIABLES		
	% CV OF FLEXTURAL STRENGTH		
	SD OF CONCRETE MODULUS		
	SD OF SUBGRADE K VALUE		
	SD OF INITIAL SERVICABILITY		
	SD OF TERMINAL SERVICABILITY		
	SD OF THICKNESS OF CONCRETE		
	OVERLAY CONSTRUCTION VARIABLES		
	TIME WHEN OL CONSTRUCT BEGINS		
	TIME WHEN OL CONSTRUCT ENDS		
	NUMBER OF CONCRETE CURE DAYS		
	TOTAL # OF LANE TO OVERLAY		
	OL LENGTH IN ONE LANE		

Table 20. PCA and California Rigid Pavement Design Procedure input and output variables.

PROGRAM	INPUT	OUTPUT	COMMENTS
PCA	TRAFFIC INFORMATION SINGLE AXLE LOAD DISTRIBUTION TANDUM AXLE LOAD DISTRIBUTION AVERAGE DAILY TRAFFIC LOAD SAFETY FACTOR DESIGN PERIOD MATERIAL PROPERTIES MODULUS OF SUBGRADE REACTION CONCRETE MODULUS OF RUPTURE LOAD TRANSFER INFORMATION TRANSVERSE JOINT LT TYPE TYPE OF SHOULDER	PAVEMENT THICKNESS FOR EACH AXLE LOAD DISTRIBUTION: EXPECTED ESAL STRESS RATIO ALLOWABLE REPETITIONS FATIGUE DEFLECTION EROSION TOTAL FATIGUE DAMAGE USED	COMPUTER SYSTEM: MICROCOMPUTER DATA INPUT METHOD: INTERACTIVE BATCH FILE CAPABILITY: YES LOADING AN EXISTING DATA FILE INTO THE PROGRAM FOR MODIFICATION CAUSES THE COMPUTER TO LOCK-UP.

PROGRAM	INPUT	OUTPUT	COMMENTS
CALIFORNIA RIGID PAVEMENT DESIGN	TRAFFIC INFORMATION TOTAL CUMULATIVE 18K ESAL TRAFFIC INDEX SUBGRADE INFORMATION R-VALUE PLASTICITY INDEX PERMEABILITY	PAVEMENT CROSS-SECTION	THE METHOD IS NOT COMPUTERIZED.

Table 21. JCS-1 and BERM input and output variables.

PROGRAM	INPUT	OUTPUT	COMMENTS
JCS1	SHOULDER DESIGN LIFE P.C.C. SLAB INFORMATION SHOULDER THICKNESS TRAFFIC LANE THICKNESS SHOULDER WIDTH MEAN PCC MODULUS OF RUPTURE (28 DAYS) COEFFICIENT OF VARIATION OF PCC MODULUS LANE/SHOULDER JOINT LOAD TRANSFER EFF. SUBGRADE INFORMATION MODULUS OF SUBGRADE REACTION ERODABILITY OF FOUNDATION SUPPORT AT BEGINNING OF DESIGN PERIOD ERODABILITY OF FOUNDATION SUPPORT AT END OF DESIGN PERIOD TRAFFIC ADT AT BEGINNING OF DESIGN PERIOD ADT AT END OF DESIGN PERIOD PERCENT TRUCKS OF ADT PERCENT TRUCKS IN DESIGN TRAVELED LANE PERCENT DIRECTIONAL DISTRIBUTION MEAN AXLES PER TRUCK LENGTH OF SURVEYED STRETCH AVERAGE LENGTH OF ENCROACHMENTS PERCENT TRUCKS PARKING ON SHOULDER SINGLE AXLE LOAD DISTRIBUTION TANDEM AXLE LOAD DISTRIBUTION	ACCUMULATED FATIGUE DAMAGE PER YEAR FATIGUE DAMAGE DUE TO PARKED TRAFFIC FATIGUE DAMAGE DUE TO ENCROACHING TRAFFIC	COMPUTER SYSTEM: MAINFRAME DATA INPUT METHOD: INPUT FILE BATCH FILE CAPABILITY: YES

PROGRAM	INPUT	OUTPUT	COMMENTS
BERM	SHOULDER TYPE RIGID/FLEXIBLE SEPARATE/MONOLITHIC DESIGN TEMPERATURE CONCRETE SHOULDER INFORMATION THICKNESS MODULUS FLEXURAL STRENGTH ASPHALT SHOULDER INFORMATION STATIC AND DYNAMIC MODULI COEFF. OR USE DEFAULT VALUES THICKNESS LOWER LAYER INFORMATION BASE MODULUS BASE THICKNESS SUBGRADE MODULUS	DESIGN LIFE - TOTAL 18K ESAL FOR RIGID SHOULDER: INNER EDGE OUTER EDGE FOR FLEXIBLE SHOULDER: ENCROACHING TRAFFIC PARKED TRAFFIC ASPHALT CONCRETE PROPERTIES DYNAMIC MODULUS CREEP MODULUS	COMPUTER SYSTEM: MICROCOMPUTER DATA INPUT METHOD: INTERACTIVE BATCH FILE CAPABILITY: YES

Table 22. Method of obtaining input variables for ILLISLAB.

PROGRAM	INPUT	METHOD OF OBTAINING DATA	PROBLEMS
ILLISLAB	P.C.C. SLAB		
	THICKNESS	CORES	
	LENGTH (MESH DIMENSIONS)	FIELD SURVEYS	
	WIDTH (MESH DIMENSIONS)	FIELD SURVEYS	
	POISSON'S RATIO	ASSUME	
	MODULUS OF ELASTICITY	BACKCALCULATE (DEFLECTION)	
	BASE COURSE INFORMATION		
	BONDING CONDITION	ASSUME	DIFFICULT TO OBTAIN IN FIELD
	POISSON'S RATIO	ASSUME	
	MODULUS OF ELASTICITY	BACKCALCULATE (DEFLECTION)	
	BASE THICKNESS	CORES	
	SUBGRADE		
	MODEL TYPE (WINKLER/SPRINGS, RESILIENT, ELASTIC SOLID, VLASOV)	FUNCTION OF ANALYSIS	
	IF WINKLER/SPRINGS, INPUT: SUBGRADE MODULUS	BACKCALCULATE (DEFLECTION)	
	IF ELASTIC SOLID, INPUT: POISSON'S RATIO	ASSUME	
	MODULUS OF ELASTICITY	BACKCALCULATE (DEFLECTION)	
	IF VLASOV, INPUT: VLASOV SHEAR PARAMETER	ASSUME VALUE BASED RECOMMENDATIONS	
	LOAD TRANSFER AT JOINTS		
	TYPE (AGG INT. OR DOWELS OR COMBO.)	FIELD SURVEYS/CONSTRUCTION RECORDS	
	IF DOWELS SPECIFIED, INPUT: JOINT WIDTH	FIELD SURVEYS	
	MODULUS OF ELASTICITY OF DOWEL BARS	ASSUME	
	DOWEL BAR INSIDE DIAMETER	CONSTRUCTION RECORDS	
	DOWEL BAR OUTSIDE DIAMETER	CONSTRUCTION RECORDS	
	DOWEL SPACING (TRANS. AND LONG.)	CONSTRUCTION RECORDS	
	DOWEL CONCRETE INTERACTION CALCULATED BY 3-DIMENSIONAL OR FRIBERG'S ANALYSIS	CALCULATE	
	IF FRIBERG'S USED, INPUT: MODULUS OF DOWEL SUPPORT		
	IF AGG INT,WITH OR WITHOUT DOWEL, INPUT: AGGREGATE INTERLOCK FACTOR	ASSUME	
	LOADING INFORMATION		
	POSITION USING MESH COORDINATES	FUNCTION OF ANALYSIS	
	TIRE PRESSURE	WIM	
	CURLING STRESS ANALYSIS		
	THERMAL GRADIENT	CALCULATE USING CMS	
	WEIGHT OF SLAB	CALCULATE	

Table 23. Methods of obtaining input variables for JSLAB.

PROGRAM	INPUT	METHOD OF OBTAINING DATA	PROBLEMS
JSLAB	P.C.C. SLAB INFORMATION		
	THICKNESS	CORES	
	LENGTH (MESH DIMENSIONS)	FIELD SURVEYS	
	WIDTH (MESH DIMENSIONS)	FIELD SURVEYS	
	POISSON'S RATIO	ASSUME	
	MODULUS OF ELASTICITY	BACKCALCULATE (DEFLECTION)	
	BASE COURSE INFORMATION		
	BONDING CONDITION	ASSUME	DIFFICULT TO OBTAIN IN THE FIELD
	POISSON'S RATIO	ASSUME	
	MODULUS OF ELASTICITY	BACKCALCULATE (DEFLECTION)	
	THICKNESS	CORES	
	SUBGRADE		
	MODULUS OF SUBGRADE REACTION	BACKCALCULATE (DEFLECTION)	
	LOAD TRANSFER AT JOINTS		
	TYPE (AGG. INT. OR DOWELS OR COMBO)	FUNCTION OF ANALYSIS	
	IF DOWELS SPECIFIED, INPUT:		
	JOINT WIDTH	FIELD SURVEYS	
	MODULUS OF ELASTICITY OF DOWEL BARS	ASSUME	
	DOWEL BAR INSIDE DIAMETER	CONSTRUCTION RECORDS	
	DOWEL BAR OUTSIDE DIAMETER	CONSTRUCTION RECORDS	
	DOWEL SPACING (TRANS. AND LONG.)	CONSTRUCTION RECORDS	
	DOWEL CONCRETE INTERACTION CALCULATED BY		
	3-DIMENSIONAL OR FRIBERG'S ANALYSIS		
	IF FRIBERG'S USED, INPUT:	CALCULATE	
	MODULUS OF DOWEL SUPPORT		
	IF AGG INT,WITH OR WITHOUT DOWEL, INPUT:		
	AGGREGATE INTERLOCK FACTOR	ASSUME	
	LOADING		
	NUMBER OF LOADS	FUNCTION OF ANALYSIS	
	POSITION OF LOADS USING MESH COORDINATES	FUNCTION OF ANALYSIS	
	TIRE PRESSURE	WIM	
	CURLING STRESS ANALYSIS		
	THERMAL GRADIENT	CMS OUTPUT	
	WEIGHT OF SLAB	CALCULATE	
	COEFFICIENT OF THERMAL EXPANSION	ASSUME	
	WARPING STRESS ANALYSIS		
	MOISTURE GRADIENT	CMS OUTPUT	

Table 24. Methods of obtaining input variables for CMS.

PROGRAM	INPUT	METHOD OF OBTAINING DATA	PROBLEMS
CMS	SURFACE/ STABILIZED LAYER INFORMATION		
	FREEZING/FROZEN/UNFROZEN THERMAL CONDUCT.	ASSUME BASED ON CMS RECOMMENDATIONS	
	FREEZING/FROZEN/UNFROZEN HEAT CAPACITIES	ASSUME BASED ON CMS RECOMMENDATIONS	
	FREEZING/FROZEN/UNFROZEN UNIT WEIGHT	ASSUME BASED ON CMS RECOMMENDATIONS	
	STIFFNESS	BACKCALCULATE (DEFLECTION)	
	GRAVIMETRIC WATER CONTENT	ASSUME BASED ON CMS RECOMMENDATIONS FOR PCC	
	RING AND BALL VALUE	ASSUME BASED ON CMS RECOMMENDATIONS FOR PCC	
	POISSON'S RATIO	ASSUME BASED ON CMS RECOMMENDATIONS FOR PCC	
	TEMPERATURE-STIFFNESS RELATIONSHIP	ASSUME BASED ON CMS RECOMMENDATIONS FOR PCC	
	PENETRATION VALUE	ASSUME BASED ON CMS RECOMMENDATIONS FOR PCC	
	SHORT-WAVE ABSORPTIVITY	ASSUME BASED ON CMS RECOMMENDATIONS FOR PCC	
	AIR CONTENT	ASSUME BASED ON CMS RECOMMENDATIONS FOR PCC	
	COARSE AGGREGATE CONTENT	ASSUME BASED ON CMS RECOMMENDATIONS FOR PCC	
	NUMBER OF LAYERS	CORES/CONSTRUCTION RECORDS	
	MATERIAL CODE	FUNCTION OF MATERIAL	
BASE COURSE/SUBBASE LAYER INFORMATION			
	UNFROZEN RESILIENT MODULUS	BACKCALCULATE (DEFLECTION)	
	UNFROZEN POISSON'S RATIO	ASSUME	
	FROZEN POISSON'S RATIO	ASSUME	
	FROZEN RESILIENT MODULUS	ASSUME	
	LENGTH OF RECOVERY PERIOD	ASSUME BASED ON PUBLISHED LITERATURE	
	DRY DENSITY	CORES/LAB TESTS	
	PERCENT PASSING NUMBER 200 SIEVE	CORES/LAB TESTS	
	MATERIAL CODE	FUNCTION OF MATERIAL	
SUBGRADE LAYER INFORMATION			
	SPECIFIC SURFACE AREA	ASSUME BASED ON PUBLISHED LITERATURE	
	CLAY LATTICE EXPANSION CONSTANT	ASSUME BASED ON PUBLISHED LITERATURE	
	INITIAL SOIL TEMPERATURE PROFILE	ASSUME BASED ON PUBLISHED LITERATURE	
	DRY HEAT CAPACITY	ASSUME BASED ON PUBLISHED LITERATURE	
	SATURATED WATER CONTENT	ASSUME BASED ON PUBLISHED LITERATURE	
	ACTIVITY RATIO	ASSUME BASED ON PUBLISHED LITERATURE	
	SOIL FREEZING TEMPERATURE	ASSUME BASED ON PUBLISHED LITERATURE	
	PLASTIC LIMIT	CORES/LAB TESTS	
	LIQUID LIMIT	CORES/LAB TESTS	
	UNFROZEN RESILIENT MODULUS	BACKCALCULATE (DEFLECTION)	
	UNFROZEN POISSON'S RATIO	ASSUME	
	FROZEN POISSON'S RATIO	ASSUME	
	FROZEN RESILIENT MODULUS	ASSUME	
	LENGTH OF RECOVERY PERIOD	ASSUME	
	DRY DENSITY	CORES/LAB TESTS	
	PERCENT PASSING NUMBER 200 SIEVE	CORES/LAB TESTS	
	MATERIAL CODE	FUNCTION OF MATERIAL	
CLIMATIC INFORMATION			
	EMISSIVITY FACTOR (SURFACE)	ASSUME BASED ON CMS RECOMMENDATIONS FOR PCC	
	DAILY EXTRATERRESTRIAL RADIATION	DETERMINE BASED ON CMS RADIATION PROGRAM	
	GEIGER LONG-WAVE BACK RADIATION FACTOR	ASSUME BASED ON CMS RECOMMENDATIONS	
	AVERAGE DAILY WIND VELOCITY	LOCAL WEATHER STATION	
	MAXIMUM GUST WIND VELOCITY	LOCAL WEATHER STATION	
	CLOUD BASE FACTOR	ASSUME BASED ON CMS RECOMMENDATIONS	
	GROUND SURFACE VAPOR PRESSURE	LOCAL WEATHER STATION	
	AIR TEMP OF FIRST OF DAY ANALYSIS	LOCAL WEATHER STATION	
	AIR TEMP OF LAST OF DAY ANALYSIS	LOCAL WEATHER STATION	
	TIME OF MAXIMUM AIR TEMPERATURE	LOCAL WEATHER STATION	
	TIME OF MINIMUM AIR TEMPERATURE	LOCAL WEATHER STATION	
	UPPER TEMP LIMIT OF FREEZING RANGE	LOCAL WEATHER STATION	
	LOWER TEMP IN FREEZING RANGE	LOCAL WEATHER STATION	
	CONSTANT DEEP GROUND TEMPERATURE	LOCAL WEATHER STATION	
	MAXIMUM AND MINIMUM DAILY AIR TEMPERAURES	LOCAL WEATHER STATION	
	AVERAGE DAILY SUNSHINE EACH DAY	LOCAL WEATHER STATION	
	TIME SUN SET EACH DAY OF ANALYSIS PERIOD	LOCAL WEATHER STATION	
	TIME SUN RISE EACH DAY OF ANALYSIS PERIOD	LOCAL WEATHER STATION	
INVENTORY/LOCATION INFORMATION			
	MODAL THICKNESS	FUNCTION OF ANALYSIS	
	NUMBER OF TERMINAL NODES	FUNCTION OF ANALYSIS	
	# DAYS IN ANALYSIS PERIOD	FUNCTION OF ANALYSIS	
	LOCATION OF ANALYSIS	FUNCTION OF ANALYSIS	
	# TIMES A DAY THAT TEMP. PROFILE RECORD	FUNCTION OF ANALYSIS	
	MAXIMUM ALLOWABLE CONVECTION COEFFICIENT	ASSUME BASED ON CMS RECOMMENDATIONS	
	TIME INCREMENT FOR TEMP CALCULATION	FUNCTION OF ANALYSIS	
	ANALYSIS DATE	FUNCTION OF ANALYSIS	
	DEPTH TO WATER TABLE FROM SURFACE	COUNTY SOILS MAP	
THICKNESS INFORMATION			
	TOTAL NUMBER OF LAYERS	CORES/CONSTRUCTION RECORDS	
	TOTAL PAVEMENT THICKNESS	CORES/CONSTRUCTION RECORDS	
	THICKNESS OF EACH LAYER	CORES/CONSTRUCTION RECORDS	

Table 25. Method of obtaining input variables for Liu-Lytton Drainage Models.

PROGRAM	INPUT	METHOD OF OBTAINING DATA	PROBLEMS
LUI-LYTTON DRAINAGE MODELS	DRAINAGE MODEL		
	CHARACTERISTICS OF BASE & SUBGRADE		
	WIDTH OF BASE	FIELD SURVEYS	
	DEPTH OF BASE	CORES	
	BASE SLOPE RATIO	???????????	
	BASE PERMEABILITY	CORES/LAB TESTS???????	
	SUBGRADE PERMEABILITY	CORES/LAB TESTS???????	
	BASE POROSITY	CORES/LAB TESTS???????	
	SUBGRADE POROSITY	CORES/LAB TESTS???????	
	MATERIAL PROPERTIES BASE & SUBGRADE		
	BASE COURSE INDEX	ASSUME BASED ON RECOMMMENDATIONS	
	PAVEMENT TYPE	FIELD SURVEYS	
	SOIL CLASSIFICATION	CORES/LAB TESTS	
	SUBGRADE SOIL HORIZON	COUNTY SOILS MAP	
	CRACK AND JOINT SURVEY INFORMATION		
	LENGTH OF JOINTS AND CRACKS	FIELD SURVEY	
	LENGTH OF SURVEY	FIELD SURVEY	
	INTENSITY-DURATION-RECURRENCE		
	EVALUATED PERIOD	FUNCTION OF ANALYSIS	
	K CONSTANT	ASSUME BASED ON RECOMMMENDATIONS	
	POWER OF RECURRENCE INTERVAL	ASSUME BASED ON RECOMMMENDATIONS	
	POWER OF RAINFALL DURATION	ASSUME BASED ON RECOMMMENDATIONS	
	RAINFALL CURVE SHAPE FACTOR	ASSUME BASED ON RECOMMMENDATIONS	
	RAINFALL QUANTITY & FREQUENCY DATA		
	NUMBER OF EVALUATION PERIODS	FUNCTION OF ANALYSIS	
	AMOUNT OF RAINFALL PER DAY	LOCAL WEATHER STATION	
	NUMBER OF CONSECUTIVE WET DAYS	LOCAL WEATHER STATION	
	NUMBER OF CONSECUTIVE DRY DAYS	LOCAL WEATHER STATION	
	INFILTRATION MODEL		
	BASE COURSE CRACKS/JOINTS		
	WIDTH OF JOINT/CRACK	FIELD SURVEYS	
	DEPTH OF JOINT/CRACK	FIELD SURVEYS	
	HORIZONTAL PERMEABILITY	CORRELATION WITH VERTICAL PERMEABILTY	
	POROSITY	CORES/LAB TESTS???????	
	CAPILLARY HEAD	CORES/LAB TESTS???????	
	WATER EVAPORATION CHARACTERISTICS		
	SUCTION OF ATMOSPHERE	LOCAL WEATHER STATION	
	INITIAL SUCTION OF BASE COURSE	CORES/LAB TESTS???????	
	DIFFUSION COEFFICIENT	CORES/LAB TESTS???????	
	SLOPE OF WATER CONTENT-SUCTION	CORES/LAB TESTS???????	
	EVAPORATION COEFFICIENT	ASSUME BASED ON RECOMMMENDATIONS	

Table 26. Method of obtaining input variables for PMARP.

PROGRAM	INPUT	METHOD OF OBTAINING DATA	PROBLEMS
PMARP	MESH INFORMATION		
	NUMBER OF SLABS	FUNCTION OF ANALYSIS	
	NUMBER OF NODES PER SLAB	FUNCTION OF ANALYSIS	
	NODAL COORDINATES	FUNCTION OF ANALYSIS	
	P.C.C. SLAB INFORMATION		
	THICKNESS	CORES/CONSTRUCTION RECORDS	
	TENSILE STRENGTH	CORES/LABORATORY TESTS	
	POISSON'S RATIO	ASSUME	
	MODULUS OF ELASTICITY	BACKCALCULATE (DEFLECTION)	
	REINFORCEMENT INFORMATION		
	REINFORCEMENT RATIO	CONSTRUCTION RECORDS	
	DIAMETER OF REINFORCING BARS	CONSTRUCTION RECORDS	
	SUBGRADE INFORMATION		
	MODULUS OF ELASTICITY	BACKCALCULATE (DEFLECTION)	
	PRESENCE OF VOIDS AT EDGE OR CORNER	FIELD SURVEYS	
	DRAINABILITY (POOR OR GOOD)	FIELD SURVEYS	
	LOAD TRANSFER AT JOINTS		
	TYPE OF LOAD TRANSFER		
	AGGREGATE INTERLOCK ONLY	CONSTRUCTION RECORDS	
	DOWELS ONLY	CONSTRUCTION RECORDS	
	COMBINATION OF ABOVE		
	KEYED ONLY	CONSTRUCTION RECORDS	
	FOR TRANSVERSE AND LONG. JOINTS		
	IF DOWELS:		
	INSIDE DOWEL DIAMETER	CONSTRUCTION RECORDS	
	OUTSIDE DOWEL DIAMETER	CONSTRUCTION RECORDS	
	DOWEL MODULUS OF ELASTICITY	ASSUME	
	DOWEL SPACING	CONSTRUCTION RECORDS	
	DOWEL LENGTH	CONSTRUCTION RECORDS	
	DOWEL POISSON'S RATIO	ASSUME	
	IF AGG. INT. OR KEYED:		
	AGGREGATE INTERLOCK FACTOR	ASSUME	
	JOINT WIDTH	FIELD SURVEYS	
	CONCRETE FATIGUE INFORMATION	CORES/LAB TESTS	
	RESILIENT MODULUS VS. PLATE DEFLECTION CURVE	ASSUME	
	PUMPING ADJUSTMENT FACTORS		
	FACTOR DUE TO RAINFALL	ASSUME BASED ON PMARP RECOMMENDATIONS	
	FACTOR DUE TO TYPE OF SUBBASE TREATMENT	ASSUME BASED ON PMARP RECOMMENDATIONS	
	FACTOR DUE TO TYPE OF DRAINAGE	ASSUME BASED ON PMARP RECOMMENDATIONS	
	ASSUMED AVERAGE VOID DEPTH	ASSUME	

Table 27. Method of obtaining input variables for PEARDARP.

PROGRAM	INPUT	METHOD OF OBTAINING DATA	PROBLEMS
PEARDARP	P.C.C SLAB INFORMATION		
	THICKNESS	CORES	
	LENGTH	FIELD SURVEYS'	
	ELASTIC MODULUS	BACKCALCULATE (DEFLECTION)	
	MODULUS OF RUPTURE	CORES/LAB TESTS	
	SUBGRADE INFORMATION		
	SUBGRADE TYPE	CORES/LAB TESTS	
	MODULUS OF SUBGRADE REACTION	BACKCALCULATE (DEFLECTION)	
	THICKNESS	CORES/LAB TESTS	
	EFFICIENCY OF DRAINAGE	FIELD SURVEYS	
	DISTRESS INFORMATION		
	CRITICAL FAULT 1	ASSUME	
	CRITICAL FAULT 2	ASSUME	
	STANDARD DEV. OF FAULTING	FIELD SURVEYS	
	AVERAGE VOID VOLUME	PHARP OUTPUT	
	SUBDRAINAGE		
	EXCELLENT/GOOD/FAIR/POOR	FIELD SURVEYS	
	SUBBASE TYPE		
	STABILIZED/UNSTABILIZED	CORES	
	SEALANT TYPE		
	LIQUID ASPHALT/LOW MODULUS	FIELD SURVEYS/CONSTRUCTION RECORDS	
	CLIMATIC REGION		
	DRY-WARM OR COLD/WET-WARM OR COLD	FUNCTION OF SECTION	
	LOAD TRANSFER DEVICE		
	UNDOWELED/DOWELED	CONSTRUCTION RECORDS	
	REINFORCEMENT		
	UNREINFORCED/REINFORCED	CONSTRUCTION RECORDS	
	TRAFFIC INFORMATION		
	ANNUAL AVERAGE DAILY TRAFFIC	WIM	
	TRUCK FACTOR	WIM	
	PROPORTION IN DESIGN LANE	WIM	
	TRAFFIC GROWTH RATE	CALCULATE USING COPES DATABASE	
	PASSENGER CAR EQUIVALENT	WIM	
	MAXIMUM SERVICE FLOW	WIM	
	NUMBER OF TRAFFIC LANES	FIELD SURVEY	
	WIDTH FACTOR	??????????????	
	DESIGN SPEED	CONSTRUCTION RECORDS	
	SPEED LIMIT	FIELD SURVEY	
	SPEED FACTOR	ASSUME	
	TRAFFIC VOLUME DISTRIBUTION	WIM	
	TRAFFIC AND ACCIDENT COST INFORMATION		
	PROPORTION OF PASS. CARS	WIM	
	PROPORTION OF P.U. TRUCKS	WIM	
	PROPORTION OF S-U TRUCKS	WIM	
	PROPORTION OF COMBINATION TRUCKS	WIM	
	PROPORTION OF DIESEL TRUCKS	WIM	
	SECTION LENGTH	FIELD SURVEYS	
	COST PER ACCIDENT	ASSUME	
	ACCIDENT RATE	ASSUME	
	USER COSTS (FOR EACH OF THE ABOVE GROUPS)		
	GASOLINE	ASSUME	
	OIL	ASSUME	
	TIRES	ASSUME	
	TIME	ASSUME	
	COST ANALYSIS INFORMATION		
	ANALYSIS PERIOD	FUNCTION OF ANALYSIS	
	LAST YEAR FOR ANALYSIS	FUNCTION OF ANALYSIS	
	INITIAL CONSTRUCTION COST	CONSTRUCTION RECORDS	
	MAINTENANCE AND REHABILITATION ACTIVITIES	FUNCTION OF ANALYSIS	

Table 28. Method of obtaining input variables for PREDICT.

PROGRAM	INPUT	METHOD OF OBTAINING DATA	PROBLEMS
PREDICT	TYPE OF PAVEMENT (PLAIN OR REINFORCED)	CONSTRUCTION RECORDS	
	SLAB AND SHOULDER DESIGN		
	SLAB THICKNESS	CORES	
	TRANSVERSE JOINT SPACING	FIELD SURVEYS	
	DIAMETER OF DOWEL BAR	CONTRUCTION RECORDS	
	MODULUS OF RUPTURE	CORES/LAB TESTS	
	IF PLAIN:		
	UNITUBE INSERT USED	FIELD SURVEYS	
	TIED CONCRETE SHOULDERS	FIELD SURVEYS	
	IF REINFORCED:		
	AREA OF REINFORCEMENT	CONSTRUCTION RECORDS	
	FOUNDATION AND DRAINAGE INPUTS		
	TYPE OF BASE COURSE	CONSTRUCTION RECORDS	
	SUBGRADE SOIL TYPE	CORES/LAB TESTS	
	MODULUS OF SUBGRADE REACTION	BACKCALCULATE (DEFLECTION)	
	IF REINFORCED:		
	LONGITUDINAL SUBDRAINS	FIELD SURVEYS/CONSTRUCTION RECORDS	
	AGE AND TRAFFIC LOADING INPUTS		
	IS ESAL/YEAR CONSTANT OVER AGE (Y/N)		
	IF NO:		
	SPECIFY AGE/ESAL COMBINATIONS	WIM	
	POTENTIAL PAVEMENT CONDITION INPUTS		
	"D" CRACKING AGGREGATE IN SLAB	FIELD SURVEYS	
	INCOMPRESSIBLES IN TRANSVERSE JOINTS	FIELD SURVEYS	
	IF REINFORCED:		
	REACTIVE AGGREGATE IN SLAB	FIELD SURVEYS	
	CLIMATIC INPUTS		
	MEAN ANNUAL PRECIPITATION	LOCAL WEATHER STATION	
	CORPS OF ENGINEERS FREEZING INDEX	LOCAL WEATHER STATION	
	MEAN ANNUAL TEMPERATURE	LOCAL WEATHER STATION	
	TEMPERATURE RANGE	LOCAL WEATHER STATION	

Table 29. Method of obtaining input variables for BERM.

PROGRAM	INPUT	METHOD OF OBTAINING DATA	PROBLEMS
BERM	SHOULDER TYPE		
	RIGID/FLEXIBLE	FIELD SURVEYS/CONSTRUCTION RECORDS	
	SEPARATE/MONOLITHIC	FIELD SURVEYS/CONSTRUCTION RECORDS	
	DESIGN TEMPERATURE	LOCAL WEATHER STATION	
	CONCRETE SHOULDER INFORMATION		
	THICKNESS	CORES/CONSTRUCTION RECORDS	
	MODULUS	BACKCALCULATION (DEFLECTION)	
	FLEXURAL STRENGTH	ASSUME SAM AS MAINLINE	
	ASPHALT SHOULDER INFORMATION		
	STATIC AND DYNAMIC MODULI COEFF. OR USE DEFAULT VALUES	DEFAULT VALUES OR BACKCALCULATE	
	THICKNESS	CONSTRUCTION RECORDS	
	LOWER LAYER INFORMATION		
	BASE MODULUS	BACKCALCULATION (DEFLECTION)	
	BASE THICKNESS	CONSTRUCTION RECORDS	
	SUBGRADE MODULUS	BACKCALCULATION (DEFLECTION)	

Table 30. Method of obtaining input variables for JCS-1.

PROGRAM	INPUT	METHOD OF OBTAINING DATA	PROBLEMS
JCS1	SHOULDER DESIGN LIFE	FUNCTION OF ANALYSIS	
	P.C.C. SLAB INFORMATION		
	SHOULDER THICKNESS	CORES	
	TRAFFIC LANE THICKNESS	CORES	
	SHOULDER WIDTH	FIELD SURVEY	
	MEAN PCC MODULUS OF RUPTURE (28 DAYS)	CORES/LABORATORY TESTS	
	COEFFICIENT OF VARIATION OF PCC MODULUS	CORES/LABORATORY TESTS	
	LANE/SHOULDER JOINT LOAD TRANSFER EFF.	FIELD TESTING	
	SUBGRADE INFORMATION		
	MODULUS OF SUBGRADE REACTION	BACKCALCULATE (DEFLECTION)	
	ERODABILITY OF FOUNDATION SUPPORT AT BEGINNING OF DESIGN PERIOD	ASSUME USING FIELD SURVEYS/PMARP?????	
	ERODABILITY OF FOUNDATION SUPPORT AT END OF DESIGN PERIOD	RESULTS OF PMARP	
	TRAFFIC		
	ADT AT BEGINNING OF DESIGN PERIOD	WIM	
	ADT AT END OF DESIGN PERIOD	ASSUME	
	PERCENT TRUCKS OF ADT	WIM	
	PERCENT TRUCKS IN DESIGN TRAVELED LANE	WIM	
	PERCENT DIRECTIONAL DISTRIBUTION	WIM	
	MEAN AXLES PER TRUCK	WIM	
	LENGTH OF SURVEYED STRETCH	FIELD SURVEYS	
	AVERAGE LENGTH OF ENCROACHMENTS	??????????????	
	PERCENT TRUCKS PARKING ON SHOULDER	??????????????	
	SINGLE AXLE LOAD DISTRIBUTION	WIM	
	TANDEM AXLE LOAD DISTRIBUTION	WIM	

Table 31. Method of obtaining input variables for JCP-1.

PROGRAM	INPUT	METHOD OF OBTAINING DATA	PROBLEMS
JCP1 <ZERO MAINTENANCE DESIGN>	DESIGN CRITERIA		
	DESIGN LIFE	CONSTRUCTION RECORDS	
	CONSTRUCTION SERVICEABILITY INDEX	CONSTRUCTION RECORDS	
	TERMINAL SERVICEABILITY INDEX	ASSUME	
	TIME SLABS OPEN TO TRAFFIC	CONSTRUCTION RECORDS	
	MONTH PAVEMENT WILL BE OPENED	CONSTRUCTION RECORDS	
	P.C.C SLAB INFORMATION		
	THICKNESS	CONSTRUCTION RECORDS/CORES	
	LENGTH	CONSTRUCTION RECORDS/FIELD SURVEYS	
	MEAN MODULUS OF RUPTURE <MR>	CONSTRUCTION RECORDS	
	COEFFICIENT OF VARIATION FOR MR	ASSUME	
	COEFFICIENT OF THERMAL EXPANSION	ASSUME	
	MODULUS OF ELASTICITY	BACKCALCULATE <DEFLECTION>	
	MONTHLY THERMAL GRADIENTS <DAY/NIGHT>	CMS OUTPUT	
	TRAFFIC INFORMATION		
	ADT AT BEGINNING OF DESIGN PERIOD	TRAFFIC RECORDS	
	ADT AT END OF DESIGN PERIOD	TRAFFIC RECORDS	
	PERCENT TRUCKS OF ADT	TRAFFIC RECORDS	
	PERCENT OF TRUCKS IN DESIGN LANE	CALCULATE USING NCHRP 1-19	
	PERCENT DIRECTIONAL DISTRIBUTION	ASSUME 0.5	
	MEAN AXLES PER TRUCK	WIM/W4 TABLES	
	PERCENT TRUCKS DURING DAYLIGHT	WIM	
	MEAN DISTANCE SLAB EDGE TO DUAL	FIELD SURVEY	
	SINGLE AXLE LOAD DISTRIBUTION	WIM/W4 TABLE	
	TANDEM AXLE LOAD DISTRIBUTION	WIM/W4 TABLE	
	MONTHLY TRUCK PERCENTAGE	WIM/W4 TABLE	
	SUBGRADE INFORMATION		
	MONTHLY MODULUS OF SUBGRADE REACTION	CMS OUTPUT	
	ERODABILITY OF FOUNDATION SUPPORT		
	AT BEGINNING OF DESIGN PERIOD	ASSUME FULL SUPPORT	
	AT END OF DESIGN PERIOD	PMARP OUTPUT/NDT TESTING	
	CLIMATIC REGIONAL FACTOR	ASSUME BASED ON JCP RECOMMENDATIONS	

PART IV. RESULTS OF SENSITIVITY ANALYSIS

This section summarizes the results of hundreds of computer runs and design procedure calculations in the form of tabular sensitivity analyses. The results of these analyses are shown in tables 32 through 64 and figures 15 and 16.

Table 32. Effect of slab thickness on pavement responses as measured by ILLISLAB, JSLAB, WESLIQID, and WESLAYER.

EFFECT OF SLAB THICKNESS ON PAVEMENT RESPONSES *

ILLISLAB OUTPUTS		STANDARD 9 IN.	VARIED SLAB THICKNESS 6 IN.	% DIFF	12 IN.	% DIFF	15 IN.	% DIFF
MINIMUM LOAD TRANSFER [%]	LONGITUDINAL	60.0	65.0	8.3	57.0	-5.0	55.0	-8.3
	TRANSVERSE	1.0	1.0	0.0	1.0	0.0	1.0	0.0
MAXIMUM PRINCIPAL TENSILE STRESS [PSI]	BOTTOM OF SLAB	185.7	278.8	50.1	131.6	-29.1	97.8	-47.3
	BOTTOM OF BASE	41.3	92.9	124.9	21.9	-47.0	13.0	-68.5
MAXIMUM SUBGRADE STRESS [PSI]		1.7	2.4	41.2	1.4	-17.6	1.1	-35.3
MAXIMUM DEFLECTION [MILS]		8.6	11.8	37.2	6.8	-20.9	5.7	-33.7

JSLAB OUTPUTS		STANDARD 9 IN.	VARIED SLAB THICKNESS 6 IN.	% DIFF	12 IN.	% DIFF	15 IN.	% DIFF
MINIMUM LOAD TRANSFER [%]	LONGITUDINAL	44.0	48.0	9.1	41.0	-6.8	40.0	-9.1
	TRANSVERSE	1.0	1.0	0.0	1.0	0.0	1.0	0.0
MAXIMUM PRINCIPAL TENSILE STRESS [PSI]	BOTTOM OF SLAB	192.4	292.3	51.9	135.7	-29.5	100.1	-48.0
	BOTTOM OF BASE	42.8	97.4	127.6	22.6	-47.2	13.3	-68.9
MAXIMUM DEFLECTION [MILS]		9.7	13.3	37.1	7.7	-20.6	6.4	-34.0

WESLAYER OUTPUTS		STANDARD 9 IN.	VARIED SLAB THICKNESS 6 IN.	% DIFF	12 IN.	% DIFF	15 IN.	% DIFF
MINIMUM LOAD TRANSFER [%]	LONGITUDINAL	74.0	74.0	0.0	73.0	-1.4	74.0	0.0
	TRANSVERSE	1.0	1.0	0.0	1.0	0.0	1.0	0.0
MAXIMUM PRINCIPAL TENSILE STRESS [PSI]	BOTTOM OF SLAB	212.7	319.2	50.1	150.5	-29.2	112.0	-47.3
	BOTTOM OF BASE	47.3	106.4	124.9	25.1	-46.9	14.9	-68.5
MAXIMUM SUBGRADE STRESS [PSI]		9.5	12.0	26.3	8.2	-13.7	7.1	-25.3
MAXIMUM DEFLECTION [MILS]		14.4	17.3	20.1	12.6	-12.5	11.4	-20.8

WESLIQUID OUTPUTS		STANDARD 9 IN.	VARIED SLAB THICKNESS 6 IN.	% DIFF	12 IN.	% DIFF	15 IN.	% DIFF
MINIMUM LOAD TRANSFER [%]	LONGITUDINAL	42.0	41.0	-2.4	41.0	-2.4	42.0	0.0
	TRANSVERSE	1.0	1.0	0.0	1.0	0.0	1.0	0.0
MAXIMUM PRINCIPAL TENSILE STRESS [PSI]	BOTTOM OF SLAB	224.2	353.1	57.5	152.3	-32.1	109.3	-51.2
	BOTTOM OF BASE	49.8	117.7	136.3	25.4	-49.0	14.6	-70.7
MAXIMUM SUBGRADE STRESS [PSI]		1.9	2.6	36.8	1.5	-21.1	1.3	-31.6
MAXIMUM DEFLECTION [MILS]		9.4	12.8	36.2	7.6	-19.1	6.6	-29.8

(1 in = 25.4 mm and 1 psi = 6.894 kPa)

* To wheel loading only

Table 33. Effect of shoulder parameters on pavement responses as measured by ILLISLAB, JSLAB, WESLIQID, and WESLAYER.

EFFECT OF SHOULDER PARAMETERS ON PAVEMENT RESPONSES *

ILLISLAB OUTPUTS		STANDARD TIED SHOULDER	NO SHOULDER	% DIFF	WIDENED LANE 15' WIDE	% DIFF
MINIMUM LOAD TRANSFER [%]	LONGITUDINAL	60.0	N/A		58.0	-3.3
	TRANSVERSE	1.0	1.0	0.0	1.0	0.0
MAXIMUM PRINCIPAL TENSILE STRESS [PSI]	BOTTOM OF SLAB	185.7	228.4	23.0	124.0	-33.2
	BOTTOM OF BASE	41.3	50.8	23.0	27.6	-33.2
MAXIMUM SUBGRADE STRESS [PSI]		1.7	2.7	58.8	1.2	-29.4
MAXIMUM DEFLECTION [MILS]		8.6	13.6	58.1	6.1	-29.1

JSLAB OUTPUTS		STANDARD TIED SHOULDER	NO SHOULDER	% DIFF	WIDENED LANE 15' WIDE	% DIFF
MINIMUM LOAD TRANSFER [%]	LONGITUDINAL	44.0	N/A		36.0	-18.2
	TRANSVERSE	1.0	1.0	0.0	1.0	0.0
MAXIMUM PRINCIPAL TENSILE STRESS [PSI]	BOTTOM OF SLAB	192.4	218.6	13.6	117.2	-39.1
	BOTTOM OF BASE	42.8	48.6	13.6	26.1	-39.0
MAXIMUM DEFLECTION [MILS]		9.7	13.8	42.3	6.1	-37.1

WESLAYER OUTPUTS		STANDARD TIED SHOULDER	NO SHOULDER	% DIFF	WIDENED LANE 15' WIDE	% DIFF
MINIMUM LOAD TRANSFER [%]	LONGITUDINAL	74.0	N/A		85.0	14.9
	TRANSVERSE	1.0	1.0	0.0	1.0	0.0
MAXIMUM PRINCIPAL TENSILE STRESS [PSI]	BOTTOM OF SLAB	212.7	238.5	12.1	132.7	-37.6
	BOTTOM OF BASE	47.3	53.0	12.1	29.5	-37.6
MAXIMUM SUBGRADE STRESS [PSI]		9.5	8.5	-10.5	2.8	-70.5
MAXIMUM DEFLECTION [MILS]		14.4	15.7	9.0	11.5	-20.1

WESLIQUID OUTPUTS		STANDARD TIED SHOULDER	NO SHOULDER	% DIFF	WIDENED LANE 15' WIDE	% DIFF
MINIMUM LOAD TRANSFER [%]	LONGITUDINAL	42.0	N/A		42.0	0.0
	TRANSVERSE	1.0	1.0	0.0	1.0	0.0
MAXIMUM PRINCIPAL TENSILE STRESS [PSI]	BOTTOM OF SLAB	224.2	250.3	11.6	127.3	-43.2
	BOTTOM OF BASE	49.8	55.6	11.6	28.3	-43.2
MAXIMUM SUBGRADE STRESS [PSI]		1.9	2.6	36.8	1.2	-36.8
MAXIMUM DEFLECTION [MILS]		9.4	13.3	41.5	5.8	-38.3

(1 in = 25.4 mm and 1 psi = 6.894 kPa)

* To wheel loading only

Table 34. Effect of subgrade strength on pavement responses as measured by ILLISLAB, JSLAB, WESLIQID, and WESLAYER.

EFFECT OF SUBGRADE STRENGTH ON PAVEMENT RESPONSES*

ILLISLAB OUTPUTS		STANDARD 200	VARIED SUBGRADE K-VALUE 50	% DIFF	100	% DIFF	500	% DIFF
MINIMUM LOAD TRANSFER [%]	LONGITUDINAL	60.0	79.0	31.7	70.0	16.7	44.0	-26.7
	TRANSVERSE	1.0	1.0	0.0	1.0	0.0	1.0	0.0
MAXIMUM PRINCIPAL TENSILE STRESS [PSI]	BOTTOM OF SLAB	185.7	223.0	20.1	205.0	10.4	161.6	-13.0
	BOTTOM OF BASE	41.3	49.5	19.9	45.6	10.4	35.9	-13.1
MAXIMUM SUBGRADE STRESS [PSI]		1.7	1.0	-41.2	1.3	-23.5	2.6	52.9
MAXIMUM DEFLECTION [MILS]		8.6	20.2	134.9	13.0	51.2	5.1	-40.7

JSLAB OUTPUTS		STANDARD 200	VARIED SUBGRADE K-VALUE 50	% DIFF	100	% DIFF	500	% DIFF
MINIMUM LOAD TRANSFER [%]	LONGITUDINAL	44.0	66.0	50.0	55.0	25.0	30.0	-31.8
	TRANSVERSE	1.0	1.0	0.0	1.0	0.0	1.0	0.0
MAXIMUM PRINCIPAL TENSILE STRESS [PSI]	BOTTOM OF SLAB	192.4	237.9	23.6	214.8	11.6	165.5	-14.0
	BOTTOM OF BASE	42.8	52.9	23.6	47.7	11.4	36.8	-14.0
MAXIMUM DEFLECTION [MILS]		9.7	22.4	131.2	14.8	52.6	5.7	-41.2

WESLAYER OUTPUTS		STANDARD 200	VARIED SUBGRADE K-VALUE 50	% DIFF	100	% DIFF	500	% DIFF
MINIMUM LOAD TRANSFER [%]	LONGITUDINAL	74.0	87.0	17.6	78.0	5.4	69.0	-6.8
	TRANSVERSE	1.0	1.0	0.0	1.0	0.0	1.0	0.0
MAXIMUM PRINCIPAL TENSILE STRESS [PSI]	BOTTOM OF SLAB	212.7	281.5	32.3	235.9	10.9	182.5	-14.2
	BOTTOM OF BASE	47.3	62.6	32.3	52.4	10.8	40.5	-14.4
MAXIMUM SUBGRADE STRESS [PSI]		9.5	3.8	-60.0	7.3	-23.2	12.8	34.7
MAXIMUM DEFLECTION [MILS]		14.4	52.4	263.9	21.5	49.3	8.3	-42.4

WESLIQUID OUTPUTS		STANDARD 200	VARIED SUBGRADE K-VALUE 50	% DIFF	100	% DIFF	500	% DIFF
MINIMUM LOAD TRANSFER [%]	LONGITUDINAL	42.0	69.0	64.3	57.0	35.7	27.0	-35.7
	TRANSVERSE	1.0	1.0	0.0	1.0	0.0	1.0	0.0
MAXIMUM PRINCIPAL TENSILE STRESS [PSI]	BOTTOM OF SLAB	224.2	258.8	15.4	242.9	8.3	198.4	-11.5
	BOTTOM OF BASE	49.8	57.5	15.5	54.0	8.4	44.1	-11.4
MAXIMUM SUBGRADE STRESS [PSI]		1.9	1.1	-42.1	1.4	-26.3	2.8	47.4
MAXIMUM DEFLECTION [MILS]		9.4	22.7	141.5	14.2	51.1	5.6	-40.4

(1 in = 25.4 mm and 1 psi = 6.894 kPa)

* To wheel loading only

Table 35. Effect of joint width and slab length on pavement responses as measured by ILLISLAB, JSLAB, WESLIQID, and WESLAYER.

EFFECT OF JOINT WIDTH AND SLAB LENGTH ON PAVEMENT RESPONSES *

ILLISLAB OUTPUTS		STANDARD 0.25/15	VARIED JOINT WIDTH/SLAB LENGTH (INCHES/FEET) 0.15/10	% DIFF	0.24/10	% DIFF	0.3/20	% DIFF	0.48/20	% DIFF
MINIMUM LOAD TRANSFER [%]	LONGITUDINAL	60.0	61.0	1.7	60.0	0.0	59.0	-1.7	57.0	-5.0
	TRANSVERSE	1.0	1.0	0.0	1.0	0.0	1.0	0.0	1.0	0.0
MAXIMUM PRINCIPAL TENSILE STRESS [PSI]	BOTTOM OF SLAB	185.7	186.5	0.4	187.0	0.7	183.0	-1.5	184.2	-0.8
	BOTTOM OF BASE	41.3	41.5	0.5	41.5	0.5	40.7	-1.5	40.9	-1.0
MAXIMUM SUBGRADE STRESS [PSI]		1.7	1.8	5.9	1.8	5.9	1.6	-5.9	1.7	0.0
MAXIMUM DEFLECTION [MILS]		8.6	9.0	4.7	9.0	4.7	8.2	-4.7	8.3	-3.5

JSLAB OUTPUTS		STANDARD 0.25/15	VARIED JOINT WIDTH/SLAB LENGTH (INCHES/FEET) 0.15/10	% DIFF	0.24/10	% DIFF	0.3/20	% DIFF	0.48/20	% DIFF
MINIMUM LOAD TRANSFER [%]	LONGITUDINAL	44.0	45.0	2.3	46.0	4.5	43.0	-2.3	43.0	-2.3
	TRANSVERSE	1.0	1.0	0.0	1.0	0.0	1.0	0.0	1.0	0.0
MAXIMUM PRINCIPAL TENSILE STRESS [PSI]	BOTTOM OF SLAB	192.4	196.2	2.0	196.1	1.9	189.4	-1.6	189.4	-1.6
	BOTTOM OF BASE	42.8	43.6	1.9	43.6	1.9	42.1	-1.6	42.1	-1.6
MAXIMUM DEFLECTION [MILS]		9.7	10.5	7.8	10.5	8.2	9.2	-5.2	9.2	-5.2

WESLAYER OUTPUTS		STANDARD 0.25/15	VARIED JOINT WIDTH/SLAB LENGTH (INCHES/FEET) 0.15/10	% DIFF	0.24/10	% DIFF	0.3/20	% DIFF	0.48/20	% DIFF
MINIMUM LOAD TRANSFER [%]	LONGITUDINAL	74.0	74.0	0.0			77.0	4.1		
	TRANSVERSE	1.0	1.0	0.0			1.0	0.0		
MAXIMUM PRINCIPAL TENSILE STRESS [PSI]	BOTTOM OF SLAB	212.7	211.8	-0.4			74.3	-65.1		
	BOTTOM OF BASE	47.3	47.1	-0.4			16.5	-65.1		
MAXIMUM SUBGRADE STRESS [PSI]		9.5	9.8	3.2			6.1	-35.8		
MAXIMUM DEFLECTION [MILS]		14.4	14.9	3.5			10.8	-25.0		

WESLIQUID OUTPUTS		STANDARD 0.25/15	VARIED JOINT WIDTH/SLAB LENGTH (INCHES/FEET) 0.15/10	% DIFF	0.24/10	% DIFF	0.3/20	% DIFF	0.48/20	% DIFF
MINIMUM LOAD TRANSFER [%]	LONGITUDINAL	42.0	46.0	9.5			41.0	-2.4		
	TRANSVERSE	1.0	1.0	0.0			1.0	0.0		
MAXIMUM PRINCIPAL TENSILE STRESS [PSI]	BOTTOM OF SLAB	224.2	219.3	-2.2			222.7	-0.7		
	BOTTOM OF BASE	49.8	48.7	-2.2			49.5	-0.6		
MAXIMUM SUBGRADE STRESS [PSI]		1.9	2.1	10.5			1.8	-5.3		
MAXIMUM DEFLECTION [MILS]		9.4	10.4	10.6			9.0	-4.3		

NOTE: Several combinations of slab length and joint width did not execute for WESLAYER and WESLIQID.
(1 in = 25.4 mm and 1 psi = 6.874 kPa)
* To wheel loading only

Table 36. Effect of load transfer on pavement responses as measured by ILLISLAB and JSLAB.

EFFECT OF LOAD TRANSFER ON PAVEMENT RESPONSES*

ILLISLAB OUTPUTS		STANDARD 1.25 IN.	VARIED DOWEL DIAMETER 1.0 IN.	% DIFF	1.5 IN.	% DIFF	AGGREGATE INTERLOCK 3.157/10	% DIFF	(LONG/TRANS)*10^4 0/0	% DIFF
MINIMUM LOAD TRANSFER [%]	LONGITUDINAL	60.0	60.0	0.0	60.0	0.0	74.0	23.3	0.0	-100.0
	TRANSVERSE	1.0	1.0	0.0	1.0	0.0	0.0	-100.0	0.0	-100.0
MAXIMUM PRINCIPAL TENSILE STRESS [PSI]	BOTTOM OF SLAB	185.7	185.7	0.0	185.7	0.0	172.3	-7.2	227.7	22.6
	BOTTOM OF BASE	41.3	41.3	0.0	41.3	0.0	38.3	-7.3	50.6	22.5
MAXIMUM SUBGRADE STRESS [PSI]		1.7	1.7	0.0	1.7	0.0	1.6	-5.9	2.8	64.7
MAXIMUM DEFLECTION [MILS]		8.6	8.6	0.0	8.6	0.0	7.9	-8.1	13.7	59.3

JSLAB OUTPUTS		STANDARD 1.25 IN.	VARIED DOWEL DIAMETER 1.0 IN.	% DIFF	1.5 IN.	% DIFF	AGGREGATE INTERLOCK 3.157/10	% DIFF	(LONG/TRANS)*10^4 0/0	% DIFF
MINIMUM LOAD TRANSFER [%]	LONGITUDINAL	44.0	43.0	-2.3	44.0	0.0	74.0	68.2	0.0	-100.0
	TRANSVERSE	1.0	1.0	0.0	1.0	0.0	0.0	-100.0	0.0	-100.0
MAXIMUM PRINCIPAL TENSILE STRESS [PSI]	BOTTOM OF SLAB	192.4	192.7	0.2	192.0	-0.2	166.6	-13.4	220.2	14.4
	BOTTOM OF BASE	42.8	42.8	0.0	42.7	-0.2	37.0	-13.6	48.9	14.3
MAXIMUM DEFLECTION [MILS]		9.7	9.6	-1.0	9.8	1.0	7.9	-18.6	13.8	42.3

Note: There are no results for WESLIQUID or WESLAYER because only a 2-slab mesh was used.

The results of the effect of load transfer may be misleading due to the distance of the joint away from the load.

(1 in = 25.4 mm and 1 psi = 6.894 kPa)

* To wheel loading only

Table 37. Effect of base type on pavement responses as measured by ILLISLAB and JSLAB.

EFFECT OF BASE TYPE ON PAVEMENT RESPONSES*

ILLISLAB OUTPUTS		STANDARD STABILIZED UNBONDED	STABILIZED BONDED	% DIFF	TYPE OF BASE, BONDING CONDITION GRANULAR	% DIFF	NO BASE	% DIFF
MINIMUM LOAD TRANSFER [%]	LONGITUDINAL	60.0	57.0	-5.0	60.0	0.0	60.0	0.0
	TRANSVERSE	1.0	1.0	0.0	1.0	0.0	1.0	0.0
MAXIMUM PRINCIPAL TENSILE STRESS [PSI]	BOTTOM OF SLAB	185.7	71.9	-61.3	195.2	5.1	195.3	5.2
	BOTTOM OF BASE	41.3	73.4	77.7	0.5	-98.8	N/A	
MAXIMUM SUBGRADE STRESS [PSI]		1.7	1.4	-17.6	1.7	0.0	1.7	0.0
MAXIMUM DEFLECTION [MILS]		8.6	6.8	-20.9	8.7	1.2	8.7	1.2

JSLAB OUTPUTS		STANDARD STABILIZED UNBONDED	STABILIZED BONDED	% DIFF	TYPE OF BASE, BONDING CONDITION GRANULAR	% DIFF	NO BASE	% DIFF
MINIMUM LOAD TRANSFER [%]	LONGITUDINAL	44.0	42.0	-4.5	44.0	0.0	44.0	0.0
	TRANSVERSE	1.0	1.0	0.0	1.0	0.0	1.0	0.0
MAXIMUM PRINCIPAL TENSILE STRESS [PSI]	BOTTOM OF SLAB	193.2	77.1	-60.1	202.3	4.7	203.2	5.2
	BOTTOM OF BASE	42.9	78.7	83.4	0.5	-98.8	N/A	
MAXIMUM DEFLECTION [MILS]		9.6	7.7	-19.8	9.9	3.1	9.8	2.1

(1 in = 25.4 mm and 1 psi = 6.894 kPa)

* To wheel loading only

Table 38. Effect of slab length/joint width, slab thickness, and shoulder parameters on pavement responses as measured by PMARP.

EFFECT OF VARIOUS INPUTS ON PAVEMENT RESPONSES

PMARP OUTPUTS		STANDARD	VARIED JOINT WIDTH/SLAB LENGTH 0.15/10	% DIFF	0.24/10	% DIFF	0.3/20	% DIFF	0.48/20	% DIFF
MINIMUM LOAD TRANSFER [%]	LONGITUDINAL	71.0	70.0	-1.4	68.0	-4.2	70.0	-1.4	68.0	-4.2
MAXIMUM PRINCIPAL TENSILE STRESS [PSI]	BOTTOM OF SLAB	217.3	216.7	-0.3	216.7	-0.3	216.3	-0.5	217.0	-0.1
MAXIMUM SUBGRADE STRESS [PSI]		2.4	2.5	4.2	2.5	4.2	2.3	-4.2	2.3	-4.2
MAXIMUM DEFLECTION [MILS]		11.3	12.0	6.2	12.0	6.2	11.0	-2.7	11.1	-1.8

PMARP OUTPUTS		STANDARD 9 IN.	VARIED SLAB THICKNESS 6 IN.	% DIFF	12 IN.	% DIFF	15 IN.	% DIFF
MINIMUM LOAD TRANSFER [%]	LONGITUDINAL	71.0	72.0	1.4	62.0	-12.7	61.0	-14.1
MAXIMUM PRINCIPAL TENSILE STRESS [PSI]	BOTTOM OF SLAB	217.3	335.1	54.2	171.9	-20.9	131.6	-39.4
MAXIMUM SUBGRADE STRESS [PSI]		2.4	3.2	33.3	1.8	-25.0	1.7	-29.2
MAXIMUM DEFLECTION [MILS]		11.3	17.1	51.3	8.8	-22.1	7.3	-35.4

PMARP OUTPUTS		STANDARD TIE BAR 0.625 IN.	AGGREGATE INTERLOCK X 10^4 3.157	% DIFF	0.0	% DIFF	NO SHOULDER	% DIFF
MINIMUM LOAD TRANSFER [%]	LONGITUDINAL	71.0	83.0	16.9	0.0	-100.0	0.0	-100.0
MAXIMUM PRINCIPAL TENSILE STRESS [PSI]	BOTTOM OF SLAB	217.3	219.5	1.0	284.9	31.1	284.9	31.1
MAXIMUM SUBGRADE STRESS [PSI]		2.4	2.9	20.8	3.9	62.5	3.9	62.5
MAXIMUM DEFLECTION [MILS]		11.3	10.2	-9.7	22.4	98.2	22.4	98.2

(1 in = 25.4 mm and 1 psi = 6.894 kPa)

Table 39. Effect of void depth, drainage factor, rainfall factor, and subbase treatment factor on pavement responses as measured by PMARP.

EFFECT OF VARIOUS PARAMETERS ON PAVEMENT RESPONSES

PMARP OUTPUTS		STANDARD 0.001 IN.	VARIED AVERAGE VOID DEPTH 0.1 IN.	% DIFF	0.5 IN.	% DIFF
MINIMUM LOAD TRANSFER [%]	LONGITUDINAL	71.0	68.0	-4.2	67.0	-5.6
MAXIMUM PRINCIPAL TENSILE STRESS [PSI]	BOTTOM OF SLAB	217.3	245.6	13.0	355.8	63.7
MAXIMUM SUBGRADE STRESS [PSI]		2.4	2.8	16.7	3.0	25.0
MAXIMUM DEFLECTION [MILS]		11.3	12.9	14.2	19.5	72.6

PMARP OUTPUTS		STANDARD 1/1/1	VARIED DRAINAGE FACTOR, RAINFALL FACTOR, AND SUBBASE FACTOR Drainage 0	% DIFF	Rainfall 0	% DIFF	Subbase 0	% DIFF
MINIMUM LOAD TRANSFER [%]	LONGITUDINAL	71.0	71.0	0.0	71.0	0.0	75.0	5.6
MAXIMUM PRINCIPAL TENSILE STRESS [PSI]	BOTTOM OF SLAB	217.3	218.5	0.6	217.4	0.0	229.2	5.5
MAXIMUM SUBGRADE STRESS [PSI]		2.4	3.0	25.0	2.5	4.2	1.5	-37.5
MAXIMUM DEFLECTION [MILS]		11.3	12.2	8.0	11.4	0.9	9.9	-12.4

EFFECT OF VARIOUS PARAMETERS ON PAVEMENT RESPONSES

PMARP OUTPUTS		STANDARD TIED SHOULDER	VARIED SHOULDER PARAMETERS NO SHOULDER	% DIFF	WIDENED LANE 15' WIDE	% DIFF
MINIMUM LOAD TRANSFER [%]	LONGITUDINAL	71.0	N/A		58.0	-18.3
MAXIMUM PRINCIPAL TENSILE STRESS [PSI]	BOTTOM OF SLAB	217.3	284.9	31.1	139.9	-35.6
MAXIMUM SUBGRADE STRESS [PSI]		2.4	3.9	62.5	1.9	-20.8
MAXIMUM DEFLECTION [MILS]		11.3	22.4	98.2	7.9	-30.1

PMARP OUTPUTS		STANDARD 1.0	VARIED TRAFFIC LEVEL (ESAL) 5×10^{-6}	% DIFF	15×10^{-6}	% DIFF
MINIMUM LOAD TRANSFER [%]	LONGITUDINAL	71.0	57.7	-18.7	43.1	-39.3
MAXIMUM PRINCIPAL TENSILE STRESS [PSI]	BOTTOM OF SLAB	217.3	253.3	16.6	313.5	44.3
MAXIMUM SUBGRADE STRESS [PSI]		2.4	2.7	12.5	3.8	58.3
MAXIMUM DEFLECTION [MILS]		11.3	11.8	4.4	19.3	70.8

(1 in = 25.4 mm and 1 psi = 6.894 kPa)

Table 40. ILLISLAB and JSLAB curling analysis.

ILLI-SLAB CURLING ANALYSIS RESULTS

PROGRAM: ILLI-SLAB
RESULTS FOR CURLING ANALYSIS WITHOUT TRAFFIC LOAD
MAXIMUM PRINCIPAL SLAB STRESS

SLAB THICKNESS (INCH)	SLAB SIZE (FT.)	SUBGRADE "K" VALUE (PCI) 50	50	200	200	500	500
		TEMPERATURE GRADIENT (DEGREES F/INCH) 1.5	-3.0	1.5	-3.0	1.5	-3.0
8.0	12 x 15	67.0	117.3	117.6	180.5	145.2	218.9
8.0	12 x 20	120.5	222.7	165.3	283.2	182.1	301.5
10.0	12 x 15	51.1	91.7	98.9	152.5	126.5	183.4
10.0	12 x 20	107.2	198.7	164.5	276.6	191.9	315.2
10.0	12 x 25	157.8	302.7	203.7	369.5	218.8	387.5
10.0	12 x 30	190.7	373.1	217.1	408.5	221.1	417.9
14.0	12 x 15	30.4	58.2	69.1	108.2	91.7	131.2
14.0	12 x 20	76.0	143.2	133.2	216.2	163.9	240.1

Note: A positive temperature gradient is defined as slab bottom temperature higher than slab top temperature.

Unit Weight of Concrete = 0.0868 lb/in^3
Concrete Coefficient of Expansion = 5.0x10^-6 in/in/f

JSLAB CURLING ANALYSIS RESULTS

PROGRAM: JSLAB
RESULTS FOR CURLING ANALYSIS WITHOUT TRAFFIC LOAD
MAXIMUM PRINCIPAL SLAB STRESS

SLAB THICKNESS (INCH)	SLAB SIZE (FT.)	SUBGRADE "K" VALUE (PCI) 50	50	200	200	500	500
		TEMPERATURE GRADIENT (DEGREES F/INCH) 1.5	-3.0	1.5	-3.0	1.5	-3.0
8.0	12 x 15	52.3	98.6	97.7	141.3	116.7	162.4
8.0	12 x 20	94.0	180.2	127.4	225.0	133.5	233.8
10.0	12 x 15	40.1	77.1	83.5	120.4	109.4	141.8
10.0	12 x 20	84.7	160.4	133.8	221.3	151.2	249.4
10.0	12 x 25	124.1	241.5	160.6	292.5	159.8	300.1
10.0	12 x 30	148.5	249.9	168.1	321.5	166.5	322.4
14.0	12 x 15	23.8	47.8	59.9	88.2	81.6	105.9
14.0	12 x 20	60.1	116.0	114.6	184.2	141.7	204.9

Note: A positive temperature gradient is defined as slab bottom temperature higher than slab top temperature.

Unit Weight of Concrete = 0.0868 lb/in^3
Concrete Coefficient of Expansion = 5.0x10^-6 in/in/f

NOTE: JSLAB models a thermal gradient by application of a calibrated moment along the slab edges due to the temperature variation. WESLIQID, WESLAYER, and ILLISLAB use an interative computation routine to model the effects of thermal gradient.

1 lb = 2.205kg, 1 psi = 6.894 kPa, and °C = 5/9(°F-32)

Table 41. WESLIQID and WESLAYER curling analysis.

WESLIQUID CURLING ANALYSIS RESULTS

PROGRAM: JSLAB
RESULTS FOR CURLING ANALYSIS WITHOUT TRAFFIC LOAD
MAXIMUM PRINCIPAL SLAB STRESS

SLAB THICKNESS (INCH)	SLAB SIZE (FT.)	SUBGRADE "K" VALUE (PCI) 50	50	200	200	500	500
		TEMPERATURE GRADIENT (DEGREES F/INCH) 1.5	-3.0	1.5	-3.0	1.5	-3.0
8.0	12 x 15	69.2	121.5	120.1	184.4	147.9	227.6
8.0	12 x 20	121.3	223.9	166.1	278.5	182.4	302.6
10.0	12 x 15	52.9	95.1	102.0	157.9	129.2	191.2
10.0	12 x 20	108.1	201.3	165.1	279.3	192.4	320.8
10.0	12 x 25	159.3	303.4	205.6	364.0	219.9	388.3
10.0	12 x 30	191.2	373.5	217.4	410.6	221.0	413.9
14.0	12 x 15	31.7	60.7	71.0	111.9	94.0	136.5
14.0	12 x 20	76.8	145.6	133.6	221.1	164.0	246.3

Note: A positive temperature gradient is defined as slab bottom temperature higher than slab top temperature.

Unit Weight of Concrete = 0.0868 lb/in^3
Concrete Coefficient of Expansion = 5.0x10^-6 in/in/f

WESLAYER CURLING ANALYSIS RESULTS

PROGRAM: WESLAYER
RESULTS FOR CURLING ANALYSIS WITHOUT TRAFFIC LOAD
MAXIMUM PRINCIPAL SLAB STRESS

SLAB THICKNESS (INCH)	SLAB SIZE (FT.)	SUBGRADE "K" VALUE (PCI) 50	50	200	200	500	500
		TEMPERATURE GRADIENT (DEGREES F/INCH) 1.5	-3.0	1.5	-3.0	1.5	-3.0
8.0	12 x 15	49.7	189.6	119.0	267.0	142.4	282.6
8.0	12 x 20	91.0	264.5	155.3	312.0	172.2	314.2
10.0	12 x 15	35.8	160.8	102.1	220.6	129.1	231.3
10.0	12 x 20	79.7	254.1	155.8	347.4	180.8	367.6
10.0	12 x 25	152.1	370.1	209.7	399.7	220.4	403.1
10.0	12 x 30	149.9	389.4	204.2	411.0	213.3	410.2
14.0	12 x 15	15.6	112.2	71.4	157.7	94.5	165.2
14.0	12 x 20	50.9	200.8	127.6	262.8	110.9	269.9

Note: A positive temperature gradient is defined as slab bottom temperature higher than slab top temperature.

Unit Weight of Concrete = 0.0868 lb/in^3
Concrete Coefficient of Expansion = 5.0x10^-6 in/in/f

(1 lb = 2.205 kg, 1 psi = 6.894 kPa and °C = 5/9 (°F-32)

Table 42. Analysis of RISC.

PAVEMENT SECTION RESPONSES	RISC ANALYSIS FOR STANDARD PAVEMENT SECTION	COMPARISON OF SINGLE SLAB ANALYSIS OF ILLISLAB (ELASTIC SOLID) TO RISC FOR THE STANDARD THICKNESS	
		RISC	ILLISLAB
DEFLECTION (in)	0.0128	0.0131	0.0120
SLAB STRESS (psi)	165.4	166.9	136.4
SUBGRADE STRESS (psi)	2.14	2.13	3.28
LOAD TRANSFER EFFICIENCY	25 %		

(1 in = 25.4 mm and 1 psi = 6.894 kPa)

NOTE: RISC was run only twice due to excessive execution times.

Table 43. Effect of subgrade strength and pavement thickness on pavement response as measured by H-51.

H-51
EFFECT OF SUBGRADE VALUE
ON PAVEMENT STRESS

POSITION	STANDARD K=200	K=500	% DIFF	K=100	% DIFF	K=50	% DIFF
LONG. A	254.2	218.9	13.9	286.4	-12.7	318.7	-25.4
TRANS. A	-27.7	-53.7	93.9	8.4	-130.3	33.2	-219.9
B	169.8	147.1	13.4	192.6	-13.4	217.7	-28.2
C	158.0	133.5	15.5	179.3	-13.5	211.9	-34.1
D	171.8	154.2	10.2	190.3	-10.8	211.8	-23.3

H-51
EFFECT OF THICKNESS
ON PAVEMENT STRESS

POSITION	STANDARD H=9 IN.	H=6 IN.	% DIFF	H=12 IN.	% DIFF	H=15 IN.	% DIFF
LONG. A	254.2	470.3	-85.0	166.0	34.7	117.2	53.9
TRANS. A	-27.7	-135.6	389.5	7.5	-127.1	14.3	-151.6
B	169.8	314.6	-85.3	111.6	34.3	80.5	52.6
C	158.0	283.6	-79.5	105.4	33.3	78.6	50.3
D	171.8	332.9	-93.8	109.8	36.1	77.7	54.8

Table 44. CMS capabilities.

C M S

DUE TO LACK OF DATA THE PROGRAM WAS RUN FOR CONDITIONS IN URBANA, ILLINOIS FOR THE MONTH OF APRIL. THE FOLLOWING GRAPH SHOWS THE TEMPERATURE GRADIENT THROUGH THE SLAB ON APRIL 13 1986 AT 11:00 PM. THE PROGRAM CALCULATES:

1) RESILENT MODULUS PROFILE WITH DEPTH OF EACH DAY AT EACH TIME SPECIFIED,
2) DEGREE DAYS PROFILE WITH DEPTH OF EACH DAY AT EACH TIME SPECIFIED,
3) MOISTURE PROFILE WITH DEPTH AT SPECIFIED TIME, AND
4) THE LOCATION OF FROST LINES AT THE SPECIFIED TIME.

(1 lb = 2.205 kg and 1 in = 25.4 mm)

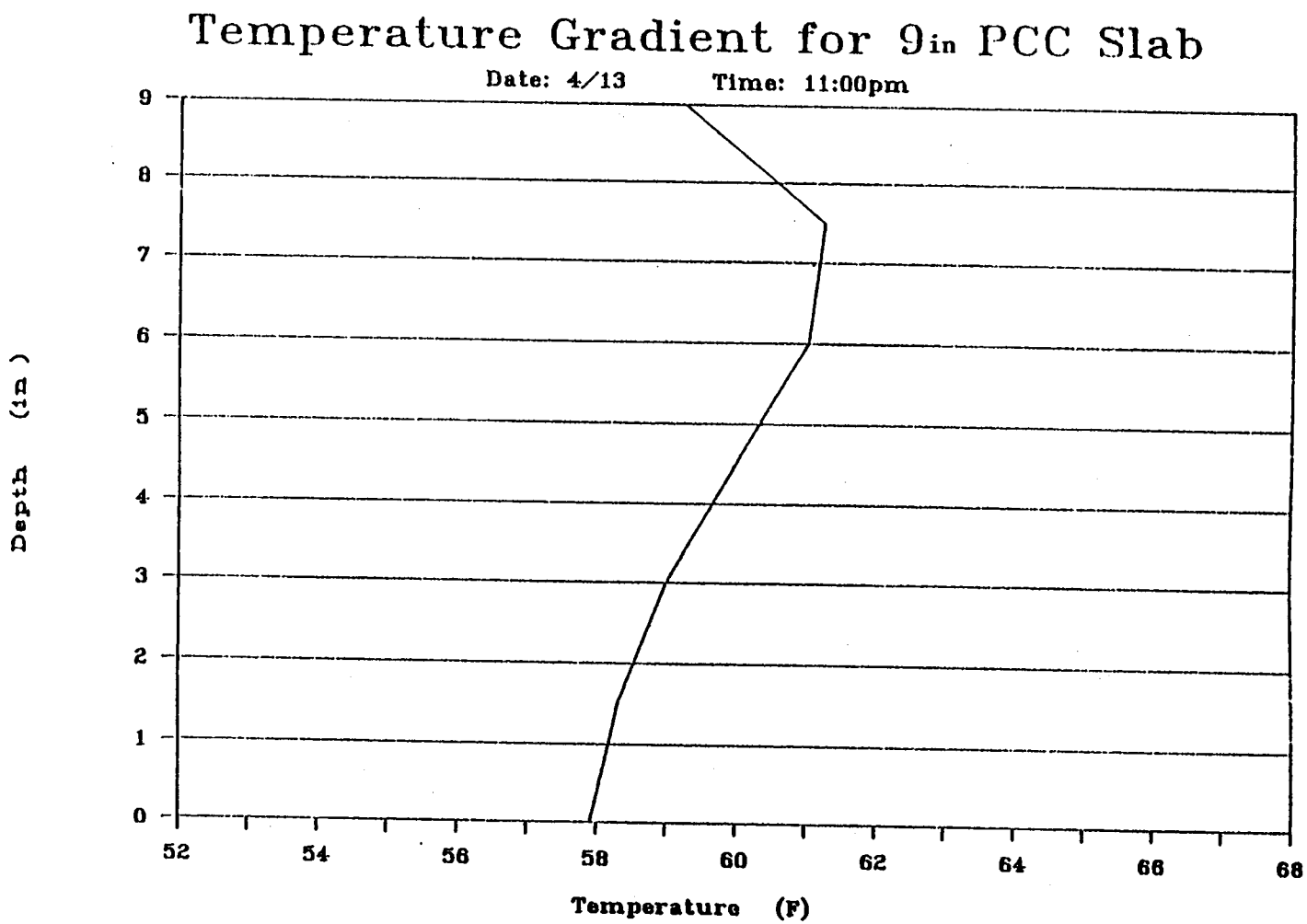

(1 in = 25.4 mm and °C = 5/9(°F-32)

Figure 15. Temperature gradient as measured by CMS.

Table 45. Effect of subgrade strength and slab thickness on cracking and PSR of JPCP as measured by PREDICT.

PREDICT
EFFECT OF K-VALUE AND SLAB THICKNESS
ON CRACKING OF JPCP

CRACKING (FT./MILE)

SUBGRADE k-VALUE	BASE COURSE	SUBGRADE SOIL	AGE/ESAL	THICKNESS 9 IN.	THICKNESS 6 IN.	% DIFF	THICKNESS 12 IN.	% DIFF	THICKNESS 15 IN.	% DIFF
200.0	GRANULAR	FINE	10/1.5	138.0	1709.0	1138.4	32.0	-76.8	10.0	-92.8
		GRAINED	20/5	367.0	17600.0	4695.6	61.0	-83.4	18.0	-95.1
100.0	GRANULAR	FINE	10/1.5	181.0	3075.0	1598.9	40.0	-77.9	12.0	-93.4
		GRAINED	20/5	549.0	17600.0	3105.8	78.0	-85.8	23.0	-95.8
50.0	GRANULAR	FINE	10/1.5	234.0	5570.0	2280.3	50.0	-78.6	15.0	-93.6
		GRAINED	20/5	825.0	17600.0	2033.3	100.0	-87.9	28.0	-96.6
400.0	STABILIZED	FINE	10/1.5	104.0	965.0	827.9	25.0	-76.0	8.0	-92.3
		GRAINED	20/5	246.0	8403.0	3315.9	47.0	-80.9	14.0	-94.3
300.0	GRANULAR	COURSE	10/1.5	117.0	1123.0	859.8	28.0	-76.1	9.0	-92.3
		GRAINED	20/5	286.0	9268.0	3140.6	52.0	-81.8	16.0	-94.4
500.0	STABILIZED	COURSE	10/1.5	94.0	765.0	713.8	23.0	-75.5	7.0	-92.6
		GRAINED	20/5	214.0	5214.0	2336.4	43.0	-79.9	13.0	-93.9

PREDICT
EFFECT OF K-VALUE AND SLAB THICKNESS
ON PSR OF JPCP

PSR (0 TO 5)

SUBGRADE k-VALUE	BASE COURSE	SUBGRADE SOIL	AGE/ESAL	THICKNESS 9 IN.	THICKNESS 6 IN.	% DIFF	THICKNESS 12 IN.	% DIFF	THICKNESS 15 IN.	% DIFF
200.0	GRANULAR	FINE	10/1.5	3.7	3.5	-5.4	4.0	8.1	4.3	16.2
		GRAINED	20/5	3.6	3.2	-11.1	3.9	8.3	4.3	19.4
100.0	GRANULAR	FINE	10/1.5	3.7	3.5	-5.4	4.0	8.1	4.2	13.5
		GRAINED	20/5	3.5	3.2	-8.6	3.9	11.4	4.2	20.0
50.0	GRANULAR	FINE	10/1.5	3.7	3.4	-8.1	3.9	5.4	4.2	13.5
		GRAINED	20/5	3.5	3.1	-11.4	3.8	8.6	4.1	17.1
400.0	STABILIZED	FINE	10/1.5	3.8	3.5	-7.9	4.1	7.9	4.3	13.2
		GRAINED	20/5	3.6	3.3	-8.3	4.0	11.1	4.4	22.2
300.0	GRANULAR	COURSE	10/1.5	3.8	3.5	-7.9	4.0	5.3	4.3	13.2
		GRAINED	20/5	3.6	3.2	-11.1	4.0	11.1	4.3	19.4
500.0	STABILIZED	COURSE	10/1.5	3.8	3.5	-7.9	4.1	7.9	4.4	15.8
		GRAINED	20/5	3.6	3.3	-8.3	4.0	11.1	4.4	22.2

(1 in = 25.4 mm, 1 kip = 80 kN, and 1 psi = 6.894 kPa)

Table 46. Effect of subgrade strength and slab thickness on pumping and faulting of JPCP as measured by PREDICT.

PREDICT
EFFECT OF K-VALUE AND SLAB THICKNESS
ON PUMPING OF JPCP

PUMPING (0=LOW,3=HIGH)

SUBGRADE k-VALUE	BASE COURSE	SUBGRADE SOIL	AGE/ESAL	THICKNESS 9 IN.	THICKNESS 6 IN.	% DIFF	THICKNESS 12 IN.	% DIFF	THICKNESS 15 IN.	% DIFF
200.0	GRANULAR	FINE	10/1.5	1.0	2.4	140.0	0.4	-60.0	0.2	-80.0
		GRAINED	20/5	1.6	3.0	87.5	0.7	-56.3	0.3	-81.3
100.0	GRANULAR	FINE	10/1.5	1.0	2.4	140.0	0.4	-60.0	0.2	-80.0
		GRAINED	20/5	1.6	3.0	87.5	0.7	-56.3	0.3	-81.3
50.0	GRANULAR	FINE	10/1.5	1.0	2.4	140.0	0.4	-60.0	0.2	-80.0
		GRAINED	20/5	1.6	3.0	87.5	0.7	-56.3	0.3	-81.3
400.0	STABILIZED	FINE	10/1.5	1.0	2.4	140.0	0.4	-60.0	0.2	-80.0
		GRAINED	20/5	1.6	3.0	87.5	0.7	-56.3	0.3	-81.3
300.0	GRANULAR	COURSE	10/1.5	0.6	2.0	233.3	0.1	-83.3	0.0	-100.0
		GRAINED	20/5	1.1	3.0	172.7	0.2	-81.8	0.0	-100.0
500.0	STABILIZED	COURSE	10/1.5	0.6	2.0	233.3	0.1	-83.3	0.0	-100.0
		GRAINED	20/5	1.1	3.0	172.7	0.2	-81.8	0.0	-100.0

PREDICT
EFFECT OF K-VALUE AND SLAB THICKNESS
ON FAULTING OF JPCP

FAULTING (INCHES)

SUBGRADE k-VALUE	BASE COURSE	SUBGRADE SOIL	AGE/ESAL	THICKNESS 9 IN.	THICKNESS 6 IN.	% DIFF	THICKNESS 12 IN.	THICKNESS 15 IN.
200	GRANULAR	FINE	10/1.5	0.02	0.04	100	0	0
		GRAINED	20/5	0.02	0.05	150	0	0
100	GRANULAR	FINE	10/1.5	0.02	0.04	100	0	0
		GRAINED	20/5	0.02	0.05	150	0	0
50	GRANULAR	FINE	10/1.5	0.02	0.04	100	0	0
		GRAINED	20/5	0.02	0.05	150	0	0
400	STABILIZED	FINE	10/1.5	0	0	0	0	0
		GRAINED	20/5	0	0.01	N/A	0	0
300	GRANULAR	COURSE	10/1.5	0.02	0.04	100	0	0
		GRAINED	20/5	0.02	0.05	150	0	0
500	STABILIZED	COURSE	10/1.5	0	0	0	0	0
		GRAINED	20/5	0	0.01	N/A	0	0

(1 in = 25.4 mm, 1 kip = 80 kN, and 1 lb = 2.205 kg)

Table 47. Effect of climatic region on distresses of JPCP as measured by PREDICT.

PREDICT
EFFECT OF CLIMATIC REGION
ON PAVEMENT DISTRESS OF JPCP

CLIMATIC REGION	AGE/ESAL	PUMPING 0=LO 3=HI	FAULTING INCHES	CRACKING FT./MILE	JT. DET. NO./MILE	PSR 0 TO 5
III-A	10/1.5	1	0.02	138	1	3.7
	20/5	1.6	0.02	367	12	3.6
II-A	10/1.5	1.1	0.02	158	1	3.7
	20/5	1.9	0.02	403	12	3.3
I-A	10/1.5	1.2	0.02	132	1	3.6
	20/5	2.1	0.02	356	12	3.1
III-B	10/1.5	0.4	0	86	1	3.8
	20/5	0.7	0	168	12	3.7
II-B	10/1.5	0.6	0	102	1	3.7
	20/5	1	0	196	12	3.4
I-B	10/1.5	0.7	0	91	1	3.6
	20/5	1.3	0	178	12	3.3
III-C	10/1.5	0.5	0	66	1	3.8
	20/5	0.8	0	128	12	3.7
II-C	10/1.5	0.6	0	71	1	3.7
	20/5	1.1	0	137	12	3.5
I-C	10/1.5	0.8	0	53	1	3.7
	20/5	1.3	0	105	12	3.3

* JOINT DETERIORATION WAS NOT AFFECTED BY THE PRESCENCE OF SUBDRAINS

+ PSR WAS NOT AFFECTED BY THE PRESCENCE OF SUBDRAINS

(1 kip = 80 kN and 1 in = 25.4 mm)

Table 48. Specific variables for the nine climatic zones.(5)

Thermal Climates	Moist Climates		
	Dry (III)	Seasonally Wet (II)	Wet (I)
Freeze (A)	III-A *Prec : 30 Frze : 650 Temp : 8.3 T.R. : 41	II-A Prec : 61 Frze : 650 Temp : 9.4 T.R. : 44	I-A Prec : 89 Frze : 650 Temp : 8.9 T.R. : 40
Freeze-Thaw (B)	III-B Prec : 46 Frze : 75 Temp : 16.7 T.R. : 33	II-B Prec : 88 Frze : 50 Temp : 15 T.R. : 36	I-B Prec : 122 Frze : 75 Temp : 15 T.R. : 34
No Freeze Activity (C)	III-C Prec : 61 Frze : 0 Temp : 21.7 T.R. : 29	II-C Prec : 102 Frze : 0 Temp : 21.1 T.R. : 30	I-C Prec : 142 Frze : 0 Temp : 18.9 T.R. : 26

*NOTES: Prec = Mean annual precipitation, cms
Frze = Corps of Engineers Freezing Index, degree-days
Temp = Mean annual temprature, degree C
T.R. = Temperature range (difference between ave. daily max temp in July and ave. daily min. temp. in January), degree C

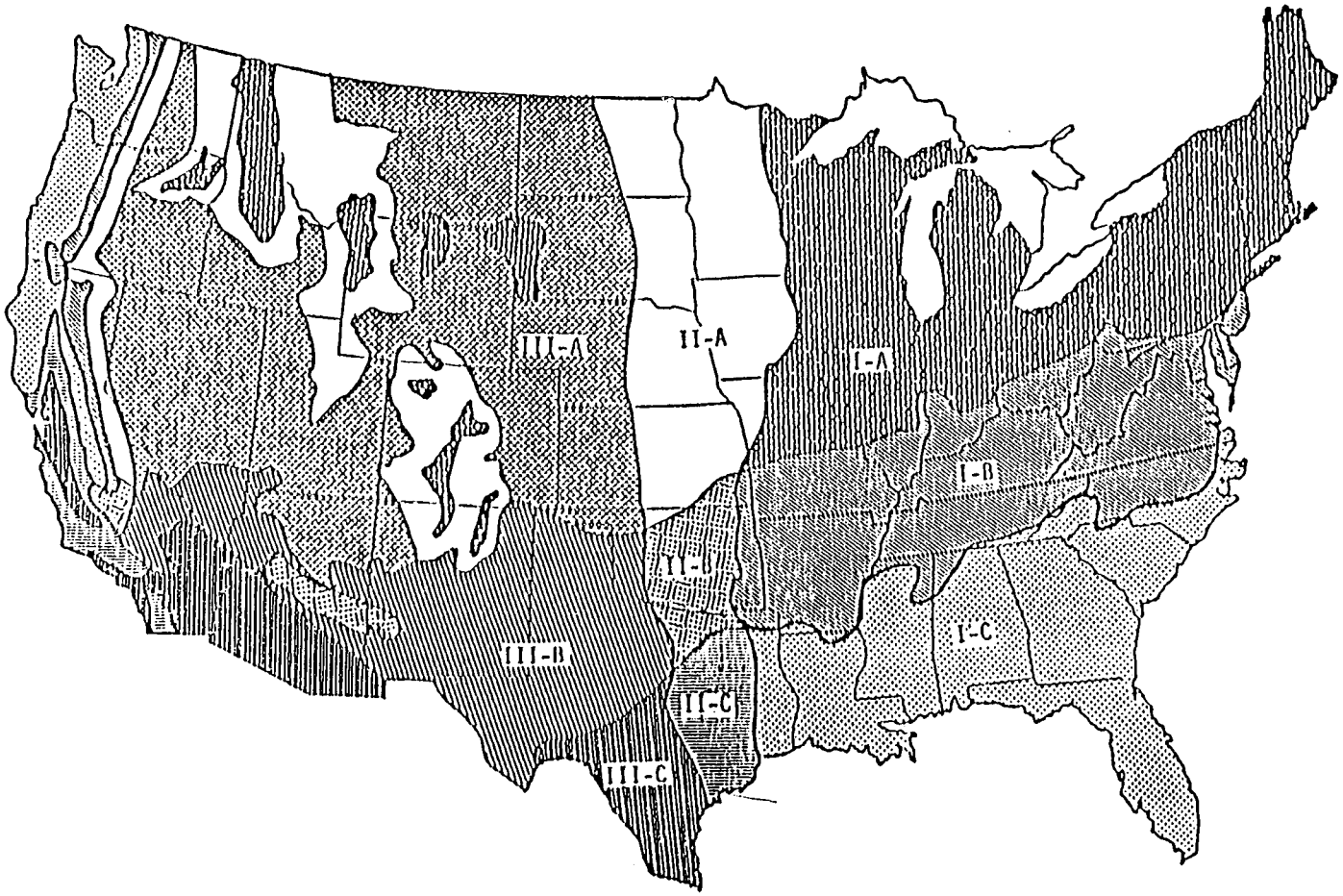

Figure 16. Climatic zones based on Thornthwaite potential evapotranspiration and moisture index and their interaction with performance, with similar performance expected in similar climatic regions.(5)

Table 49. Effect of climatic region on distresses of JRCP as measured by PREDICT.

PREDICT
EFFECT OF CLIMATIC REGION
ON PAVEMENT DISTRESS OF JRCP

CLIMATIC REGION	AGE/ESAL	PUMPING	FAULTING	CRACKING	JOINT DETER.	PSR
III-A	10/1.5	0.0	0.0	75.0	8.0	3.9
	20/5	0.0	0.0	265.0	43.0	3.5
II-A	10/1.5	0.3	0.0	75.0	8.0	3.8
	20/5	0.7	0.1	266.0	43.0	3.4
I-A	10/1.5	0.6	0.0	75.0	8.0	3.8
	20/5	1.4	0.1	280.0	43.0	3.2
III-B	10/1.5	0.0	0.0	74.0	6.0	3.9
	20/5	0.0	0.0	264.0	31.0	3.4
II-B	10/1.5	0.4	0.0	74.0	6.0	3.8
	20/5	1.0	0.0	266.0	31.0	3.3
I-B	10/1.5	0.7	0.0	75.0	6.0	3.7
	20/5	1.6	0.1	295.0	31.0	3.1
III-C	10/1.5	0.0	0.0	74.0	6.0	3.9
	20/5	0.0	0.0	263.0	30.0	3.4
II-C	10/1.5	0.3	0.0	74.0	6.0	3.8
	20/5	0.6	0.0	264.0	30.0	3.3
I-C	10/1.5	0.5	0.0	74.0	6.0	3.7
	20/5	1.2	0.1	270.0	30.0	3.1

RESULTS FOR PAVEMENT WITH SUBDRAINS

(1 kip = 80 kN and 1 in = 25.4 mm)

Table 50. Effect of climatic region on distress of JRCP as measured by PREDICT.

PREDICT
EFFECT OF CLIMATIC REGION
ON PAVEMENT DISTRESS OF JRCP

CLIMATIC REGION	AGE/ESAL	PUMPING	FAULTING	CRACKING	JOINT DETER.	PSR
III-A	10/1.5	0.00	0.02	75.00	8.00	3.90
	20/5	0.00	0.04	265.00	43.00	3.50
II-A	10/1.5	0.50	0.03	75.00	8.00	3.80
	20/5	1.10	0.05	269.00	43.00	3.40
I-A	10/1.5	0.80	0.03	75.00	8.00	3.80
	20/5	1.80	0.06	315.00	43.00	3.20
III-B	10/1.5	0.10	0.02	74.00	6.00	3.90
	20/5	0.20	0.04	264.00	31.00	3.40
II-B	10/1.5	0.60	0.02	74.00	6.00	3.80
	20/5	1.30	0.05	276.00	31.00	3.30
I-B	10/1.5	0.90	0.03	76.00	6.00	3.70
	20/5	2.00	0.06	353.00	31.00	3.10
III-C	10/1.5	0.00	0.02	74.00	6.00	3.90
	20/5	0.00	0.04	263.00	30.00	3.40
II-C	10/1.5	0.40	0.02	74.00	6.00	3.80
	20/5	1.00	0.04	266.00	30.00	3.30
I-C	10/1.5	0.70	0.02	74.00	6.00	3.70
	20/5	1.60	0.05	290.00	30.00	3.10

RESULTS FOR PAVEMENT WITHOUT SUBDRAINS

(1 kip = 80 kN and 1 in = 25.4 mm)

Table 51. Effect of subdrainage on JRCP distress as measured by PREDICT.

PREDICT RESULTS IN THE 9 CLIMATIC REGIONS (REINFORCED PAVEMENT) FOR:

CLIMATIC REGION	AGE/ESAL	PUMPING (0-LOW,3-HIGH) LONG. SUBDRAINS YES	PUMPING LONG. SUBDRAINS NO	PUMPING PERCENT DIFF	FAULTING (INCHES) LONG. SUBDRAINS YES	FAULTING LONG. SUBDRAINS NO	FAULTING PERCENT DIFF	CRACKING (FT./MILE) LONG. SUBDRAINS YES	CRACKING LONG. SUBDRAINS NO	CRACKING PERCENT DIFF	JOINT DETER. (NO/MILE) * NO LONG SUBDRAINS	PSR (0 TO 5) + NO LONG. SUBDRAINS
III-A	10/1.5	0.0	0.0	0.0	0.0	0.0	0.0	75.0	75.0	0.0	8.0	3.9
	20/5	0.0	0.0	0.0	0.0	0.0	0.0	265.0	265.0	0.0	43.0	3.5
II-A	10/1.5	0.3	0.5	66.7	0.0	0.0	50.0	75.0	75.0	0.0	8.0	3.8
	20/5	0.7	1.1	57.1	0.1	0.1	0.0	266.0	269.0	1.1	43.0	3.4
I-A	10/1.5	0.6	0.8	33.3	0.0	0.0	0.0	75.0	75.0	0.0	8.0	3.8
	20/5	1.4	1.8	28.6	0.1	0.1	20.0	280.0	315.0	12.5	43.0	3.2
III-B	10/1.5	0.0	0.1	N/A	0.0	0.0	0.0	74.0	74.0	0.0	6.0	3.9
	20/5	0.0	0.2	N/A	0.0	0.0	0.0	264.0	264.0	0.0	31.0	3.4
II-B	10/1.5	0.4	0.6	50.0	0.0	0.0	0.0	74.0	74.0	0.0	6.0	3.8
	20/5	1.0	1.3	30.0	0.0	0.1	25.0	266.0	276.0	3.8	31.0	3.3
I-B	10/1.5	0.7	0.9	28.6	0.0	0.0	50.0	75.0	76.0	1.3	6.0	3.7
	20/5	1.6	2.0	25.0	0.1	0.1	20.0	295.0	353.0	19.7	31.0	3.1
III-C	10/1.5	0.0	0.0	0.0	0.0	0.0	0.0	74.0	74.0	0.0	6.0	3.9
	20/5	0.0	0.0	0	0.0	0.0	0.0	263.0	263.0	0.0	30.0	3.4
II-C	10/1.5	0.3	0.4	33.3	0.0	0.0	0.0	74.0	74.0	0.0	6.0	3.8
	20/5	0.6	1.0	66.7	0.0	0.0	0.0	264.0	266.0	0.8	30.0	3.3
I-C	10/1.5	0.5	0.7	40.0	0.0	0.0	0.0	74.0	74.0	0.0	6.0	3.7
	20/5	1.2	1.6	33.3	0.1	0.1	0.0	270.0	290.0	7.4	30.0	3.1

* JOINT DETERIORATION WAS NOT AFFECTED BY THE PRESCENCE OF SUBDRAINS

\+ PSR WAS NOT AFFECTED BY THE PRESCENCE OF SUBDRAINS

(1 kip = 80 kN and 1 in = 25.4 mm)

Table 52. Effect of subgrade strength on JPCP distress as measured by PEARDARP.

PEARDARP: EFFECT OF SUBGRADE STRENGTH ON PAVEMENT DISTRESSES

FAULTING (AVG. IN.)

YEAR END	ESAL MILLIONS	STANDARD STAB K=200	STAB K=400	% DIFF	STAB K=500	% DIFF	UNSTAB K=300	% DIFF
5.0	3.389	0.024	0.024	0.000	0.024	0.000	0.025	4.167
10.0	7.512	0.028	0.028	0.000	0.028	0.000	0.030	7.143
15.0	12.528	0.033	0.033	0.000	0.033	0.000	0.035	6.061

SPALLS (NO. OF JOINTS)

YEAR END	ESAL MILLIONS	STANDARD STAB K=200	STAB K=400	% DIFF	STAB K=500	% DIFF	UNSTAB K=300	% DIFF
5.0	3.389	6.000	6.000	0.000	6.000	0.000	6.000	0.000
10.0	7.512	45.000	45.000	0.000	45.000	0.000	45.000	0.000
15.0	12.528	133.000	133.000	0.000	133.000	0.000	133.000	0.000

CRACKING (FEET)

YEAR END	ESAL MILLIONS	STANDARD STAB K=200	STAB K=400	% DIFF	STAB K=500	% DIFF	UNSTAB K=300	% DIFF
5.0	3.389	217.000	0.000	-100.000	0.000	-100.000	579.000	166.820
10.0	7.512	472.000	0.000	-100.000	0.000	-100.000	785.000	66.314
15.0	12.528	621.000	0.000	-100.000	0.000	-100.000	895.000	44.122

PUMPING (JOINTS)

YEAR END	ESAL MILLIONS	STANDARD STAB K=200	STAB K=400	% DIFF	STAB K=500	% DIFF	UNSTAB K=300	% DIFF
5.0	3.389	84.000	84.000	0.000	84.000	0.000	112.000	33.333
10.0	7.512	171.000	171.000	0.000	171.000	0.000	212.000	23.977
15.0	12.528	270.000	270.000	0.000	270.000	0.000	318.000	17.778

PUMPING (VOLUME FEET^3)

YEAR END	ESAL MILLIONS	STANDARD STAB K=200	STAB K=400	% DIFF	STAB K=500	% DIFF	UNSTAB K=300	% DIFF
5.0	3.389	251.000	251.000	0.000	251.000	0.000	337.000	34.263
10.0	7.512	514.000	514.000	0.000	514.000	0.000	637.000	23.930
15.0	12.528	810.000	810.000	0.000	810.000	0.000	955.000	17.901

PSI

YEAR END	ESAL MILLIONS	STANDARD STAB K=200	STAB K=400	% DIFF	STAB K=500	% DIFF	UNSTAB K=300	% DIFF
5.0	3.389	4.420	4.500	1.810	4.500	1.810	4.330	-2.036
10.0	7.512	3.840	4.170	8.594	4.190	9.115	3.810	-0.781
15.0	12.528	3.280	3.690	12.500	3.730	13.720	3.290	0.305

(1 kip = 80 kN, 1 in = 25.4 mm, 1 lb. = 2.205 kg)

Table 53. Effect of pavement thickness on JPCP distress as measured by PEARDARP.

PEARDARP: EFFECT OF THICKNESS ON PAVEMENT DISTRESSES

FAULTING (AVG. IN.)

YEAR END	ESAL MILLIONS	STANDARD 9 IN.	12 IN.	% DIFF	15 IN.	% DIFF	6 IN.	% DIFF
5.0	3.389	0.024	0.016	-33.333	0.014	-41.666		
10.0	7.512	0.028	0.016	-42.857	0.012	-57.142		
15.0	12.528	0.033	0.016	-51.515	0.012	-63.636		

SPALLS (NO. OF JOINTS)

YEAR END	ESAL MILLIONS	STANDARD 9 IN.	12 IN.	% DIFF	15 IN.	% DIFF	6 IN.	% DIFF
5.0	3.389	6	6	0	6	0		
10.0	7.512	45	45	0	45	0		
15.0	12.528	133	133	0	133	0		

CRACKING (FEET)

YEAR END	ESAL MILLIONS	STANDARD 9 IN.	12 IN.	% DIFF	15 IN.	% DIFF	6 IN.	% DIFF
5.0	3.389	217	0	-100	0	-100		
10.0	7.512	472	0	-100	0	-100		
15.0	12.528	621	0	-100	0	-100		

PUMPING (JOINTS)

YEAR END	ESAL MILLIONS	STANDARD 9 IN.	12 IN.	% DIFF	15 IN.	% DIFF	6 IN.	% DIFF
5.0	3.389	84	14	-83.333	2	-97.619		
10.0	7.512	171	29	-83.040	5	-97.076		
15.0	12.528	270	46	-82.962	7	-97.407		

PUMPING (VOLUME FEET^3)

YEAR END	ESAL MILLIONS	STANDARD 9 IN.	12 IN.	% DIFF	15 IN.	% DIFF	6 IN.	% DIFF
5.0	3.389	251	41	-83.665	6	-97.609		
10.0	7.512	514	86	-83.268	14	-97.276		
15.0	12.528	810	138	-82.962	22	-97.283		

PSI

YEAR END	ESAL MILLIONS	STANDARD 9 IN.	12 IN.	% DIFF	15 IN.	% DIFF	6 IN.	% DIFF
5.0	3.389	4.42	4.5	1.80995	4.5	1.80995		
10.0	7.512	3.84	4.5	17.1875	4.5	17.1875		
15.0	12.528	3.28	4.45	35.6707	4.5	37.1951		

(1 kip = 80 kN and 1 in = 25.4 mm)

Table 54. Effect of various inputs on fatigue damage as measured by JCP-1.

JCP1: EFFECT OF PAVEMENT THICKNESS ON FATIGUE DAMAGE

YEAR END	STANDARD 9 IN.	6 IN.	12 IN.	15 IN.
5.0	3.14E+03	3.60E+08	2.37E-01	1.84E-03
10.0	2.55E+03	3.90E+08	2.16E-01	1.84E-03
15.0	2.73E+03	4.68E+08	2.25E-01	1.95E-03
20.0	3.13E+03	5.73E+08	2.41E-01	2.08E-03

JCP1: EFFECT OF SUBGRADE STRENGTH ON FATIGUE DAMAGE

YEAR END	STANDARD K=200	K=50	K=100	K=500
5.0	3.14E+03	1.82E+04	1.02E+04	7.04E+02
10.0	2.55E+03	1.43E+04	8.11E+03	5.87E+02
15.0	2.73E+03	1.54E+04	8.67E+03	6.25E+02
20.0	3.13E+03	1.80E+04	1.00E+04	7.10E+02

JCP1: EFFECT OF CLIMATIC ZONE ON FATIGUE DAMAGE

YEAR END	STANDARD WTFZ/DRFZ	WET NO FREZ	DRY NO FREZ
5.0	3.14E+03	3.12E+03	2.20E+03
10.0	2.55E+03	2.53E+03	1.82E+03
15.0	2.73E+03	2.73E+03	1.98E+03
20.0	3.13E+03	3.18E+03	2.32E+03

JCP1: EFFECT OF SLAB LENGTH ON FATIGUE DAMAGE

YEAR END	STANDARD 15 FT.	10 FT.	20 FT.
5.0	3.14E+03	5.71E+02	1.61E+04
10.0	2.55E+03	4.64E+02	1.32E+04
15.0	2.73E+03	4.90E+02	1.43E+04
20.0	3.13E+03	5.56E+02	1.67E+04

(1 in = 25.4 mm and 1 lb = 2.205 kg)

Table 55. Effect of various inputs on serviceability as measured by JCP-1.

JCP1: EFFECT OF PAVEMENT THICKNESS ON SERVICEABILITY

YEAR END	STANDARD 9 IN.	12 IN.	% DIFF	15 IN.	% DIFF
5.0	4.1	4.3	4.9	4.4	7.3
10.0	3.4	4.1	20.6	4.2	23.5
15.0	2.7	3.7	37.0	4.1	51.9
20.0	2.2	3.4	54.5	3.9	77.3

NOTE: FOR 6 INCH PAVEMENT SERVICEABILITY WAS TOO LOW FOR THE PAVEMENT TO BE CONSIDERED AN "ADEQUATE STRUCTURE"

JCP1: EFFECT OF SUBGRADE STRENGTH ON SERVICEABILITY

YEAR END	STANDARD K=200	K=50	% DIFF	K=100	% DIFF	K=500	% DIFF
5.0	4.1	4.0	-2.4	4.1	0.0	4.1	0.0
10.0	3.4	3.0	-11.8	3.2	-5.9	3.6	5.9
15.0	2.7	2.2	-18.5	2.4	-11.1	3.0	11.1
20.0	2.2	N/A		2.1	-4.5	2.6	18.2

JCP1: EFFECT CLIMATIC ZONE ON SERVICEABILITY

YEAR END	STANDARD WTFZ/DRFZ	WET NO FREZ	% DIFF	DRY NO FREZ	% DIFF
5.0	4.1	4.1	0.0	4.1	0.0
10.0	3.4	3.4	0.0	3.4	0.0
15.0	2.7	2.7	0.0	2.7	0.0
20.0	2.2	2.2	0.0	2.2	0.0

JCP1:EFFECT OF SLAB LENGTH ON SERVICEABILITY

YEAR END	STANDARD 15 FT.	10 FT.	% DIFF	20 FT.	% DIFF
5.0	4.1	4.1	0.0	4.1	0.0
10.0	3.4	3.4	0.0	3.4	0.0
15.0	2.7	2.7	0.0	2.7	0.0
20.0	2.2	2.2	0.0	2.2	0.0

Table 56. Effect of various inputs on DNPS86 design outputs.

AASHTO: EFFECT OF RESILIENT MODULUS ON DESIGN

AASHTO OUTPUTS	STANDARD 10000	RESILIENT MODULUS 2000	% DIFF	5000	% DIFF	20000	% DIFF	VARIED	% DIFF
EFFECTIVE MODULUS OF SUBGRADE REACTION (K)	263.0	83.0	-68.4	160.0	-39.2	432.0	64.3	174.0	-33.8
REQUIRED SLAB THICKNESS (INCHES)	8.3	8.8	6.2	8.6	3.1	8.0	-3.8	8.5	2.6
ALLOWABLE 18-KIP ESAL REPETITIONS (MILLION)	3.7	3.7	0.0	3.7	0.0	3.7	0.0	3.7	0.0

AASHTO: EFFECT OF RELIABILITY LEVEL ON DESIGN

AASHTO OUTPUTS	STANDARD 95%	RELIABILITY LEVEL 50%	% DIFF	80%	% DIFF	99%	% DIFF
EFFECTIVE MODULUS OF SUBGRADE REACTION (K)	263.0	263.0	0.0	263.0	0.0	263.0	0.0
REQUIRED SLAB THICKNESS (INCHES)	8.3	6.3	-23.9	7.3	-11.9	9.2	10.8
ALLOWABLE 18-KIP ESAL REPETITIONS (MILLION)	3.7	3.7	0.0	3.7	0.0	3.7	0.0

AASHTO: EFFECT OF SWELLING AND/OR FROST HEAVE ON DESIGN

AASHTO OUTPUTS	STANDARD NONE	WITH SWELL	% DIFF	WITH FROST HEAVE	% DIFF	WITH BOTH	% DIFF
EFFECTIVE MODULUS OF SUBGRADE REACTION (K)	263.0	263.0	0.0	263.0	0.0	263.0	0.0
REQUIRED SLAB THICKNESS (INCHES)	8.3	8.6	3.6	8.5	2.5	8.9	6.7
ALLOWABLE 18-KIP ESAL REPETITIONS (MILLION)	3.7	3.7	0.0	3.7	0.0	3.7	0.0

AASHTO: EFFECT OF BASE AND SLAB REINFORCEMENT ON DESIGN

AASHTO OUTPUTS	STANDARD STAB.	GRAN. BASE	% DIFF	NO BASE	% DIFF	REINFORCED SLAB	% DIFF
EFFECTIVE MODULUS OF SUBGRADE REACTION (K)	263.0	148.0	-43.7	160.0	-39.2	263.0	0.0
REQUIRED SLAB THICKNESS (INCHES)	8.3	8.6	3.5	8.6	3.1	8.3	0.0
ALLOWABLE 18-KIP ESAL REPETITIONS (MILLION)	3.7	3.7	0.0	3.7	0.0	3.7	0.0

(1 lb = 2.205 kg, 1 in = 25.4 mm, and 1 kip = 80 kN)

Table 57. Effect of loss of support, drainage factor, and ESAL's on design using DNPS 86.

AASHTO: EFFECT OF LOSS OF SUPPORT AND DRAINAGE ON

AASHTO OUTPUTS	STANDARD 1.0/6.00	LOSS OF SUPPORT/DRAINAGE FACTORS 0.5/6.00	% DIFF	1.0/0	% DIFF
EFFECTIVE MODULUS OF SUBGRADE REACTION (K)	263.0	483.0	83.7	263.0	0.0
REQUIRED SLAB THICKNESS (INCHES)	8.3	7.9	-4.9	8.3	0.0
ALLOWABLE 18-KIP ESAL REPETITIONS (MILLION)	3.7	3.7	0.0	3.7	0.0

AASHTO: EFFECT OF INITIAL ESAL ON DESIGN

AASHTO OUTPUTS	STANDARD 1.0/6.00	INITIAL ESAL 750000	% DIFF
EFFECTIVE MODULUS OF SUBGRADE REACTION (K)	263.0	263.0	0.0
REQUIRED SLAB THICKNESS (INCHES)	8.3	10.0	19.8
ALLOWABLE 18-KIP ESAL REPETITIONS (MILLION)	3.7	11.2	200.0

Table 58. Effect of various inputs on RPS-3 outputs.

RPS-3: EFFECT OF SUBGRADE STRENGTH ON DESIGN REQUIREMENTS

DESIGN REQUIREMENTS	STANDARD K=200				K=50				K=100				K=500			
	1	2	3	4	1	2	3	1	2	3	4	5	1	2	3	4
SLAB THICKNESS (IN.)	13.00	12.00	11.00	13.00	13.00	13.00	12.00	13.00	13.00	12.00	11.00	12.00	13.00	12.00	11.00	10.00
SUBBASE THICKNESS (IN.)	0.00	3.00	5.00	3.00	0.00	3.00	3.00	0.00	3.00	3.00	9.00	10.00	0.00	3.00	3.00	7.00
INITIAL LIFE (YEARS)	20.40	21.07	21.01	43.73	25.65	20.50	22.90	26.71	30.59	25.64	21.17	20.13	30.66	26.15	23.70	20.00
TOTAL PERFORMANCE LIFE (YEARS)	20.40	21.07	21.01	43.73	25.65	20.50	22.90	26.71	30.59	25.64	21.17	20.13	30.66	26.15	23.70	20.00
SPACING TRANS. JOINTS (FT.)	60.00	60.00	40.00	40.00	60.00	60.00	40.00	60.00	60.00	40.00	40.00	60.00	60.00	60.00	40.00	50.00
SPACING LONG. JOINTS (FT.)	12.00	12.00	12.00	12.00	12.00	12.00	12.00	12.00	12.00	12.00	12.00	12.00	12.00	12.00	12.00	12.00

RPS-3: EFFECT OF CONFIDENCE LEVEL ON DESIGN REQUIREMENTS

DESIGN REQUIREMENTS	STANDARD				50%				80%				99%			
	1	2	3	4	1	2	3	4	1	2	3	4	1	2	3	4
SLAB THICKNESS (IN.)	13.00	12.00	11.00	13.00	10.00	9.00	10.00	8.00	11.00	10.00	11.00	9.00	13.00	12.00	11.00	13.00
SUBBASE THICKNESS (IN.)	0.00	3.00	5.00	3.00	0.00	3.00	3.00	7.00	0.00	3.00	3.00	10.00	0.00	3.00	5.00	3.00
INITIAL LIFE (YEARS)	20.40	21.07	21.01	43.73	25.11	25.70	29.44	20.06	21.23	21.91	25.00	20.19	20.40	21.07	21.01	43.73
TOTAL PERFORMANCE LIFE (YEARS)	20.40	21.07	21.01	43.73	25.11	25.70	29.44	20.06	21.23	21.91	25.00	20.19	20.40	21.07	21.01	43.73
SPACING TRANS. JOINTS (FT.)	60.00	60.00	40.00	40.00	70.00	50.00	70.00	50.00	60.00	50.00	60.00	50.00	60.00	60.00	40.00	40.00
SPACING LONG. JOINTS (FT.)	12.00	12.00	12.00	12.00	12.00	12.00	12.00	12.00	12.00	12.00	12.00	12.00	12.00	12.00	12.00	12.00

RPS-3: EFFECT OF CLIMATIC REGION ON DESIGN REQUIREMENTS

DESIGN REQUIREMENTS	STANDARD WET-FREEZE				DRY-FREEZE				WET-NONFREEZE				DRY-NONFREEZE			
	1	2	3	4	1	2	3	4	1	2	3	4	1	2	3	4
SLAB THICKNESS (IN.)	13.00	12.00	11.00	13.00	13.00	12.00	11.00	13.00	13.00	12.00	11.00	13.00	13.00	12.00	11.00	13.00
SUBBASE THICKNESS (IN.)	0.00	3.00	5.00	3.00	0.00	3.00	5.00	3.00	0.00	3.00	5.00	3.00	0.00	3.00	5.00	3.00
INITIAL LIFE (YEARS)	20.40	21.07	21.01	43.73	20.40	21.07	21.01	43.73	20.40	21.07	21.01	43.73	20.40	21.07	21.01	43.73
TOTAL PERFORMANCE LIFE (YEARS)	20.40	21.07	21.01	43.73	20.40	21.07	21.01	43.73	20.40	21.07	21.01	43.73	20.40	21.07	21.01	43.73
SPACING TRANS. JOINTS (FT.)	60.00	60.00	40.00	40.00	60.00	60.00	40.00	40.00	60.00	60.00	40.00	40.00	60.00	60.00	40.00	40.00
SPACING LONG. JOINTS (FT.)	12.00	12.00	12.00	12.00	12.00	12.00	12.00	12.00	12.00	12.00	12.00	12.00	12.00	12.00	12.00	12.00

(1 lb = 2.205 kg and 1 in = 25.4 mm)

Table 59. Effect of subgrade strength and load transfer on PCA design outputs.

PCA: EFFECT OF MODULUS OF SUBGRADE REACTION ON DESIGN

PCA OUTPUTS	STANDARD 200	50	% DIFF	MODULUS OF SUBGRADE REACTION 100	% DIFF	500	% DIFF
REQUIRED SLAB THICKNESS (INCHES)	9.5	10.5	10.5	10.0	5.3	8.0	-15.8
TOTAL FATIGUE LIFE USED (%)	90.5	98.8	9.2	95.3	5.3	91.3	0.9

PCA: EFFECT OF LONGITUDINAL AND TRANSVERSE LOAD TRANSFER ON DESIGN

PCA OUTPUTS	STANDARD DOWEL/TIE	NO DOWEL	% DIFF	LOAD TRANSFER NO TIE	% DIFF
REQUIRED SLAB THICKNESS (INCHES)	9.5	11.5	21.1	10.5	10.5
TOTAL FATIGUE LIFE USED (%)	90.5	95.8	5.9	88.5	-2.2

(1 lb = 2.205 kg and 1 in = 25.4 mm)

Table 60. Effect of subgrade strength on California rigid pavement design outputs.

CALIFORNIA RIGID DESIGN: EFFECT OF R-VALUE ON DESIGN

OUTPUTS					
	II II	25	II II	43	III III
REQUIRED SLAB THICKNESS (INCHES)	II II	10.2	II II	10.2	III III
SUBBASE TYPE	II II	CTB/ASB	II II	CTB	III III
SUBBASE THICKNESS	II II	6"/8.4"	II II	6"	III III
R-VALUE	II II	25	II II	43	III III

NOTE: · The surface thickness is a function of the traffic.
The subbase types and thicknesses vary with subgrade conditions.

(1 in = 25.4 mm)

Table 61. Effect of shoulder type and thickness on BERM shoulder design outputs

BERM: EFFECT OF SHOULDER TYPE AND THICKNESS RIGID SHOULDER DESIGN

SHOULDER TYPE	STANDARD TIED	TIED	% DIFF	TIED	TIED	% DIFF	TIED	TIED	% DIFF	TIED	TIED	% DIFF	TIED/ KEYED	TIED	% DIFF	TIED/ KEYED	TIED	% DIFF
THICKNESS (INCHES)	9.0	10.0		11.0			6.0			7.0			8.0			9.0		
DESIGN LIFE (MILLION EAL)																		
INNER EDGE	3.9	6.9		76.9	11.8	202.6	0.5		-88.2	1.0		-74.4	3.8		-2.6	7.5		92.3
OUTER EDGE	3.9	6.9		76.9	11.8	202.6	0.5		-88.2	1.0		-74.4	2.1		-46.2	3.9		0.0

(1 in = 25.4 mm)

Table 62. Effect of various inputs on JCS-1 design outputs.

JCS1: EFFECT OF LOAD TRANSFER EFFICIENCY ON FATIGUE DAMAGE

	PARKED TRAFFIC			ENCROACHED TRAFFIC		
YEAR END	STANDARD 50%	0%	100%	STANDARD 50%	0%	100%
5.0	2.26E+10	2.26E+10	2.28E+10	3.11E-05	2.30E+11	2.31E+11
10.0	2.81E+10	2.81E+10	2.83E+10	2.25E-04	2.86E+12	2.87E+12
15.0	3.37E+10	3.37E+10	3.38E+10	1.58E-03	3.41E+13	3.43E+13
20.0	3.92E+10	3.92E+10	3.94E+10	1.09E-02	3.98E+14	3.99E+14

JCS1: EFFECT OF PAVEMENT THICKNESS ON FATIGUE DAMAGE

	PARKED TRAFFIC				ENCROACHED TRAFFIC			
YEAR END	STANDARD 9 IN.	6 IN.	12 IN.	15 IN.	STANDARD 9 IN.	6 IN.	12 IN.	15 IN.
5.0	2.26E+10	2.26E+10	2.26E+10	2.26E+10	3.11E-05	2.41E-01	3.35E-08	3.06E-10
10.0	2.81E+10	2.81E+10	2.81E+10	2.81E+10	2.25E-04	2.45E+00	1.61E-07	8.47E-10
15.0	3.37E+10	3.37E+10	3.37E+10	3.37E+10	1.58E-03	2.41E+01	7.75E-07	2.43E-09
20.0	3.92E+10	3.92E+10	3.92E+10	3.92E+10	1.09E-02	2.32E+02	3.72E-06	7.25E-09

JCS1: EFFECT OF SUBGRADE STRENGTH ON FATIGUE DAMAGE

	PARKED TRAFFIC				ENCROACHED TRAFFIC			
YEAR END	STANDARD K=200	K=50	K=100	K=500	STANDARD K=200	K=50	K=100	K=500
5.0	2.26E+10	1.82E+04	1.02E+04	7.04E+02	3.11E-05	1.82E+04	1.02E+04	7.04E+02
10.0	2.81E+10	1.43E+04	8.11E+03	5.87E+02	2.25E-04	1.43E+04	8.11E+03	5.87E+02
15.0	3.37E+10	1.54E+04	8.67E+03	6.25E+02	1.58E-03	1.54E+04	8.67E+03	6.25E+02
20.0	3.92E+10	1.80E+04	1.00E+04	7.10E+02	1.09E-02	1.80E+04	1.00E+04	7.10E+02

JCS1: EFFECT OF SHOULDER THICKNESS ON FATIGUE DAMAGE

	PARKED TRAFFIC					ENCROACHED TRAFFIC				
YEAR END	STANDARD 6 IN.	5 IN.	7 IN.	8 IN.	9 IN.	STANDARD 6 IN.	5 IN.	7 IN.	8 IN.	9 IN.
5.0	2.26E+10	1.65E+23	1.32E+03	4.17E-02	4.12E-05	3.11E-05	3.10E-02	9.84E-07	1.21E-07	2.81E-09
10.0	2.81E+10	2.05E+23	1.64E+03	5.18E-02	5.12E-05	2.25E-04	3.02E-01	5.60E-06	5.65E-07	1.11E-07
15.0	3.37E+10	2.45E+23	1.96E+03	6.20E-02	6.12E-05	1.58E-03	2.04E+00	3.12E-05	2.60E-06	4.36E-07
20.0	3.92E+10	2.86E+23	2.28E+03	7.21E-02	7.12E-05	1.09E-02	2.61E+01	1.71E-04	1.19E-05	1.71E-06

(1 in = 25.4 mm and 1 lb = 2.205 kg)

Table 63. Effect of various inputs on the Liu-Lytton drainage models outputs.

LUI-LYTTON DRAINANGE MODELS: EFFECT OPEN JOINTS ON SUBBASE MODULUS

SUBBASE TYPE	PERCENT JOINTS SEALED *	AVERAGE SUBBASE COURSE MODULUS WET STATE (KSI)	AVERAGE SUBBASE COURSE MODULUS DRY STATE (KSI)
CTB 0 % Clay Fines	100%	422.03	425.28
	50%	335.36	424.76
	0%	309.04	424.78
CTB 10 % Clay Fines	100%	422.03	425.28
	50%	335.36	424.76
	0%	309.04	424.61
Crushed Limestone 0 % Clay Fines	100%	207.78	209.29
	50%	168.27	209.05
	0%	155.58	208.98
Crushed Limestone 10 % Clay Fines	100%	207.78	209.29
	50%	168.27	209.01
	0%	155.58	209.92
Gravel 0 % Clay Fines	100%	64.13	64.60
	50%	51.94	64.52
	0%	48.02	64.50
Gravel 10 % Clay Fines	100%	64.13	64.60
	50%	51.94	64.51
	0%	48.02	64.48

* - 100-foot long survey section with 10-foot joint spacing

(1 psi = 6.894 kPa)

Table 64. Effect of various inputs on JRCP4 outputs.

JRCP4: EFFECT OF TEMPERATURE, SLAB LENGTH, AND SLAB THICKNESS.

SLAB LENGTH	SLAB THICKNESS 8"	10"	12"
20'	16.50 * .03241 **	12.76 .03203	10.33 .03192
40'	45.12 .05800	36.73 .05838	30.57 .05904
60'	76.03 .07573	62.43 .07826	53.20 .08042

* Maximum Concrete Stress in the Center of the Slab Before the Crack Occurs (PSI).
** Joint Movement (IN).
Curing Temperature = 45 F.
Minimum Temperature = 5 F.

JRCP4: EFFECT OF TEMPERATURE, SLAB LENGTH, AND SLAB THICKNESS.

SLAB LENGTH	SLAB THICKNESS 8"	10"	12"
20'	14.53 * .02446 **	11.24 .02402	9.12 .02387
40'	38.79 .04311	31.17 .0433	26.41 .04364
60'	64.17 .05543	53.05 .05702	45.14 .05869

* Maximum Concrete Stress in the Center of the Slab Before the Crack Occurs (PSI).
** Joint Movement (IN).
Curing Temperature = 100 F.
Minimum Temperature = 70 F.

(1 im = 25.4 mm and °C = 5/9 (°F-32), and 1 psi = 6.894 kPa)

APPENDIX D

SUMMARY OF ANALYSIS DATA FOR THE EVALUATION OF PREDICTIVE MODELS

1. INTRODUCTION

Under this study, several predictive models were evaluated. These models include the AASHTO design equation, the PEARDARP models, the COPES models, and the PFAULT models. The predictive models were used to generate the predicted values based on site-specific inputs which were obtained from field surveys, construction records, and previously published reports. The actual performance data were measured during the field surveys. This appendix presents the summary tables and graphs resulting from the comprehensive statistical analyses performed to evaluate the predictive models. The design and performance information gathered for each section is summarized in volume IV. Volume II presents the methodology employed in these analyses as well as a detailed explanation of the results.

2. DESCRIPTION OF TABLES AND FIGURES

A multitude of tables and graphs are presented herein to supplement the discussion of volume II. Tables 65 through 69 and figures 17 through 21 represent the results of the analyses of the AASHTO design equation. The results of the analyses of the PEARDARP models are presented in tables 70 through 101 and figures 22 through 52. Tables 102 through 146 and figures 53 through 97 illustrate the analyses of the COPES models, while tables 147 through 157 and figures 98 through 108 represent the results of the PFAULT analysis. Table 158 is an itemized listing of all of the input variables for each section which were used to analyze the various models.

Table 65. Actual ESAL's (based on ADT) versus ESAL's as predicted using the AASHTO design equation for all Phase I sections.

Section ID	Actual ESAL's	Predicted ESAL's	Difference
AZ 1-1	3968618	5390854	1422236
AZ 1-2	3414954	48472076	45057122
AZ 1-4	2387085	73223621	70836536
AZ 1-5	2801246	27569140	24767894
AZ 1-6	2012173	20088394	18076221
AZ 1-7	1522951	15829304	14306353
AZ 2	1622817	26346047	24723230
CA 1-1	7621830	3397328	4224502
CA 1-3	7621830	3998471	3623359
CA 1-5	7621830	96074941	88453111
CA 1-7	7621830	9589304	1967474
CA 1-9	7621830	8719466	1097636
CA 2-2	4423827	4364140	59687
CA 2-3	4423827	706241	3717586
CA 3-1	3641197	2758625	882572
CA 3-2	3641197	5001246	1360049
CA 3-5	3641197	5245140	1603943
CA 6	4434338	7348331	2913993
CA 7	10524966	1445695	9079271
CA 8	5263439	5115692	147747
FL 2	2005755	47913163	45907408
FL 3	5967175	5231660	735515
MI 1-1a	885249	9870400	8985151
MI 1-1b	885249	5551862	4666613
MI 1-4a	885249	4244329	3359080
MI 1-7a	885249	6361392	5476143
MI 1-7b	885249	2468056	1582807
MI 1-10a	885249	2720817	1835568
MI 1-10b	885249	3180672	2295423
MI 1-25	885249	2160668	1275419
MI 3	2768818	5856575	3087757
MI 4-1	4367392	6276089	1908697
MI 4-2	4367392	6420228	2052836
MI 5	3123694	7872373	4748679
MN-1	5518188	3035032	2483156
MN 1-2	5518188	14781654	9263466
MN 1-3	5518188	2122105	3396083
MN 1-4	5518188	2344959	3173229
MN 1-5	5518188	773411	4744777
MN 1-6	5518188	1348804	4169384
MN 1-7	5518188	1302798	4215390
MN 1-8	5518188	4645086	873102
MN 1-9	5518188	1404908	4113280
MN 1-10	5518188	5347315	170873

Table 65. Actual ESAL's (based on ADT) versus ESAL's as predicted using the AASHTO design equation for all Phase I sections (continued).

Section ID	Actual ESAL's	Predicted ESAL's	Difference
MN 1-11	5518188	649608	4868580
MN 1-12	5518188	2337369	3180819
MN 2-1	2785505	3943992	1158487
MN 2-2	2785505	948723	1836782
MN 2-3	2785505	2089325	696180
MN 2-4	2785505	2456677	328828
MN 3	1495624	1963278	467654
MN 4b	218813	907487	688674
MN 5	5518188	5317725	200463
MN 6a	845032	1245151	400119
NJ 2	34813131	12175454	22637677
NJ 3-1	4181394	10146071	5964677
NJ 3-2	4181394	11988764	7807370
NY 1-1	3136345	1338290	1798055
NY 1-3	3136345	4721918	1585573
NY 1-4	3136345	1928422	1207923
NY 1-6	3136345	876615	2259730
NY 1-8a	3136345	1910165	1226180
NY 1-8b	3136345	3092095	44250
NY 2-3	1428074	8862139	7434065
NY 2-9	1428074	4835568	3407494
NY 2-11	1428074	4187432	2759358
NY 2-15	1428074	1986258	558184
NC 1-1	9137389	2254068	6883321
NC 1-2	9137389	3854366	5283023
NC 1-3	9137389	2050734	7086655
NC 1-4	9137389	5128565	4008824
NC 1-5	9137389	1969204	7168185
NC 1-6	9137389	1134801	8002588
NC 1-7	9137389	2041842	7095547
NC 1-8	9137389	1818467	7318922
NC 2	5755336	14685777	8930441
OH 1-1	3424613	2616350	808263
OH 1-3	3424613	1719740	1704873
OH 1-4	3424613	2407985	1016628
OH 1-6	3424613	2595204	829409
OH 1-7	3424613	7018721	3594108
OH 1-9	3424613	4157382	732769
OH 1-10	3424613	5467127	2042514
OH 2-33a	3295668	87540724	84245056
OH 2-33b	3295668	68000765	64705097
PA 1-1	603407	4015023	3411616
PA 1-2	270228	28375209	28104981
PA 1-3	270228	23476741	23206513

Table 65. Actual ESAL's (based on ADT) versus ESAL's as predicted using the AASHTO design equation for all Phase I sections (continued).

Section ID	Actual ESAL's	Predicted ESAL's	Difference
PA 1-4	270228	20266347	19996119
PA 1-5	270228	9456488	9186260
ONT 1-1a	1011133	10920554	9909421
ONT 1-1b	1011133	10920554	9909421
ONT 1-2a	1011133	1164537	153404
ONT 1-2b	1011133	1309615	298482
ONT 1-3a	1011133	1639857	628724
ONT 1-3b	1011133	1639857	628724
ONT 1-4a	1011133	1001419	9714
ONT 1-4b	1011133	908542	102591
ONT 2	35649275	2310396	33338879

Analysis Variable : DIFESAL

N Obs	Mean	Std Error	T	Prob>|T|
99	8845439.92	1672589.92	5.2884690	0.0001

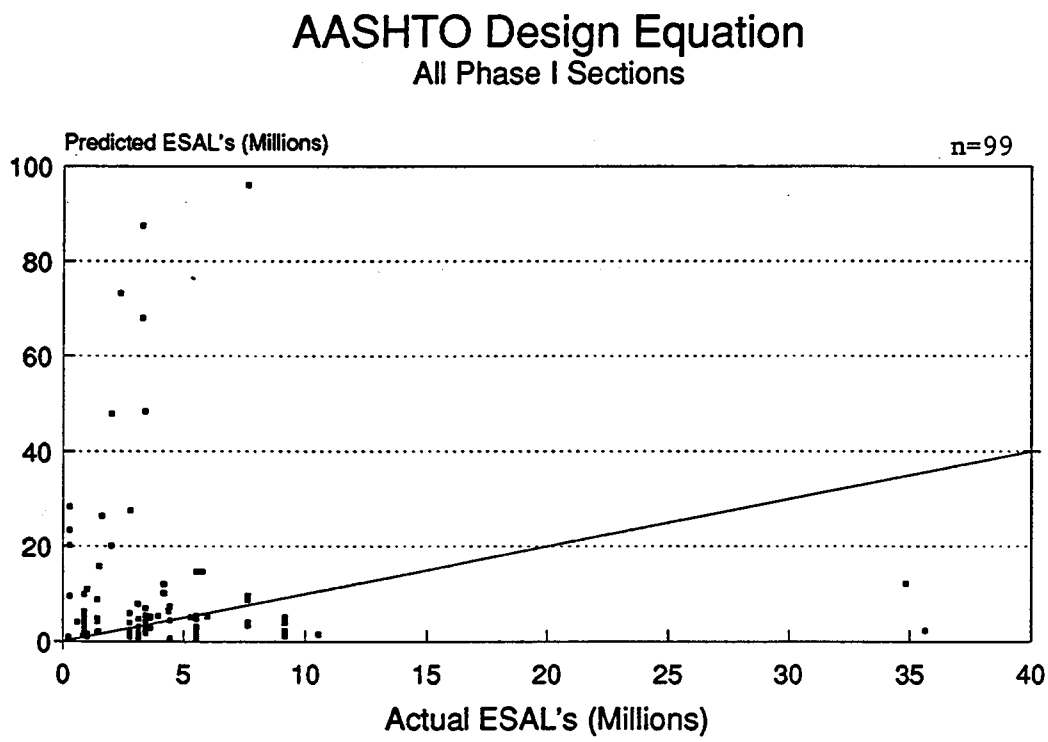

Figure 17. Actual ESAL's (based on ADT) versus ESAL's as predicted using the AASHTO design equation for all Phase I sections.

Table 66. Actual ESAL's (based on ADT) versus ESAL's as predicted using the AASHTO design equation for the dry-freeze region.

Section ID	Actual ESAL's	Predicted ESAL's	Difference
MN 1-1	5518188	3035032	2483156
MN 1-2	5518188	14781654	9263466
MN 1-3	5518188	2122105	3396083
MN 1-4	5518188	2344959	3173229
MN 1-5	5518188	773411	4744777
MN 1-6	5518188	1348804	4169384
MN 1-7	5518188	1302798	4215390
MN 1-8	5518188	4645086	873102
MN 1-9	5518188	1404908	4113280
MN 1-10	5518188	5347315	170873
MN 1-11	5518188	649608	4868580
MN 1-12	5518188	2337369	3180819
MN 2-1	2785505	3943992	1158487
MN 2-2	2785505	948723	1836782
MN 2-3	2785505	2089325	696180
MN 2-4	2785505	2456677	328828
MN 3	1495624	1963278	467654
MN 4b	218813	907487	688674
MN 5	5518188	5317725	200463
MN 6a	845032	1245151	400119

Analysis Variable : DIFESAL

N Obs	Mean	Std Error	T	Prob>|T|
20	2521466.30	517646.83	4.8710166	0.0001

Table 67. Actual ESAL's (based on ADT) versus ESAL's as predicted using the AASHTO design equation for the dry-nonfreeze region.

Section ID	Actual ESAL's	Predicted ESAL's	Difference
AZ 1-1	3968618	5390854	1422236
AZ 1-2	3414954	48472076	45057122
AZ 1-4	2387085	73223621	70836536
AZ 1-5	2801246	27569140	24767894
AZ 1-6	2012173	20088394	18076221
AZ 1-7	1522951	15829304	14306353
AZ 2	1622817	26346047	24723230
CA 1-1	7621830	3397328	4224502
CA 1-3	7621830	3998471	3623359
CA 1-5	7621830	96074941	88453111
CA 1-7	7621830	9589304	1967474
CA 1-9	7621830	8719466	1097636
CA 2-2	4423827	4364140	59687
CA 2-3	4423827	706241	3717586
CA 6	4434338	7348331	2913993
CA 7	10524966	1445695	9079271
CA 8	5263439	5115692	147747

Analysis Variable : DIFESAL

N Obs	Mean	Std Error	T	Prob>|T|
17	18498468.12	6345904.66	2.9150246	0.0101

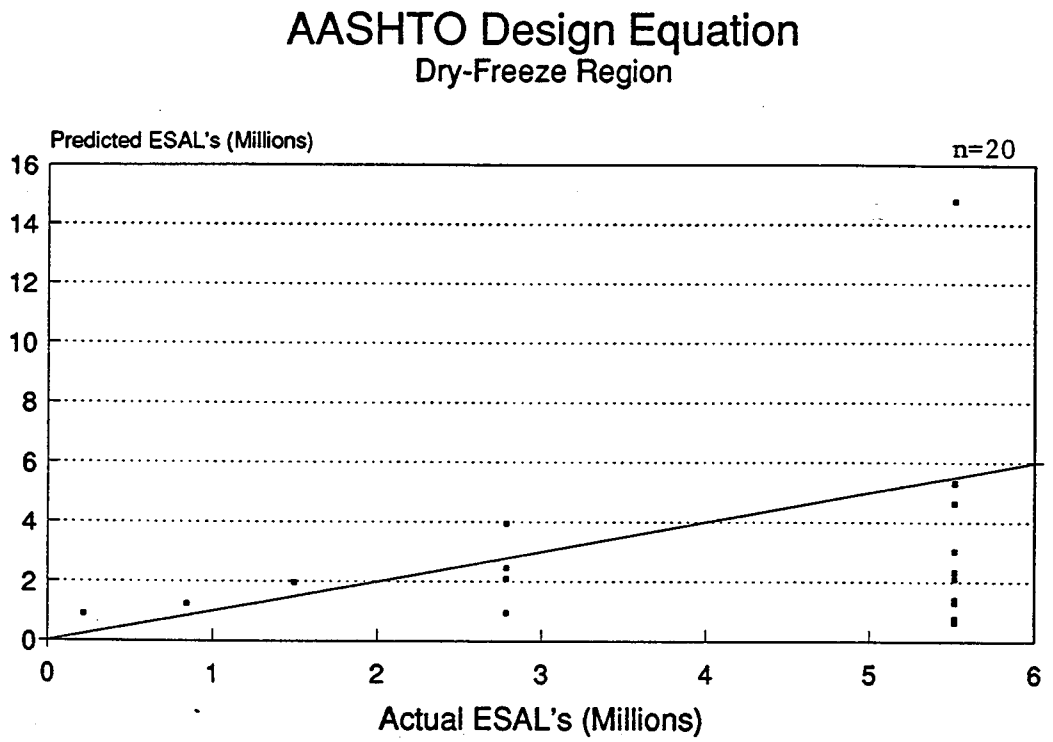

Figure 18. Actual ESAL's (based on ADT) versus ESAL's predicted using the AASHTO Design equation for the dry-freeze region.

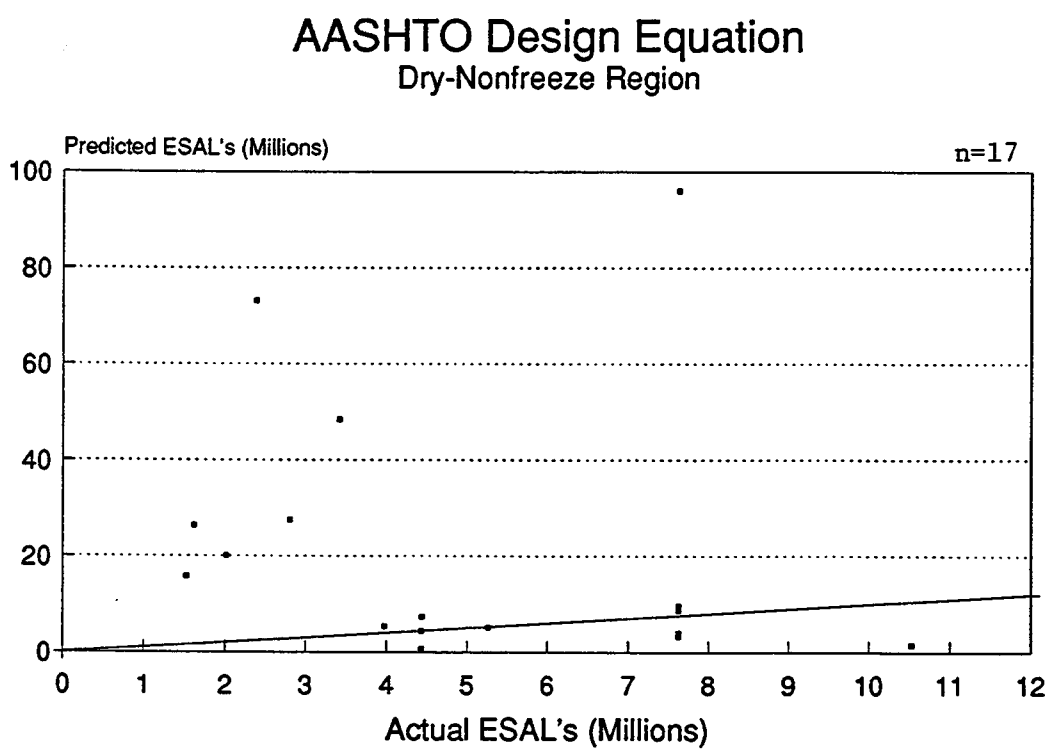

Figure 19. Actual ESAL's (based on ADT) versus ESAL's predicted using the AASHTO design equation for the dry-nonfreeze region.

Table 68. Actual ESAL's (based on ADT) versus ESAL's as predicted using the AASHTO design equation for the wet-freeze region.

Section ID	Actual ESAL's	Predicted ESAL's	Difference
MI 1-1a	885249	9870400	8985151
MI 1-1b	885249	5551862	4666613
MI 1-4a	885249	4244329	3359080
MI 1-7a	885249	6361392	5476143
MI 1-7b	885249	2468056	1582807
MI 1-10a	885249	2720817	1835568
MI 1-10b	885249	3180672	2295423
MI 1-25	885249	2160668	1275419
MI 3	2768818	5856575	3087757
MI 4-1	4367392	6276089	1908697
MI 4-2	4367392	6420228	2052836
MI 5	3123694	7872373	4748679
NJ 2	34813131	12175454	22637677
NJ 3-1	4181394	10146071	5964677
NJ 3-2	4181394	11988764	7807370
NY 1-1	3136345	1338290	1798055
NY 1-3	3136345	4721918	1585573
NY 1-4	3136345	1928422	1207923
NY 1-6	3136345	876615	2259730
NY 1-8a	3136345	1910165	1226180
NY 1-8b	3136345	3092095	44250
NY 2-3	1428074	8862139	7434065
NY 2-9	1428074	4835568	3407494
NY 2-11	1428074	4187432	2759358
NY 2-15	1428074	1986258	558184
OH 1-1	3424613	2616350	808263
OH 1-3	3424613	1719740	1704873
OH 1-4	3424613	2407985	1016628
OH 1-6	3424613	2595204	829409
OH 1-7	3424613	7018721	3594108
OH 1-9	3424613	4157382	732769
OH 1-10	3424613	5467127	2042514
OH 2-33a	3295668	87540724	84245056
OH 2-33b	3295668	68000765	64705097
PA 1-1	603407	4015023	3411616
PA 1-2	270228	28375209	28104981
PA 1-3	270228	23476741	23206513
PA 1-4	270228	20266347	19996119
PA 1-5	270228	9456488	9186260
ONT 1-1a	1011133	10920554	9909421
ONT 1-1b	1011133	10920554	9909421
ONT 1-2a	1011133	1164537	153404
ONT 1-2b	1011133	1309615	298482
ONT 1-3a	1011133	1639857	628724

Table 68. Actual ESAL's (based on ADT) versus ESAL's as predicted using the AASHTO design equation for the wet-freeze region (continued).

Section ID	Actual ESAL's	Predicted ESAL's	Difference
ONT 1-3b	1011133	1639857	628724
ONT 1-4a	1011133	1001419	9714
ONT 1-4b	1011133	908542	102591
ONT 2	35649275	2310396	33338879

Analysis Variable : DIFESAL

N Obs	Mean	Std Error	T	Prob>|T|
48	8302672.40	2308752.11	3.5961732	0.0008

Table 69. Actual ESAL's (based on ADT) versus ESAL's as predicted using the AASHTO design equation for the wet-nonfreeze region.

Section ID	Actual ESAL's	Predicted ESAL's	Difference
CA 3-1	3641197	2758625	882572
CA 3-2	3641197	5001246	1360049
CA 3-5	3641197	5245140	1603943
FL 2	2005755	47913163	45907408
FL 3	5967175	5231660	735515
NC 1-1	9137389	2254068	6883321
NC 1-2	9137389	3854366	5283023
NC 1-3	9137389	2050734	7086655
NC 1-4	9137389	5128565	4008824
NC 1-5	9137389	1969204	7168185
NC 1-6	9137389	1134801	8002588
NC 1-7	9137389	2041842	7095547
NC 1-8	9137389	1818467	7318922
NC 2	5755336	14685777	8930441

Analysis Variable : DIFESAL

N Obs	Mean	Std Error	T	Prob>|T|
14	8019070.93	3014277.08	2.6603629	0.0196

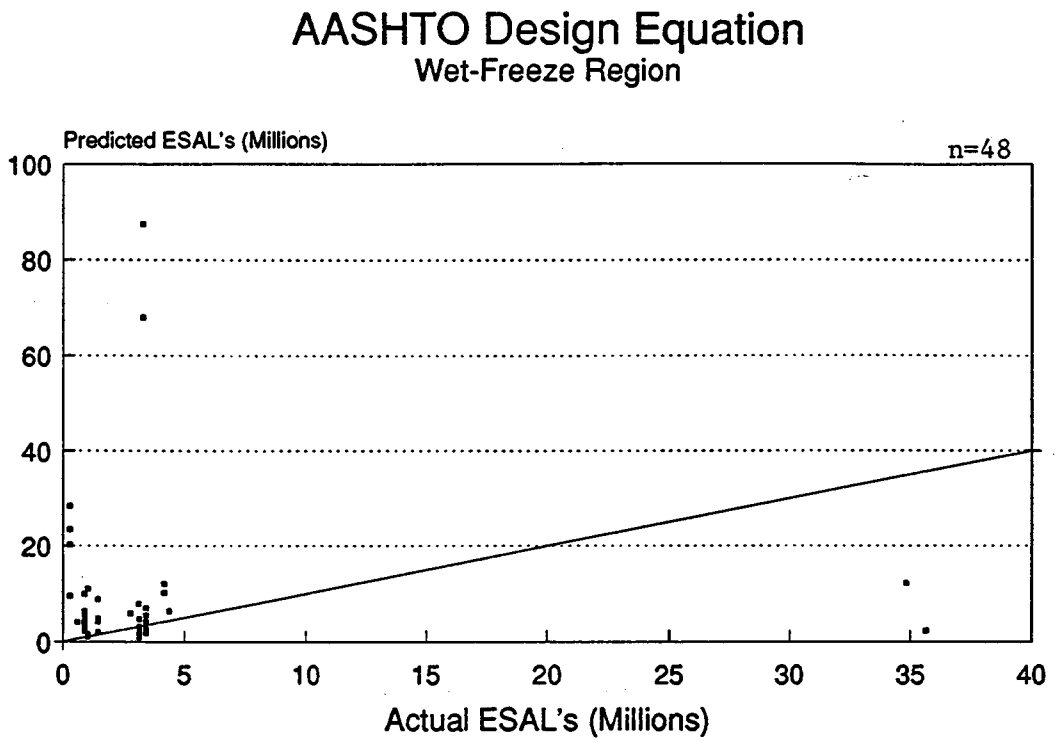

Figure 20. Actual ESAL's (based on ADT) versus ESAL's as predicted using the AASHTO design equation for the wet-freeze region.

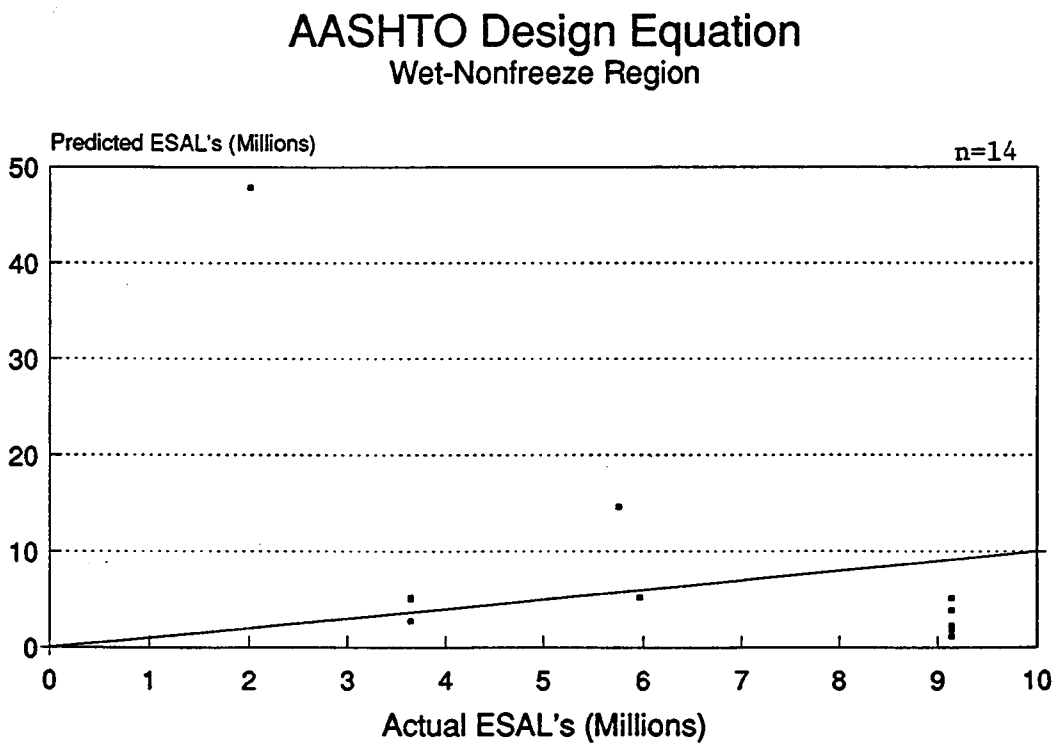

Figure 21. Actual ESAL's (based on ADT) versus ESAL's as predicted using the AASHTO design equation for the wet-nonfreeze region.

Table 70. Actual PSR as determined by a panel of users versus PSI as predicted by the PEARDARP PSI model for all Phase I sections.

Section ID	Measured PSR	Predicted PSI	Difference
AZ 1-1	3.4	3.83840	0.43840
AZ 1-2	3.8	4.61179	0.81179
AZ 1-4	3.6	4.02162	0.42162
AZ 1-5	3.8	4.27845	0.47845
AZ 1-6	3.5	4.09450	0.59450
AZ 1-7	3.8	4.18487	0.38487
AZ 2	3.6	4.50871	0.90871
CA 1-1	2.9	4.01136	1.11136
CA 1-3	3.0	4.09483	1.09483
CA 1-5	2.7	3.75125	1.05125
CA 1-7	2.7	3.97884	1.27884
CA 1-9	2.5	3.76244	1.26244
CA 2-2	3.8	3.95092	0.15092
CA 2-3	4.1	4.01003	0.08997
CA 3-1	3.6	3.51742	0.08258
CA 3-2	3.9	3.98322	0.08322
CA 3-5	3.8	3.97460	0.17460
CA 6	3.4	3.30703	0.09297
CA 7	3.8	4.18935	0.38935
CA 8	3.8	4.16959	0.36959
FL 2	3.7	4.62917	0.92917
FL 3	3.2	4.21346	1.01346
MI 1-1a	3.6	4.09540	0.49540
MI 1-1b	3.3	4.16516	0.86516
MI 1-4a	3.9	4.90967	1.00967
MI 1-7a	3.6	4.73423	1.13423
MI 1-7b	3.7	5.00000	1.30000
MI 1-10a	2.9	4.07975	1.17975
MI 1-10b	2.8	3.97914	1.17914
MI 1-25	2.9	3.31366	0.41366
MI 3	4.8	5.00000	0.20000
MI 4-1	2.4	3.54548	1.14548
MI 4-2	2.4	3.79985	1.39985
MI 5	4.2	5.00000	0.80000
MN 1-1	3.7	4.81157	1.11157
MN 1-2	3.3	3.96843	0.66843
MN 1-3	3.4	4.94663	1.54663
MN 1-4	3.3	3.87900	0.57900
MN 1-5	3.4	4.87743	1.47743
MN 1-6	3.4	3.89595	0.49595
MN 1-7	3.6	5.00000	1.40000
MN 1-8	3.4	4.08421	0.68421
MN 1-9	3.7	4.87483	1.17483
MN 1-10	3.3	3.89619	0.59619
MN 1-11	3.7	4.83348	1.13348
MN 1-12	3.5	3.85523	0.35523
MN 2-1	3.8	4.49176	0.69176
MN 2-2	3.9	4.31084	0.41084

Table 70. Actual PSR as determined by a panel of users versus PSI as predicted by the PEARDARP PSI model for all Phase I sections (continued).

Section ID	Measured PSR	Predicted PSI	Difference
MN 2-3	4.0	4.42467	0.42467
MN 2-4	4.0	4.09948	0.09948
MN 3	3.8	4.97845	1.17845
MN 4b	4.7	5.00000	0.30000
MN 5	3.3	3.98914	0.68914
MN 6a	4.5	4.85733	0.35733
NJ 2	3.8	4.61139	0.81139
NJ 3-1	3.6	3.60393	0.00393
NJ 3-2	3.5	3.39049	0.10951
NY 1-1	4.0	4.76943	0.76943
NY 1-3	3.6	4.36094	0.76094
NY 1-4	3.4	4.18630	0.78630
NY 1-6	3.9	4.30671	0.40671
NY 1-8a	4.1	4.61931	0.51931
NY 1-8b	3.8	4.61179	0.81179
NY 2-3	4.2	4.63033	0.43033
NY 2-9	4.0	4.55597	0.55597
NY 2-11	4.1	4.40455	0.30455
NY 2-15	4.0	4.63557	0.63557
NC 1-1	3.4	4.31035	0.91035
NC 1-2	3.5	4.32475	0.82475
NC 1-3	3.6	4.33677	0.73677
NC 1-4	3.4	4.27845	0.87845
NC 1-5	3.2	3.96187	0.76187
NC 1-6	3.8	4.54283	0.74283
NC 1-7	3.4	4.25623	0.85623
NC 1-8	3.7	4.08872	0.38872
NC 2	4.2	4.61523	0.41523
OH 1-1	4.2	3.88380	0.31620
OH 1-3	4.2	3.96489	0.23511
OH 1-4	4.1	3.70739	0.39261
OH 1-6	4.2	3.96700	0.23300
OH 1-7	4.2	3.79489	0.40511
OH 1-9	4.2	3.86923	0.33077
OH 1-10	4.2	3.72167	0.47833
OH 2-33a	3.4	4.18999	0.78999
OH 2-33b	3.5	4.26394	0.76394
PA 1-1	4.2	4.41345	0.21345
PA 1-2	3.8	4.18487	0.38487
PA 1-3	3.7	3.86887	0.16887
PA 1-4	4.1	3.92323	0.17677
PA 1-5	4.1	4.32643	0.22643
ONT 1-1a	3.8	4.20025	0.40025
ONT 1-1b	3.8	4.65600	0.85600
ONT 1-2a	3.8	4.39160	0.59160
ONT 1-2b	3.7	4.52574	0.82574

Table 70. Actual PSR as determined by a panel of users versus PSI as predicted by the PEARDARP PSI model for all Phase I sections (continued).

Section ID	Measured PSR	Predicted PSI	Difference
ONT 1-3a	3.8	4.72767	0.92767
ONT 1-3b	3.8	4.55802	0.75802
ONT 1-4a	3.7	4.57997	0.87997
ONT 1-4b	3.8	4.45336	0.65336
ONT 2	3.9	3.98322	0.08322

Analysis Variable : DIFPSR

N Obs	Mean	Std Error	T	Prob>|T|
99	0.6487074	0.0375570	17.2726296	0.0001

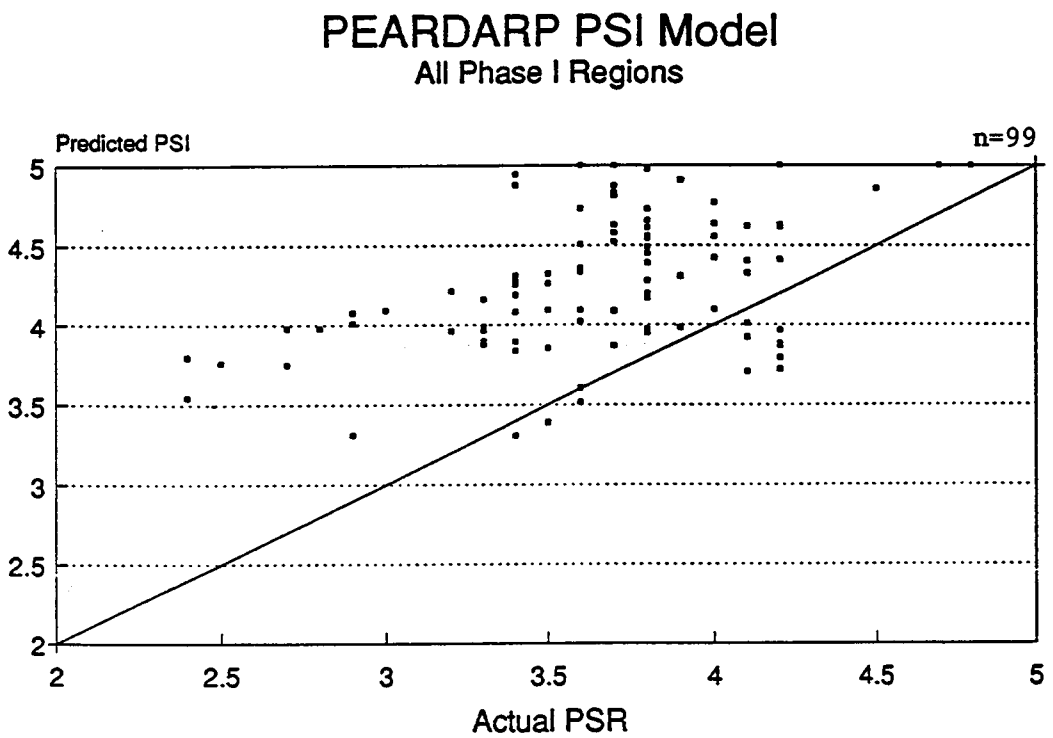

Figure 22. Actual PSR as determined by a panel of users versus PSI as predicted by the PEARDARP PSI model for all Phase I sections.

Table 71. Actual PSR as determined by a panel of users versus PSI as predicted by the PEARDARP PSI model for the dry-freeze region.

Section ID	Actual PSR	Predicted PSI	Difference
MN 1-1	3.7	4.81157	1.11157
MN 1-2	3.3	3.96843	0.66843
MN 1-3	3.4	4.94663	1.54663
MN 1-4	3.3	3.87900	0.57900
MN 1-5	3.4	4.87743	1.47743
MN 1-6	3.4	3.89595	0.49595
MN 1-7	3.6	5.00000	1.40000
MN 1-8	3.4	4.08421	0.68421
MN 1-9	3.7	4.87483	1.17483
MN 1-10	3.3	3.89619	0.59619
MN 1-11	3.7	4.83348	1.13348
MN 1-12	3.5	3.85523	0.35523
MN 2-1	3.8	4.49176	0.69176
MN 2-2	3.9	4.31084	0.41084
MN 2-3	4.0	4.42467	0.42467
MN 2-4	4.0	4.09948	0.09948
MN 3	3.8	4.97845	1.17845
MN 4b	4.7	5.00000	0.30000
MN 5	3.3	3.98914	0.68914
MN 6a	4.5	4.85733	0.35733

Analysis Variable : DIFPSR

N Obs	Mean	Std Error	T	Prob>|T|
20	0.7687315	0.0961522	7.9949480	0.0001

Table 72. Actual PSR as determined by a panel of users versus PSI as predicted by the PEARDARP PSI model for the dry-nonfreeze region.

Section ID	Actual PSR	Predicted PSI	Difference
AZ 1-1	3.4	3.83840	0.43840
AZ 1-2	3.8	4.61179	0.81179
AZ 1-4	3.6	4.02162	0.42162
AZ 1-5	3.8	4.27845	0.47845
AZ 1-6	3.5	4.09450	0.59450
AZ 1-7	3.8	4.18487	0.38487
AZ 2	3.6	4.50871	0.90871
CA 1-1	2.9	4.01136	1.11136
CA 1-3	3.0	4.09483	1.09483
CA 1-5	2.7	3.75125	1.05125
CA 1-7	2.7	3.97884	1.27884
CA 1-9	2.5	3.76244	1.26244
CA 2-2	3.8	3.95092	0.15092
CA 2-3	4.1	4.01003	0.08997
CA 6	3.4	3.30703	0.09297
CA 7	3.8	4.18935	0.38935
CA 8	3.8	4.16959	0.36959

Analysis Variable : DIFPSR

N Obs	Mean	Std Error	T	Prob>|T|
17	0.6429329	0.0987758	6.5090146	0.0001

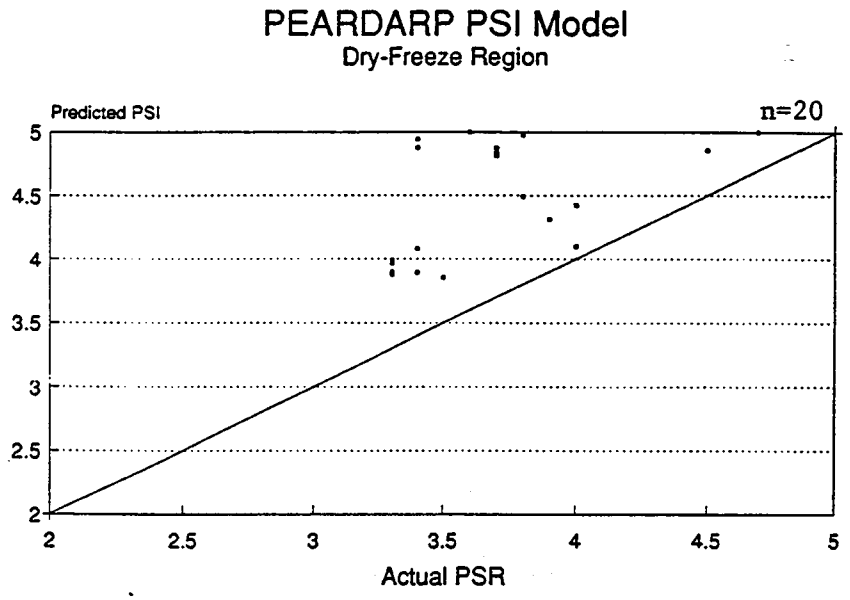

Figure 23. Actual PSR as determined by a panel of users versus PSI as predicted by the PEARDARP PSI model for the dry-freeze region.

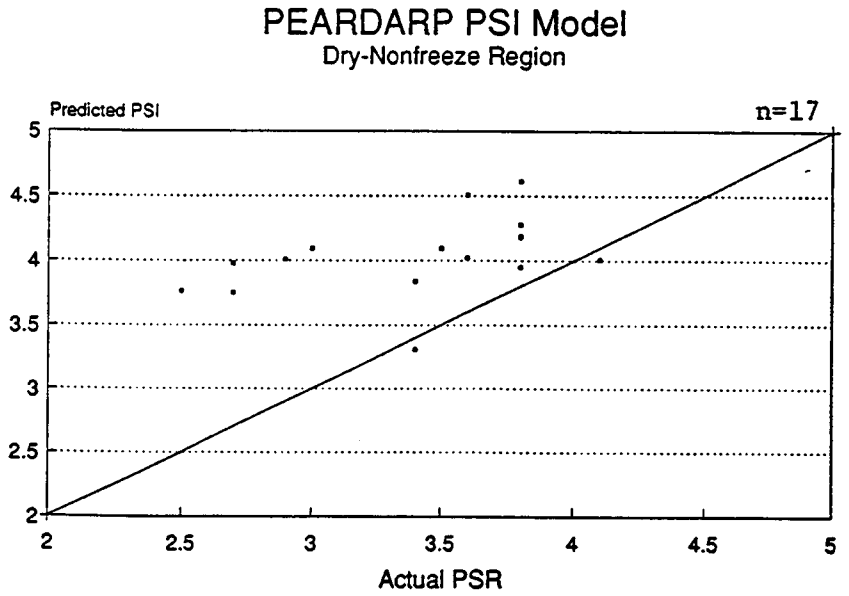

Figure 24. Actual PSR as determined by a panel of users versus PSI as predicted by the PEARDARP PSI model for the dry-nonfreeze region.

Table 73. Actual PSR as determined by a panel of users versus PSI as predicted by the PEARDARP PSI model for the wet-freeze region.

Section ID	Actual PSR	Predicted PSI	Difference
MI 1-1a	3.6	4.09540	0.49540
MI 1-1b	3.3	4.16516	0.86516
MI 1-4a	3.9	4.90967	1.00967
MI 1-7a	3.6	4.73423	1.13423
MI 1-7b	3.7	5.00000	1.30000
MI 1-10a	2.9	4.07975	1.17975
MI 1-10b	2.8	3.97914	1.17914
MI 1-25	2.9	3.31366	0.41366
MI 3	4.8	5.00000	0.20000
MI 4-1	2.4	3.54548	1.14548
MI 4-2	2.4	3.79985	1.39985
MI 5	4.2	5.00000	0.80000
NJ 2	3.8	4.61139	0.81139
NJ 3-1	3.6	3.60393	0.00393
NJ 3-2	3.5	3.39049	0.10951
NY 1-1	4.0	4.76943	0.76943
NY 1-3	3.6	4.36094	0.76094
NY 1-4	3.4	4.18630	0.78630
NY 1-6	3.9	4.30671	0.40671
NY 1-8a	4.1	4.61931	0.51931
NY 1-8b	3.8	4.61179	0.81179
NY 2-3	4.2	4.63033	0.43033
NY 2-9	4.0	4.55597	0.55597
NY 2-11	4.1	4.40455	0.30455
NY 2-15	4.0	4.63557	0.63557
OH 1-1	4.2	3.88380	0.31620
OH 1-3	4.2	3.96489	0.23511
OH 1-4	4.1	3.70739	0.39261
OH 1-6	4.2	3.96700	0.23300
OH 1-7	4.2	3.79489	0.40511
OH 1-9	4.2	3.86923	0.33077
OH 1-10	4.2	3.72167	0.47833
OH 2-33a	3.4	4.18999	0.78999
OH 2-33b	3.5	4.26394	0.76394
PA 1-1	4.2	4.41345	0.21345
PA 1-2	3.8	4.18487	0.38487
PA 1-3	3.7	3.86887	0.16887
PA 1-4	4.1	3.92323	0.17677
PA 1-5	4.1	4.32643	0.22643
ONT 1-1a	3.8	4.20025	0.40025
ONT 1-1b	3.8	4.65600	0.85600
ONT 1-2a	3.8	4.39160	0.59160
ONT 1-2b	3.7	4.52574	0.82574
ONT 1-3a	3.8	4.72767	0.92767
ONT 1-3b	3.8	4.55802	0.75802

Table 73. Actual PSR as determined by a panel of users versus PSI as predicted by the PEARDARP PSI model for the wet-freeze region (continued).

Section ID	Actual PSR	Predicted PSI	Difference
ONT 1-4a	3.7	4.57997	0.87997
ONT 1-4b	3.8	4.45336	0.65336
ONT 2	3.9	3.98322	0.08322

Analysis Variable : DIFPSR

N Obs	Mean	Std Error	T	Prob>|T|
48	0.6066526	0.0503567	12.0470978	0.0001

Table 74. Actual PSR as determined by a panel of users versus PSI as predicted by the PEARDARP PSI model for the wet-nonfreeze region.

Section ID	Actual PSR	Predicted PSI	Difference
CA 3-1	3.6	3.51742	0.08258
CA 3-2	3.9	3.98322	0.08322
CA 3-5	3.8	3.97460	0.17460
FL 2	3.7	4.62917	0.92917
FL 3	3.2	4.21346	1.01346
NC 1-1	3.4	4.31035	0.91035
NC 1-2	3.5	4.32475	0.82475
NC 1-3	3.6	4.33677	0.73677
NC 1-4	3.4	4.27845	0.87845
NC 1-5	3.2	3.96187	0.76187
NC 1-6	3.8	4.54283	0.74283
NC 1-7	3.4	4.25623	0.85623
NC 1-8	3.7	4.08872	0.38872
NC 2	4.2	4.61523	0.41523

Analysis Variable : DIFPSR

N Obs	Mean	Std Error	T	Prob>|T|
14	0.6284444	0.0882623	7.1201886	0.0001

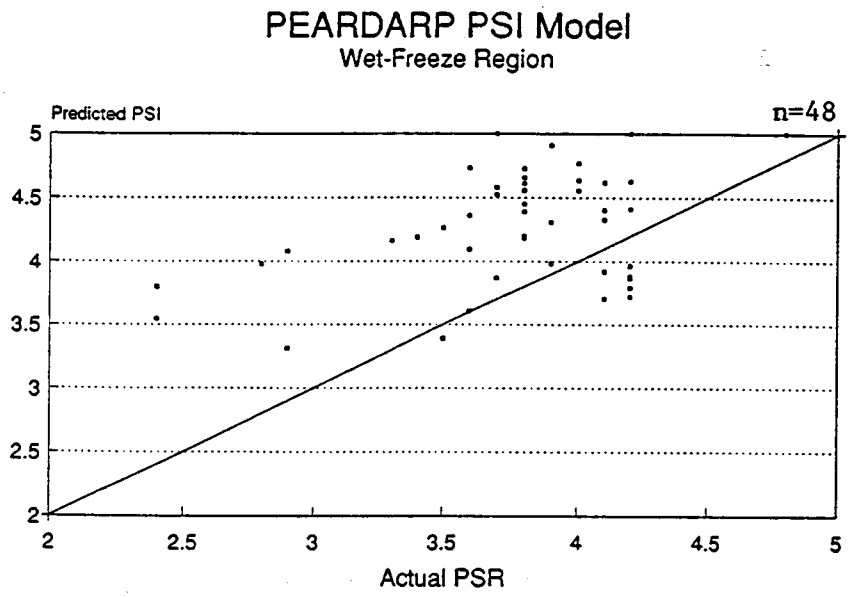

Figure 25. Actual PSR as determined by a panel of users versus PSI as predicted by the PEARDARP PSI model for the wet-freeze region.

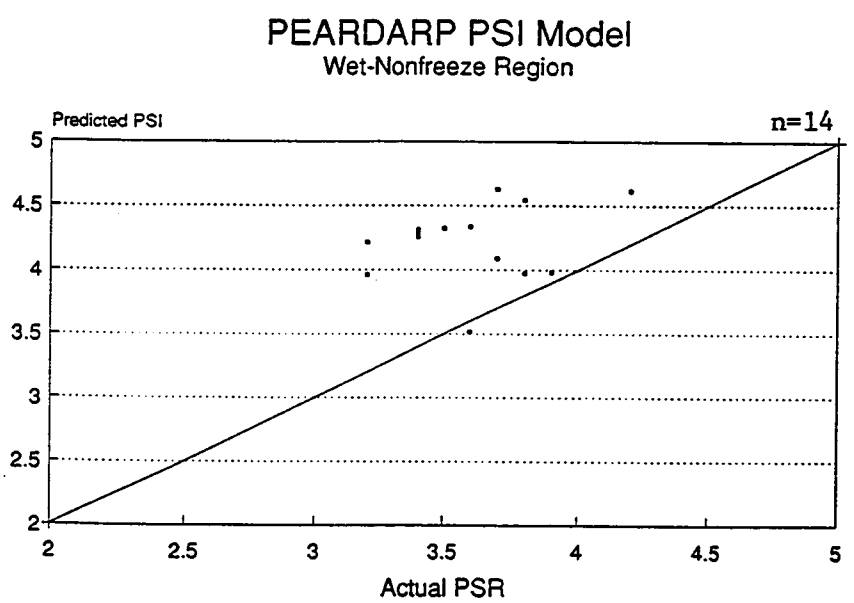

Figure 26. Actual PSR as determined by a panel of users versus PSI as predicted by the PEARDARP PSI model for the wet-nonfreeze region.

Table 75. Actual field measured roughness versus roughness as predicted using the PEARDARP roughness model for all Phase I sections.

Section ID	Actual Mays Roughness	Predicted Roughness	Difference
AZ 1-1	114	190	76
AZ 1-2	65	162	97
AZ 1-4	102	143	41
AZ 1-5	85	155	70
AZ 1-6	97	136	39
AZ 1-7	91	114	23
AZ 2	71	117	46
CA 1-1	102	233	131
CA 1-3	94	220	126
CA 1-5	122	169	47
CA 1-7	102	214	112
CA 1-9	116	215	99
CA 2-2	107	199	92
CA 2-3	98	208	110
CA 3-1	134	191	57
CA 3-2	104	183	79
CA 3-5	102	179	77
CA 6	158	195	37
CA 7	87	216	129
CA 8	92	190	98
FL 2	64	133	69
FL 3	84	215	131
MI 1-1a	96	76	20
MI 1-1b	91	69	22
MI 1-4a	48	77	29
MI 1-7a	58	74	16
MI 1-7b	36	68	32
MI 1-10a	98	70	28
MI 1-10b	104	72	32
MI 1-25	159	72	87
MI 3	37	160	123
MI 4-1	132	207	75
MI 4-2	112	198	86
MI 5	36	174	138
MN 1-1	53	219	166
MN 1-2	104	205	101
MN 1-3	44	225	181
MN 1-4	110	202	92
MN 1-5	46	225	179
MN 1-6	107	215	108
MN 1-7	32	217	185
MN 1-8	93	213	120
MN 1-9	50	216	166
MN 1-10	108	207	99
MN 1-11	50	224	174
MN 1-12	111	225	114
MN 2-1	72	161	89

Table 75. Actual field measured roughness versus roughness as predicted using the PEARDARP roughness model for all Phase I sections (continued).

Section ID	Actual Mays Roughness	Predicted Roughness	Difference
MN 2-2	82	98	16
MN 2-3	76	165	89
MN 2-4	96	160	64
MN 3	44	94	50
MN 4b	37	38	1
MN 5	100	220	120
MN 6a	51	44	7
NJ 2	63	201	138
NJ 3-1	134	199	65
NJ 3-2	153	199	46
NY 1-1	56	177	121
NY 1-3	78	171	93
NY 1-4	90	177	87
NY 1-6	82	177	95
NY 1-8a	64	176	112
NY 1-8b	65	177	112
NY 2-3	61	109	48
NY 2-9	66	104	38
NY 2-11	76	107	31
NY 2-15	63	95	32
NC 1-1	83	201	118
NC 1-2	79	214	135
NC 1-3	77	204	127
NC 1-4	85	203	118
NC 1-5	105	209	104
NC 1-6	69	223	154
NC 1-7	85	244	159
NC 1-8	95	204	109
NC 2	64	186	122
OH 1-1	109	184	75
OH 1-3	106	186	80
OH 1-4	123	185	62
OH 1-6	104	180	76
OH 1-7	115	176	61
OH 1-9	109	176	67
OH 1-10	122	179	57
OH 2-33a	90	156	66
OH 2-33b	85	156	71
PA 1-1	75	66	9
PA 1-2	91	49	42
PA 1-3	113	49	64
PA 1-4	109	50	59
PA 1-5	82	49	33
ONT 1-1a	90	89	1
ONT 1-1b	62	89	27
ONT 1-2a	78	58	20
ONT 1-2b	70	58	12

Table 75. Actual field measured roughness versus roughness as predicted using the PEARDARP roughness model for all Phase I sections (continued).

Section ID	Actual Mays Roughness	Predicted Roughness	Difference
ONT 1-3a	57	58	1
ONT 1-3b	66	58	8
ONT 1-4a	65	36	29
ONT 1-4b	72	36	36
ONT 2	104	214	110

Analysis Variable : DIFRGH

N Obs	Mean	Std Error	T	Prob>|T|
99	79.0404040	4.6819020	16.8821143	0.0001

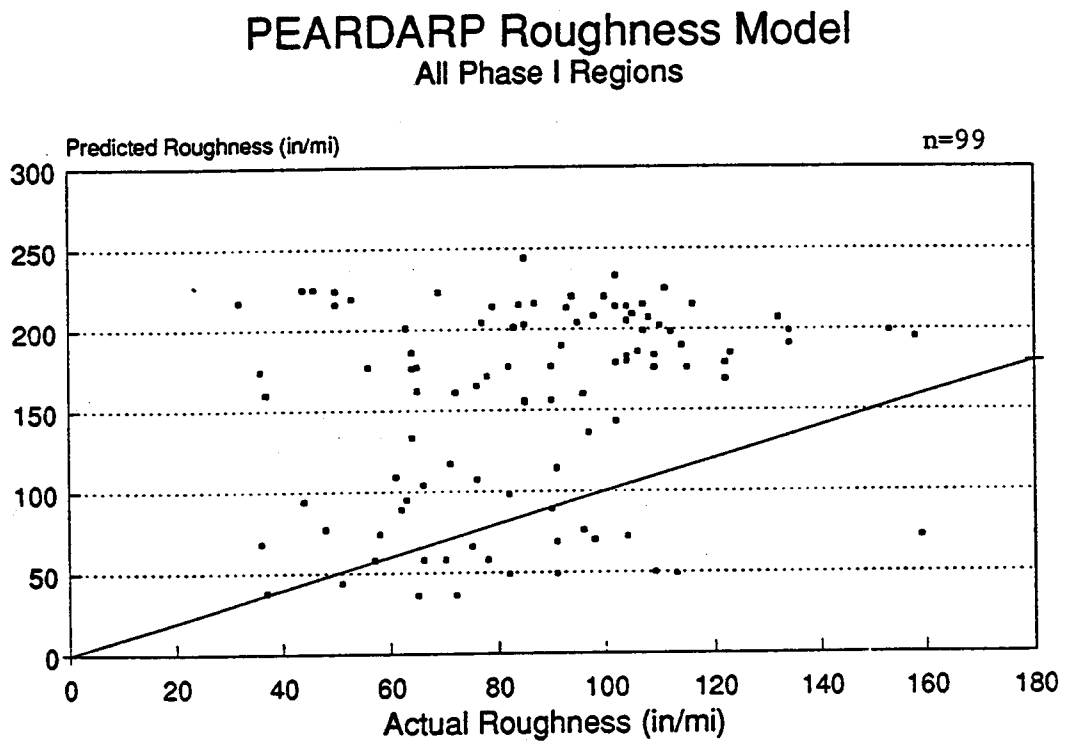

Figure 27. Actual field measured roughness versus roughness as predicted using the PEARDARP roughness model for all Phase I sections.

Table 76. Actual field measured roughness versus roughness as predicted using the PEARDARP roughness model for the dry-freeze region.

Section ID	Actual Mays Roughness	Predicted Roughness	Difference
MN 1-1	53	219	166
MN 1-2	104	205	101
MN 1-3	44	225	181
MN 1-4	110	202	92
MN 1-5	46	225	179
MN 1-6	107	215	108
MN 1-7	32	217	185
MN 1-8	93	213	120
MN 1-9	50	216	166
MN 1-10	108	207	99
MN 1-11	50	224	174
MN 1-12	111	225	114
MN 2-1	72	161	89
MN 2-2	82	98	16
MN 2-3	76	165	89
MN 2-4	96	160	64
MN 3	44	94	50
MN 4b	37	38	1
MN 5	100	220	120
MN 6a	51	44	7

Analysis Variable : DIFRGH

N Obs	Mean	Std Error	T	Prob>|T|
20	106.0500000	12.9932118	8.1619542	0.0001

Table 77. Actual field measured roughness versus roughness as predicted using the PEARDARP roughness model for the dry-nonfreeze region.

Section ID	Actual Mays Roughness	Predicted Roughness	Difference
AZ 1-1	114	190	76
AZ 1-2	65	162	97
AZ 1-4	102	143	41
AZ 1-5	85	155	70
AZ 1-6	97	136	39
AZ 1-7	91	114	23
AZ 2	71	117	46
CA 1-1	102	233	131
CA 1-3	94	220	126
CA 1-5	122	169	47
CA 1-7	102	214	112
CA 1-9	116	215	99
CA 2-2	107	199	92
CA 2-3	98	208	110
CA 6	158	195	37
CA 7	87	216	129
CA 8	92	190	98

Analysis Variable : DIFRGH

N Obs	Mean	Std Error	T	Prob>|T|
17	80.7647059	8.7470707	9.2333432	0.0001

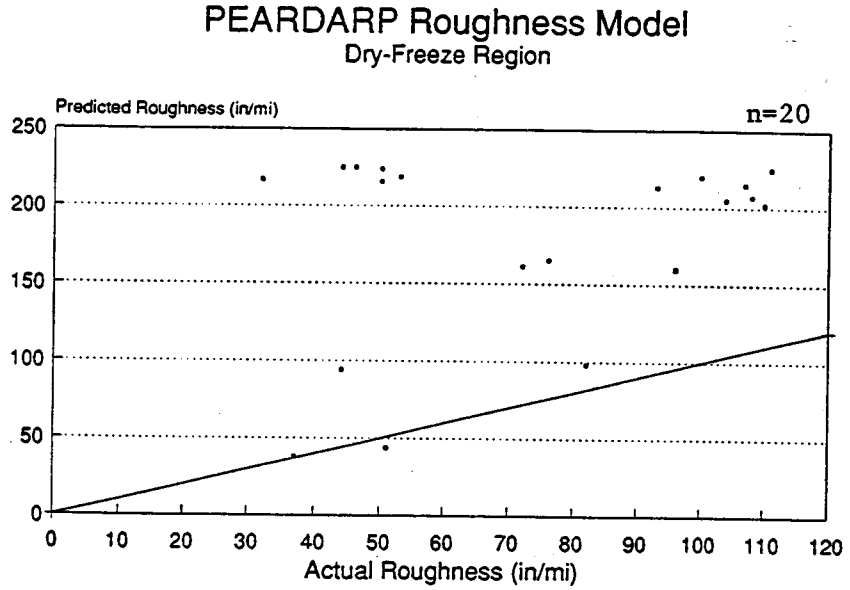

Figure 28 . Actual field measured roughness versus roughness as predicted using the PEARDARP roughness model for the dry-freeze region.

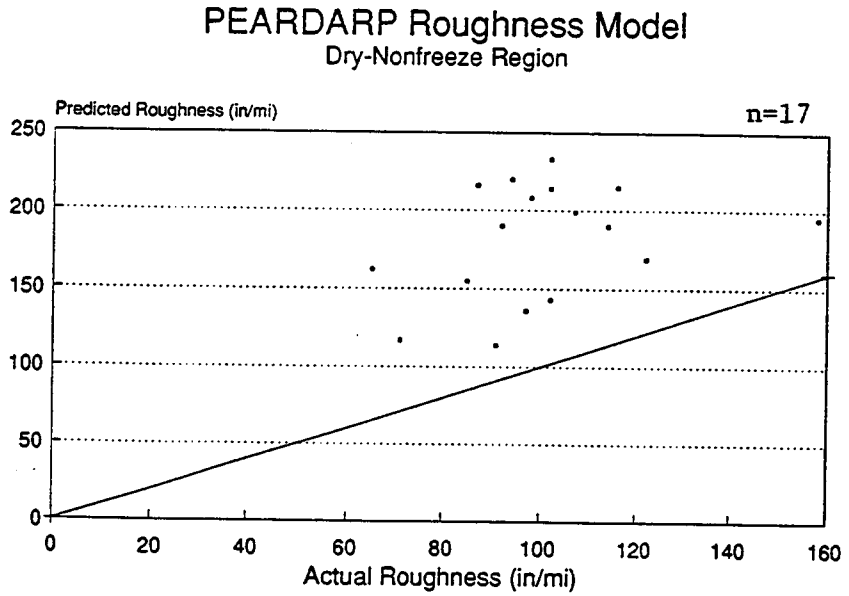

Figure 29. Actual field measured roughness versus roughness as predicted using the PEARDARP roughness model for the dry-nonfreeze region.

Table 78. Actual field measured roughness versus roughness as predicted using the PEARDARP roughness model for the wet-freeze region.

Section ID	Actual Mays Roughness	Predicted Roughness	Difference
MI 1-1a	96	76	20
MI 1-1b	91	69	22
MI 1-4a	48	77	29
MI 1-7a	58	74	16
MI 1-7b	36	68	32
MI 1-10a	98	70	28
MI 1-10b	104	72	32
MI 1-25	159	72	87
MI 3	37	160	123
MI 4-1	132	207	75
MI 4-2	112	198	86
MI 5	36	174	138
NJ 2	63	201	138
NJ 3-1	134	199	65
NJ 3-2	153	199	46
NY 1-1	56	177	121
NY 1-3	78	171	93
NY 1-4	90	177	87
NY 1-6	82	177	95
NY 1-8a	64	176	112
NY 1-8b	65	177	112
NY 2-3	61	109	48
NY 2-9	66	104	38
NY 2-11	76	107	31
NY 2-15	63	95	32
OH 1-1	109	184	75
OH 1-3	106	186	80
OH 1-4	123	185	62
OH 1-6	104	180	76
OH 1-7	115	176	61
OH 1-9	109	176	67
OH 1-10	122	179	57
OH 2-33a	90	156	66
OH 2-33b	85	156	71
PA 1-1	75	66	9
PA 1-2	91	49	42
PA 1-3	113	49	64
PA 1-4	109	50	59
PA 1-5	82	49	33
ONT 1-1a	90	89	1
ONT 1-1b	62	89	27
ONT 1-2a	78	58	20
ONT 1-2b	70	58	12

Table 78. Actual field measured roughness versus roughness as predicted using the PEARDARP roughness model for the wet-freeze region (continued).

Section ID	Actual Mays Roughness	Predicted Roughness	Difference
ONT 1-3a	57	58	1
ONT 1-3b	66	58	8
ONT 1-4a	65	36	29
ONT 1-4b	72	36	36
ONT 2	104	214	110

Analysis Variable : DIFRGH

N Obs	Mean	Std Error	T	Prob>|T|
48	57.7500000	5.3333472	10.8280969	0.0001

Table 79. Actual field measured roughness versus roughness as predicted using the PEARDARP roughness model for the wet-nonfreeze region.

Section ID	Actual Mays Roughness	Predicted Roughness	Difference
CA 3-1	134	191	57
CA 3-2	104	183	79
CA 3-5	102	179	77
FL 2	64	133	69
FL 3	84	215	131
NC 1-1	83	201	118
NC 1-2	79	214	135
NC 1-3	77	204	127
NC 1-4	85	203	118
NC 1-5	105	209	104
NC 1-6	69	223	154
NC 1-7	85	244	159
NC 1-8	95	204	109
NC 2	64	186	122

Analysis Variable : DIFRGH

N Obs	Mean	Std Error	T	Prob>|T|
14	111.3571429	8.2924613	13.4287203	0.0001

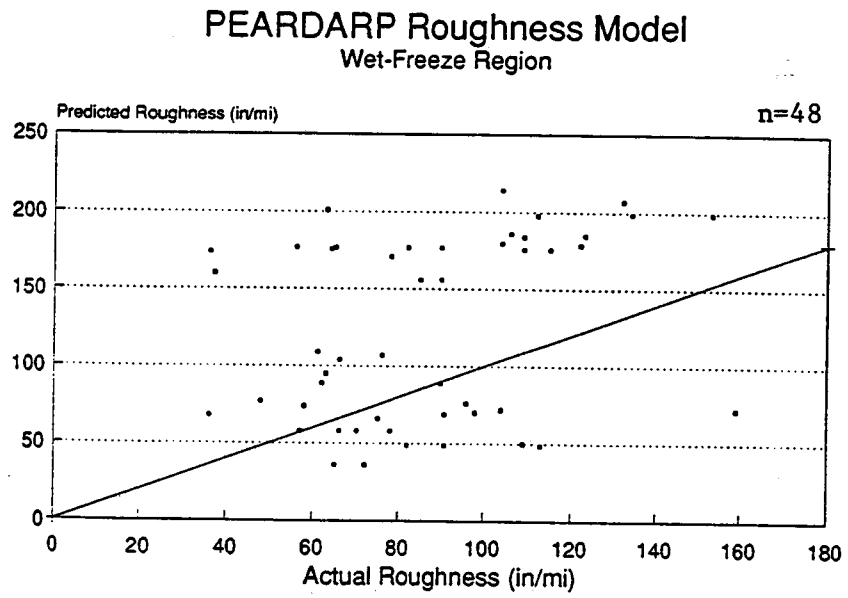

Figure 30. Actual field measured roughness versus roughness as predicted using the PEARDARP roughness model for the wet-freeze region.

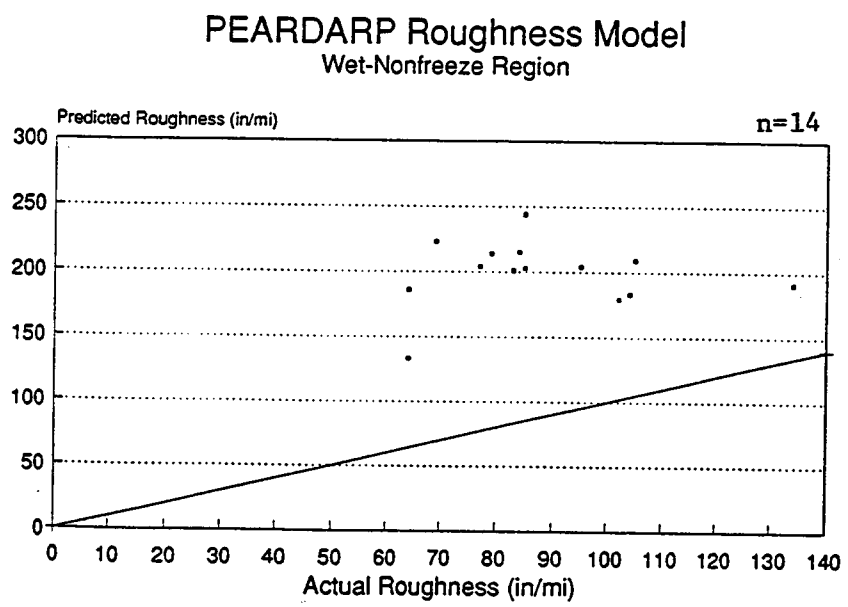

Figure 31. Actual field measured roughness versus roughness as predicted using the PEARDARP roughness model for the wet-nonfreeze region.

Table 80. Comparison of actual field observed pumping with the normalized pumping index, volume of pumping, number of joints pumping, and volume of undersealing material required as predicted by the PEARDARP pumping model for all Phase I sections.

Section ID	Measured Pumping	Normalized Pumping Index	Volume Pumping	Number of Joints	Volume Undersealing
AZ 1-1	N	0.74069	27.161	301.788	379.161
AZ 1-2	N	0.01833	0.672	84.039	352.672
AZ 1-4	N	0.00895	0.328	41.003	352.328
AZ 1-5	N	0.13556	4.971	55.231	356.971
AZ 1-6	N	0.40208	14.744	163.825	366.744
AZ 1-7	N	0.25415	9.320	103.553	361.320
AZ 2	N	0.38896	14.263	158.480	366.263
CA 1-1	M	2.77250	101.668	676.923	778.591
CA 1-3	N	2.77250	101.668	340.645	442.313
CA 1-5	L	0.25521	9.358	103.982	350.004
CA 1-7	H	2.77250	101.668	340.645	442.313
CA 1-9	L	2.77250	101.668	340.645	442.313
CA 2-2	N	1.96170	71.936	340.645	412.581
CA 2-3	N	1.96170	71.936	340.645	412.581
CA 3-1	N	1.97865	72.557	340.645	413.202
CA 3-2	N	1.97865	72.557	340.645	413.202
CA 3-5	N	1.97865	72.557	340.645	413.202
CA 6	N	0.8654	31.735	352.615	422.846
CA 7	N	1.4711	53.945	340.645	394.590
CA 8	N	0.7469	27.390	304.338	418.501
FL 2	N	0.3946	14.471	160.794	355.117
FL 3	M	3.7212	136.456	270.769	407.226
MI 1-1a	N	8.4082	308.329	74.157	382.486
MI 1-1b	N	8.4082	308.329	74.157	382.486
MI 1-4a	N	0.1796	6.587	73.188	347.232
MI 1-7a	N	0.6492	23.806	264.516	387.944
MI 1-7b	N	0.6492	23.806	264.516	390.473
MI 1-10a	L	0.1796	6.587	73.188	347.232
MI 1-10b	L	0.1796	6.587	73.188	347.232
MI 1-25	L	0.1796	6.587	73.188	347.232
MI 3	N	9.8977	362.950	128.780	491.730
MI 4-1	N	19.6409	720.230	74.157	794.388
MI 4-2	N	19.6409	720.230	74.157	794.388
MI 5	N	10.5595	387.216	128.780	515.996
MN 1-1	L	1.12517	41.260	195.556	236.815
MN 1-2	N	1.12517	41.260	195.556	236.815
MN 1-3	L	3.83444	140.609	195.556	336.165
MN 1-4	L	3.83444	140.609	195.556	336.165
MN 1-5	L	2.87583	105.457	195.556	301.012
MN 1-6	N	2.87583	105.457	195.556	301.012
MN 1-7	M	0.82137	30.120	195.556	225.675
MN 1-8	N	0.82137	30.120	195.556	225.675
MN 1-9	L	0.82137	30.120	195.556	225.675
MN 1-10	L	0.82137	30.120	195.556	225.675

Table 80. Comparison of actual field observed pumping with the normalized pumping index, volume of pumping, number of joints pumping, and volume of undersealing material required as predicted by the PEARDARP pumping model for all Phase I sections (continued).

Section ID	Measured Pumping	Normalized Pumping Index	Volume Pumping	Number of Joints	Volume Undersealing
MN 1-11	L	2.87583	105.457	195.556	301.012
MN 1-12	M	2.87583	105.457	195.556	301.012
MN 2-1	N	0.59995	22.000	244.446	362.645
MN 2-2	N	1.23234	45.190	340.645	385.835
MN 2-3	N	1.48121	54.316	195.556	249.871
MN 2-4	N	1.48121	54.316	195.556	249.871
MN 3	N	1.40937	51.681	195.556	247.237
MN 4b	N	0.1807	6.63	73.620	358.63
MN 5	L	1.1252	41.26	195.556	236.82
MN 6a	N	1.9483	71.44	195.556	267.00
NJ 2	N	33.3053	1221.30	67.261	1288.57
NJ 3-1	N	19.2164	704.66	67.261	771.92
NJ 3-2	N	14.0279	514.40	67.261	581.67
NY 1-1	N	1.2800	46.94	264.000	310.94
NY 1-3	M	12.1163	444.30	86.842	531.15
NY 1-4	N	16.5976	608.64	86.842	695.48
NY 1-6	N	1.7312	63.48	264.000	327.48
NY 1-8a	N	1.2800	46.94	264.000	310.94
NY 1-8b	N	1.2800	46.94	264.000	310.94
NY 2-3	N	0.9756	35.77	264.000	299.77
NY 2-9	N	0.9756	35.77	264.000	299.77
NY 2-11	N	0.9756	35.77	197.753	233.53
NY 2-15	N	10.9382	401.10	83.150	484.25
NC 1-1	N	17.0353	624.69	176.000	800.69
NC 1-2	N	3.0058	110.22	176.000	286.22
NC 1-3	N	3.3706	123.60	176.000	299.60
NC 1-4	N	3.6525	133.94	176.000	309.94
NC 1-5	N	4.3673	160.15	176.000	336.15
NC 1-6	N	3.3706	123.60	176.000	299.60
NC 1-7	N	31.5273	1156.11	88.000	1244.11
NC 1-8	N	4.0957	150.19	176.000	326.19
NC 2	H	1.7059	62.56	249.057	311.61
OH 1-1	N	17.3646	636.76	132.000	768.76
OH 1-3	N	12.6761	464.83	251.429	716.26
OH 1-4	N	12.6761	464.83	132.000	596.83
OH 1-6	N	17.3646	636.76	251.429	888.19
OH 1-7	N	17.3646	636.76	132.000	768.76
OH 1-9	N	17.3646	636.76	132.000	768.76
OH 1-10	N	17.3646	636.76	251.429	888.19
OH 2-33a	L	1.0300	37.77	264.000	301.77
OH 2-33b	M	1.0300	37.77	264.000	301.77

Table 80. Comparison of actual field observed pumping with the normalized pumping index, volume of pumping, number of joints pumping, and volume of undersealing material required as predicted by the PEARDARP pumping model for all Phase I sections (continued).

Section ID	Measured Pumping	Normalized Pumping Index	Volume Pumping	Number of Joints	Volume Undersealing
PA 1-1	N	2.9972	109.908	113.548	223.457
PA 1-2	N	1.8744	68.736	113.548	182.284
PA 1-3	N	2.6401	96.811	113.548	210.360
PA 1-4	N	2.6401	96.811	113.548	210.360
PA 1-5	N	2.6401	96.811	113.548	210.360
ONT 1-1a	L	0.0902	3.309	220.588	343.954
ONT 1-1b	L	0.0902	3.309	220.588	343.954
ONT 1-2a	M	1.1404	41.819	340.645	382.465
ONT 1-2b	M	1.1404	41.819	340.645	382.465
ONT 1-3a	L	1.1404	41.819	340.645	382.465
ONT 1-3b	L	1.1404	41.819	340.645	382.465
ONT 1-4a	N	2.2147	81.214	340.645	421.859
ONT 1-4b	N	2.2147	81.214	340.645	421.859
ONT 2	N	11.9089	436.700	340.645	777.346

Table 81. Actual field measured spalling versus spalling as predicted using the PEARDARP spalling model for all Phase I sections.

Section ID	Measured Spalling	Predicted Spalling	Difference
AZ 1-1	22	38	16
AZ 1-2	1	21	20
AZ 1-4	0	7	7
AZ 1-5	0	7	7
AZ 1-6	1	3	2
AZ 1-7	0	3	3
AZ 2	0	0	0
CA 1-1	2	0	2
CA 1-3	0	46	46
CA 1-5	3	46	43
CA 1-7	9	46	37
CA 1-9	3	46	43
CA 2-2	0	5	5
CA 2-3	0	5	5
CA 3-1	2	23	21
CA 3-2	3	23	20
CA 3-5	6	23	17
CA 6	3	4	1
CA 7	0	7	7
CA 8	0	1	1
FL 2	0	0	0
FL 3	2	3	1
MI 1-1a	0	88	88
MI 1-1b	0	88	88
MI 1-4a	9	23	14
MI 1-7a	12	20	8
MI 1-7b	11	20	9
MI 1-10a	41	23	18
MI 1-10b	63	23	40
MI 1-25	75	23	52
MI 3	0	0	0
MI 4-1	0	99	99
MI 4-2	6	99	93
MI 5	0	2	2
MN 1-1	4	85	81
MN 1-2	14	85	71
MN 1-3	8	85	77
MN 1-4	15	85	70
MN 1-5	24	85	61
MN 1-6	31	85	54
MN 1-7	15	85	70
MN 1-8	69	85	16
MN 1-9	4	85	81
MN 1-10	6	85	79

Table 81. Actual field measured spalling versus spalling as predicted using the PEARDARP spalling model for all Phase I sections (continued).

Section ID	Measured Spalling	Predicted Spalling	Difference
MN 1-11	37	85	48
MN 1-12	29	85	56
MN 2-1	3	18	15
MN 2-2	9	18	9
MN 2-3	3	39	36
MN 2-4	8	39	31
MN 3	0	1	1
MN 4b	0	0	0
MN 5	36	85	49
MN 6a	0	2	2
NJ 2	20	100	80
NJ 3-1	0	50	50
NJ 3-2	43	50	7
NY 1-1	6	90	84
NY 1-3	73	100	27
NY 1-4	9	100	91
NY 1-6	13	90	77
NY 1-8a	0	90	90
NY 1-8b	0	90	90
NY 2-3	0	34	34
NY 2-9	0	34	34
NY 2-11	0	47	47
NY 2-15	0	85	85
NC 1-1	0	95	95
NC 1-2	0	95	95
NC 1-3	0	95	95
NC 1-4	0	95	95
NC 1-5	0	95	95
NC 1-6	0	95	95
NC 1-7	0	100	100
NC 1-8	0	95	95
NC 2	0	3	3
OH 1-1	0	83	83
OH 1-3	13	51	38
OH 1-4	0	83	83
OH 1-6	0	51	51
OH 1-7	0	83	83
OH 1-9	0	83	83
OH 1-10	0	51	51
OH 2-33a	15	34	19
OH 2-33b	23	34	11
PA 1-1	0	22	22
PA 1-2	0	22	22
PA 1-3	0	22	22
PA 1-4	0	22	22
PA 1-5	0	22	22

Table 81. Actual field measured spalling versus spalling as predicted using the PEARDARP spalling model for all Phase I sections (continued).

Section ID	Measured Spalling	Predicted Spalling	Difference
ONT 1-1a	0	2	2
ONT 1-1b	0	2	2
ONT 1-2a	0	2	2
ONT 1-2b	0	2	2
ONT 1-3a	0	2	2
ONT 1-3b	0	2	2
ONT 1-4a	0	2	2
ONT 1-4b	0	2	2
ONT 2	0	53	53

Analysis Variable : DIFSPALL

N Obs	Mean	Std Error	T	Prob>|T|
99	40.090371	3.4917113	11.4742244	0.0001

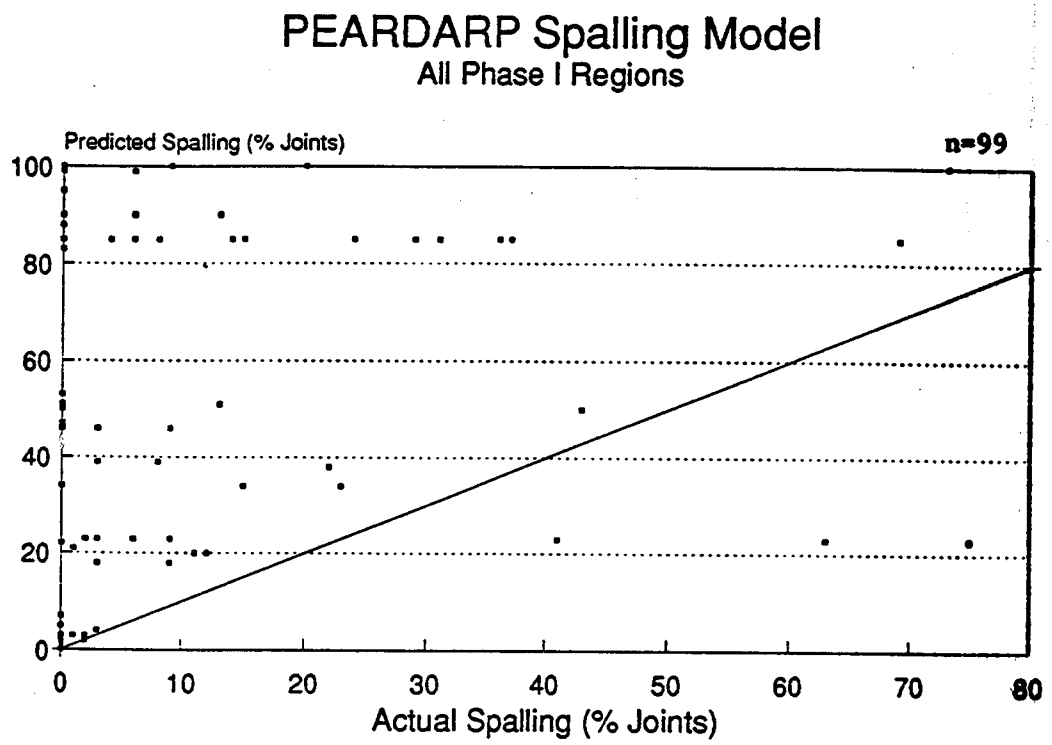

Figure 32. Actual field measured spalling versus spalling as predicted using the PEARDARP spalling model for all Phase I sections.

Table 82. Actual field measured spalling versus spalling as predicted using the PEARDARP spalling model for the dry-freeze region.

Section ID	Predicted Spalling	Measured Spalling	Difference
MN 1-1	4	85	81
MN 1-2	14	85	71
MN 1-3	8	85	77
MN 1-4	15	85	70
MN 1-5	24	85	61
MN 1-6	31	85	54
MN 1-7	15	85	70
MN 1-8	69	85	16
MN 1-9	4	85	81
MN 1-10	6	85	79
MN 1-11	37	85	48
MN 1-12	29	85	56
MN 2-1	3	18	15
MN 2-2	9	18	9
MN 2-3	3	39	36
MN 2-4	8	39	31
MN 3	0	1	1
MN 4b	0	0	0
MN 5	36	85	49
MN 6a	0	2	2

Analysis Variable : DIFSPALL

N Obs	Mean	Std Error	T	Prob>|T|
20	45.3500000	6.5499196	6.9237491	0.0001

Table 83. Actual field measured spalling versus spalling as predicted using the PEARDARP spalling model for the dry-nonfreeze region.

Section ID	Predicted Spalling	Measured Spalling	Difference
AZ 1-1	22	38	16
AZ 1-2	1	21	20
AZ 1-4	0	7	7
AZ 1-5	0	7	7
AZ 1-6	1	3	2
AZ 1-7	0	3	3
AZ 2	0	0	0
CA 1-1	2	0	2
CA 1-3	0	46	46
CA 1-5	3	46	43
CA 1-7	9	46	37
CA 1-9	3	46	43
CA 2-2	0	5	5
CA 2-3	0	5	5
CA 6	3	4	1
CA 7	0	7	7
CA 8	0	1	1

Analysis Variable : DIFSPALL

N Obs	Mean	Std Error	T	Prob>|T|
17	14.4705	4.001013	3.413111	0.0026

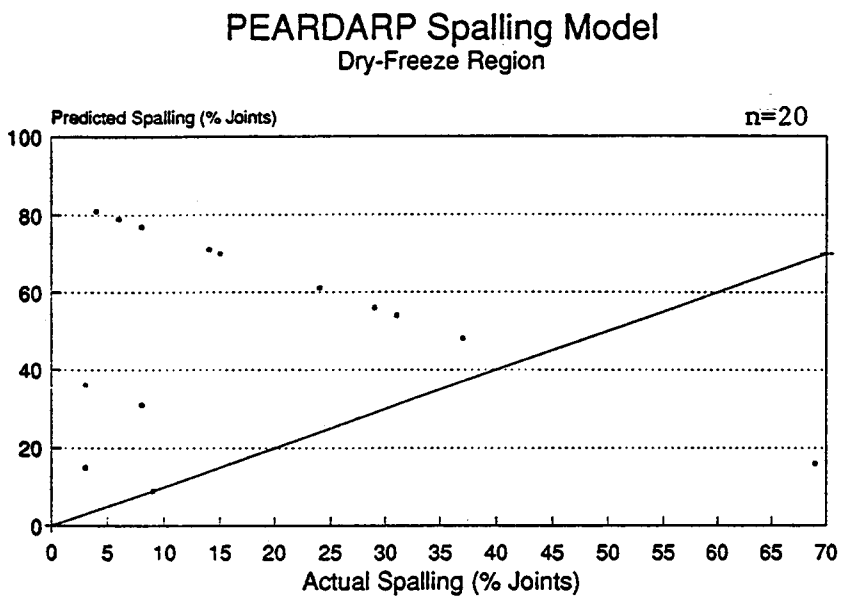

Figure 33. Actual field measured spalling versus spalling as predicted using the PEARDARP spalling model for the dry-freeze region.

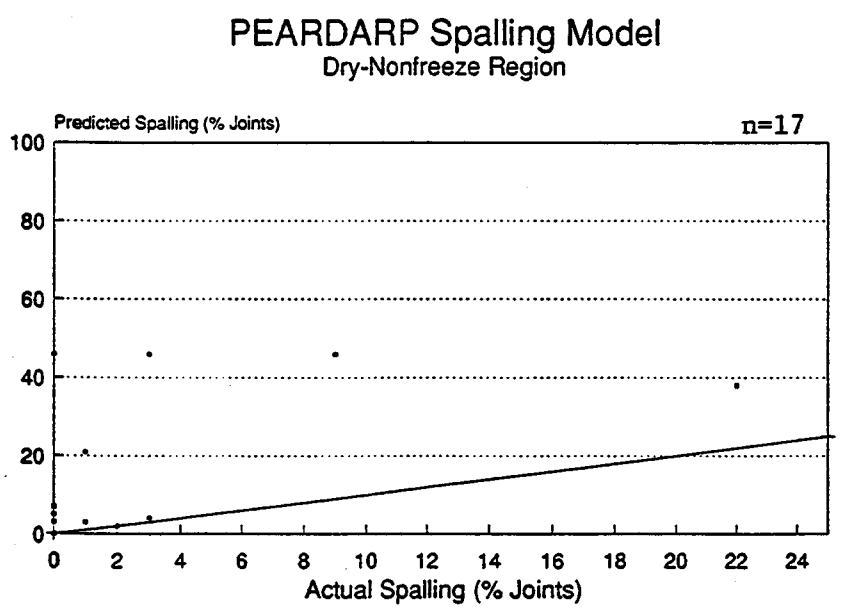

Figure 34. Actual field measured spalling versus spalling as predicted using the PEARDARP spalling model for the dry-nonfreeze region.

Table 84. Actual field measured spalling versus spalling as predicted using the PEARDARP spalling model for the wet-freeze region.

Section ID	Predicted Spalling	Measured Spalling	Difference
MI 1-1a	0	88	88
MI 1-1b	0	88	88
MI 1-4a	9	23	14
MI 1-7a	12	20	8
MI 1-7b	11	20	9
MI 1-10a	41	23	18
MI 1-10b	63	23	40
MI 1-25	75	23	52
MI 3	0	0	0
MI 4-1	0	99	99
MI 4-2	6	99	93
MI 5	0	2	2
NJ 2	20	100	80
NJ 3-1	0	50	50
NJ 3-2	43	50	7
NY 1-1	6	90	84
NY 1-3	73	100	27
NY 1-4	9	100	91
NY 1-6	13	90	77
NY 1-8a	0	90	90
NY 1-8b	0	90	90
NY 2-3	0	34	34
NY 2-9	0	34	34
NY 2-11	0	47	47
NY 2-15	0	85	85
OH 1-1	0	83	83
OH 1-3	13	51	38
OH 1-4	0	83	83
OH 1-6	0	51	51
OH 1-7	0	83	83
OH 1-9	0	83	83
OH 1-10	0	51	51
OH 2-33a	15	34	19
OH 2-33b	23	34	11
PA 1-1	0	22	22
PA 1-2	0	22	22
PA 1-3	0	22	22
PA 1-4	0	22	22
PA 1-5	0	22	22
ONT 1-1a	0	2	2
ONT 1-1b	0	2	2
ONT 1-2a	0	2	2
ONT 1-2b	0	2	2
ONT 1-3a	0	2	2
ONT 1-3b	0	2	2

Table 84. Actual field measured spalling versus spalling as predicted using the PEARDARP spalling model for the wet-freeze region (continued).

Section ID	Predicted Spalling	Measured Spalling	Difference
ONT 1-4a	0	2	2
ONT 1-4b	0	2	2
ONT 2	0	53	53

Analysis Variable : DIFSPALL

N Obs	Mean	Std Error	T	Prob>|T|
48	41.4166667	4.9559078	8.3570292	0.0001

Table 85. Actual field measured spalling versus spalling as predicted using the PEARDARP spalling model for the wet-nonfreeze region.

Section ID	Predicted Spalling	Measured Spalling	Difference
CA 3-1	2	23	21
CA 3-2	3	23	20
CA 3-5	6	23	17
FL 2	0	0	0
FL 3	2	3	1
NC 1-1	0	95	95
NC 1-2	0	95	95
NC 1-3	0	95	95
NC 1-4	0	95	95
NC 1-5	0	95	95
NC 1-6	0	95	95
NC 1-7	0	100	100
NC 1-8	0	95	95
NC 2	0	3	3

Analysis Variable : DIFSPALL

N Obs	Mean	Std Error	T	Prob>|T|
14	59.0714286	11.8281952	4.9941202	0.0002

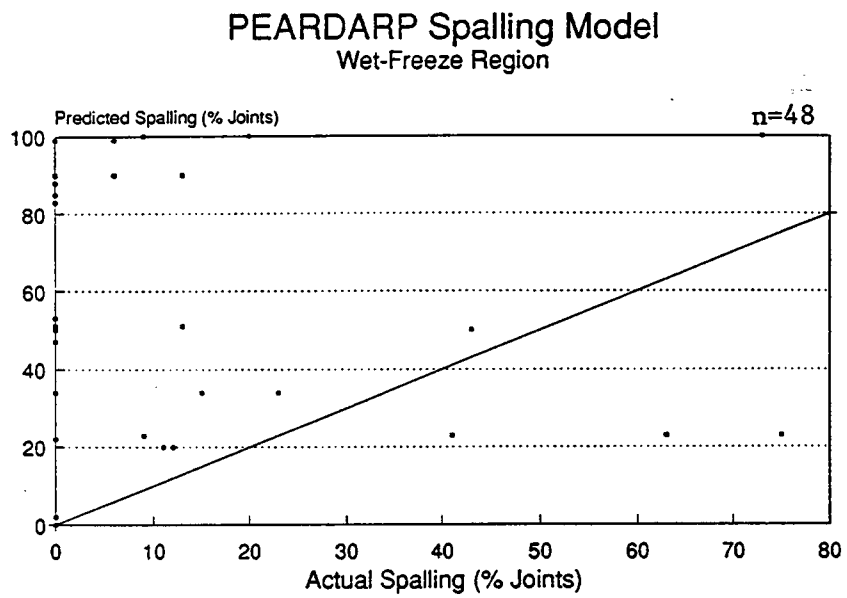

Figure 35. Actual field measured spalling versus spalling as predicted using the PEARDARP spalling model for the wet-freeze region.

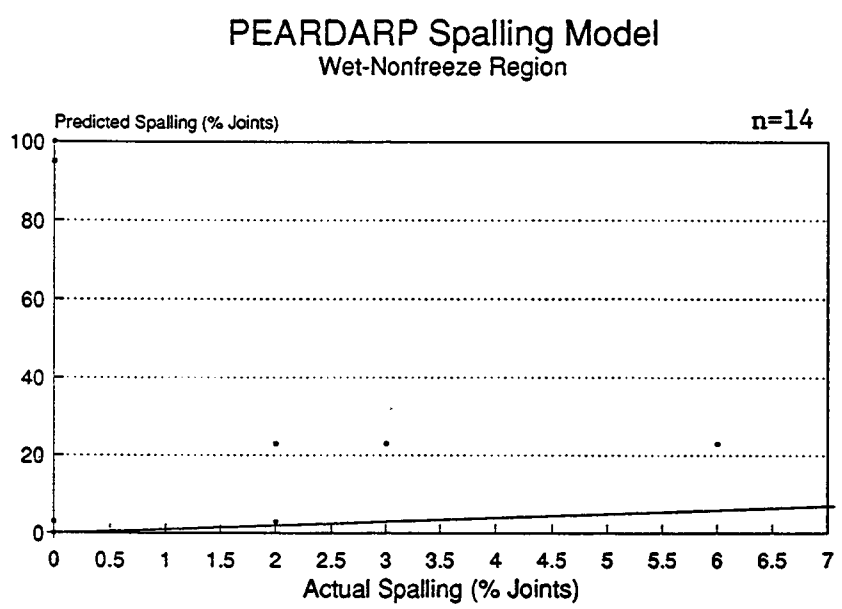

Figure 36. Actual field measured spalling versus spalling as predicted using the PEARDARP spalling model for the wet-nonfreeze region.

Table 86. Actual field measured faulting versus faulting as predicted using the PEARDARP faulting models for all Phase I sections.

Section ID	Measured Faulting	Precicted Faulting	Difference
AZ 1-1	0.08	0.062442	0.017558
AZ 1-2	0.01	0.043220	0.033220
AZ 1-4	0.01	0.041664	0.031664
AZ 1-5	0.03	0.043387	0.013387
AZ 1-6	0.01	0.044050	0.034050
AZ 1-7	0.02	0.041420	0.021420
AZ 2	0.01	0.028689	0.018689
CA 1-1	0.06	0.040313	0.019687
CA 1-3	0.10	0.094215	0.005785
CA 1-5	0.11	0.052014	0.057986
CA 1-7	0.06	0.055448	0.004552
CA 1-9	0.13	0.078814	0.051186
CA 2-2	0.11	0.060802	0.049198
CA 2-3	0.11	0.068998	0.041002
CA 3-1	0.08	0.063730	0.016270
CA 3-2	0.11	0.063730	0.046270
CA 3-5	0.10	0.06373	0.03627
CA 6	0.15	0.04031	0.10969
CA 7	0.06	0.05662	0.00338
CA 8	0.04	0.04031	0.00031
FL 2	0.01	0.02866	0.01866
FL 3	0.08	0.02146	0.05854
MI 1-1a	0.05	0.06154	0.01154
MI 1-1b	0.08	0.06154	0.01846
MI 1-4a	0.03	0.09039	0.06039
MI 1-7a	0.04	0.03013	0.00987
MI 1-7b	0.04	0.02966	0.01034
MI 1-10a	0.14	0.11041	0.02959
MI 1-10b	0.19	0.11041	0.07959
MI 1-25	0.20	0.11041	0.08959
MI 3	0.02	0.02904	0.00904
MI 4-1	0.12	0.02971	0.09029
MI 4-2	0.06	0.029714	0.03029
MI 5	0.05	0.022408	0.02759
MN 1-1	0.31	0.074832	0.23517
MN 1-2	0.06	0.019322	0.04068
MN 1-3	0.31	0.094959	0.21504
MN 1-4	0.06	0.024518	0.03548
MN 1-5	0.37	0.085301	0.28470
MN 1-6	0.00	0.022025	0.02202
MN 1-7	0.31	0.068731	0.24127
MN 1-8	0.06	0.017746	0.04225
MN 1-9	0.37	0.068731	0.30127
MN 1-10	0.13	0.017746	0.11225
MN 1-11	0.50	0.085301	0.41470
MN 1-12	0.06	0.022025	0.03798
MN 2-1	0.06	0.016240	0.04376
MN 2-2	0.06	0.018924	0.04108

Table 86. Actual field measured faulting versus faulting as predicted using the PEARDARP faulting models for all Phase I sections (continued).

Section ID	Measured Faulting	Precicted Faulting	Difference
MN 2-3	0.05	0.01893	0.031070
MN 2-4	0.06	0.01893	0.041070
MN 3	0.02	0.02192	0.001921
MN 4b	0.01	0.02865	0.018646
MN 5	0.09	0.02594	0.064059
MN 6a	0.01	0.01881	0.008808
NJ 2	0.06	0.13677	0.076769
NJ 3-1	0.05	0.01440	0.035602
NJ 3-2	0.06	0.01385	0.046153
NY 1-1	0.02	0.07400	0.053997
NY 1-3	0.14	0.07656	0.063437
NY 1-4	0.09	0.11993	0.029926
NY 1-6	0.03	0.08966	0.059659
NY 1-8a	0.01	0.07400	0.063997
NY 1-8b	0.03	0.06437	0.034373
NY 2-3	0.01	0.01450	0.004496
NY 2-9	0.02	0.01450	0.00550
NY 2-11	0.01	0.01511	0.00511
NY 2-15	0.02	0.01660	0.00340
NC 1-1	0.12	0.17830	0.05830
NC 1-2	0.16	0.02643	0.13357
NC 1-3	0.13	0.11820	0.01180
NC 1-4	0.13	0.03987	0.09013
NC 1-5	0.16	0.11820	0.04180
NC 1-6	0.05	0.11820	0.06820
NC 1-7	0.15	0.07171	0.07829
NC 1-8	0.22	0.17830	0.04170
NC 2	0.02	0.01826	0.00174
OH 1-1	0.13	0.02556	0.10444
OH 1-3	0.06	0.01782	0.04218
OH 1-4	0.07	0.01818	0.05182
OH 1-6	0.03	0.02159	0.00841
OH 1-7	0.07	0.021234	0.04877
OH 1-9	0.14	0.025565	0.11444
OH 1-10	0.10	0.018395	0.08161
OH 2-33a	0.11	0.045915	0.06409
OH 2-33b	0.11	0.045915	0.06409
PA 1-1	0.03	0.014937	0.01506
PA 1-2	0.02	0.014472	0.00553
PA 1-3	0.03	0.014699	0.01530
PA 1-4	0.03	0.014878	0.01512
PA 1-5	0.03	0.014878	0.01512
ONT 1-1a	0.05	0.041091	0.00891
ONT 1-1b	0.07	0.041091	0.02891
ONT 1-2a	0.05	0.043596	0.00640
ONT 1-2b	0.06	0.043596	0.01640

Table 86. Actual field measured faulting versus faulting as predicted using the PEARDARP faulting models for all Phase I sections (continued).

Section ID	Measured Faulting	Precicted Faulting	Difference
ONT 1-3a	0.04	0.043596	0.00360
ONT 1-3b	0.09	0.043596	0.04640
ONT 1-4a	0.04	0.045840	0.005840
ONT 1-4b	0.07	0.045840	0.024160
ONT 2	0.01	0.068245	0.058245

Analysis Variable : DIFFLT

N Obs	Mean	Std Error	T	Prob>|T|
99	0.0529429	0.0067659	7.8249659	0.0001

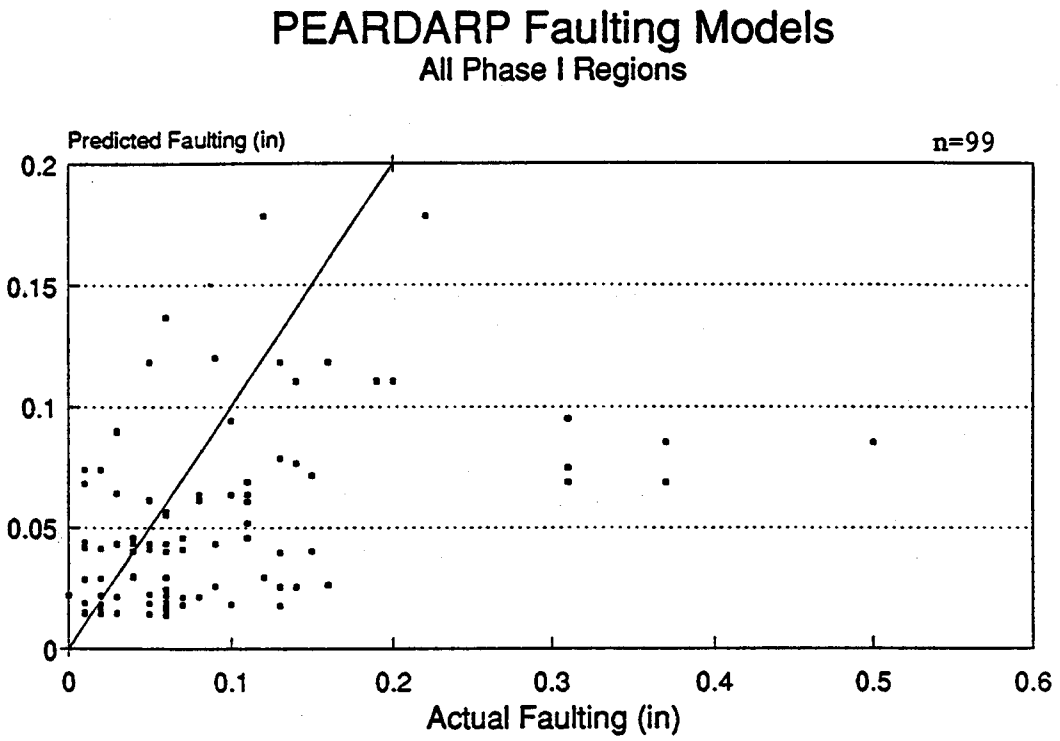

Figure 37. Actual field measured faulting versus faulting as predicted using the PEARDARP faulting models for all Phase I sections.

Table 87. Actual field measured faulting versus faulting as predicted using the PEARDARP faulting models for the dry-freeze region.

Section ID	Measured Faulting	Predicted Faulting	Difference
MN 1-1	0.31	0.074832	0.23517
MN 1-2	0.06	0.019322	0.04068
MN 1-3	0.31	0.094959	0.21504
MN 1-4	0.06	0.024518	0.03548
MN 1-5	0.37	0.085301	0.28470
MN 1-6	0.00	0.022025	0.02202
MN 1-7	0.31	0.068731	0.24127
MN 1-8	0.06	0.017746	0.04225
MN 1-9	0.37	0.068731	0.30127
MN 1-10	0.13	0.017746	0.11225
MN 1-11	0.50	0.085301	0.41470
MN 1-12	0.06	0.022025	0.03798
MN 2-1	0.06	0.016240	0.04376
MN 2-2	0.06	0.018924	0.04108
MN 2-3	0.05	0.018930	0.03107
MN 2-4	0.06	0.018930	0.04107
MN 3	0.02	0.021921	0.001921
MN 4b	0.01	0.028646	0.018646
MN 5	0.09	0.025941	0.064059
MN 6a	0.01	0.018808	0.008808

Analysis Variable : DIFFLT

N Obs	Mean	Std Error	T	Prob>|T|
20	0.1116612	0.0273476	4.0830317	0.0006

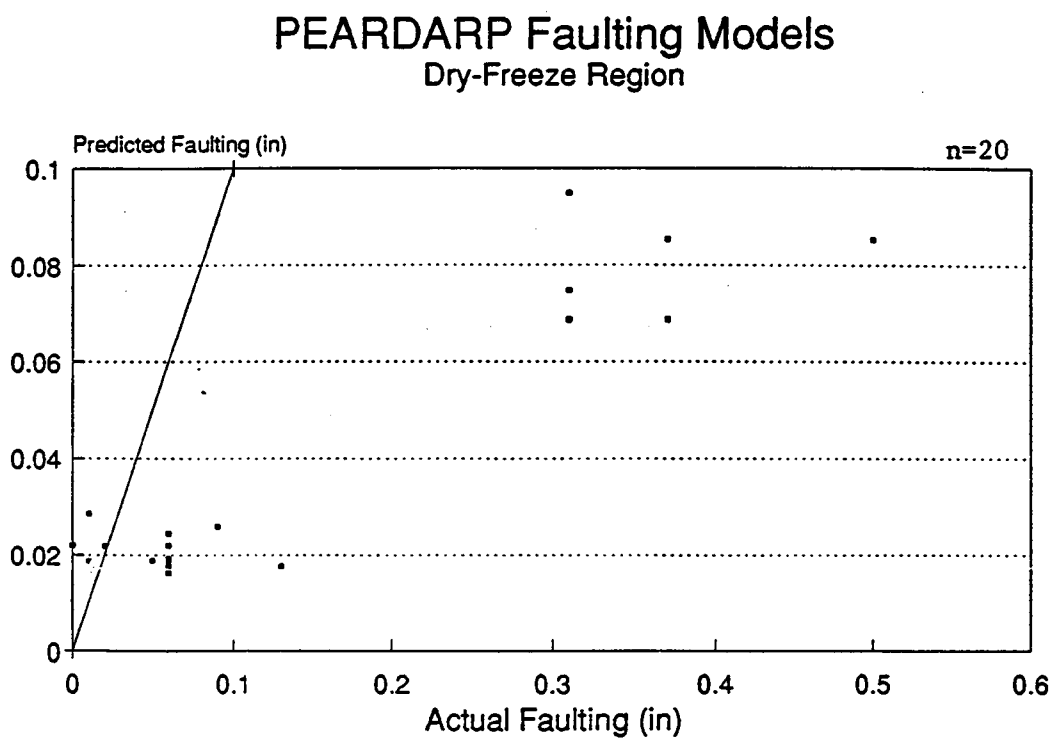

Figure 38. Actual field measured faulting versus faulting as predicted using the PEARDARP faulting models for the dry-freeze region.

Table 88. Actual field measured faulting versus faulting as predicted using the PEARDARP faulting models for doweled pavement for the dry-freeze region.

Section ID	Measured Faulting	Predicted Faulting	Difference
MN 1-2	0.06	0.019322	0.04068
MN 1-4	0.06	0.024518	0.03548
MN 1-6	0.00	0.022025	0.02202
MN 1-8	0.06	0.017746	0.04225
MN 1-10	0.13	0.017746	0.11225
MN 1-12	0.06	0.022025	0.03798
MN 2-1	0.06	0.016240	0.04376
MN 2-2	0.06	0.018924	0.04108
MN 2-3	0.05	0.018930	0.03107
MN 2-4	0.06	0.018930	0.04107
MN 3	0.02	0.021921	0.00192
MN 4b	0.01	0.028646	0.01865
MN 5	0.09	0.025941	0.06406
MN 6a	0.01	0.018808	0.00881

Analysis Variable : DIFFLT

N Obs	Mean	Std Error	T	Prob>|T|
14	0.0386485	0.0070719	5.4650645	0.0001

Table 89. Actual field measured faulting versus faulting as predicted using the PEARDARP faulting models for nondoweled pavement for the dry-freeze region.

Section ID	Measured Faulting	Predicted Faulting	Difference
MN 1-1	0.31	0.074832	0.23517
MN 1-3	0.31	0.094959	0.21504
MN 1-5	0.37	0.085301	0.28470
MN 1-7	0.31	0.068731	0.24127
MN 1-9	0.37	0.068731	0.30127
MN 1-11	0.50	0.085301	0.41470

Analysis Variable : DIFFLT

N Obs	Mean	Std Error	T	Prob>|T|
6	0.2820243	0.0296217	9.5208638	0.0002

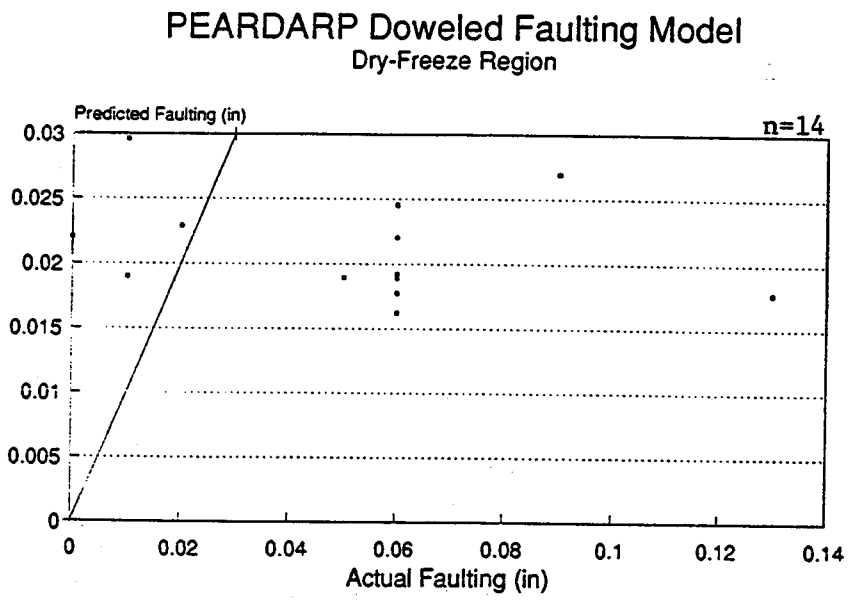

Figure 39 . Actual field measured faulting versus faulting as predicted using the PEARDARP faulting models for doweled pavements for the dry-freeze region.

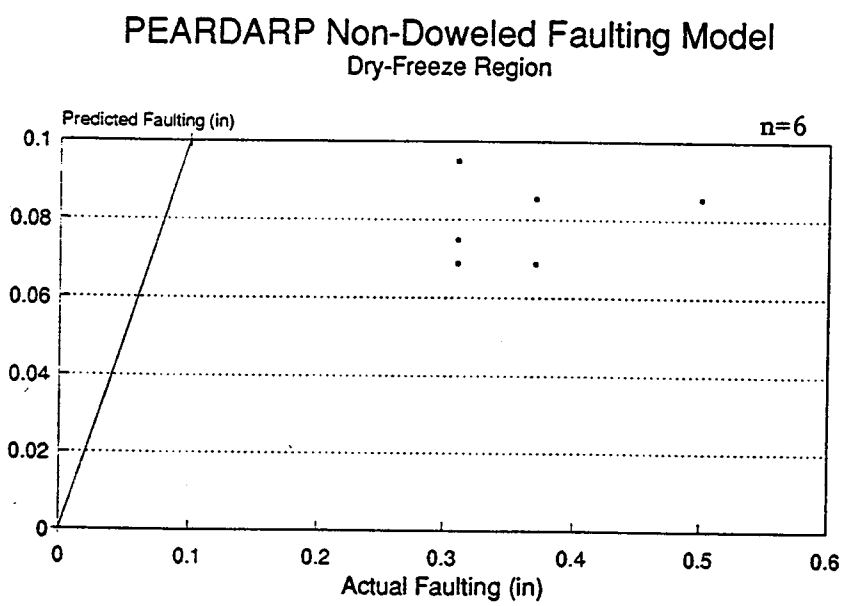

Figure 40. Actual field measured faulting versus faulting as predicted using the PEARDARP faulting models for nondoweled pavements for the dry-freeze region.

Table 90. Actual field measured faulting versus faulting as predicted using the PEARDARP faulting models for the dry-nonfreeze region.

Section ID	Measured Faulting	Predicted Faulting	Difference
AZ 1-1	0.08	0.062442	0.01756
AZ 1-2	0.01	0.043220	0.03322
AZ 1-4	0.01	0.041664	0.03166
AZ 1-5	0.03	0.043387	0.01339
AZ 1-6	0.01	0.044050	0.03405
AZ 1-7	0.02	0.041420	0.02142
AZ 2	0.01	0.028689	0.01869
CA 1-1	0.06	0.040313	0.01969
CA 1-3	0.10	0.094215	0.00579
CA 1-5	0.11	0.052014	0.05799
CA 1-7	0.06	0.055448	0.00455
CA 1-9	0.13	0.078814	0.05119
CA 2-2	0.11	0.060802	0.04920
CA 2-3	0.11	0.068998	0.04100
CA 6	0.15	0.040313	0.10969
CA 7	0.06	0.056622	0.00338
CA 8	0.04	0.040313	.0003125

Analysis Variable : DIFFLT

N Obs	Mean	Std Error	T	Prob>|T|
17	0.0301625	0.0065484	4.6061117	0.0003

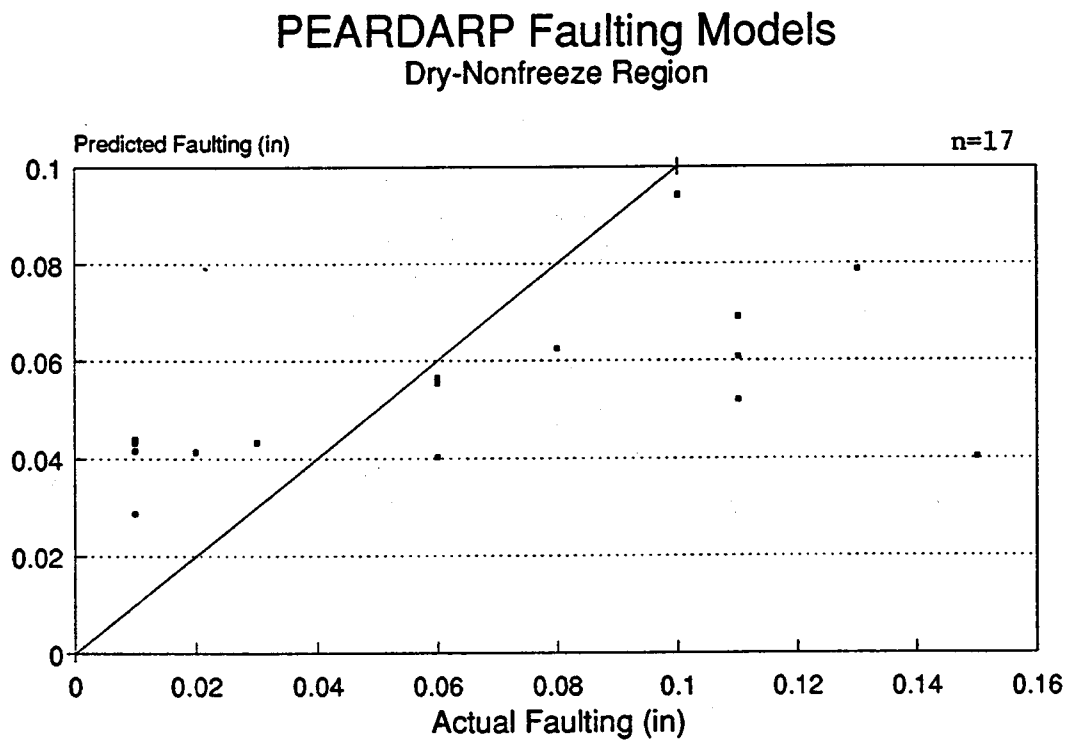

Figure 41. Actual field measured faulting versus faulting as predicted using the PEARDARP faulting models for the dry-nonfreeze region.

Table 91. Actual field measured faulting versus faulting as predicted using the PEARDARP faulting models for the wet-freeze region.

Section ID	Measured Faulting	Predicted Faulting	Difference
MI 1-1a	0.05	0.06154	0.011538
MI 1-1b	0.08	0.06154	0.018462
MI 1-4a	0.03	0.09039	0.060386
MI 1-7a	0.04	0.03013	0.009869
MI 1-7b	0.04	0.02966	0.010344
MI 1-10a	0.14	0.11041	0.029585
MI 1-10b	0.19	0.11041	0.079585
MI 1-25	0.20	0.11041	0.089585
MI 3	0.02	0.02904	0.009042
MI 4-1	0.12	0.02971	0.090286
MI 4-2	0.06	0.02971	0.030286
MI 5	0.05	0.02241	0.027592
NJ 2	0.06	0.13677	0.076769
NJ 3-1	0.05	0.01440	0.035602
NJ 3-2	0.06	0.01385	0.046153
NY 1-1	0.02	0.07400	0.053997
NY 1-3	0.14	0.07656	0.06344
NY 1-4	0.09	0.11993	0.02993
NY 1-6	0.03	0.08966	0.05966
NY 1-8a	0.01	0.07400	0.06400
NY 1-8b	0.03	0.06437	0.03437
NY 2-3	0.01	0.01450	0.00450
NY 2-9	0.02	0.01450	0.00550
NY 2-11	0.01	0.01511	0.00511
NY 2-15	0.02	0.01660	0.00340
OH 1-1	0.13	0.02556	0.10444
OH 1-3	0.06	0.01782	0.04218
OH 1-4	0.07	0.01818	0.05182
OH 1-6	0.03	0.02159	0.00841
OH 1-7	0.07	0.02123	0.04877
OH 1-9	0.14	0.02556	0.11444
OH 1-10	0.10	0.01839	0.08161
OH 2-33a	0.11	0.045915	0.064085
OH 2-33b	0.11	0.045915	0.064085
PA 1-1	0.03	0.014937	0.015063
PA 1-2	0.02	0.014472	0.005528
PA 1-3	0.03	0.014699	0.015301
PA 1-4	0.03	0.014878	0.015122
PA 1-5	0.03	0.014878	0.015122
ONT 1-1a	0.05	0.041091	0.008909
ONT 1-1b	0.07	0.041091	0.028909
ONT 1-2a	0.05	0.043596	0.006404
ONT 1-2b	0.06	0.043596	0.016404
ONT 1-3a	0.04	0.043596	0.003596
ONT 1-3b	0.09	0.043596	0.046404

Table 91. Actual field measured faulting versus faulting as predicted using the PEARDARP faulting models for the wet-freeze region (continued).

Section ID	Measured Faulting	Predicted Faulting	Difference
ONT 1-4a	0.04	0.045840	0.005840
ONT 1-4b	0.07	0.045840	0.024160
ONT 2	0.01	0.068245	0.058245

Analysis Variable : DIFFLT

N Obs	Mean	Std Error	T	Prob>|T|
48	0.0373712	0.0043467	8.5975476	0.0001

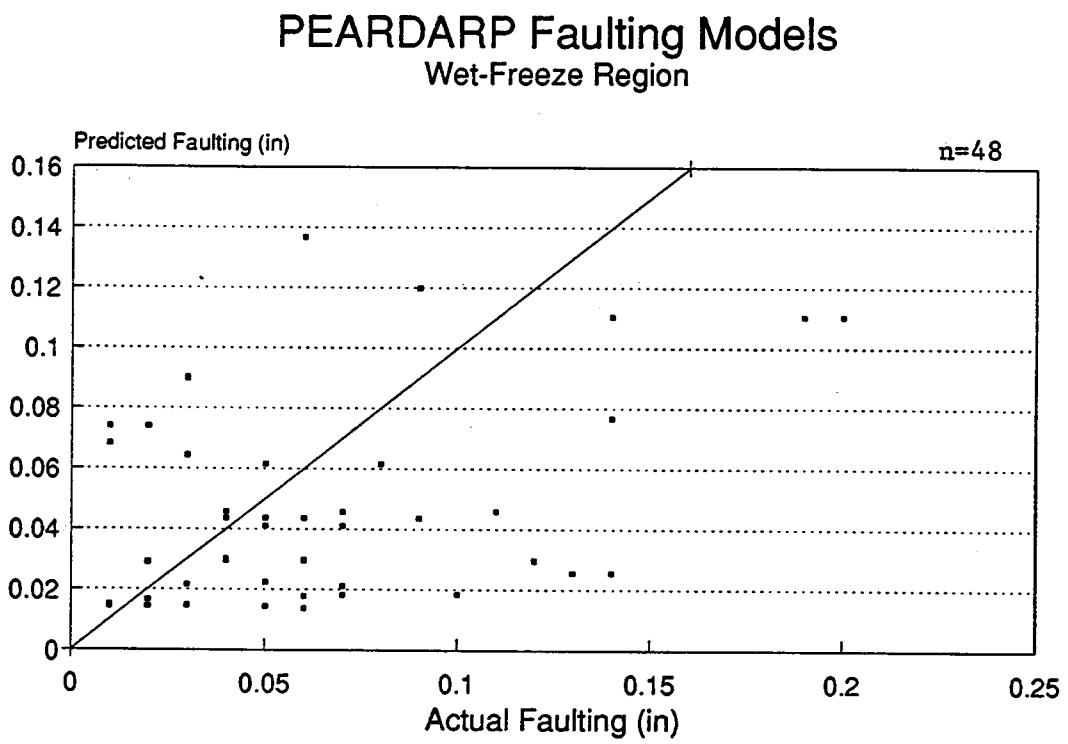

Figure 42. Actual field measured faulting versus faulting as predicted using the PEARDARP faulting model for the wet-freeze region.

Table 92. Actual field measured faulting versus faulting as predicted using the PEARDARP faulting models for doweled pavements for the wet-freeze region.

Section ID	Measured Faulting	Predicted Faulting	Difference
MI 1-1a	0.05	0.06154	0.01154
MI 1-1b	0.08	0.06154	0.01846
MI 1-7a	0.04	0.03013	0.00987
MI 1-7b	0.04	0.02966	0.01034
MI 3	0.02	0.02904	0.00904
MI 4-1	0.12	0.02971	0.09029
MI 4-2	0.06	0.02971	0.03029
MI 5	0.05	0.02241	0.02759
NJ 2	0.06	0.13677	0.07677
NJ 3-1	0.05	0.01440	0.03560
NJ 3-2	0.06	0.01385	0.04615
NY 2-3	0.01	0.01450	0.00450
NY 2-9	0.02	0.01450	0.00550
NY 2-11	0.01	0.01511	0.00511
NY 2-15	0.02	0.01660	0.00340
OH 1-1	0.13	0.02556	0.10444
OH 1-3	0.06	0.017821	0.04218
OH 1-4	0.07	0.018175	0.05182
OH 1-6	0.03	0.021589	0.00841
OH 1-7	0.07	0.021234	0.04877
OH 1-9	0.14	0.025565	0.11444
OH 1-10	0.10	0.018395	0.08161
PA 1-1	0.03	0.014937	0.01506
PA 1-2	0.02	0.014472	0.00553
PA 1-3	0.03	0.014699	0.01530
PA 1-4	0.03	0.014878	0.01512
PA 1-5	0.03	0.014878	0.01512
ONT 2	0.01	0.068245	0.05824

Analysis Variable : DIFFLT

N Obs	Mean	Std Error	T	Prob>|T|
28	0.0343032	0.0061869	5.5444690	0.0001

Table 93. Actual field measured faulting versus faulting as predicted using the PEARDARP faulting models for nondoweled pavements for the wet-freeze region.

Section ID	Measured Faulting	Predicted Faulting	Difference
MI 1-4a	0.03	0.09039	0.060386
MI 1-10a	0.14	0.11041	0.029585
MI 1-10b	0.19	0.11041	0.079585
MI 1-25	0.20	0.11041	0.089585
NY 1-1	0.02	0.07400	0.053997
NY 1-3	0.14	0.07656	0.063437
NY 1-4	0.09	0.11993	0.029926
NY 1-6	0.03	0.08966	0.059659
NY 1-8a	0.01	0.07400	0.063997
NY 1-8b	0.03	0.06437	0.034373
OH 2-33a	0.11	0.04591	0.064085
OH 2-33b	0.11	0.04591	0.064085
ONT 1-1a	0.05	0.04109	0.008909
ONT 1-1b	0.07	0.04109	0.028909
ONT 1-2a	0.05	0.04360	0.006404
ONT 1-2b	0.06	0.04360	0.016404
ONT 1-3a	0.04	0.043596	0.003596
ONT 1-3b	0.09	0.043596	0.046404
ONT 1-4a	0.04	0.045840	0.005840
ONT 1-4b	0.07	0.045840	0.024160

Analysis Variable : DIFFLT

N Obs	Mean	Std Error	T	Prob>|T|
20	0.0416663	0.0058612	7.1088928	0.0001

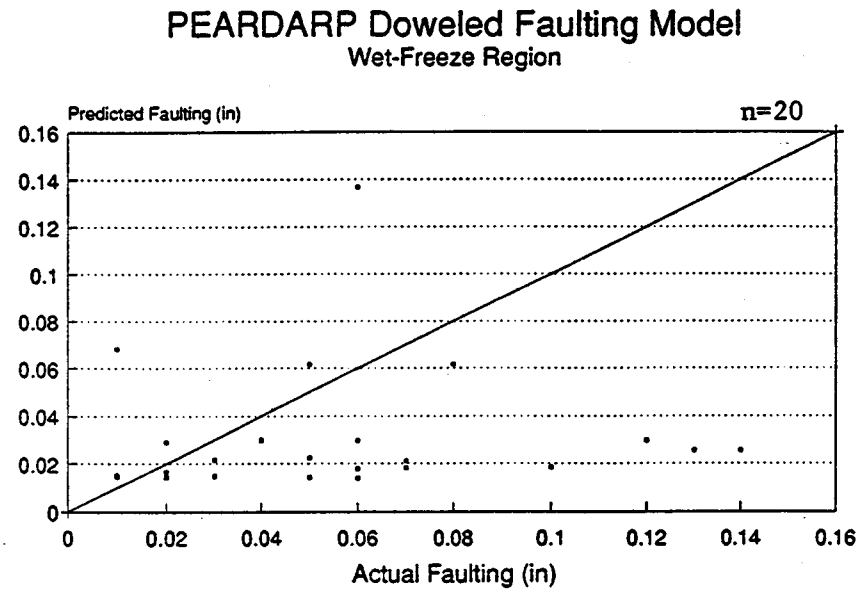

Figure 43. Actual field measured faulting versus faulting as predicted using the PEARDARP faulting models for doweled pavements for the wet-freeze region.

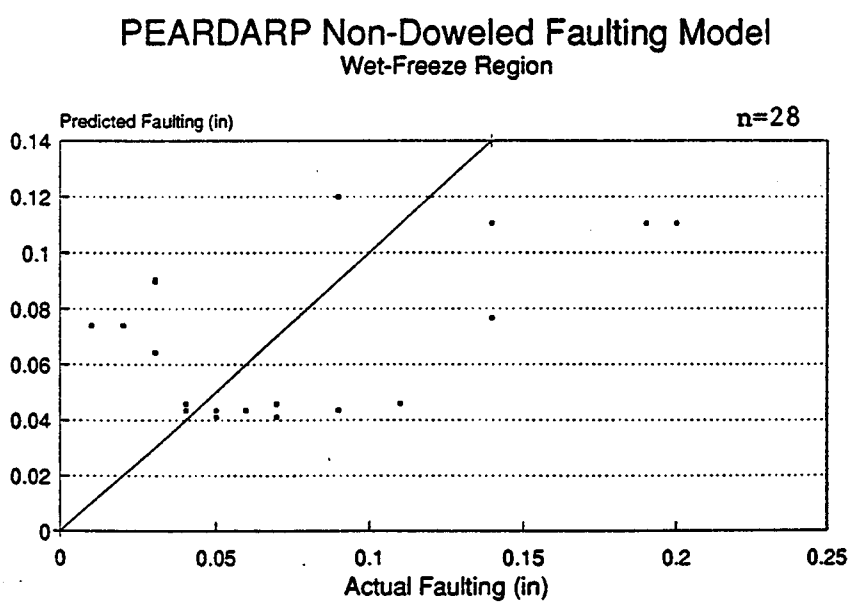

Figure 44. Actual field measured faulting versus faulting as predicted using the PEARDARP faulting models for nondoweled pavements for wet-freeze region.

Table 94. Actual field measured faulting versus faulting as predicted using the PEARDARP faulting models for the wet-nonfreeze region.

Section ID	Measured Faulting	Predicted Faulting	Difference
CA 3-1	0.08	0.06373	0.01627
CA 3-2	0.11	0.06373	0.04627
CA 3-5	0.10	0.06373	0.03627
FL 2	0.01	0.02866	0.01866
FL 3	0.08	0.02146	0.05854
NC 1-1	0.12	0.17830	0.05830
NC 1-2	0.16	0.02643	0.13357
NC 1-3	0.13	0.11820	0.01180
NC 1-4	0.13	0.03987	0.09013
NC 1-5	0.16	0.11820	0.04180
NC 1-6	0.05	0.11820	0.06820
NC 1-7	0.15	0.07171	0.07829
NC 1-8	0.22	0.17830	0.04170
NC 2	0.02	0.01826	0.00174

Analysis Variable : DIFFLT

N Obs	Mean	Std Error	T	Prob>|T|
14	0.0501105	0.0094095	5.3254929	0.0001

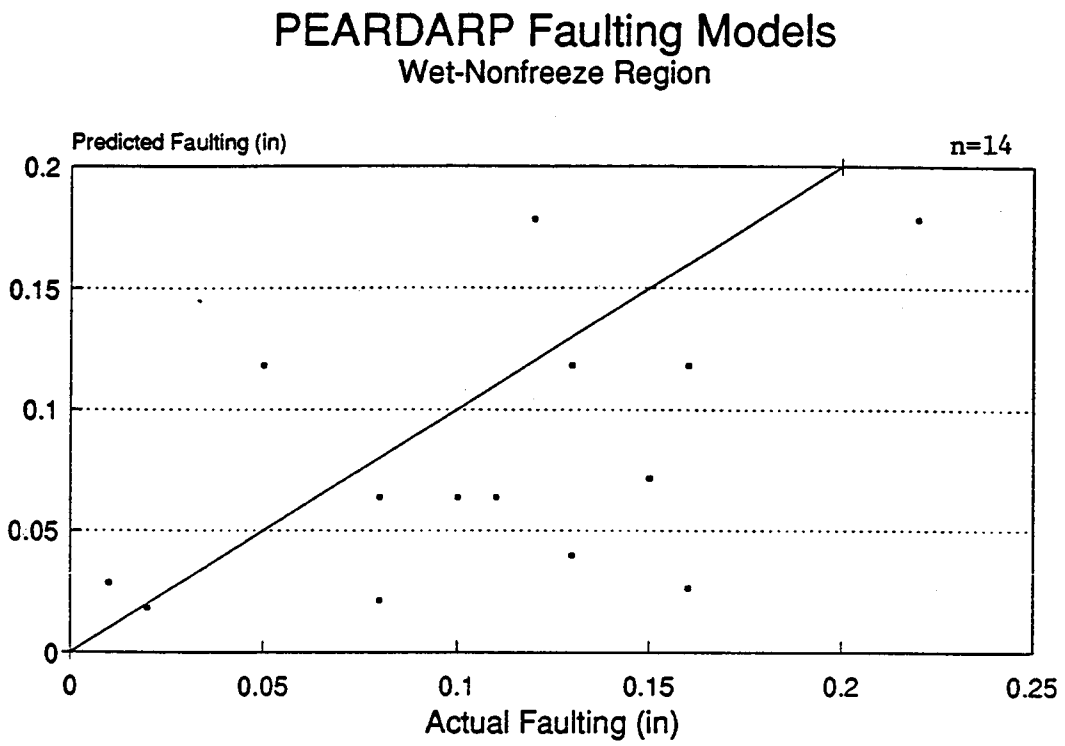

Figure 45. Actual field measured faulting versus faulting as predicted using the PEARDARP faulting models for the wet-nonfreeze region.

Table 95. Actual field measured faulting versus faulting as predicted using the PEARDARP faulting models for doweled pavements for the wet-nonfreeze region.

Section ID	Measured Faulting	Predicted Faulting	Difference
FL 2	0.01	0.028663	0.01866
FL 3	0.08	0.021456	0.05854
NC 1-2	0.16	0.026430	0.13357
NC 1-4	0.13	0.039868	0.09013
NC 1-7	0.15	0.071711	0.07829
NC 2	0.02	0.018263	0.00174

Analysis Variable : DIFFLT

N Obs	Mean	Std Error	T	Prob>|T|
6	0.0634892	0.0197377	3.2166425	0.0236

Table 96. Actual field measured faulting versus faulting as predicted using the PEARDARP faulting models for nondoweled pavements for the wet-nonfreeze region.

Section ID	Measured Faulting	Predicted Faulting	Difference
CA 3-1	0.08	0.06373	0.016270
CA 3-2	0.11	0.06373	0.046270
CA 3-5	0.10	0.06373	0.036270
NC 1-1	0.12	0.17830	0.058295
NC 1-3	0.13	0.11820	0.011802
NC 1-5	0.16	0.11820	0.041802
NC 1-6	0.05	0.11820	0.068198
NC 1-8	0.22	0.17830	0.041705

Analysis Variable : DIFFLT

N Obs	Mean	Std Error	T	Prob>|T|
8	0.0400764	0.0067446	5.9419636	0.0006

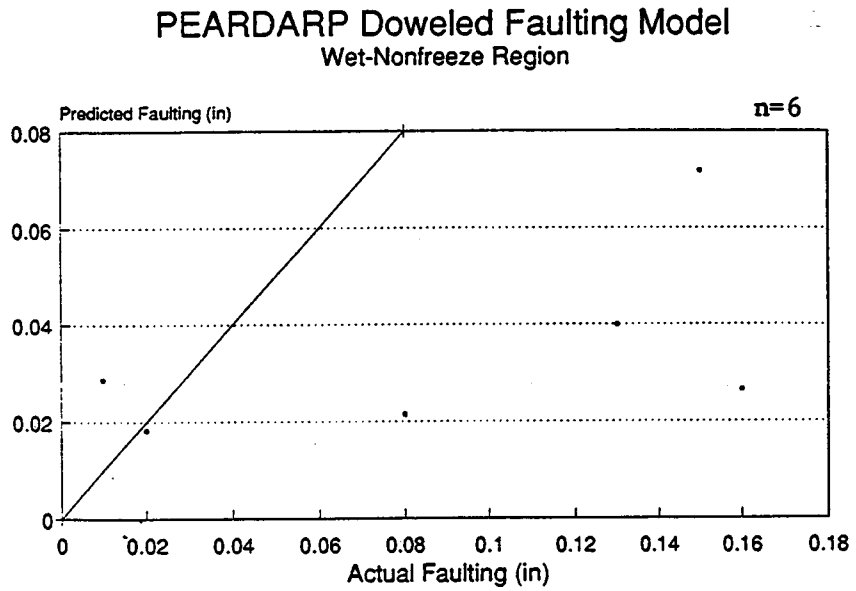

Figure 46. Actual field measured faulting versus faulting as predicted using the PEARDARP faulting models for doweled pavements for the wet-nonfreeze region.

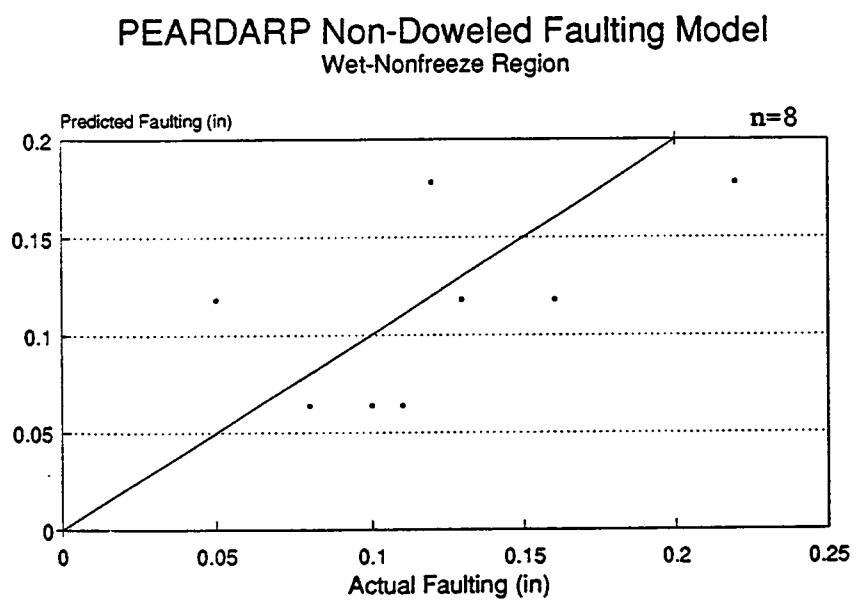

Figure 47. Actual field measured faulting versus faulting as predicted using the PEARDARP faulting models for nondoweled pavements for the wet-nonfreeze region.

Table 97. Actual field measured cracking versus cracking as predicted using the PEARDARP cracking model for all Phase I sections.

Section ID	Measured Crack	Predicted Crack	Difference
AZ 1-1	47	392	345
AZ 1-2	0	0	0
AZ 1-4	0	1	1
AZ 1-5	0	258	258
AZ 1-6	0	383	383
AZ 1-7	0	382	382
AZ 2	0	369	369
CA 1-1	19	415	396
CA 1-3	385	412	27
CA 1-5	0	324	324
CA 1-7	357	411	54
CA 1-9	862	413	449
CA 2-2	0	388	388
CA 2-3	947	404	543
CA 3-1	95	398	303
CA 3-2	19	397	378
CA 3-5	426	395	31
CA 6	186	399	213
CA 7	646	377	269
CA 8	0	368	368
FL 2	0	0	0
FL 3	1275	395	880
MI 1-1a	38	364	326
MI 1-1b	76	369	293
MI 1-4a	0	380	380
MI 1-7a	0	370	370
MI 1-7b	0	372	372
MI 1-10a	0	381	381
MI 1-10b	38	379	341
MI 1-25	38	382	344
MI 3	19	362	343
MI 4-1	1319	387	932
MI 4-2	1326	394	932
MI 5	1136	358	778
MN 1-1	19	396	377
MN 1-2	114	397	283
MN 1-3	191	412	221
MN 1-4	170	412	242
MN 1-5	647	417	230
MN 1-6	570	417	153
MN 1-7	551	401	150
MN 1-8	882	401	481
MN 1-9	0	401	401
MN 1-10	246	401	155
MN 1-11	276	418	142
MN 1-12	300	418	118
MN 2-1	0	395	395
MN 2-2	47	413	366

Table 97. Actual field measured cracking versus cracking as predicted using the PEARDARP cracking model for all Phase I sections (continued).

Section ID	Measured Crack	Predicted Crack	Difference
MN 2-3	0	392	392
MN 2-4	19	391	372
MN 3	0	379	379
MN 4b	0	399	399
MN 5	718	398	320
MN 6a	0	408	408
NJ 2	230	385	155
NJ 3-1	0	381	381
NJ 3-2	0	401	401
NY 1-1	0	389	389
NY 1-3	19	391	372
NY 1-4	0	362	362
NY 1-6	76	354	278
NY 1-8a	19	387	368
NY 1-8b	0	389	389
NY 2-3	511	371	140
NY 2-9	267	358	91
NY 2-11	76	375	299
NY 2-15	24	377	353
NC 1-1	0	374	374
NC 1-2	496	403	93
NC 1-3	991	399	592
NC 1-4	0	372	372
NC 1-5	57	396	339
NC 1-6	0	395	395
NC 1-7	96	419	323
NC 1-8	246	376	130
NC 2	38	342	304
OH 1-1	303	371	68
OH 1-3	0	393	393
OH 1-4	189	391	202
OH 1-6	133	372	239
OH 1-7	436	380	56
OH 1-9	568	379	189
OH 1-10	170	375	205
OH 2-33a	21	0	21
OH 2-33b	41	0	41
PA 1-1	152	323	171
PA 1-2	0	282	282
PA 1-3	0	243	243
PA 1-4	0	168	168
PA 1-5	0	243	243
ONT 1-1a	0	67	67
ONT 1-1b	13	67	54
ONT 1-2a	0	405	405
ONT 1-2b	0	405	405
ONT 1-3a	114	405	291
ONT 1-3b	259	405	146

Table 97. Actual field measured cracking versus cracking as predicted using the PEARDARP cracking model for all Phase I sections (continued).

Section ID	Measured Crack	Predicted Crack	Difference
ONT 1-4a	197	421	224
ONT 1-4b	287	421	134
ONT 2	19	411	392

Analysis Variable : DIFCRACK

N Obs	Mean	Std Error	T	Prob>|T|
99	299.7575758	17.9199881	16.7275544	0.0001

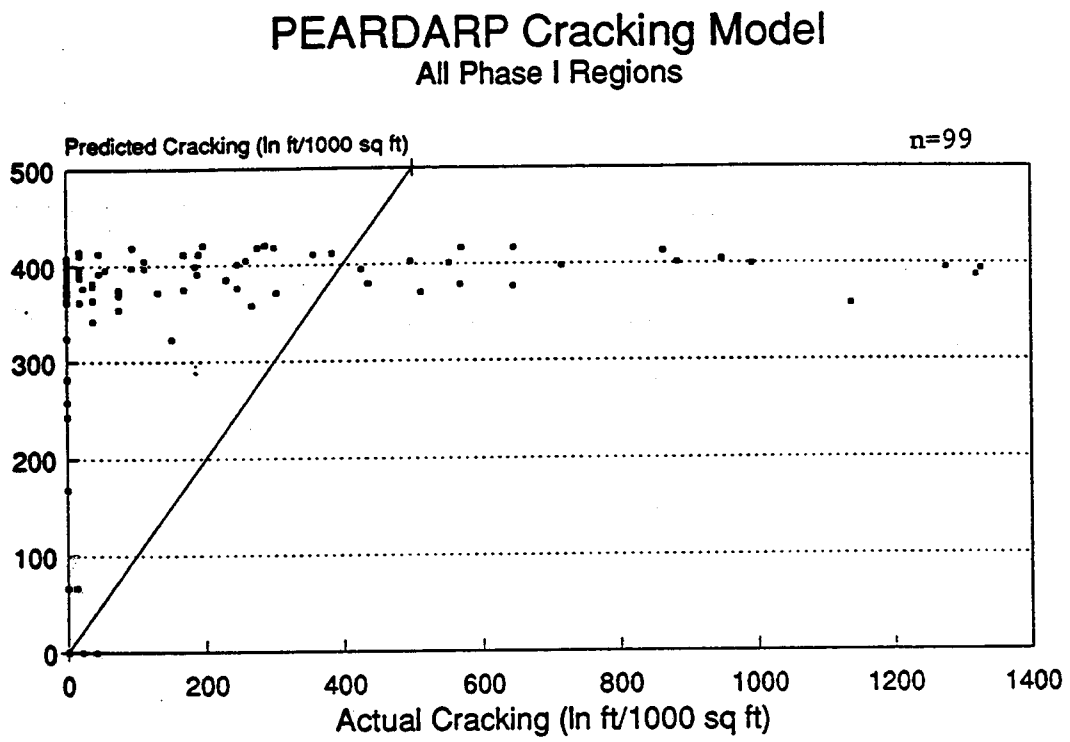

Figure 48. Actual field measured cracking versus cracking as predicted using the PEARDARP cracking model for all Phase I sections.

Table 98. Actual field measured cracking versus cracking as predicted using the PEARDARP cracking model for the dry-freeze region.

Section ID	Measured Crack	Predicted Crack	Difference
MN 1-1	19	396	377
MN 1-2	114	397	283
MN 1-3	191	412	221
MN 1-4	170	412	242
MN 1-5	647	417	230
MN 1-6	570	417	153
MN 1-7	551	401	150
MN 1-8	882	401	481
MN 1-9	0	401	401
MN 1-10	246	401	155
MN 1-11	276	418	142
MN 1-12	300	418	118
MN 2-1	0	395	395
MN 2-2	47	413	366
MN 2-3	0	392	392
MN 2-4	19	391	372
MN 3	0	379	379
MN 4b	0	399	399
MN 5	718	398	320
MN 6a	0	408	408

Analysis Variable : DIFCRACK

N Obs	Mean	Std Error	T	Prob>|T|
20	299.2000000	25.2372532	11.8554899	0.0001

Table 99. Actual field measured cracking versus cracking as predicted using the PEARDARP cracking model for the dry-nonfreeze region.

Section ID	Measured Crack	Predicted Crack	Difference
AZ 1-1	47	392	345
AZ 1-2	0	0	0
AZ 1-4	0	1	1
AZ 1-5	0	258	258
AZ 1-6	0	383	383
AZ 1-7	0	382	382
AZ 2	0	369	369
CA 1-1	19	415	396
CA 1-3	385	412	27
CA 1-5	0	324	324
CA 1-7	357	411	54
CA 1-9	862	413	449
CA 2-2	0	388	388
CA 2-3	947	404	543
CA 6	186	399	213
CA 7	646	377	269
CA 8	0	368	368

Analysis Variable : DIFCRACK

N Obs	Mean	Std Error	T	Prob>|T|
17	280.5294118	40.3160417	6.9582578	0.0001

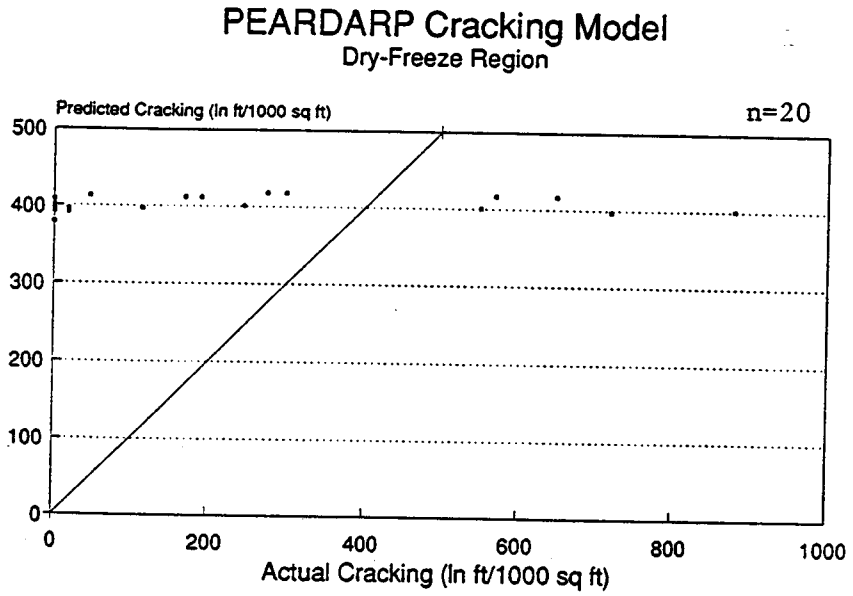

Figure 49. Actual field measured cracking versus cracking as predicted using the PEARDARP cracking model for the dry-freeze region.

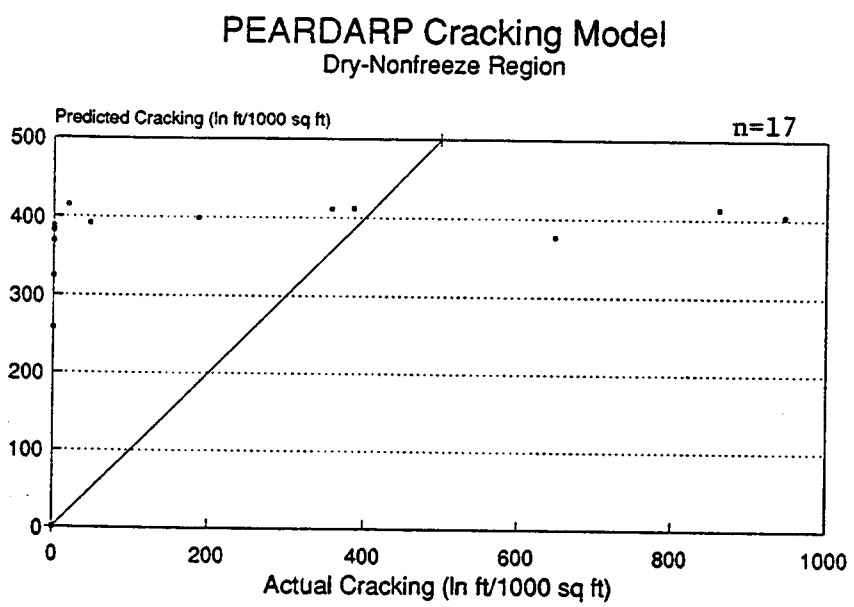

Figure 50. Actual field measured cracking versus cracking as predicted using the PEARDARP cracking model for the dry-nonfreeze region.

Table 100. Actual field measured cracking versus cracking as predicted using the PEARDARP cracking model for the wet-freeze region (continued).

Section ID	Measured Crack	Predicted Crack	Difference
MI 1-1a	38	364	326
MI 1-1b	76	369	293
MI 1-4a	0	380	380
MI 1-7a	0	370	370
MI 1-7b	0	372	372
MI 1-10a	0	381	381
MI 1-10b	38	379	341
MI 1-25	38	382	344
MI 3	19	362	343
MI 4-1	1319	387	932
MI 4-2	1326	394	932
MI 5	1136	358	778
NJ 2	230	385	155
NJ 3-1	0	381	381
NJ 3-2	0	401	401
NY 1-1	0	389	389
NY 1-3	19	391	372
NY 1-4	0	362	362
NY 1-6	76	354	278
NY 1-8a	19	387	368
NY 1-8b	0	389	389
NY 2-3	511	371	140
NY 2-9	267	358	91
NY 2-11	76	375	299
NY 2-15	24	377	353
OH 1-1	303	371	68
OH 1-3	0	393	393
OH 1-4	189	391	202
OH 1-6	133	372	239
OH 1-7	436	380	56
OH 1-9	568	379	189
OH 1-10	170	375	205
OH 2-33a	21	0	21
OH 2-33b	41	0	41
PA 1-1	152	323	171
PA 1-2	0	282	282
PA 1-3	0	243	243
PA 1-4	0	168	168
PA 1-5	0	243	243
ONT 1-1a	0	67	67
ONT 1-1b	13	67	54
ONT 1-2a	0	405	405
ONT 1-2b	0	405	405
ONT 1-3a	114	405	291
ONT 1-3b	259	405	146

Table 100. Actual field measured cracking versus cracking as predicted using the PEARDARP cracking model for the wet-freeze region (continued).

Section ID	Measured Crack	Predicted Crack	Difference
ONT 1-4a	197	421	224
ONT 1-4b	287	421	134
ONT 2	19	411	392

Analysis Variable : DIFCRACK

N Obs	Mean	Std Error	T	Prob>|T|
48	300.1875000	27.7827128	10.8048304	0.0001

Table 101. Actual field measured cracking versus cracking as predicted using the PEARDARP cracking model for the wet-nonfreeze region.

Section ID	Measured Crack	Predicted Crack	Difference
CA 3-1	95	398	303
CA 3-2	19	397	378
CA 3-5	426	395	31
FL 2	0	0	0
FL 3	1275	395	880
NC 1-1	0	374	374
NC 1-2	496	403	93
NC 1-3	991	399	592
NC 1-4	0	372	372
NC 1-5	57	396	339
NC 1-6	0	395	395
NC 1-7	96	419	323
NC 1-8	246	376	130
NC 2	38	342	304

Analysis Variable : DIFCRACK

N Obs	Mean	Std Error	T	Prob>|T|
14	322.4285714	60.9708735	5.2882393	0.0001

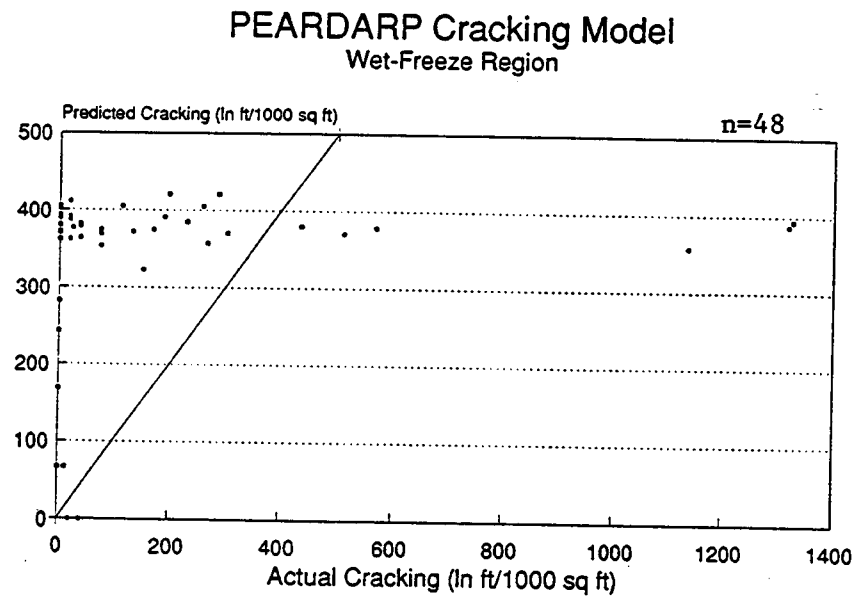

Figure 51. Actual field measured cracking versus cracking as predicted using the PEARDARP cracking model for the wet-freeze region.

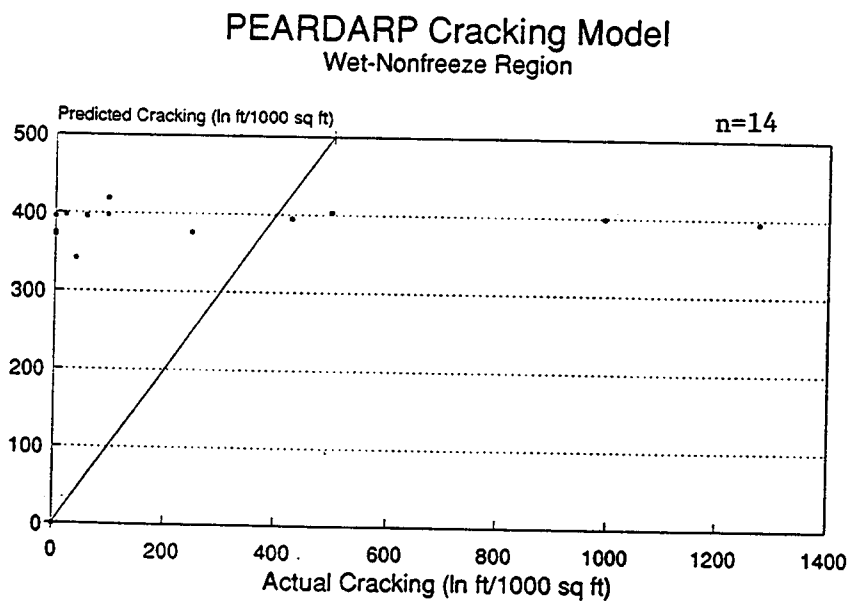

Figure 52. Actual field measured cracking versus cracking as predicted using the PEARDARP cracking model for the wet-nonfreeze region.

Table 102. Actual field observed pumping versus pumping as predicted using COPES pumping models for all Phase I sections.

Section ID	Actual Pumping	Integer Pumping	Predicted Pumping	Difference
AZ 1-1	N	0	0	0
AZ 1-2	N	0	0	0
AZ 1-4	N	0	0	0
AZ 1-5	N	0	0	0
AZ 1-6	N	0	0	0
AZ 1-7	N	0	0	0
AZ 2	N	0	0	0
CA 1-1	M	2	0	2
CA 1-3	N	0	0	0
CA 1-5	L	1	0	1
CA 1-7	H	3	0	3
CA 1-9	L	1	0	1
CA 2-2	N	0	0	0
CA 2-3	N	0	0	0
CA 3-1	N	0	0	0
CA 3-2	N	0	0	0
CA 3-5	N	0	0	0
CA 6	N	0	0	0
CA 7	N	0	0	0
CA 8	N	0	0	0
FL 2	N	0	0	0
FL 3	M	2	0	2
MI 1-1a	N	0	0	0
MI 1-1b	N	0	0	0
MI 1-4a	N	0	1	1
MI 1-7a	N	0	1	1
MI 1-7b	N	0	1	1
MI 1-10a	L	1	1	0
MI 1-10b	L	1	1	0
MI 1-25	L	1	1	0
MI 3	N	0	0	0
MI 4-1	N	0	0	0
MI 4-2	N	0	0	0
MI 5	N	0	0	0
MN 1-1	L	1	0	1
MN 1-2	N	0	0	0
MN 1-3	L	1	0	1
MN 1-4	L	1	0	1
MN 1-5	L	1	0	1
MN 1-6	N	0	0	0
MN 1-7	M	2	0	2
MN 1-8	N	0	0	0
MN 1-9	L	1	0	1
MN 1-10	L	1	0	1
MN 1-11	L	1	0	1
MN 1-12	M	2	0	2

Table 102. Actual field observed pumping versus pumping as predicted using COPES pumping models for all Phase I sections (continued).

Section ID	Actual Pumping	Integer Pumping	Predicted Pumping	Difference
MN 2-1	N	0	3	3
MN 2-2	N	0	3	3
MN 2-3	N	0	0	0
MN 2-4	N	0	0	0
MN 3	N	0	0	0
MN 4b	N	0	1	1
MN 5	L	1	0	1
MN 6a	N	0	0	0
NJ 2	N	0	0	0
NJ 3-1	N	0	0	0
NJ 3-2	N	0	0	0
NY 1-1	N	0	1	1
NY 1-3	M	2	0	2
NY 1-4	N	0	0	0
NY 1-6	N	0	1	1
NY 1-8a	N	0	1	1
NY 1-8b	N	0	1	1
NY 2-3	N	0	0	0
NY 2-9	N	0	0	0
NY 2-11	N	0	0	0
NY 2-15	N	0	0	0
NC 1-1	N	0	0	0
NC 1-2	N	0	0	0
NC 1-3	N	0	0	0
NC 1-4	N	0	0	0
NC 1-5	N	0	0	0
NC 1-6	N	0	0	0
NC 1-7	N	0	0	0
NC 1-8	N	0	0	0
NC 2	H	3	0	3
OH 1-1	N	0	0	0
OH 1-3	N	0	0	0
OH 1-4	N	0	0	0
OH 1-6	N	0	0	0
OH 1-7	N	0	0	0
OH 1-9	N	0	0	0
OH 1-10	N	0	0	0
OH 2-33a	L	1	0	1
OH 2-33b	M	2	0	2
PA 1-1	N	0	0	0
PA 1-2	N	0	0	0
PA 1-3	N	0	0	0
PA 1-4	N	0	0	0
PA 1-5	N	0	0	0
ONT 1-1a	L	1	1	0
ONT 1-1b	L	1	1	0
ONT 1-2a	M	2	1	1
ONT 1-2b	M	2	1	1

Table 102. Actual field observed pumping versus pumping as predicted using COPES pumping models for all Phase I sections (continued).

Section ID	Actual Pumping	Integer Pumping	Predicted Pumping	Difference
ONT 1-3a	L	1	1	0
ONT 1-3b	L	1	1	0
ONT 1-4a	N	0	2	2
ONT 1-4b	N	0	2	2
ONT 2	N	0	3	3

Analysis Variable : DIFPUMP

N Obs	Mean	Std Error	T	Prob>|T|
99	0.5252525	0.0853569	6.1536021	0.0001

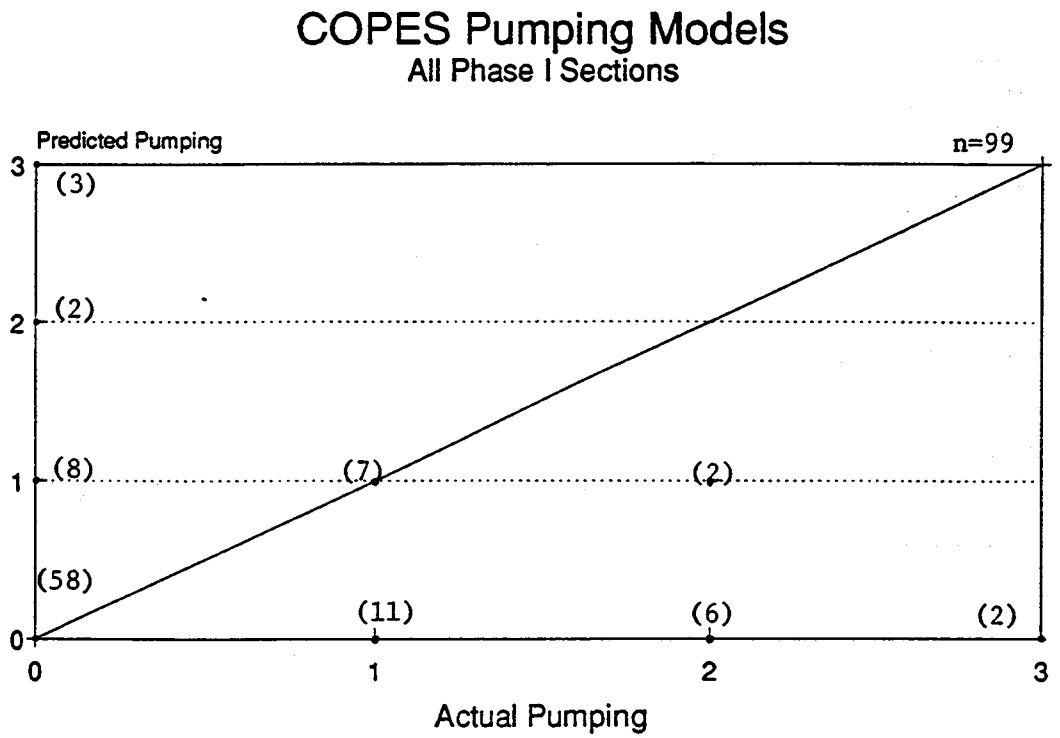

Figure 53. Actual field observed pumping versus pumping as predicted using COPES pumping models for all Phase I sections.

Table 103. Actual field observed pumping versus pumping as predicted using COPES pumping models for the dry-freeze region.

Section ID	Actual Pumping	Integer Pumping	Predicted Pumping	Difference
MN 1-1	L	1	0	1
MN 1-2	N	0	0	0
MN 1-3	L	1	0	1
MN 1-4	L	1	0	1
MN 1-5	L	1	0	1
MN 1-6	N	0	0	0
MN 1-7	M	2	0	2
MN 1-8	N	0	0	0
MN 1-9	L	1	0	1
MN 1-10	L	1	0	1
MN 1-11	L	1	0	1
MN 1-12	M	2	0	2
MN 2-1	N	0	3	3
MN 2-2	N	0	3	3
MN 2-3	N	0	0	0
MN 2-4	N	0	0	0
MN 3	N	0	0	0
MN 4b	N	0	1	1
MN 5	L	1	0	1
MN 6a	N	0	0	0

Analysis Variable : DIFPUMP

N Obs	Mean	Std Error	T	Prob>|T|
20	0.9500000	0.2111996	4.4981150	0.0002

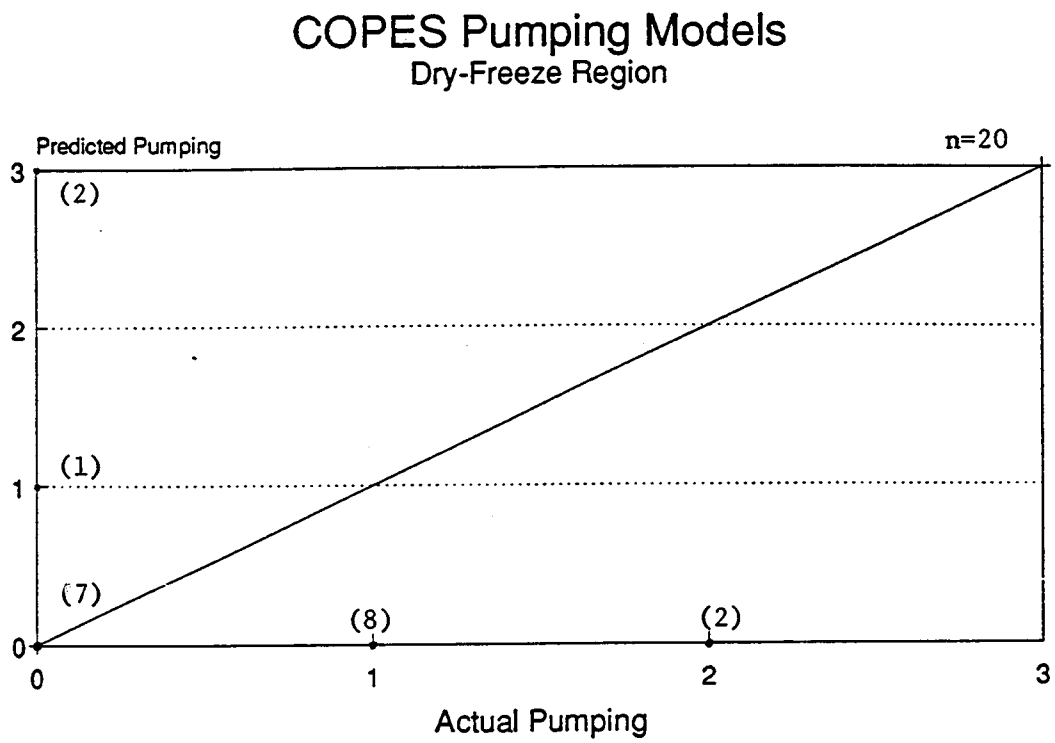

Figure 54. Actual field observed pumping versus pumping as predicted using COPES pumping models for the dry-freeze region.

Table 104. Actual field observed pumping versus pumping as predicted using COPES JPCP pumping model for the dry-freeze region.

Section ID	Actual Pumping	Integer Pumping	Predicted Pumping	Difference
MN 2-1	N	0	3	3
MN 2-2	N	0	3	3
MN 4b	N	0	1	1

Analysis Variable : DIFPUMP

N Obs	Mean	Std Error	T	Prob>|T|
3	2.3333333	0.6666667	3.5000000	0.0728

Table 105. Actual field observed pumping versus pumping as predicted using COPES JRCP pumping model for the dry-freeze region.

Section ID	Actual Pumping	Integer Pumping	Predicted Pumping	Difference
MN 1-1	L	1	0	1
MN 1-2	N	0	0	0
MN 1-3	L	1	0	1
MN 1-4	L	1	0	1
MN 1-5	L	1	0	1
MN 1-6	N	0	0	0
MN 1-7	M	2	0	2
MN 1-8	N	0	0	0
MN 1-9	L	1	0	1
MN 1-10	L	1	0	1
MN 1-11	L	1	0	1
MN 1-12	M	2	0	2
MN 2-3	N	0	0	0
MN 2-4	N	0	0	0
MN 3	N	0	0	0
MN 5	L	1	0	1
MN 6a	N	0	0	0

Analysis Variable : DIFPUMP

N Obs	Mean	Std Error	T	Prob>|T|
17	0.7058824	0.1663781	4.2426407	0.0006

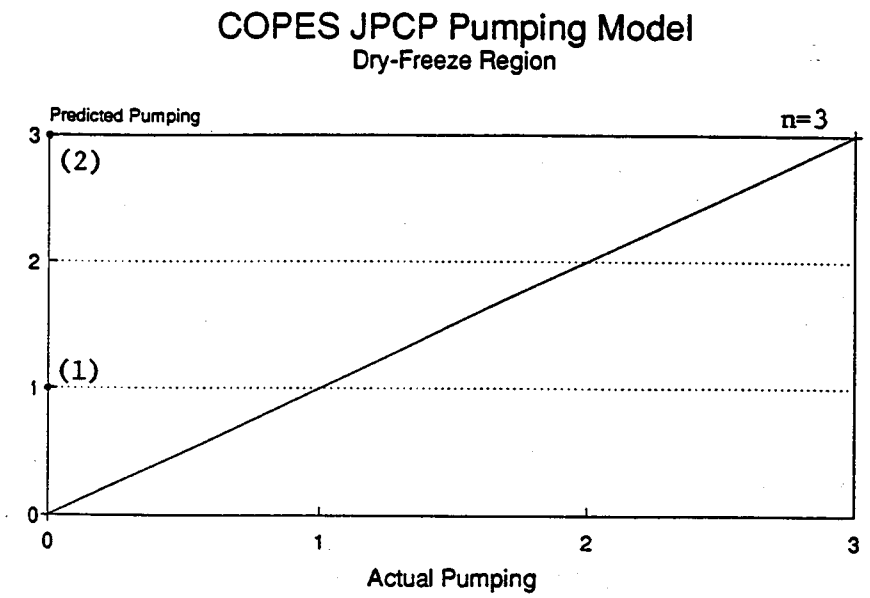

Figure 55. Actual field observed pumping versus pumping as predicted using COPES JPCP pumping model for the dry-freeze region.

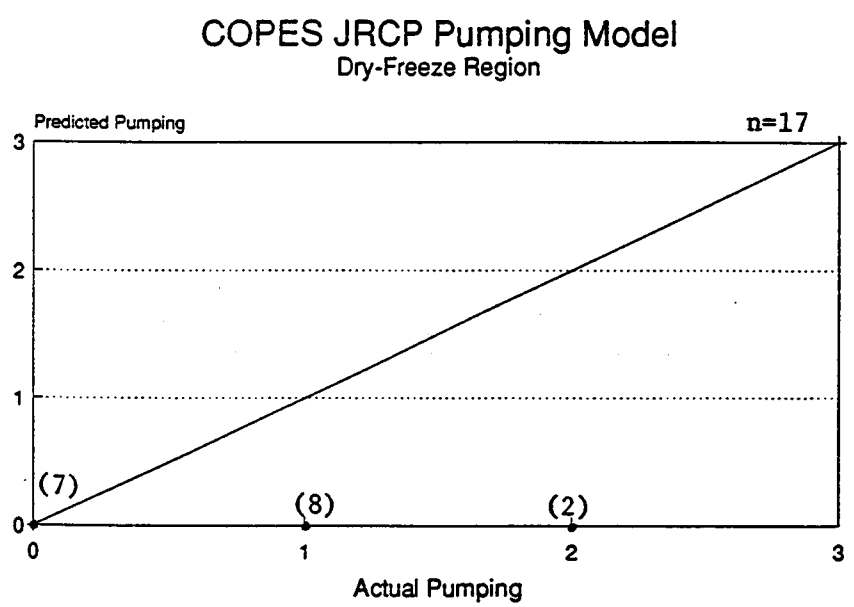

Figure 56. Actual field observed pumping versus pumping as predicted using COPES JRCP pumping model for the dry-freeze region.

Table 106. Actual field observed pumping versus pumping as predicted using COPES pumping model for the dry-nonfreeze region.

Section ID	Actual Pumping	Integer Pumping	Predicting Pumping	Difference
AZ 1-1	N	0	0	0
AZ 1-2	N	0	0	0
AZ 1-4	N	0	0	0
AZ 1-5	N	0	0	0
AZ 1-6	N	0	0	0
AZ 1-7	N	0	0	0
AZ 2	N	0	0	0
CA 1-1	M	2	0	2
CA 1-3	N	0	0	0
CA 1-5	L	1	0	1
CA 1-7	H	3	0	3
CA 1-9	L	1	0	1
CA 2-2	N	0	0	0
CA 2-3	N	0	0	0
CA 6	N	0	0	0
CA 7	N	0	0	0
CA 8	N	0	0	0

Analysis Variable : DIFPUMP

N Obs	Mean	Std Error	T	Prob>|T|
17	0.4117647	0.2110691	1.9508524	0.0688

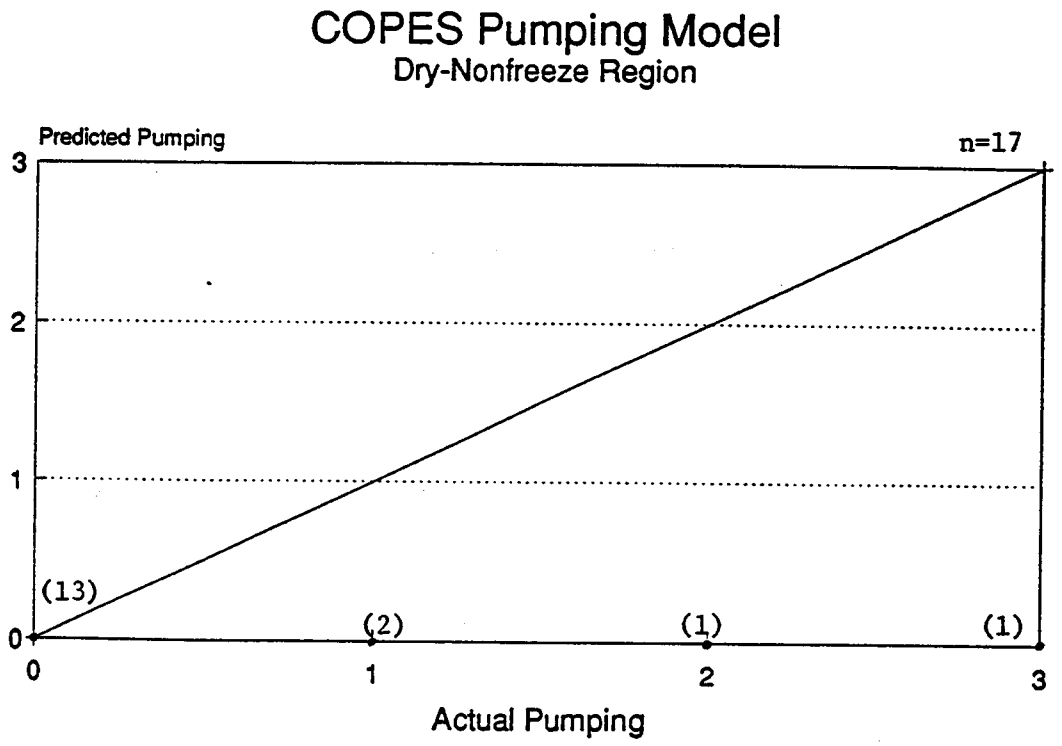

Figure 57. Actual field observed pumping versus pumping as predicted using COPES pumping model for the dry-nonfreeze region.

Table 107. Actual field observed pumping versus pumping as predicted using COPES pumping models for the wet-freeze region.

Section ID	Actual Pumping	Integer Pumping	Predicted Pumping	Difference
MI 1-1a	N	0	0	0
MI 1-1b	N	0	0	0
MI 1-4a	N	0	1	1
MI 1-7a	N	0	1	1
MI 1-7b	N	0	1	1
MI 1-10a	L	1	1	0
MI 1-10b	L	1	1	0
MI 1-25	L	1	1	0
MI 3	N	0	0	0
MI 4-1	N	0	0	0
MI 4-2	N	0	0	0
MI 5	N	0	0	0
NJ 2	N	0	0	0
NJ 3-1	N	0	0	0
NJ 3-2	N	0	0	0
NY 1-1	N	0	1	1
NY 1-3	M	2	0	2
NY 1-4	N	0	0	0
NY 1-6	N	0	1	1
NY 1-8a	N	0	1	1
NY 1-8b	N	0	1	1
NY 2-3	N	0	0	0
NY 2-9	N	0	0	0
NY 2-11	N	0	0	0
NY 2-15	N	0	0	0
OH 1-1	N	0	0	0
OH 1-3	N	0	0	0
OH 1-4	N	0	0	0
OH 1-6	N	0	0	0
OH 1-7	N	0	0	0
OH 1-9	N	0	0	0
OH 1-10	N	0	0	0
OH 2-33a	L	1	0	1
OH 2-33b	M	2	0	2
PA 1-1	N	0	0	0
PA 1-2	N	0	0	0
PA 1-3	N	0	0	0
PA 1-4	N	0	0	0
PA 1-5	N	0	0	0
ONT 1-1a	L	1	1	0
ONT 1-1b	L	1	1	0
ONT 1-2a	M	2	1	1
ONT 1-2b	M	2	1	1
ONT 1-3a	L	1	1	0
ONT 1-3b	L	1	1	0

Table 107. Actual field observed pumping versus pumping as predicted using COPES pumping models for the wet-freeze region (continued).

Section ID	Actual Pumping	Integer Pumping	Predicted Pumping	Difference
ONT 1-4a	N	0	2	2
ONT 1-4b	N	0	2	2
ONT 2	N	0	3	3

Analysis Variable : DIFPUMP

N Obs	Mean	Std Error	T	Prob>|T|
48	0.4375000	0.1069659	4.0900872	0.0002

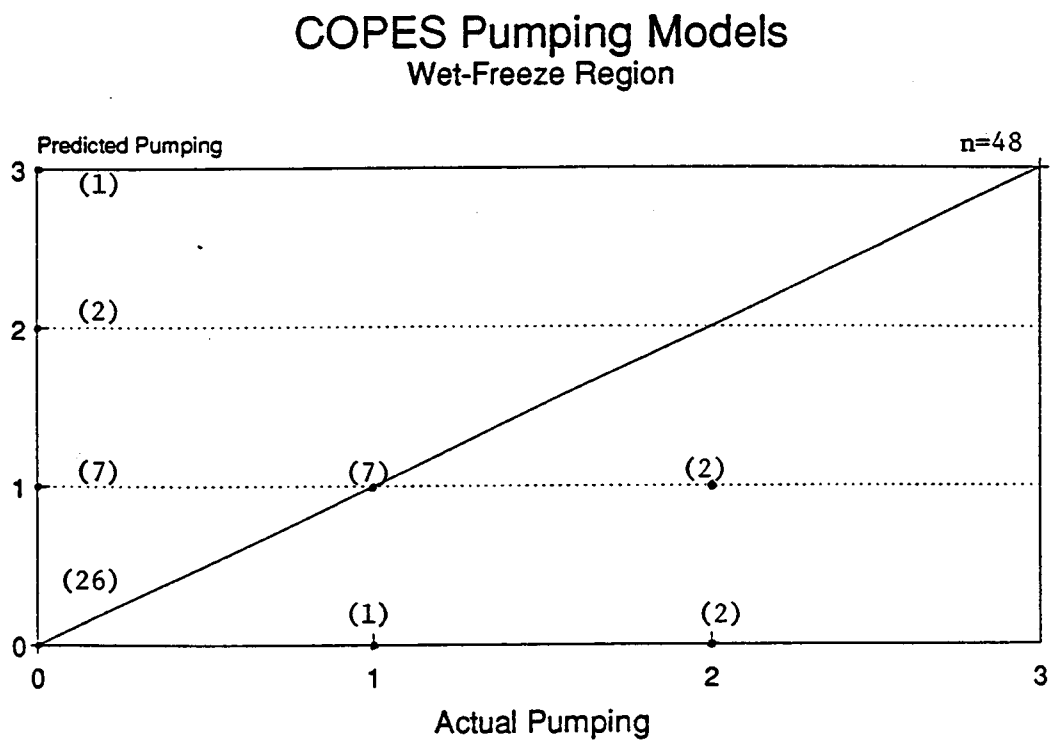

Figure 58. Actual field observed pumping versus pumping as predicted using COPES pumping models for the wet-freeze region.

Table 108. Actual field observed pumping versus pumping as predicted using COPES JPCP pumping model for the wet-freeze region.

Section ID	Actual Pumping	Integer Pumping	Predicted Pumping	Difference
MI 1-4a	N	0	1	1
MI 1-7a	N	0	1	1
MI 1-7b	N	0	1	1
MI 1-10a	L	1	1	0
MI 1-10b	L	1	1	0
MI 1-25	L	1	1	0
NY 1-1	N	0	1	1
NY 1-6	N	0	1	1
NY 1-8a	N	0	1	1
NY 1-8b	N	0	1	1
NY 2-3	N	0	0	0
NY 2-9	N	0	0	0
NY 2-11	N	0	0	0
ONT 1-1a	L	1	1	0
ONT 1-1b	L	1	1	0
ONT 1-2a	M	2	1	1
ONT 1-2b	M	2	1	1
ONT 1-3a	L	1	1	0
ONT 1-3b	L	1	1	0
ONT 1-4a	N	0	2	2
ONT 1-4b	N	0	2	2
ONT 2	N	0	3	3

Analysis Variable : DIFPUMP

N Obs	Mean	Std Error	T	Prob>|T|
22	0.7272727	0.1763239	4.1246404	0.0005

Table 109. Actual field observed pumping versus pumping as predicted using COPES JRCP pumping model for the wet-freeze region.

Section ID	Actual Pumping	Integer Pumping	Predicted Pumping	Difference
MI 1-1a	N	0	0	0
MI 1-1b	N	0	0	0
MI 3	N	0	0	0
MI 4-1	N	0	0	0
MI 4-2	N	0	0	0
MI 5	N	0	0	0
NJ 2	N	0	0	0
NJ 3-1	N	0	0	0
NJ 3-2	N	0	0	0
NY 1-3	M	2	0	2
NY 1-4	N	0	0	0
NY 2-15	N	0	0	0
OH 1-1	N	0	0	0
OH 1-3	N	0	0	0
OH 1-4	N	0	0	0
OH 1-6	N	0	0	0
OH 1-7	N	0	0	0
OH 1-9	N	0	0	0
OH 1-10	N	0	0	0
OH 2-33a	L	1	0	1
OH 2-33b	M	2	0	2
PA 1-1	N	0	0	0
PA 1-2	N	0	0	0
PA 1-3	N	0	0	0
PA 1-4	N	0	0	0
PA 1-5	N	0	0	0

Analysis Variable : DIFPUMP

N Obs	Mean	Std Error	T	Prob>|T|
26	0.1923077	0.1112064	1.7292862	0.0961

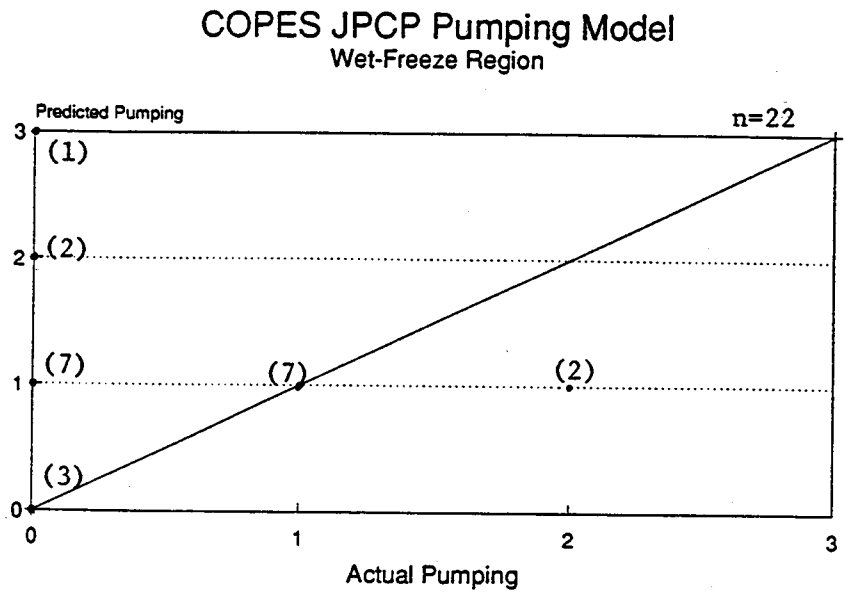

Figure 59. Actual field observed pumping versus pumping as predicted using COPES JPCP pumping model for the wet-freeze region.

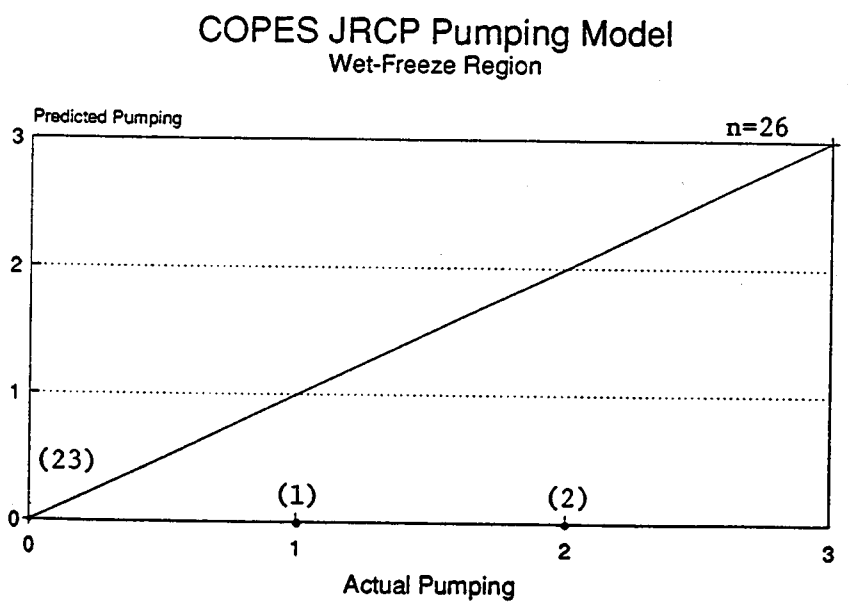

Figure 60. Actual field observed pumping versus pumping as predicted using COPES JRCP pumping model for the wet-freeze region.

Table 110. Actual field observed pumping versus pumping as predicted using COPES pumping model for the wet-nonfreeze region.

Section ID	Actual Pumping	Integer Pumping	Predicted Pumping	Difference
CA 3-1	N	0	0	0
CA 3-2	N	0	0	0
CA 3-5	N	0	0	0
FL 2	N	0	0	0
FL 3	M	2	0	2
NC 1-1	N	0	0	0
NC 1-2	N	0	0	0
NC 1-3	N	0	0	0
NC 1-4	N	0	0	0
NC 1-5	N	0	0	0
NC 1-6	N	0	0	0
NC 1-7	N	0	0	0
NC 1-8	N	0	0	0
NC 2	H	3	0	3

Analysis Variable : DIFPUMP

N Obs	Mean	Std Error	T	Prob>|T|
14	0.3571429	0.2482276	1.4387716	0.1739

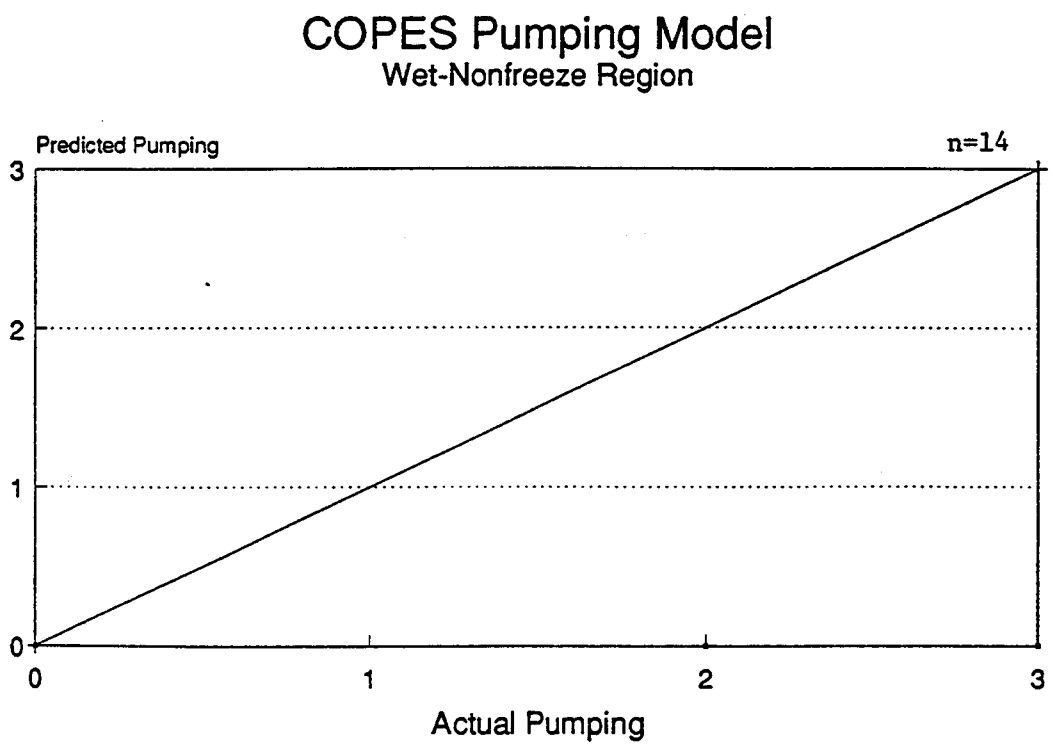

Figure 61. Actual field observed pumping versus pumping as predicted using COPES pumping models for the wet-nonfreeze region.

Table III. Actual field measured faulting versus faulting as predicted using the COPES faulting models for all Phase I sections.

Section ID	Measured Faulting	Predicted Faulting	Difference
AZ 1-1	0.08	0.0594	0.0206
AZ 1-2	0.01	0.0194	0.0094
AZ 1-4	0.01	0.0185	0.0085
AZ 1-5	0.03	0.0264	0.0036
AZ 1-6	0.01	0.0028	0.0072
AZ 1-7	0.02	0.0027	0.0173
AZ 2	0.01	0.0000	0.0100
CA 1-1	0.06	0.0704	0.0104
CA 1-3	0.10	0.0704	0.0296
CA 1-5	0.11	0.0523	0.0577
CA 1-7	0.06	0.0704	0.0104
CA 1-9	0.13	0.0704	0.0596
CA 2-2	0.11	0.0650	0.0450
CA 2-3	0.11	0.0650	0.0450
CA 3-1	0.08	0.0037	0.0763
CA 3-2	0.11	0.0037	0.1063
CA 3-5	0.10	0.0037	0.0963
CA 6	0.15	0.0603	0.0897
CA 7	0.06	0.0610	0.0010
CA 8	0.04	0.0552	0.0152
FL 2	0.01	0.0000	0.0100
FL 3	0.08	0.0000	0.0800
MI 1-1a	0.05	0.0340	0.0160
MI 1-1b	0.08	0.0340	0.0460
MI 1-4a	0.03	0.0907	0.0607
MI 1-7a	0.04	0.0659	0.0259
MI 1-7b	0.04	0.0659	0.0259
MI 1-10a	0.14	0.0907	0.0493
MI 1-10b	0.19	0.0907	0.0993
MI 1-25	0.20	0.0453	0.1547
MI 3	0.02	0.0577	0.0377
MI 4-1	0.12	0.1017	0.0183
MI 4-2	0.06	0.1017	0.0417
MI 5	0.05	0.0410	0.0090
MN 1-1	0.31	0.1101	0.1999
MN 1-2	0.06	0.0314	0.0286
MN 1-3	0.31	0.1162	0.1938
MN 1-4	0.06	0.0482	0.0118
MN 1-5	0.37	0.1375	0.2325
MN 1-6	0.00	0.0482	0.0482
MN 1-7	0.31	0.1314	0.1786
MN 1-8	0.06	0.0313	0.0286
MN 1-9	0.37	0.0758	0.2942
MN 1-10	0.13	0.0313	0.0986
MN 1-11	0.50	0.0819	0.4181
MN 1-12	0.06	0.0482	0.0118
MN 2-1	0.06	0.0638	0.0038

Table III. Actual field measured faulting versus faulting as predicted using the COPES faulting models for all Phase I sections (continued).

Section ID	Measured Faulting	Predicted Faulting	Difference
MN 2-2	0.06	0.0700	0.0100
MN 2-3	0.05	0.0258	0.0242
MN 2-4	0.06	0.0257	0.0342
MN 3	0.02	0.0179	0.0021
MN 4b	0.01	0.0877	0.0777
MN 5	0.09	0.0381	0.5169
MN 6a	0.01	0.0234	0.0134
NJ 2	0.06	0.2867	0.2267
NJ 3-1	0.05	0.0809	0.0309
NJ 3-2	0.06	0.0809	0.0209
NY 1-1	0.02	0.0994	0.0794
NY 1-3	0.14	0.0974	0.0426
NY 1-4	0.09	0.1310	0.0410
NY 1-6	0.03	0.1330	0.1030
NY 1-8a	0.01	0.0994	0.0894
NY 1-8b	0.03	0.0994	0.0694
NY 2-3	0.01	0.0334	0.0234
NY 2-9	0.02	0.0334	0.0134
NY 2-11	0.01	0.0334	0.0234
NY 2-15	0.02	0.0762	0.0562
NC 1-1	0.12	0.1061	0.0139
NC 1-2	0.16	0.0201	0.1399
NC 1-3	0.13	0.0669	0.0631
NC 1-4	0.13	0.0593	0.0707
NC 1-5	0.16	0.0682	0.0918
NC 1-6	0.05	0.0669	0.0169
NC 1-7	0.15	0.1524	0.0023
NC 1-8	0.22	0.1061	0.1139
NC 2	0.02	0.0000	0.0200
OH 1-1	0.13	0.0332	0.0967
OH 1-3	0.06	0.0000	0.0600
OH 1-4	0.07	0.0332	0.0367
OH 1-6	0.03	0.0000	0.0300
OH 1-7	0.07	0.0332	0.0367
OH 1-9	0.14	0.0332	0.1067
OH 1-10	0.10	0.0000	0.1000
OH 2-33a	0.11	0.0492	0.0608
OH 2-33b	0.11	0.1040	0.0060
PA 1-1	0.03	0.0057	0.0243
PA 1-2	0.02	0.0122	0.0078
PA 1-3	0.03	0.0122	0.0178
PA 1-4	0.03	0.0039	0.0026
PA 1-5	0.03	0.0122	0.0178
ONT 1-1a	0.05	0.1117	0.0617
ONT 1-1b	0.07	0.1117	0.0417
ONT 1-2a	0.05	0.1008	0.0508
ONT 1-2b	0.06	0.1008	0.0408

Table III. Actual field measured faulting versus faulting as predicted using the COPES faulting models for all Phase I sections (continued).

Section ID	Measured Faulting	Predicted Faulting	Difference
ONT 1-3a	0.04	0.0545	0.0145
ONT 1-3b	0.09	0.0545	0.0355
ONT 1-4a	0.04	0.0609	0.0209
ONT 1-4b	0.07	0.0609	0.0091
ONT 2	0.01	0.1054	0.0954

Analysis Variable : DIFCFLT

N Obs	Mean	Std Error	T	Prob>|T|
99	1.5981416	0.3822610	4.1807597	0.0001

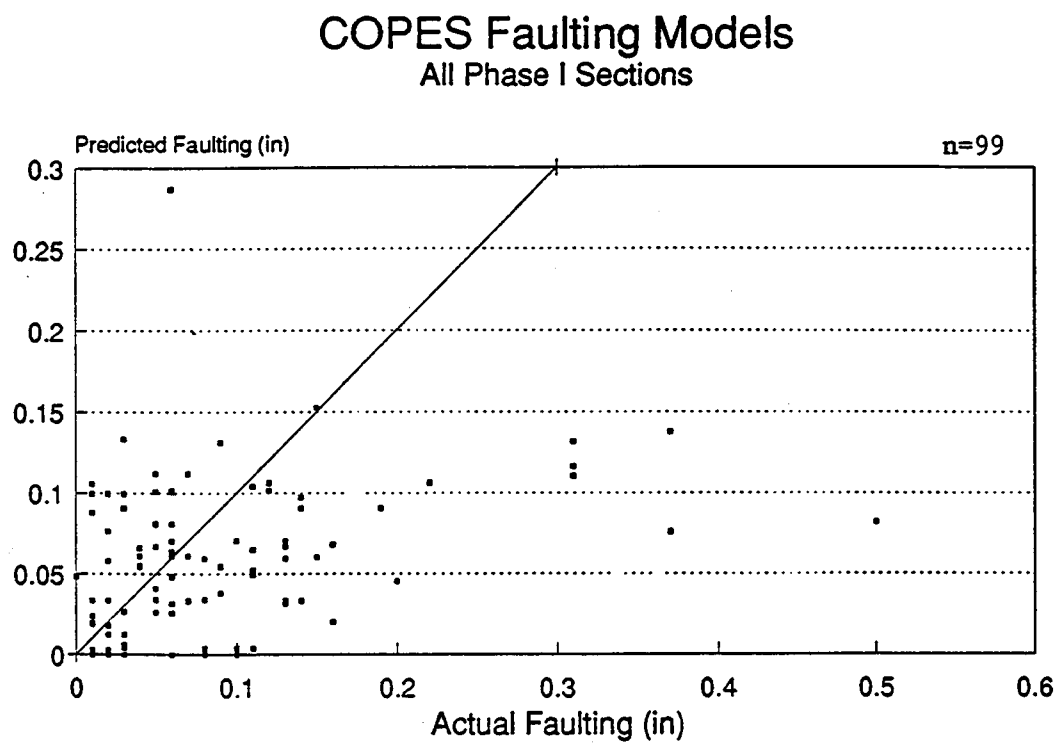

Figure 62. Actual field measured faulting versus faulting as predicted using the COPES faulting models for all Phase I sections.

Table 112. Actual field measured faulting versus faulting as predicted using the COPES faulting models for the dry-freeze region.

Section ID	Measured Faulting	Predicted Faulting	Difference
MN 1-1	0.31	0.11013	0.19987
MN 1-2	0.06	0.03139	0.02861
MN 1-3	0.31	0.11624	0.19376
MN 1-4	0.06	0.04819	0.01181
MN 1-5	0.37	0.13754	0.23246
MN 1-6	0.00	0.04819	0.04819
MN 1-7	0.31	0.13144	0.17856
MN 1-8	0.06	0.03139	0.02861
MN 1-9	0.37	0.07583	0.29417
MN 1-10	0.13	0.03139	0.09861
MN 1-11	0.50	0.08194	0.41806
MN 1-12	0.06	0.04819	0.01181
MN 2-1	0.06	0.06382	0.00382
MN 2-2	0.06	0.07003	0.01003
MN 2-3	0.05	0.02578	0.02422
MN 2-4	0.06	0.02578	0.03422
MN 3	0.02	0.01794	0.00206
MN 4b	0.01	0.08775	0.07775
MN 5	0.09	0.03831	0.05169
MN 6a	0.01	0.02335	0.01335

Analysis Variable : DIFCFLT

N Obs	Mean	Std Error	T	Prob>|T|
20	0.0980837	0.0260088	3.7711794	0.0013

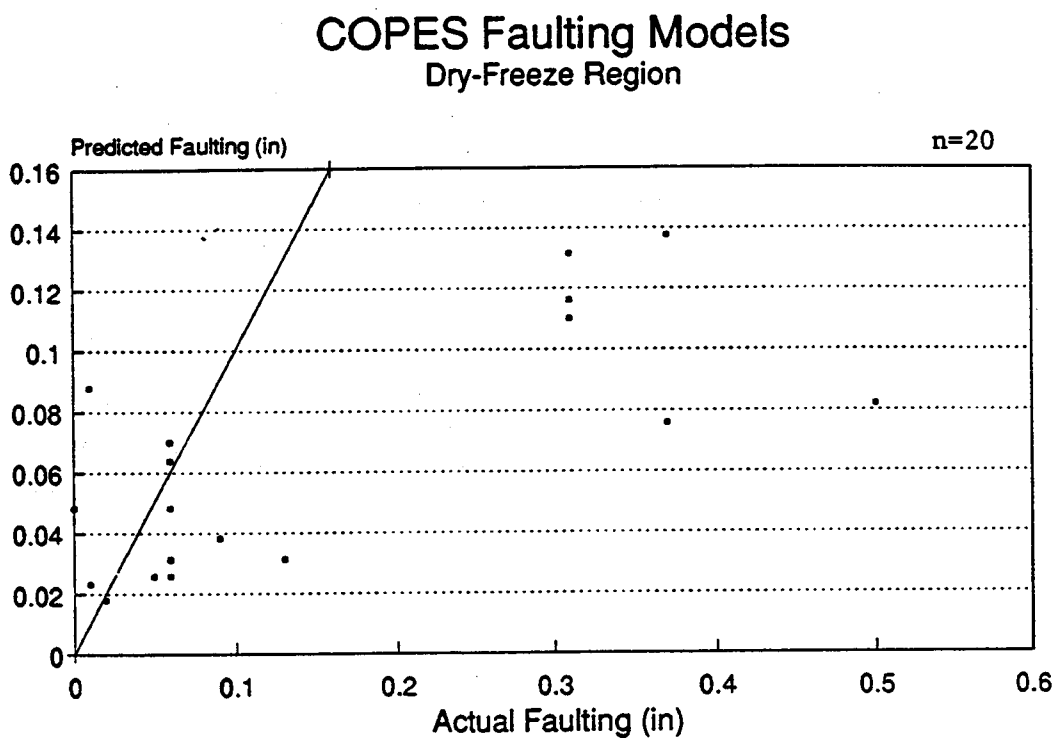

Figure 63. Actual field measured faulting versus faulting as predicted using the COPES faulting models for the dry-freeze region.

Table 113. Actual field measured faulting versus faulting as predicted using the COPES JPCP faulting model for the dry-freeze region.

Section ID	Measured Faulting	Predicted Faulting	Difference
MN 2-1	0.06	0.063820	0.003820
MN 2-2	0.06	0.070029	0.010029
MN 4b	0.01	0.087745	0.077745

Analysis Variable : DIFCFLT

N Obs	Mean	Std Error	T	Prob>|T|
3	0.0305316	0.0236749	2.9096188	0.0112

Table 114. Actual field measured faulting versus faulting as predicted using the COPES JRCP faulting model for the dry-freeze region.

Section ID	Measured Faulting	Predicted Faulting	Difference
MN 1-1	0.31	0.11013	0.19987
MN 1-2	0.06	0.03139	0.02861
MN 1-3	0.31	0.11624	0.19376
MN 1-4	0.06	0.04819	0.01181
MN 1-5	0.37	0.13754	0.23246
MN 1-6	0.00	0.04819	0.04819
MN 1-7	0.31	0.13144	0.17856
MN 1-8	0.06	0.03139	0.02861
MN 1-9	0.37	0.07583	0.29417
MN 1-10	0.13	0.03139	0.09861
MN 1-11	0.50	0.08194	0.41806
MN 1-12	0.06	0.04819	0.01181
MN 2-3	0.05	0.02578	0.02422
MN 2-4	0.06	0.02578	0.03422
MN 3	0.02	0.01794	0.00206
MN 5	0.09	0.03831	0.05169
MN 6a	0.01	0.02335	0.01335

Analysis Variable : DIFCFLT

N Obs	Mean	Std Error	T	Prob>|T|
17	0.1100047	0.0295546	3.7220875	0.0019

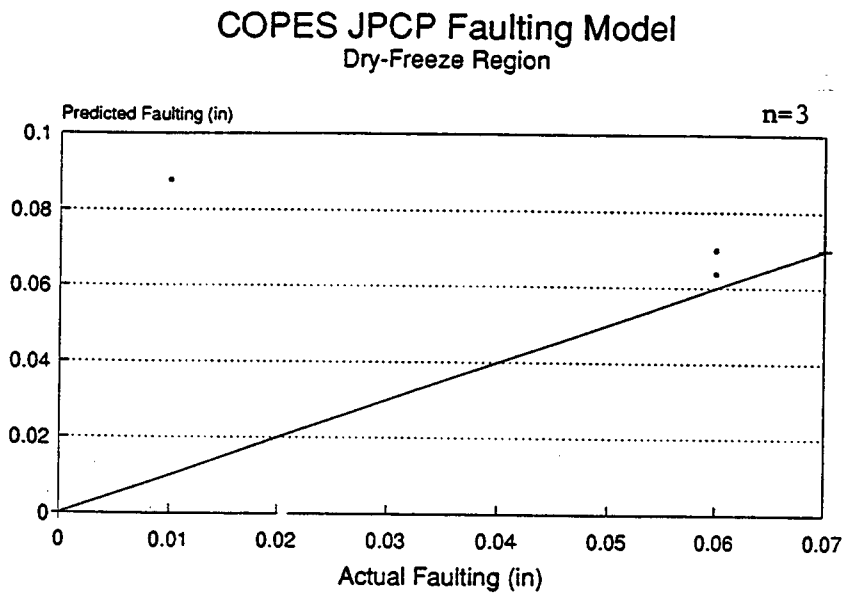

Figure 64. Actual field measured faulting versus faulting as predicted using the COPES JPCP faulting model for the dry-freeze region.

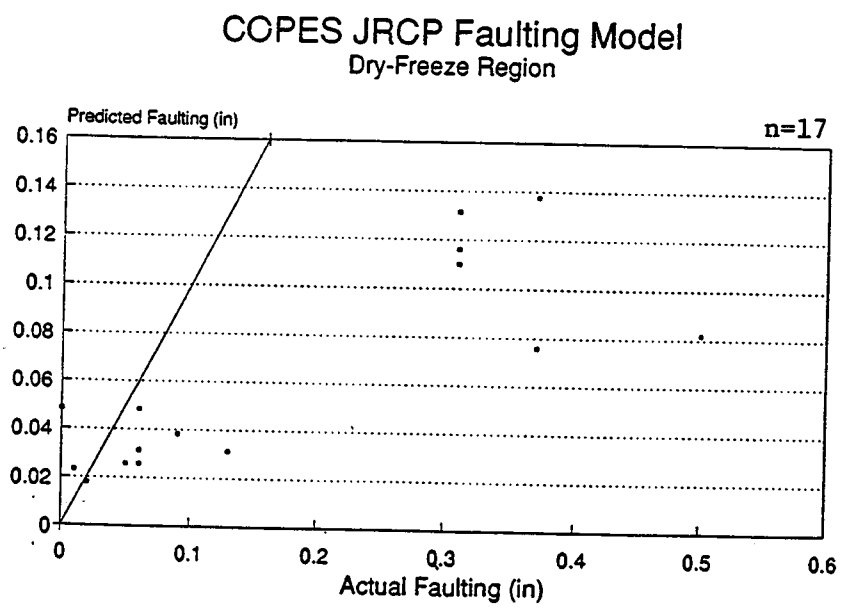

Figure 65. Actual field measured faulting versus faulting as predicted using the COPES JRCP faulting model for the dry-freeze region.

Table 115. Actual field measured faulting versus faulting as predicted using the COPES faulting models for the dry-nonfreeze region.

Section ID	Measured Faulting	Predicted Faulting	Difference
AZ 1-1	0.08	0.059444	0.020556
AZ 1-2	0.01	0.019442	0.009442
AZ 1-4	0.01	0.018465	0.008465
AZ 1-5	0.03	0.026374	0.003626
AZ 1-6	0.01	0.002786	0.007214
AZ 1-7	0.02	0.002668	0.017332
AZ 2	0.01	0.000000	0.010000
CA 1-1	0.06	0.070359	0.010359
CA 1-3	0.10	0.070359	0.029641
CA 1-5	0.11	0.052291	0.057709
CA 1-7	0.06	0.070359	0.010359
CA 1-9	0.13	0.070359	0.059641
CA 2-2	0.11	0.064993	0.045007
CA 2-3	0.11	0.064993	0.045007
CA 6	0.15	0.060289	0.089711
CA 7	0.06	0.061005	0.001005
CA 8	0.04	0.055211	0.015211

Analysis Variable : DIFCFLT

N Obs	Mean	Std Error	T	Prob>|T|
17	0.0258991	0.0060507	4.2803282	0.0006

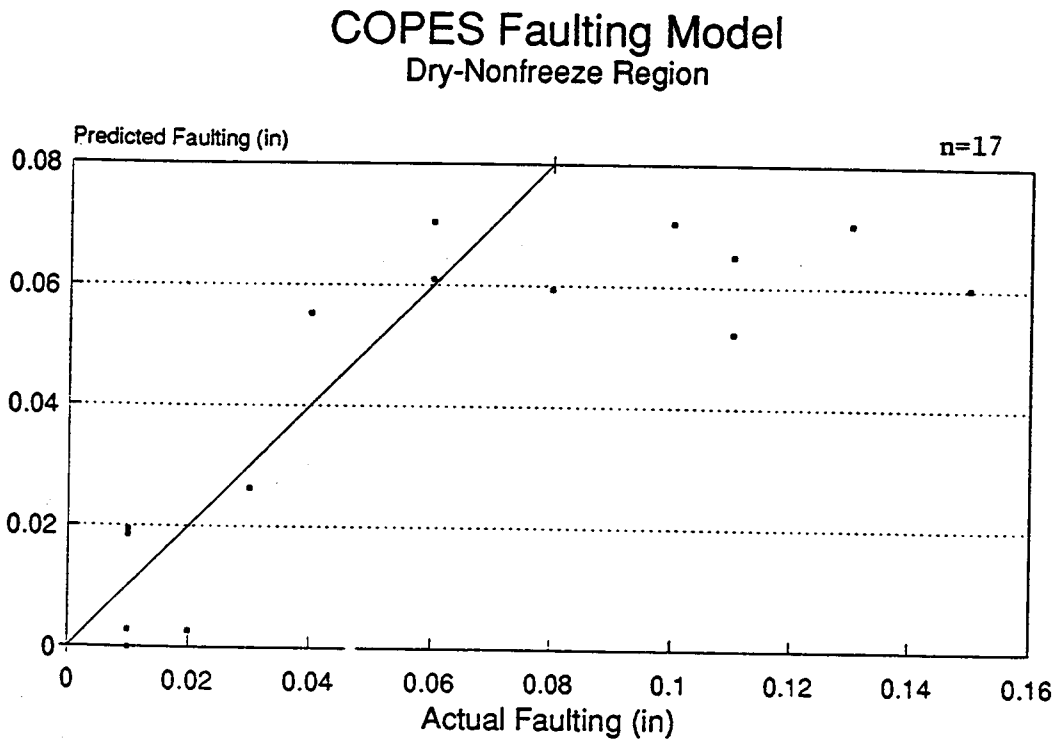

Figure 66. Actual field measured faulting versus faulting as predicted using the COPES faulting models for the dry-nonfreeze region.

Table 116. Actual field measured faulting versus faulting as predicted using the COPES faulting models for the wet-freeze region.

Section ID	Measured Faulting	Predicted Faulting	Difference
MI 1-1a	0.05	0.03401	0.01599
MI 1-1b	0.08	0.03401	0.04599
MI 1-4a	0.03	0.09074	0.06074
MI 1-7a	0.04	0.06585	0.02585
MI 1-7b	0.04	0.06585	0.02585
MI 1-10a	0.14	0.09074	0.04926
MI 1-10b	0.19	0.09074	0.09926
MI 1-25	0.20	0.04534	0.15466
MI 3	0.02	0.05769	0.03769
MI 4-1	0.12	0.10171	0.01829
MI 4-2	0.06	0.10171	0.04171
MI 5	0.05	0.00041	0.04959
NJ 2	0.06	0.28671	0.22671
NJ 3-1	0.05	0.08093	0.03093
NJ 3-2	0.06	0.08093	0.02093
NY 1-1	0.02	0.09938	0.07938
NY 1-3	0.14	0.09738	0.04262
NY 1-4	0.09	0.13098	0.04098
NY 1-6	0.03	0.13298	0.10298
NY 1-8a	0.01	0.09938	0.08938
NY 1-8b	0.03	0.09938	0.06938
NY 2-3	0.01	0.03336	0.02336
NY 2-9	0.02	0.03336	0.01336
NY 2-11	0.01	0.03336	0.02336
NY 2-15	0.02	0.07618	0.05618
OH 1-1	0.13	0.03328	0.09672
OH 1-3	0.06	0.00000	0.06000
OH 1-4	0.07	0.03328	0.03672
OH 1-6	0.03	0.00000	0.03000
OH 1-7	0.07	0.03328	0.03672
OH 1-9	0.14	0.03328	0.10672
OH 1-10	0.10	0.00000	0.10000
OH 2-33a	0.11	0.04918	0.06082
OH 2-33b	0.11	0.10404	0.00596
PA 1-1	0.03	0.00573	0.02427
PA 1-2	0.02	0.01219	0.00781
PA 1-3	0.03	0.01219	0.01781
PA 1-4	0.03	0.00392	0.02608
PA 1-5	0.03	0.01219	0.01781
ONT 1-1a	0.05	0.11167	0.06167
ONT 1-1b	0.07	0.11167	0.04167
ONT 1-2a	0.05	0.10079	0.05079

Table 116. Actual field measured faulting versus faulting as predicted using the COPES faulting models for the wet-freeze region (continued).

Section ID	Measured Faulting	Predicted Faulting	Difference
ONT 1-2b	0.06	0.10079	0.04079
ONT 1-3a	0.04	0.05451	0.01451
ONT 1-3b	0.09	0.05451	0.03549
ONT 1-4a	0.04	0.06089	0.02089
ONT 1-4b	0.07	0.06089	0.00911
ONT 2	0.01	0.10537	0.09537

Analysis Variable : DIFCFLT

N Obs	Mean	Std Error	T	Prob>|T|
48	0.0508778	0.0059633	8.5318361	0.0001

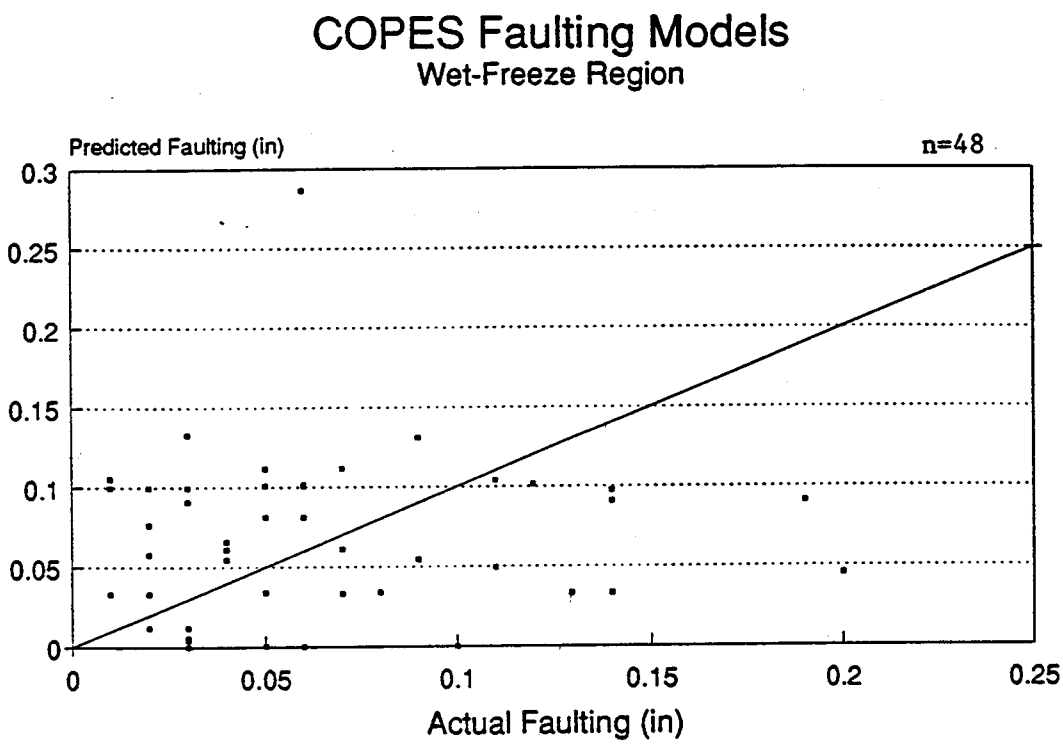

Figure 67. Actual field measured faulting versus faulting as predicted using the COPES faulting models for the wet-freeze region.

Table 117. Actual field measured faulting versus faulting as predicted using the COPES JPCP faulting model for the wet-freeze region.

Section ID	Measured Faulting	Predicted Faulting	Difference
MI 1-4a	0.03	0.09074	0.06074
MI 1-7a	0.04	0.06585	0.02585
MI 1-7b	0.04	0.06585	0.02585
MI 1-10a	0.14	0.09074	0.04926
MI 1-10b	0.19	0.09074	0.09926
MI 1-25	0.20	0.04534	0.15466
NY 1-1	0.02	0.09938	0.07938
NY 1-6	0.03	0.13298	0.10298
NY 1-8a	0.01	0.09938	0.08938
NY 1-8b	0.03	0.09938	0.06938
NY 2-3	0.01	0.03336	0.02336
NY 2-9	0.02	0.03336	0.01336
NY 2-11	0.01	0.03336	0.02336
ONT 1-1a	0.05	0.11167	0.06167
ONT 1-1b	0.07	0.11167	0.04167
ONT 1-2a	0.05	0.10079	0.05079
ONT 1-2b	0.06	0.10079	0.04079
ONT 1-3a	0.04	0.05451	0.01451
ONT 1-3b	0.09	0.05451	0.03549
ONT 1-4a	0.04	0.06089	0.02089
ONT 1-4b	0.07	0.06089	0.00911
ONT 2	0.01	0.10537	0.09537

Analysis Variable : DIFCFLT

N Obs	Mean	Std Error	T	Prob>|T|
22	0.0539593	0.0079247	6.8090333	0.0001

Table 118. Actual field measured faulting versus faulting as predicted using the COPES JRCP faulting model for the wet-freeze region.

Section ID	Measured Faulting	Predicted Faulting	Difference
MI 1-1a	0.05	0.03401	0.01599
MI 1-1b	0.08	0.03401	0.04599
MI 3	0.02	0.05769	0.03769
MI 4-1	0.12	0.10171	0.01829
MI 4-2	0.06	0.10171	0.04171
MI 5	0.05	0.00041	0.04959
NJ 2	0.06	0.28671	0.22671
NJ 3-1	0.05	0.08093	0.03093
NJ 3-2	0.06	0.08093	0.02093
NY 1-3	0.14	0.09738	0.04262
NY 1-4	0.09	0.13098	0.04098
NY 2-15	0.02	0.07618	0.05618
OH 1-1	0.13	0.03328	0.09672
OH 1-3	0.06	0.00000	0.06000
OH 1-4	0.07	0.03328	0.03672
OH 1-6	0.03	0.00000	0.03000
OH 1-7	0.07	0.03328	0.03672
OH 1-9	0.14	0.03328	0.10672
OH 1-10	0.10	0.00000	0.10000
OH 2-33a	0.11	0.04918	0.06082
OH 2-33b	0.11	0.10404	0.00596
PA 1-1	0.03	0.00573	0.02427
PA 1-2	0.02	0.01219	0.00781
PA 1-3	0.03	0.01219	0.01781
PA 1-4	0.03	0.00392	0.02608
PA 1-5	0.03	0.01219	0.01781

Analysis Variable : DIFCFLT

N Obs	Mean	Std Error	T	Prob>|T|
26	0.0482703	0.0088427	5.4587770	0.0001

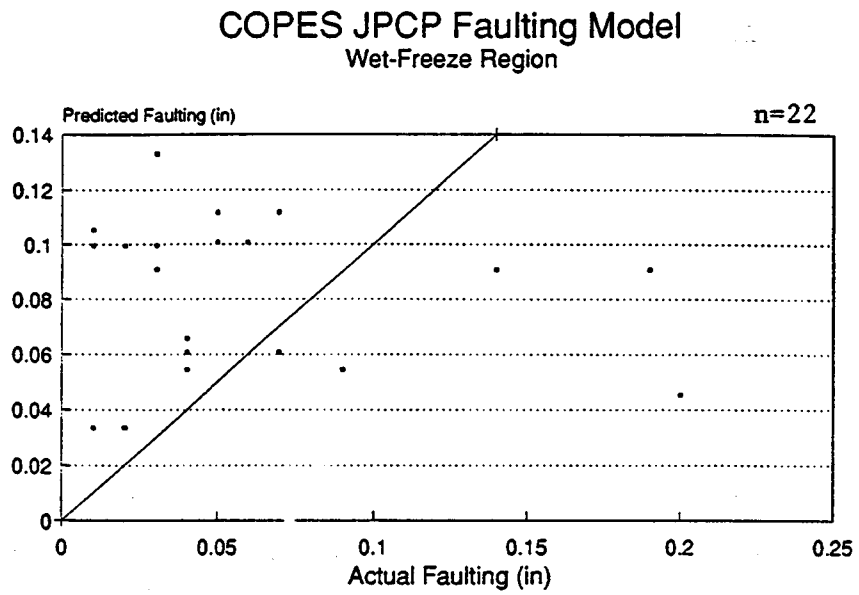

Figure 68. Actual field measured faulting versus faulting as predicted using the COPES JPCP faulting model for the wet-freeze region.

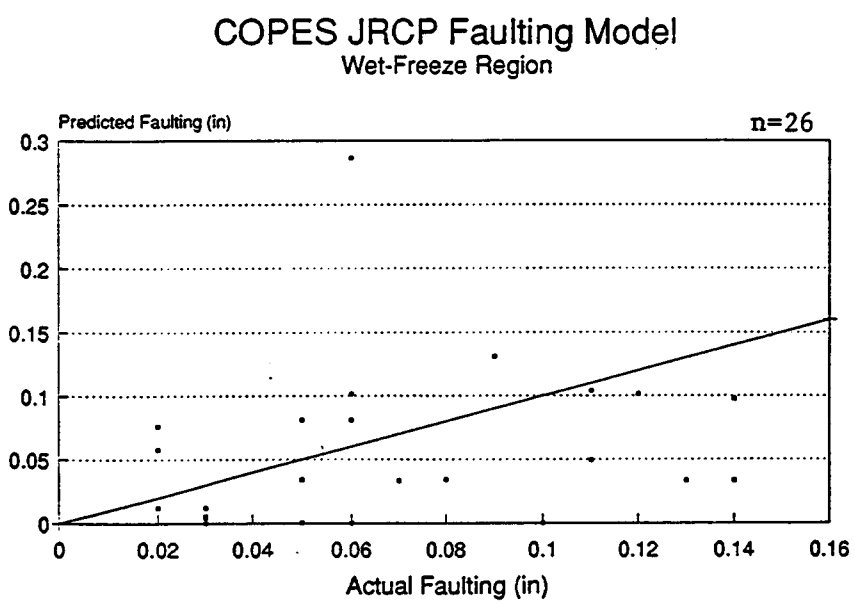

Figure 69. Actual field measured faulting versus faulting as predicted using the COPES JRCP faulting model for the wet-freeze region.

Table 119. Actual field measured faulting versus faulting as predicted using the COPES faulting models for the wet-nonfreeze region.

Section ID	Measured Faulting	Predicted Faulting	Difference
CA 3-1	0.08	0.00373	0.07627
CA 3-2	0.11	0.00375	0.10625
CA 3-5	0.10	0.00375	0.09625
FL 2	0.01	0.00000	0.01000
FL 3	0.08	0.00000	0.08000
NC 1-1	0.12	0.10610	0.01390
NC 1-2	0.16	0.02015	0.13985
NC 1-3	0.13	0.06690	0.06310
NC 1-4	0.13	0.05934	0.07066
NC 1-5	0.16	0.06824	0.09176
NC 1-6	0.05	0.06690	0.01690
NC 1-7	0.15	0.15238	0.00238
NC 1-8	0.22	0.10610	0.11390
NC 2	0.02	0.00000	0.02000

Analysis Variable : DIFCFLT

N Obs	Mean	Std Error	T	Prob>|T|
14	0.0643744	0.0118755	5.4207839	0.0001

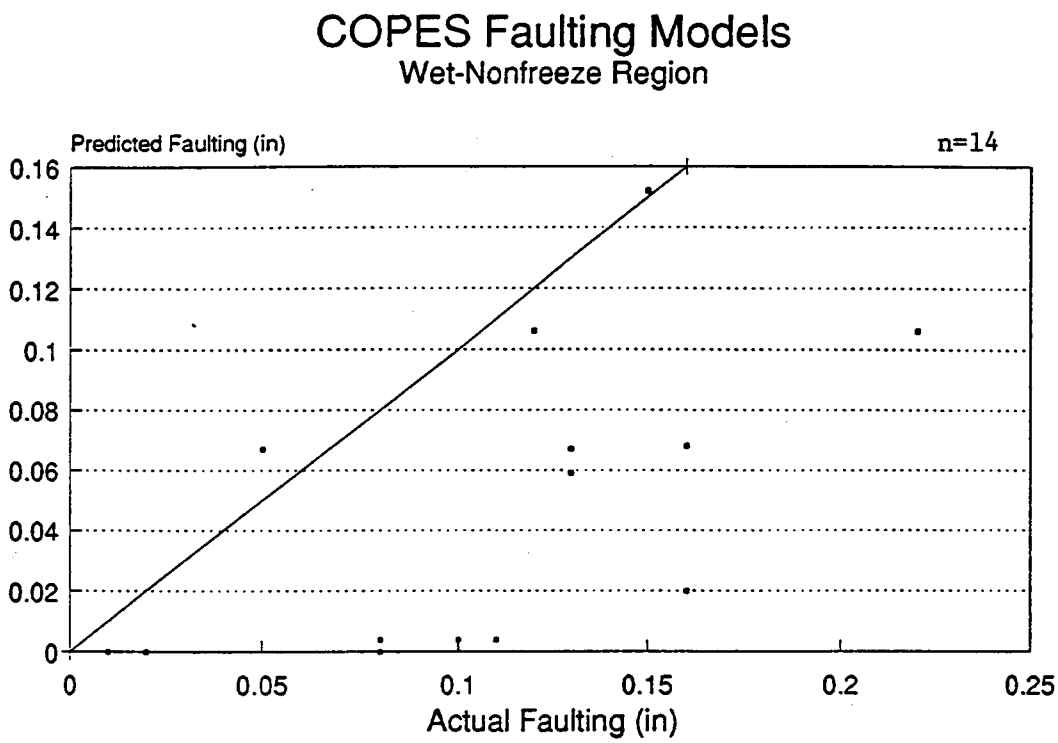

Figure 70. Actual field measured faulting versus faulting as predicted using the COPES faulting models for the wet-nonfreeze region.

Table 120. Actual field measured spalling versus joint deterioration (spalling) as predicted using the COPES spalling models for all Phase I sections.

Section ID	Measured Spalling	Predicted Spalling	Difference
AZ 1-1	22	0	22
AZ 1-2	1	0	1
AZ 1-4	0	0	0
AZ 1-5	0	1	1
AZ 1-6	1	0	1
AZ 1-7	0	0	0
AZ 2	0	0	0
CA 1-1	2	6	4
CA 1-3	0	6	6
CA 1-5	3	6	3
CA 1-7	9	6	3
CA 1-9	3	6	3
CA 2-2	0	0	0
CA 2-3	0	0	0
CA 3-1	2	0	2
CA 3-2	3	3	0
CA 3-5	6	3	3
CA 6	3	0	3
CA 7	0	1	1
CA 8	0	0	0
FL 2	0	0	0
FL 3	2	0	2
MI 1-1a	0	22	22
MI 1-1b	0	22	22
MI 1-4a	9	66	57
MI 1-7a	12	66	54
MI 1-7b	11	66	55
MI 1-10a	41	66	25
MI 1-10b	63	68	5
MI 1-25	75	66	9
MI 3	0	0	0
MI 4-1	0	32	32
MI 4-2	6	32	26
MI 5	0	0	0
MN 1-1	4	29	25
MN 1-2	14	29	15
MN 1-3	8	29	21
MN 1-4	15	29	14
MN 1-5	24	29	5
MN 1-6	31	29	2
MN 1-7	15	29	14
MN 1-8	69	29	40
MN 1-9	4	29	25
MN 1-10	6	35	29
MN 1-11	37	35	2
MN 1-12	29	35	6
MN 2-1	3	2	1
MN 2-2	9	2	7

Table 120. Actual field measured spalling versus joint deterioration (spalling) as predicted using the COPES spalling models for all Phase I sections (continued).

Section ID	Measured Spalling	Predicted Spalling	Difference
MN 2-3	3	1	2
MN 2-4	8	1	7
MN 3	0	0	0
MN 4b	0	0	0
MN 5	36	9	27
MN 6a	0	0	0
NJ 2	20	46	26
NJ 3-1	0	0	0
NJ 3-2	43	0	43
NY 1-1	6	0	6
NY 1-3	73	21	52
NY 1-4	9	21	12
NY 1-6	13	0	13
NY 1-8a	0	0	0
NY 1-8b	0	0	0
NY 2-3	0	0	0
NY 2-9	0	0	0
NY 2-11	0	0	0
NY 2-15	0	5	5
NC 1-1	0	40	40
NC 1-2	0	0	0
NC 1-3	0	0	0
NC 1-4	0	0	0
NC 1-5	0	0	0
NC 1-6	0	0	0
NC 1-7	0	19	19
NC 1-8	0	0	0
NC 2	0	0	0
OH 1-1	0	13	13
OH 1-3	13	18	5
OH 1-4	0	9	9
OH 1-6	0	18	18
OH 1-7	0	9	9
OH 1-9	0	9	9
OH 1-10	0	18	18
OH 2-33a	15	18	3
OH 2-33b	23	18	5
PA 1-1	0	2	2
PA 1-2	0	2	2
PA 1-3	0	2	2
PA 1-4	0	2	2
PA 1-5	0	2	2
ONT 1-1a	0	0	0
ONT 1-1b	0	0	0
ONT 1-2a	0	0	0
ONT 1-2b	0	0	0

Table 120. Actual field measured spalling versus joint deterioration (spalling) as predicted using the COPES spalling models for all Phase I sections (continued).

Section ID	Measured Spalling	Predicted Spalling	Difference
ONT 1-3a	0	0	0
ONT 1-3b	0	0	0
ONT 1-4a	0	0	0
ONT 1-4b	0	0	0

Analysis Variable : DIFJD

N Obs	Mean	Std Error	T	Prob>|T|
99	9.2828283	1.3995641	6.6326567	0.0001

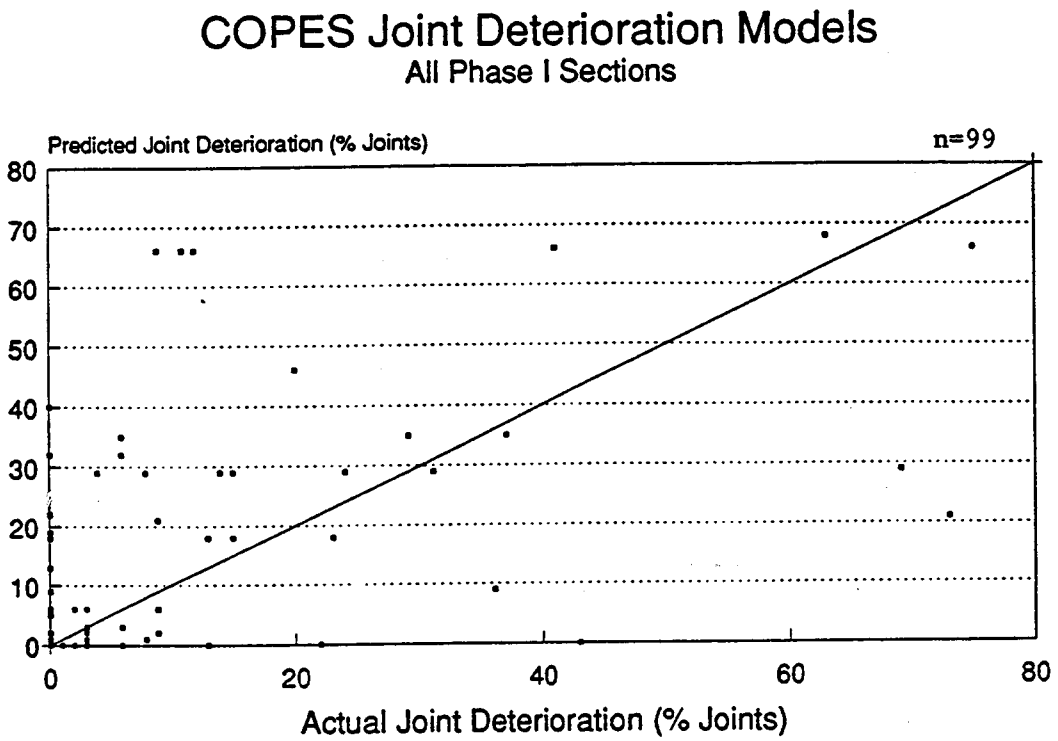

Figure 71. Actual field measured spalling versus joint deterioration (spalling) as predicted using the COPES spalling models for all Phase I sections.

Table 121. Actual field measured spalling versus joint deterioration (spalling) as predicted using the COPES spalling models for the dry-freeze region.

Section ID	Measured Spalling	Predicted Spalling	Difference
MN 1-1	4	29	25
MN 1-2	14	29	15
MN 1-3	8	29	21
MN 1-4	15	29	14
MN 1-5	24	29	5
MN 1-6	31	29	2
MN 1-7	15	29	14
MN 1-8	69	29	40
MN 1-9	4	29	25
MN 1-10	6	35	29
MN 1-11	37	35	2
MN 1-12	29	35	6
MN 2-1	3	2	1
MN 2-2	9	2	7
MN 2-3	3	1	2
MN 2-4	8	1	7
MN 3	0	0	0
MN 4b	0	0	0
MN 5	36	9	27
MN 6a	0	0	0

Analysis Variable : DIFJD

N Obs	Mean	Std Error	T	Prob>|T|
20	12.1000000	2.6763093	4.5211515	0.0002

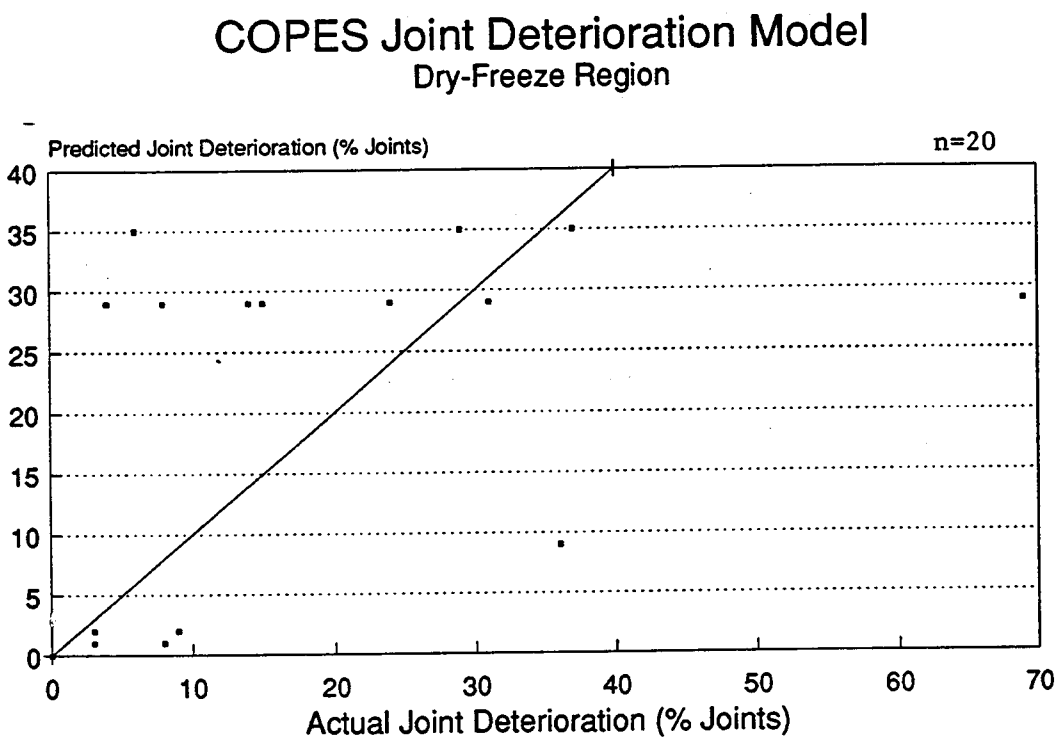

Figure 72. Actual field measured spalling versus joint deterioration (spalling) as predicted using the COPES spalling models for the dry-freeze region.

Table 122. Actual field measured spalling versus joint deterioration (spalling) as predicted using the COPES JPCP joint deterioration model for the dry-freeze region.

Section ID	Measured Spalling	Predicted Spalling	Difference
MN 2-1	3	2	1
MN 2-2	9	2	7
MN 4b	0	0	0

Analysis Variable : DIFJD

N Obs	Mean	Std Error	T	Prob>|T|
3	2.6666667	2.1858128	1.2199886	0.3468

Table 123. Actual field measured spalling versus joint deterioration (spalling) as predicted using the COPES JRCP joint deterioration model for the dry-freeze region.

Section ID	Measured Spalling	Predicted Spalling	Difference
MN 1-1	4	29	25
MN 1-2	14	29	15
MN 1-3	8	29	21
MN 1-4	15	29	14
MN 1-5	24	29	5
MN 1-6	31	29	2
MN 1-7	15	29	14
MN 1-8	69	29	40
MN 1-9	4	29	25
MN 1-10	6	35	29
MN 1-11	37	35	2
MN 1-12	29	35	6
MN 2-3	3	1	2
MN 2-4	8	1	7
MN 3	0	0	0
MN 5	36	9	27
MN 6a	0	0	0

Analysis Variable : DIFJD

N Obs	Mean	Std Error	T	Prob>|T|
17	13.7647059	2.9574550	4.6542403	0.0003

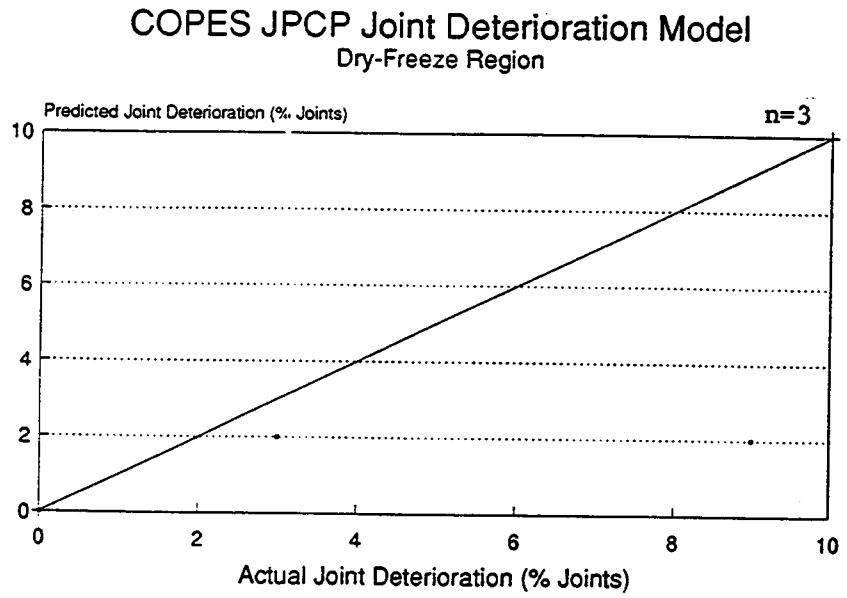

Figure 73. Actual field measured spalling versus joint deterioration (spalling) as predicted using the COPES JPCP joint deterioration model for the dry-freeze region.

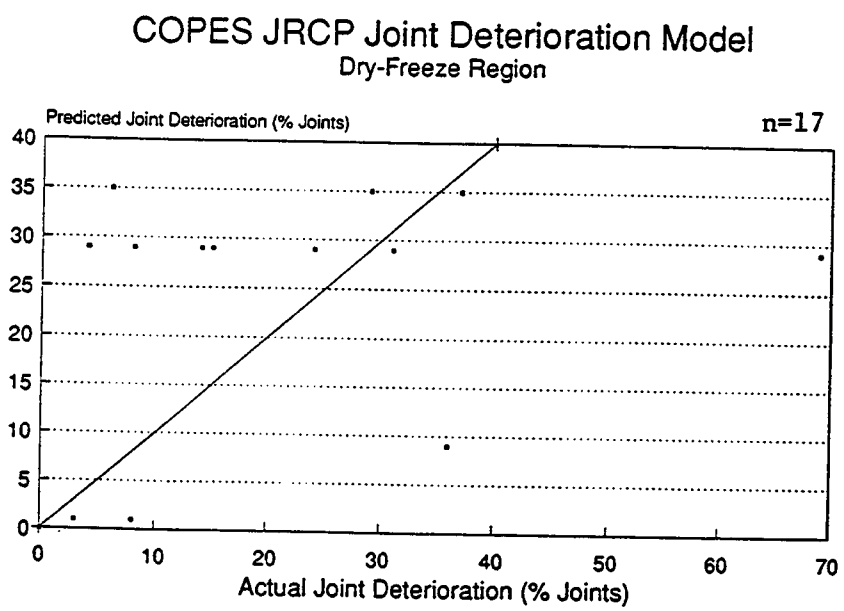

Figure 74. Actual field measured spalling versus joint deterioration (spalling) as predicted using the COPES JRCP joint deterioration model for the dry-freeze region.

Table 124. Actual field measured spalling versus joint deterioration (spalling) as predicted using the COPES spalling models for the dry-nonfreeze region.

Section ID	Measured Spalling	Predicted Spalling	Difference
AZ 1-1	22	0	22
AZ 1-2	1	0	1
AZ 1-4	0	0	0
AZ 1-5	0	1	1
AZ 1-6	1	0	1
AZ 1-7	0	0	0
AZ 2	0	0	0
CA 1-1	2	6	4
CA 1-3	0	6	6
CA 1-5	3	6	3
CA 1-7	9	6	3
CA 1-9	3	6	3
CA 2-2	0	0	0
CA 2-3	0	0	0
CA 6	3	0	3
CA 7	0	1	1
CA 8	0	0	0

Analysis Variable : DIFJD

N Obs	Mean	Std Error	T	Prob>|T|
17	2.8235294	1.2725475	2.2188008	0.0413

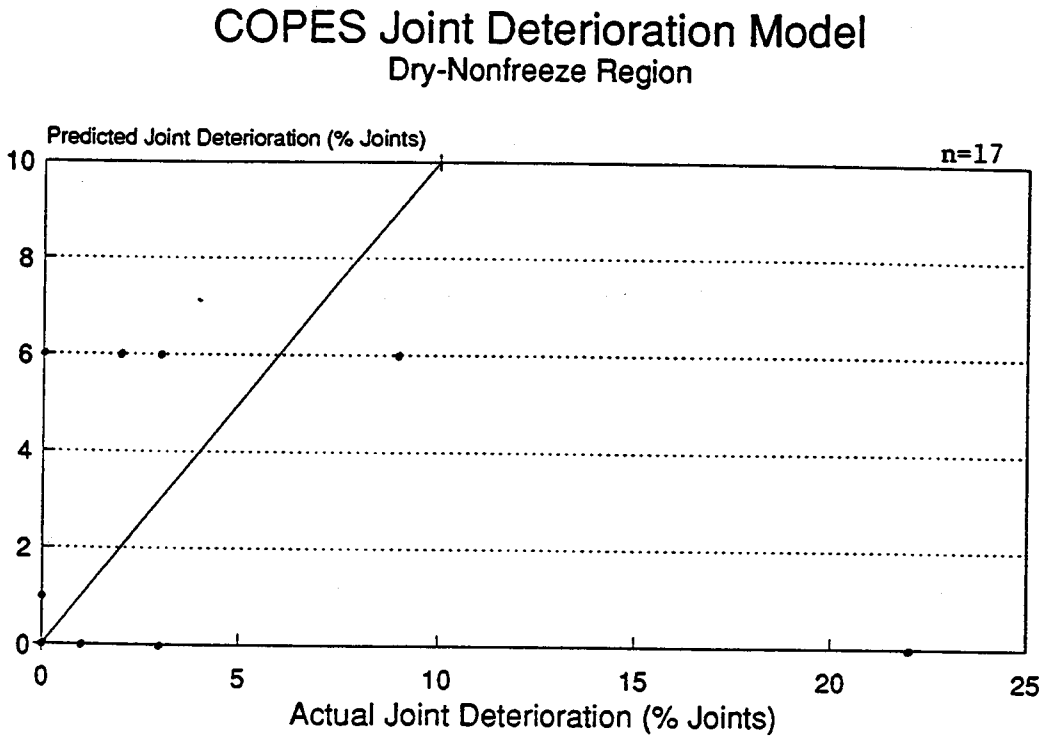

Figure 75. Actual field measured spalling versus joint deterioration (spalling) as predicted using the COPES spalling models for the dry-nonfreeze region.

Table 125. Actual field measured spalling versus joint deterioration (spalling) as predicted using the COPES spalling models for the wet-freeze region.

Section ID	Measured Spalling	Predicted Spalling	Difference
MI 1-1a	0	22	22
MI 1-1b	0	22	22
MI 1-4a	9	66	57
MI 1-7a	12	66	54
MI 1-7b	11	66	55
MI 1-10a	41	66	25
MI 1-10b	63	68	5
MI 1-25	75	66	9
MI 3	0	0	0
MI 4-1	0	32	32
MI 4-2	6	32	26
MI 5	0	0	0
NJ 2	20	46	26
NJ 3-1	0	0	0
NJ 3-2	43	0	43
NY 1-1	6	0	6
NY 1-3	73	21	52
NY 1-4	9	21	12
NY 1-6	13	0	13
NY 1-8a	0	0	0
NY 1-8b	0	0	0
NY 2-3	0	0	0
NY 2-9	0	0	0
NY 2-11	0	0	0
NY 2-15	0	5	5
OH 1-1	0	13	13
OH 1-3	13	18	5
OH 1-4	0	9	9
OH 1-6	0	18	18
OH 1-7	0	9	9
OH 1-9	0	9	9
OH 1-10	0	18	18
OH 2-33a	15	18	3
OH 2-33b	23	18	5
PA 1-1	0	2	2
PA 1-2	0	2	2
PA 1-3	0	2	2
PA 1-4	0	2	2
PA 1-5	0	2	2
ONT 1-1a	0	0	0
ONT 1-1b	0	0	0
ONT 1-2a	0	0	0
ONT 1-2b	0	0	0
ONT 1-3a	0	0	0
ONT 1-3b	0	0	0

Table 125. Actual field measured spalling versus joint deterioration (spalling) as predicted using the COPES spalling models for the wet-freeze region (continued).

Section ID	Measured Spalling	Predicted Spalling	Difference
ONT 1-4a	0	0	0
ONT 1-4b	0	0	0
ONT 2	0	0	0

Analysis Variable : DIFJD

N Obs	Mean	Std Error	T	Prob>|T|
48	11.7291667	2.3752080	4.9381640	0.0001

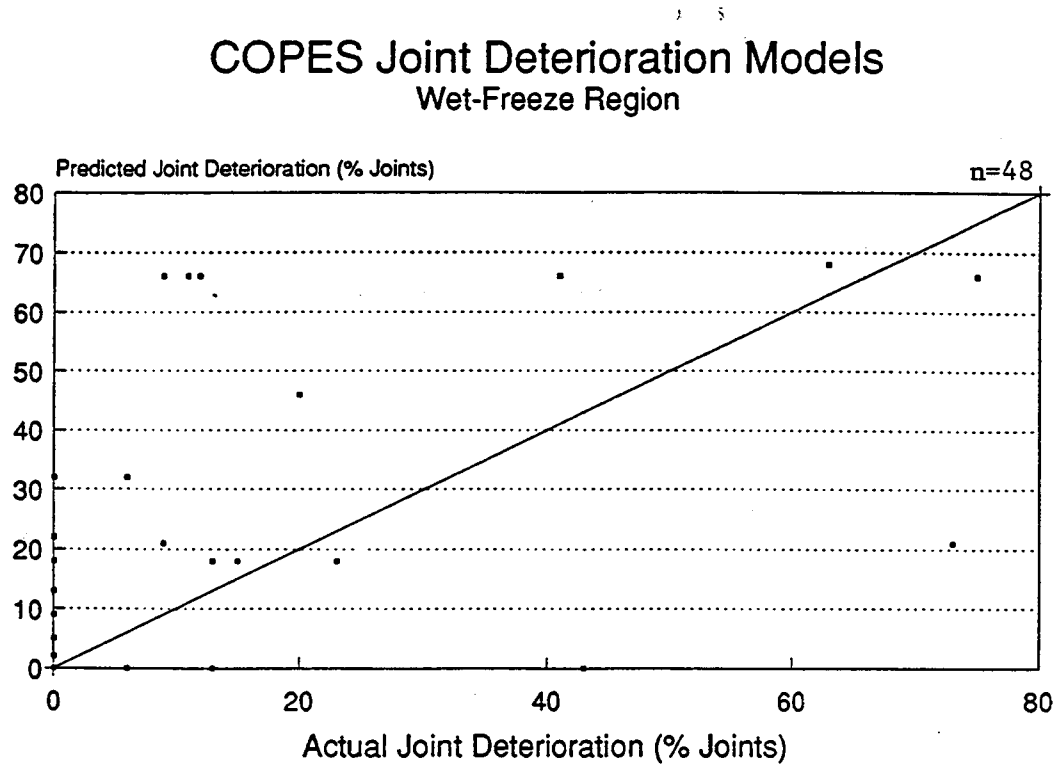

Figure 76. Actual field measured spalling versus joint deterioration (spalling) as predicted using the COPES spalling models for the wet-freeze region.

Table 126. Actual field measured spalling versus joint deterioration (spalling) as predicted using the COPES JPCP joint deterioration model for the wet-freeze region.

Section ID	Measured Spalling	Predicted Spalling	Difference
MI 1-4a	9	66	57
MI 1-7a	12	66	54
MI 1-7b	11	66	55
MI 1-10a	41	66	25
MI 1-10b	63	68	5
MI 1-25	75	66	9
NY 1-1	6	0	6
NY 1-6	13	0	13
NY 1-8a	0	0	0
NY 1-8b	0	0	0
NY 2-3	0	0	0
NY 2-9	0	0	0
NY 2-11	0	0	0
ONT 1-1a	0	0	0
ONT 1-1b	0	0	0
ONT 1-2a	0	0	0
ONT 1-2b	0	0	0
ONT 1-3a	0	0	0
ONT 1-3b	0	0	0
ONT 1-4a	0	0	0
ONT 1-4b	0	0	0
ONT 2	0	0	0

Analysis Variable : DIFJD

N Obs	Mean	Std Error	T	Prob>|T|
22	10.1818182	4.1208142	2.7408268	0.0221

Table 127. Actual field measured spalling versus joint deterioration (spalling) as predicted using the COPES JRCP joint deterioration model for the wet-freeze region.

Section ID	Measured Spalling	Predicted Spalling	Difference
MI 1-1a	0	22	22
MI 1-1b	0	22	22
MI 3	0	0	0
MI 4-1	0	32	32
MI 4-2	6	32	26
MI 5	0	0	0
NJ 2	20	46	26
NJ 3-1	0	0	0
NJ 3-2	43	0	43
NY 1-3	73	21	52
NY 1-4	9	21	12
NY 2-15	0	5	5
OH 1-1	0	13	13
OH 1-3	13	18	5
OH 1-4	0	9	9
OH 1-6	0	18	18
OH 1-7	0	9	9
OH 1-9	0	9	9
OH 1-10	0	18	18
OH 2-33a	15	18	3
OH 2-33b	23	18	5
PA 1-1	0	2	2
PA 1-2	0	2	2
PA 1-3	0	2	2
PA 1-4	0	2	2
PA 1-5	0	2	2

Analysis Variable : DIFJD

N Obs	Mean	Std Error	T	Prob>|T|
26	13.0384615	2.7132046	4.8055578	0.0001

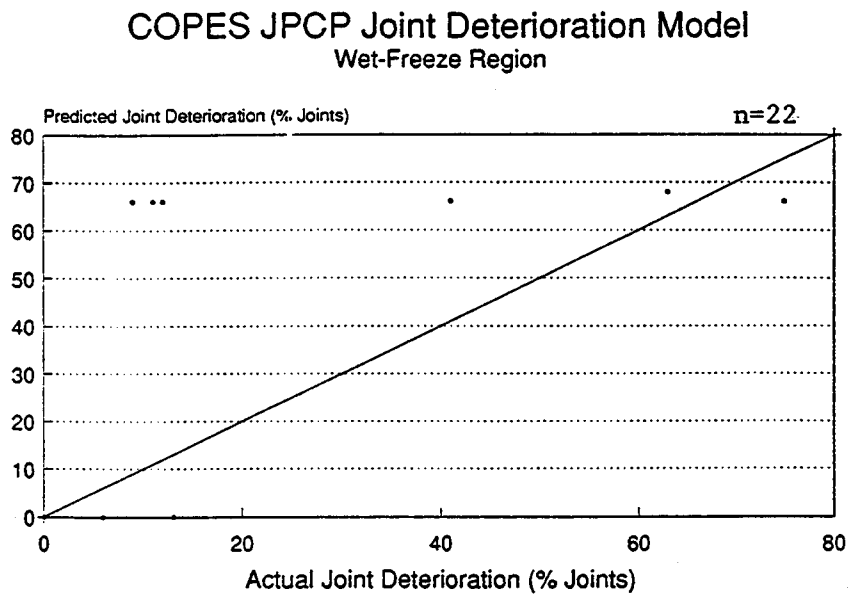

Figure 77. Actual field measured spalling versus joint deterioration (spalling) as predicted using the COPES JPCP joint deterioration model for the wet-freeze region.

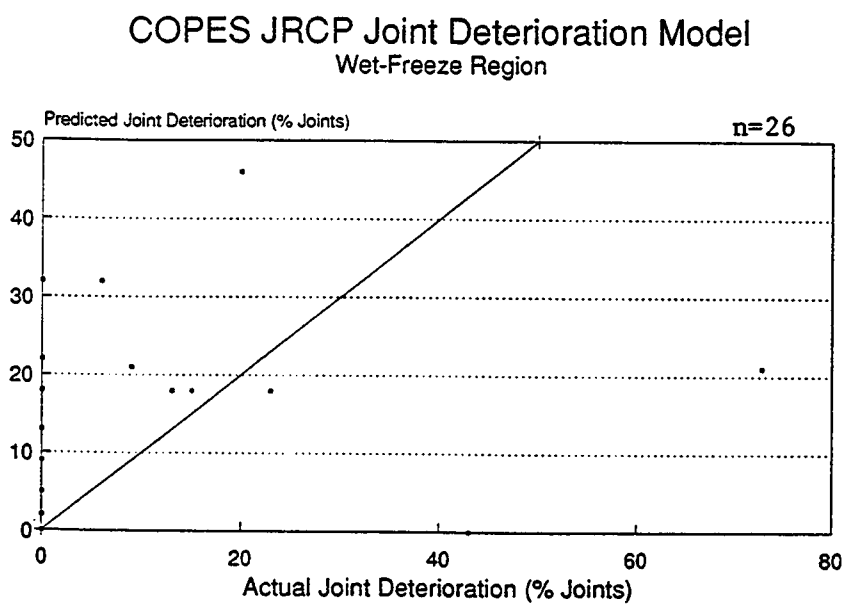

Figure 78. Actual field measured spalling versus joint deterioration (spalling) as predicted using the COPES JRCP joint deterioration model for the wet-freeze region.

Table 128. Actual field measured spalling versus joint deterioration (spalling) as predicted using the COPES spalling models for the wet-nonfreeze region.

Section ID	Measured Spalling	Predicted Spalling	Difference
CA 3-1	2	0	2
CA 3-2	3	3	0
CA 3-5	6	3	3
FL 2	0	0	0
FL 3	2	0	2
NC 1-1	0	40	40
NC 1-2	0	0	0
NC 1-3	0	0	0
NC 1-4	0	0	0
NC 1-5	0	0	0
NC 1-6	0	0	0
NC 1-7	0	19	19
NC 1-8	0	0	0
NC 2	0	0	0

Analysis Variable : DIFJD

N Obs	Mean	Std Error	T	Prob>|T|
14	4.7142857	3.0263106	1.5577667	0.1433

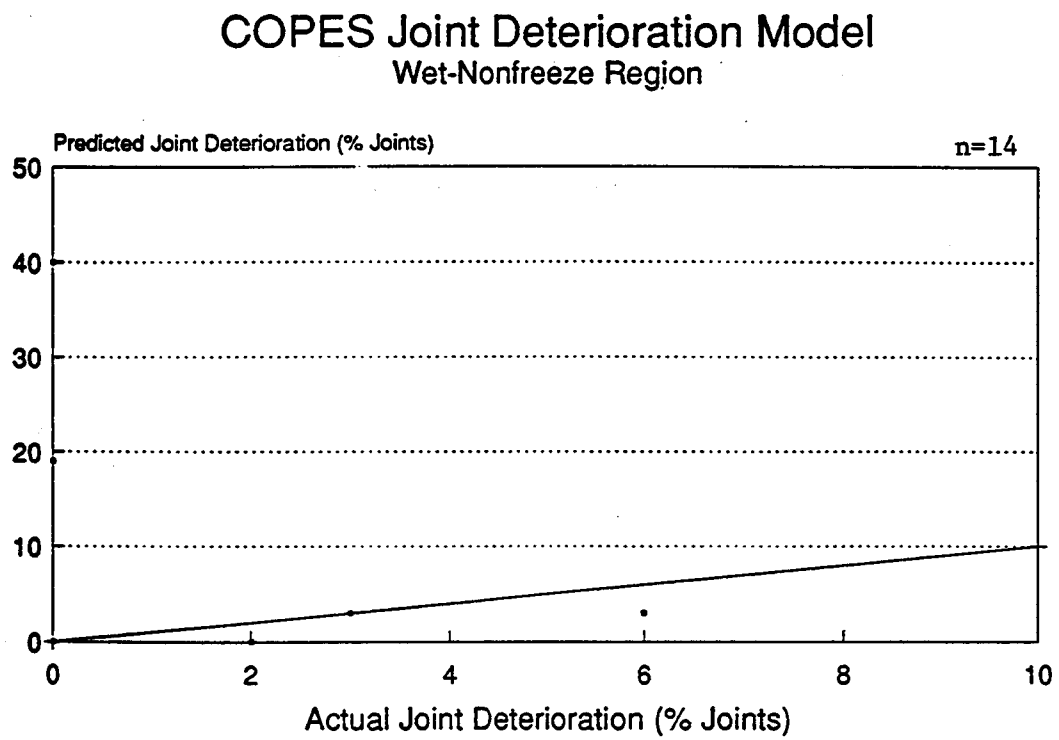

Figure 79. Actual field measured spalling versus joint deterioration (spalling) as predicted using the COPES spalling models for the wet-nonfreeze region.

Table 129. Actual field measured cracking versus cracking as measured by the COPES cracking models for all Phase I sections.

Section ID	Measured Cracking	Predicted Cracking	Difference
AZ 1-1	30	334.24	304.24
AZ 1-2	0	71.12	71.12
AZ 1-4	0	53.68	53.68
AZ 1-5	0	91.60	91.60
AZ 1-6	0	120.50	120.50
AZ 1-7	0	109.71	109.71
AZ 2	0	186.41	186.41
CA 1-1	12	1051.01	1039.01
CA 1-3	244	560.47	316.47
CA 1-5	0	65.40	65.40
CA 1-7	226	441.16	215.16
CA 1-9	546	480.12	65.88
CA 2-2	0	184.87	184.87
CA 2-3	600	338.43	261.57
CA 3-1	60	308.45	248.45
CA 3-2	12	176.58	164.58
CA 3-5	270	140.15	129.85
CA 6	118	355.88	237.88
CA 7	409	601.41	192.41
CA 8	0	60.69	60.69
FL 2	0	21.81	21.81
FL 3	808	241.79	566.21
MI 1-1a	0	53.81	53.81
MI 1-1b	12	53.81	41.81
MI 1-4a	0	175.88	175.88
MI 1-7a	0	223.05	223.05
MI 1-7b	0	334.76	334.76
MI 1-10a	0	285.15	285.15
MI 1-10b	24	255.03	231.03
MI 1-25	24	261.45	237.45
MI 3	0	68.42	68.42
MI 4-1	540	259.95	280.05
MI 4-2	444	259.95	184.05
MI 5	348	79.34	268.66
MN 1-1	0	160.65	160.65
MN 1-2	36	160.65	124.65
MN 1-3	97	238.41	141.41
MN 1-4	96	238.41	142.41
MN 1-5	168	223.84	55.84
MN 1-6	27	223.84	196.84
MN 1-7	49	146.08	97.08
MN 1-8	383	146.08	236.92
MN 1-9	0	146.08	146.08
MN 1-10	132	146.08	14.08
MN 1-11	104	223.84	119.84
MN 1-12	72	223.84	151.84
MN 2-1	0	1055.60	1055.60

Table 129. Actual field measured cracking versus cracking as measured by the COPES cracking models for all Phase I sections (continued).

Section ID	Measured Cracking	Predicted Cracking	Difference
MN 2-2	30	3235.46	3205.46
MN 2-3	0	108.52	108.52
MN 2-4	12	108.52	96.52
MN 3	0	98.07	98.07
MN 4b	0	282.41	282.41
MN 5	141	451.92	310.92
MN 6a	0	0.00	0.00
NJ 2	62	4837.11	4775.11
NJ 3-1	0	253.61	253.61
NJ 3-2	0	233.72	233.72
NY 1-1	0	418.48	418.48
NY 1-3	0	114.79	114.79
NY 1-4	0	125.48	125.48
NY 1-6	48	525.35	477.35
NY 1-8a	12	348.62	336.62
NY 1-8b	0	421.88	421.88
NY 2-3	324	152.98	171.02
NY 2-9	169	244.63	75.63
NY 2-11	48	204.67	156.67
NY 2-15	15	532.52	517.52
NC 1-1	60	0.00	60.00
NC 1-2	314	578.09	264.09
NC 1-3	628	404.90	223.10
NC 1-4	0	385.73	385.73
NC 1-5	36	487.92	451.92
NC 1-6	0	773.01	773.01
NC 1-7	0	774.20	774.20
NC 1-8	156	408.51	252.51
NC 2	24	167.47	143.47
OH 1-1	0	188.11	188.11
OH 1-3	0	98.28	98.28
OH 1-4	24	175.18	151.18
OH 1-6	12	111.20	99.20
OH 1-7	192	188.11	3.89
OH 1-9	96	188.11	92.11
OH 1-10	0	111.20	111.20
OH 2-33a	13	0.00	13.00
OH 2-33b	7	0.00	7.00
PA 1-1	0	24.07	24.07
PA 1-2	0	11.80	11.80
PA 1-3	0	11.85	11.85
PA 1-4	0	11.85	11.85
PA 1-5	0	11.85	11.85
ONT 1-1a	0	51.64	51.64
ONT 1-1b	8	51.64	43.64
ONT 1-2a	0	355.71	355.71
ONT 1-2b	0	355.71	355.71
ONT 1-3a	72	355.71	283.71

Table 129. Actual field measured cracking versus cracking as measured by the COPES cracking models for all Phase I sections (continued).

Section ID	Measured Cracking	Predicted Cracking	Difference
ONT 1-3b	164	355.71	191.71
ONT 1-4a	125	691.55	566.55
ONT 1-4b	182	691.55	509.55
ONT 2	12	19080.95	19068.95

Analysis Variable : DIFCRACK

N Obs	Mean	Std Error	T	Prob>|T|
99	496.3928338	208.5014922	7.3070008	0.0074

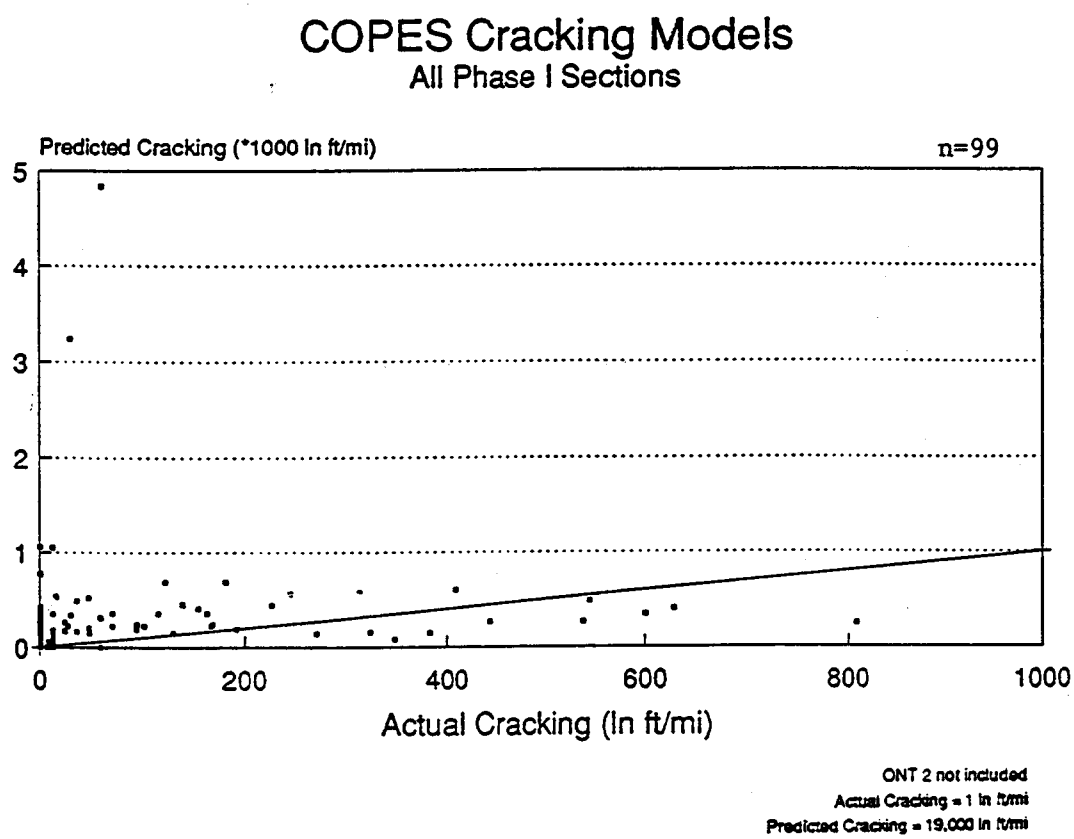

Figure 80. Actual field measured cracking versus cracking as predicted by the COPES cracking models for all Phase I sections.

Table 130. Actual field measured cracking versus cracking as predicted by the COPES cracking models for the dry-freeze region.

Section ID	Measured Cracking	Predicted Cracking	Difference
MN 1-1	0	160.65	160.65
MN 1-2	36	160.65	124.65
MN 1-3	97	238.41	141.41
MN 1-4	96	238.41	142.41
MN 1-5	168	223.84	55.84
MN 1-6	27	223.84	196.84
MN 1-7	49	146.08	97.08
MN 1-8	383	146.08	236.92
MN 1-9	0	146.08	146.08
MN 1-10	132	146.08	14.08
MN 1-11	104	223.84	119.84
MN 1-12	72	223.84	151.84
MN 2-1	0	1055.60	1055.60
MN 2-2	30	3235.46	3205.46
MN 2-3	0	108.52	108.52
MN 2-4	12	108.52	96.52
MN 3	0	98.073	98.073
MN 4b	0	282.413	282.413
MN 5	141	451.920	310.920
MN 6a	0	0.000	0.000

Analysis Variable : DIFCRACK

N Obs	Mean	Std Error	T	Prob>|T|
20	337.2578876	158.6917996	2.9252383	0.0064

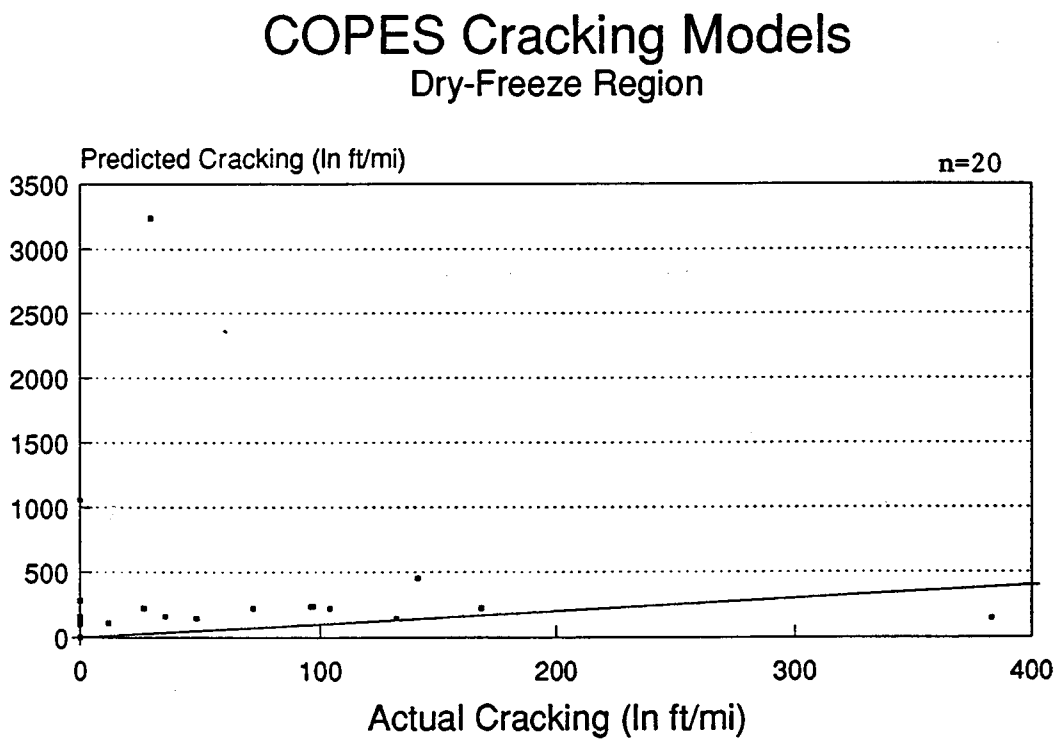

Figure 81. Actual field measured cracking versus cracking as predicted by the COPES cracking models for the dry-freeze region.

Table 131. Actual field measured cracking versus cracking as predicted by the COPES JPCP cracking model for the dry-freeze region.

Section ID	Measured Cracking	Predicted Cracking	Difference
MN 2-1	0	1055.60	1055.60
MN 2-2	30	3235.46	3205.46
MN 4b	0	282.41	282.41

Analysis Variable : DIFCRACK

N Obs	Mean	Std Error	T	Prob>|T|
3	1514.49	874.4513263	3.7919338	0.0054

Table 131. Actual field measured cracking versus cracking as predicted by the COPES JRCP cracking model for the dry-freeze region.

Section ID	Measured Cracking	Predicted Cracking	Difference
MN 1-1	0	160.647	160.647
MN 1-2	36	160.647	124.647
MN 1-3	97	238.414	141.414
MN 1-4	96	238.414	142.414
MN 1-5	168	223.842	55.842
MN 1-6	27	223.842	196.842
MN 1-7	49	146.076	97.076
MN 1-8	383	146.076	236.924
MN 1-9	0	146.076	146.076
MN 1-10	132	146.076	14.076
MN 1-11	104	223.842	119.842
MN 1-12	72	223.842	151.842
MN 2-3	0	108.524	108.524
MN 2-4	12	108.524	96.524
MN 3	0	98.073	98.073
MN 5	141	451.920	310.920
MN 6a	0	0	0

Analysis Variable : DIFCRACK

N Obs	Mean	Std Error	T	Prob>|T|
17	129.5107303	18.2146655	7.1102448	0.0001

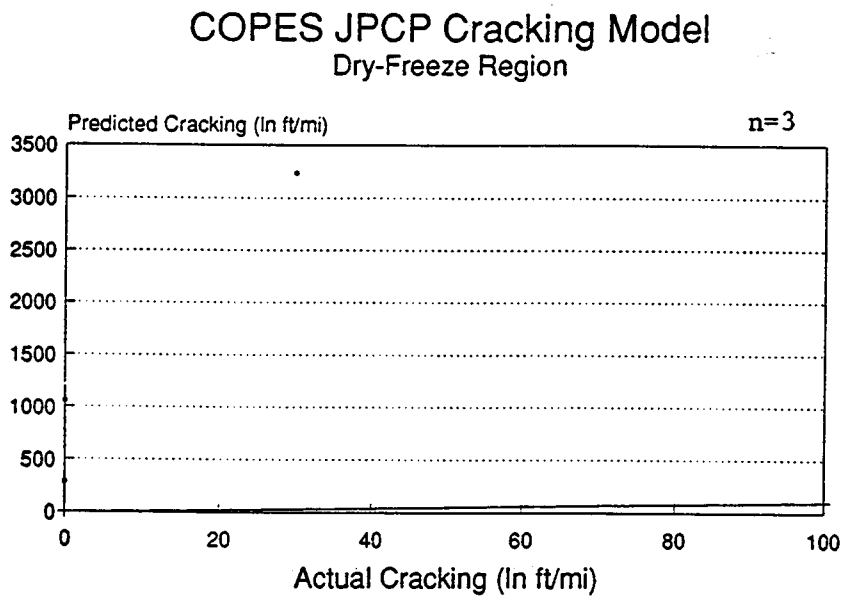

Figure 82. Actual field measured cracking versus cracking as predicted by the COPES JPCP cracking model for the dry-freeze region.

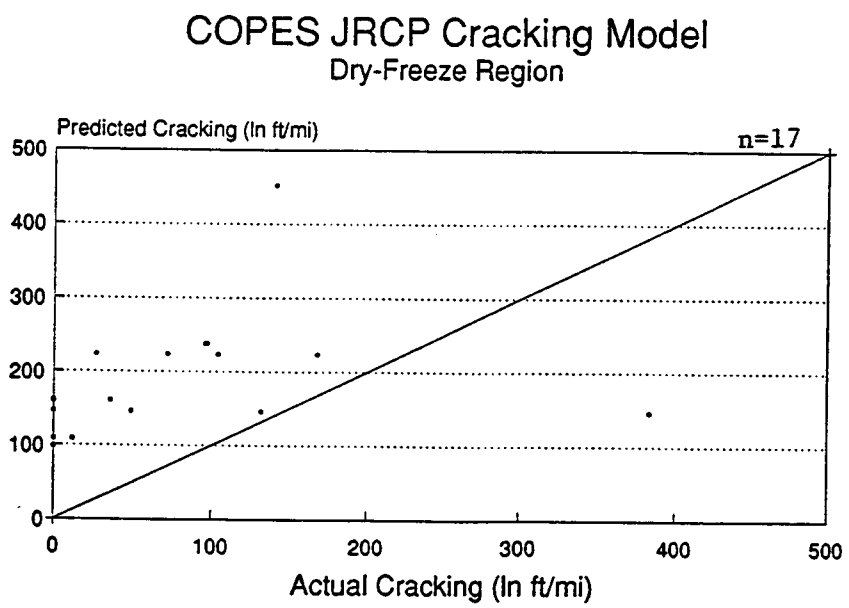

Figure 83. Actual field measured cracking versus cracking as predicted by the COPES JRCP cracking model for the dry-freeze region.

Table 133. Actual field measured cracking versus cracking as predicted by the COPES cracking models for the dry-nonfreeze region.

Section ID	Measured Cracking	Predicted Cracking	Difference
AZ 1-1	30	334.24	304.24
AZ 1-2	0	71.12	71.12
AZ 1-4	0	53.68	53.68
AZ 1-5	0	91.60	91.60
AZ 1-6	0	120.50	120.50
AZ 1-7	0	109.71	109.71
AZ 2	0	186.41	186.41
CA 1-1	12	1051.01	1039.01
CA 1-3	244	560.47	316.47
CA 1-5	0	65.40	65.40
CA 1-7	226	441.16	215.16
CA 1-9	546	480.12	65.88
CA 2-2	0	184.87	184.87
CA 2-3	600	338.43	261.57
CA 6	118	355.88	237.88
CA 7	409	601.41	192.41
CA 8	0	60.68	60.68

Analysis Variable : DIFCRACK

N Obs	Mean	Std Error	T	Prob>|T|
17	210.3885588	55.9747162	1.8986356	0.1917

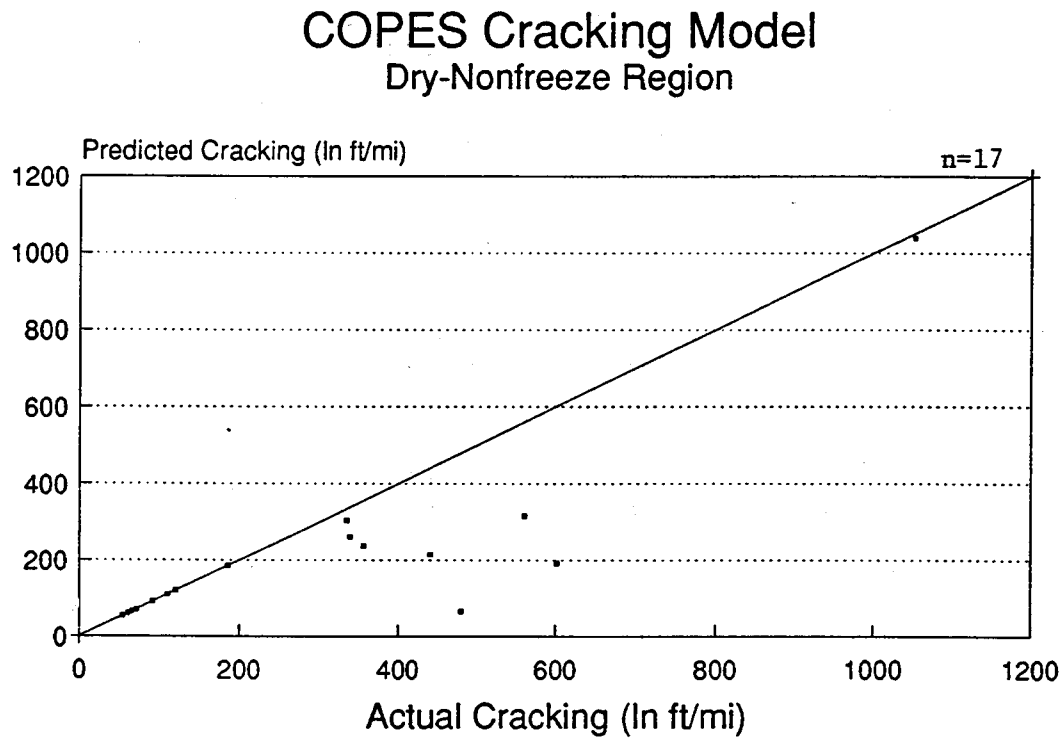

Figure 84. Actual field measured cracking versus cracking as predicted by the COPES cracking models for the dry-nonfreeze region.

Table 134. Actual field measured cracking versus cracking as predicted by the COPES cracking models for the wet-freeze region.

Section ID	Measured Cracking	Predicted Cracking	Difference
MI 1-1a	0	53.81	53.81
MI 1-1b	12	53.81	41.81
MI 1-4a	0	175.88	175.88
MI 1-7a	0	223.05	223.05
MI 1-7b	0	334.76	334.76
MI 1-10a	0	285.15	285.15
MI 1-10b	24	255.03	231.03
MI 1-25	24	261.45	237.45
MI 3	0	68.42	68.42
MI 4-1	540	259.95	280.05
MI 4-2	444	259.95	184.05
MI 5	348	79.34	268.66
NJ 2	62	4837.11	4775.11
NJ 3-1	0	253.61	253.61
NJ 3-2	0	233.72	233.72
NY 1-1	0	418.48	418.48
NY 1-3	0	114.795	114.795
NY 1-4	0	125.483	125.483
NY 1-6	48	525.351	477.351
NY 1-8a	12	348.622	336.622
NY 1-8b	0	421.880	421.880
NY 2-3	324	152.980	171.020
NY 2-9	169	244.633	75.633
NY 2-11	48	204.674	156.674
NY 2-15	15	532.516	517.516
OH 1-1	0	188.106	188.106
OH 1-3	0	98.280	98.280
OH 1-4	24	175.182	151.182
OH 1-6	12	111.205	99.205
OH 1-7	192	188.106	3.894
OH 1-9	96	188.106	92.106
OH 1-10	0	111.205	111.205
OH 2-33a	13	0.00	13.00
OH 2-33b	7	0.00	7.00
PA 1-1	0	24.07	24.07
PA 1-2	0	11.80	11.80
PA 1-3	0	11.85	11.85
PA 1-4	0	11.85	11.85
PA 1-5	0	11.85	11.85
ONT 1-1a	0	51.64	51.64
ONT 1-1b	8	51.64	43.64
ONT 1-2a	0	355.71	355.71
ONT 1-2b	0	355.71	355.71
ONT 1-3a	72	355.71	283.71
ONT 1-3b	164	355.71	191.71

Table 134. Actual field measured cracking versus cracking as predicted by the COPES cracking models for the wet-freeze region (continued).

Section ID	Measured Cracking	Predicted Cracking	Difference
ONT 1-4a	125	691.55	566.55
ONT 1-4b	182	691.55	509.55
ONT 2	12	19080.95	19068.95

Analysis Variable : DIFCRACK

N Obs	Mean	Std Error	T	Prob>|T|
48	681.7620513	403.2881124	3.6905087	0.0076

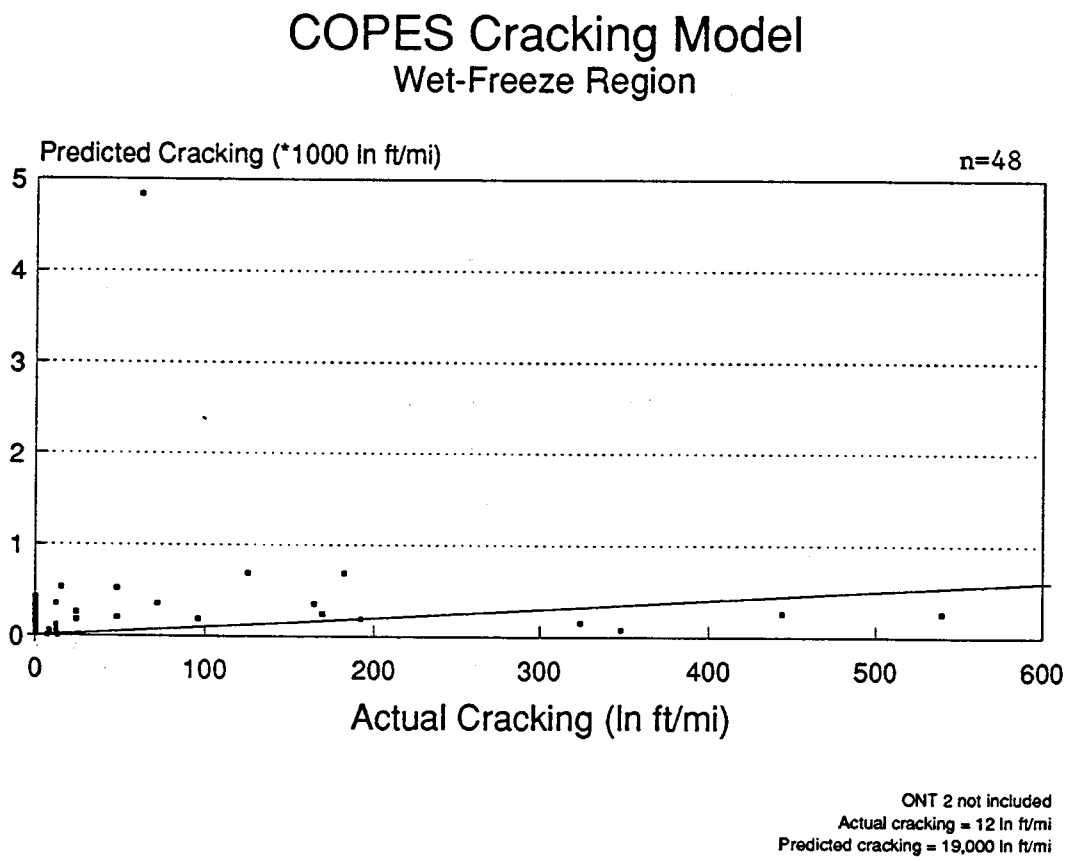

Figure 85. Actual field measured cracking versus cracking as predicted by the COPES cracking models for the wet-freeze region.

Table 135. Actual field measured cracking versus cracking as predicted by the COPES JPCP cracking model for the wet-freeze region.

Section ID	Measured Cracking	Predicted Cracking	Difference
MI 1-4a	0	175.877	175.877
MI 1-7a	0	223.045	223.045
MI 1-7b	0	334.763	334.763
MI 1-10a	0	285.151	285.151
MI 1-10b	24	255.028	231.028
MI 1-25	24	261.450	237.450
NY 1-1	0	418.481	418.481
NY 1-6	48	525.351	477.351
NY 1-8a	12	348.622	336.622
NY 1-8b	0	421.880	421.880
NY 2-3	324	152.980	171.020
NY 2-9	169	244.633	75.633
NY 2-11	48	204.674	156.674
ONT 1-1a	0	51.637	51.637
ONT 1-1b	8	51.637	43.637
ONT 1-2a	0	355.709	355.709
ONT 1-2b	0	355.71	355.71
ONT 1-3a	72	355.71	283.71
ONT 1-3b	164	355.71	191.71
ONT 1-4a	125	691.55	566.55
ONT 1-4b	182	691.55	509.55
ONT 2	12	19080.95	19068.95

Analysis Variable : DIFCRACK

N Obs	Mean	Std Error	T	Prob>|T|
22	1135.10	854.5424847	3.8983097	0.0083

Table 136. Actual field measured cracking versus cracking as predicted by the COPES JRCP cracking model for the wet-freeze region.

Section ID	Measured Cracking	Predicted Cracking	Difference
MI 1-1a	0	53.81	53.81
MI 1-1b	12	53.81	41.81
MI 3	0	68.42	68.42
MI 4-1	540	259.95	280.05
MI 4-2	444	259.95	184.05
MI 5	348	79.34	268.66
NJ 2	62	4837.11	4775.11
NJ 3-1	0	253.61	253.61
NJ 3-2	0	233.72	233.72
NY 1-3	0	114.79	114.79
NY 1-4	0	125.48	125.48
NY 2-15	15	532.52	517.52
OH 1-1	0	188.11	188.11
OH 1-3	0	98.28	98.28
OH 1-4	24	175.18	151.18
OH 1-6	12	111.20	99.20
OH 1-7	192	188.106	3.894
OH 1-9	96	188.106	92.106
OH 1-10	0	111.205	111.205
OH 2-33a	13	0.000	13.000
OH 2-33b	7	0.000	7.000
PA 1-1	0	24.072	24.072
PA 1-2	0	11.797	11.797
PA 1-3	0	11.851	11.851
PA 1-4	0	11.851	11.851
PA 1-5	0	11.851	11.851

Analysis Variable : DIFCRACK

N Obs	Mean	Std Error	T	Prob>|T|
26	298.1708684	180.5955978	3.6510417	0.0012

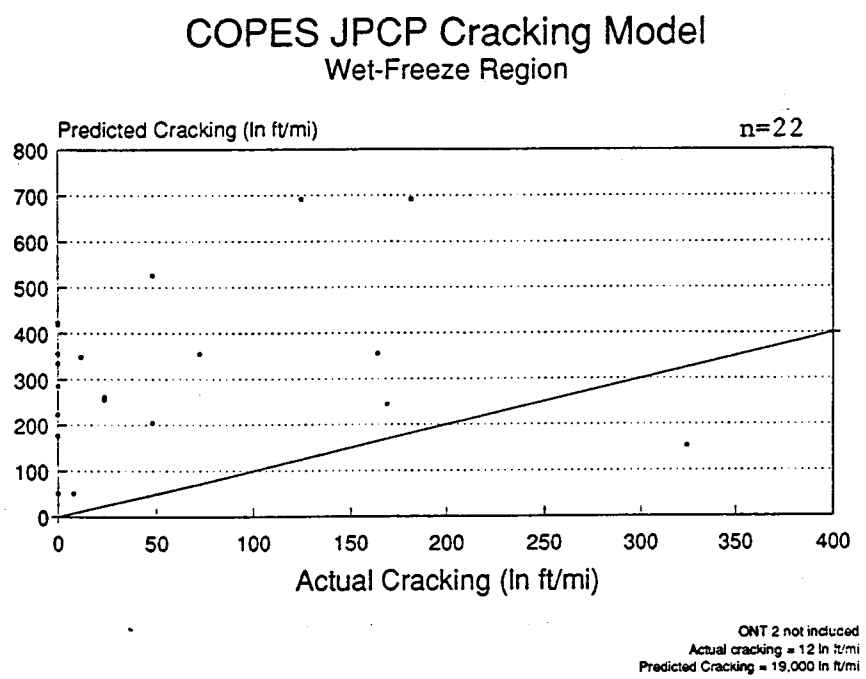

Figure 86. Actual field measured cracking versus cracking as predicted by the COPES JPCP cracking model for the wet-freeze region.

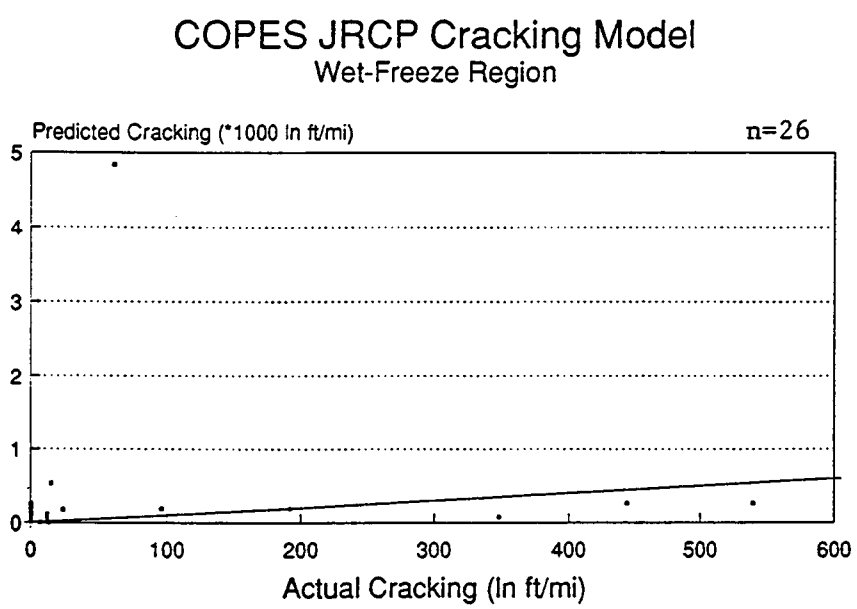

Figure 87. Actual field measured cracking versus cracking as predicted by the COPES JRCP cracking model for the wet-freeze region.

Table 137. Actual field measured cracking versus cracking as predicted by the COPES cracking models for the wet-nonfreeze region.

Section ID	Measured Cracking	Predicted Cracking	Difference
CA 3-1	60	308.450	248.450
CA 3-2	12	176.578	164.578
CA 3-5	270	140.146	129.854
FL 2	0	21.806	21.806
FL 3	808	241.795	566.205
NC 1-1	60	0.000	60.000
NC 1-2	314	578.085	264.085
NC 1-3	628	404.905	223.095
NC 1-4	0	385.728	385.728
NC 1-5	36	487.919	451.919
NC 1-6	0	773.014	773.014
NC 1-7	0	774.197	774.197
NC 1-8	156	408.509	252.509
NC 2	24	167.466	143.466

Analysis Variable : DIFCRACK

N Obs	Mean	Std Error	T	Prob>|T|
14	338.3773938	66.6050632	5.0803554	0.0003

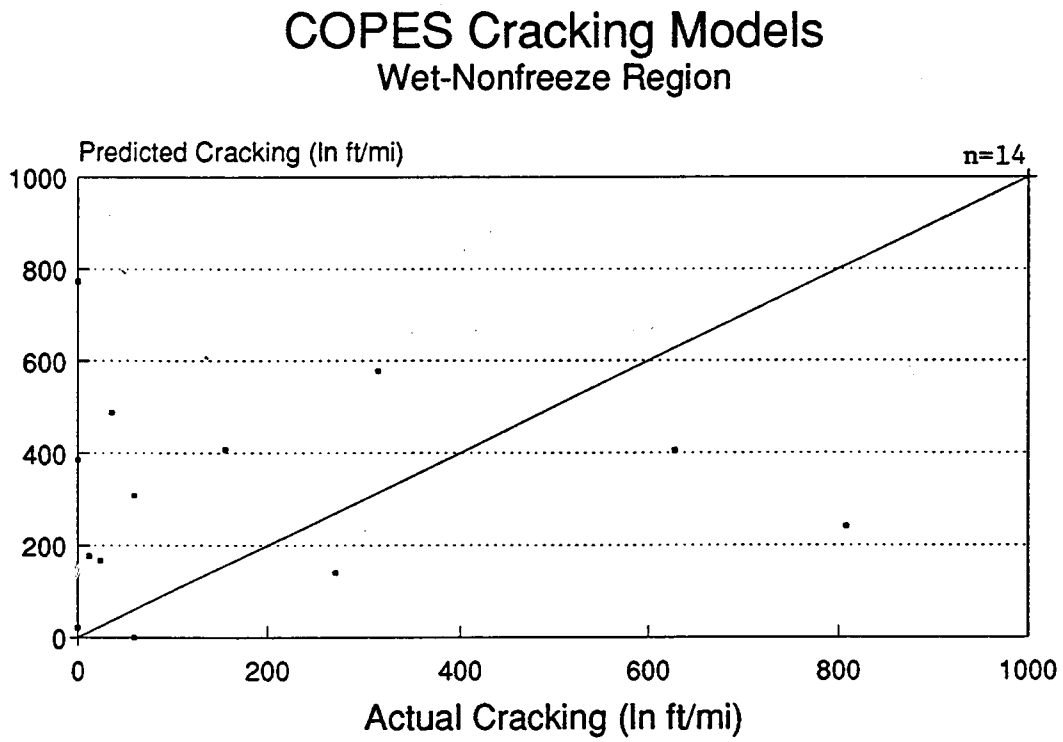

Figure 88. Actual field measured cracking versus cracking as predicted by the COPES cracking models for the wet-freeze region.

Table 138. Actual PSR as determined by a panel of users versus PSR as predicted by the COPES PSR models for all Phase I sections.

Section ID	Actual PSR	Predicted PSR	Difference
AZ 1-1	3.4	4.00695	0.60695
AZ 1-2	3.8	4.36878	0.56878
AZ 1-4	3.6	4.33839	0.73839
AZ 1-5	3.8	4.24284	0.44284
AZ 1-6	3.5	4.10210	0.60210
AZ 1-7	3.8	4.07014	0.27014
AZ 2	3.6	3.96170	0.36170
CA 1-1	2.9	3.80456	0.90456
CA 1-3	3.0	3.93104	0.93104
CA 1-5	2.7	4.57064	1.87064
CA 1-7	2.7	3.98799	1.28799
CA 1-9	2.5	3.96736	1.46736
CA 2-2	3.8	3.99735	0.19735
CA 2-3	4.1	3.86599	0.23401
CA 3-1	3.6	3.89058	0.29058
CA 3-2	3.9	4.01175	0.11175
CA 3-5	3.8	4.06597	0.26597
CA 6	3.4	3.99465	0.59465
CA 7	3.8	3.97484	0.17484
CA 8	3.8	4.11389	0.31389
FL 2	3.7	4.24266	0.54266
FL 3	3.2	3.90931	0.70931
MI 1-1a	3.6	4.00076	0.40076
MI 1-1b	3.3	3.84963	0.54963
MI 1-4a	3.9	3.92404	0.02404
MI 1-7a	3.6	3.88818	0.28818
MI 1-7b	3.7	3.83044	0.13044
MI 1-10a	2.9	3.85272	0.95272
MI 1-10b	2.8	3.86863	1.06863
MI 1-25	2.9	3.86506	0.96506
MI 3	4.8	4.15033	0.64967
MI 4-1	2.4	3.04593	0.64593
MI 4-2	2.4	3.48948	1.08948
MI 5	4.2	4.00151	0.19849
MN 1-1	3.7	3.20581	0.49419
MN 1-2	3.3	3.60511	0.30511
MN 1-3	3.4	2.50188	0.89812
MN 1-4	3.3	1.27563	2.02437
MN 1-5	3.4	2.63738	0.76262
MN 1-6	3.4	1.98083	1.41917
MN 1-7	3.6	3.40512	0.19488
MN 1-8	3.4	3.54900	0.14900
MN 1-9	3.7	3.47246	0.22754
MN 1-10	3.3	3.70563	0.40563
MN 1-11	3.7	2.58123	1.11877
MN 1-12	3.5	3.26538	0.23462
MN 2-1	3.8	3.81557	0.01557
MN 2-2	3.9	3.68496	0.21504

Table 138. Actual PSR as determined by a panel of users versus PSR as predicted by the COPES PSR models for all Phase I sections (continued).

Section ID	Actual PSR	Predicted PSR	Difference
MN 2-3	4.0	3.78901	0.21099
MN 2-4	4.0	3.54447	0.45553
MN 3	3.8	3.80362	0.00362
MN 4b	4.7	3.83882	0.86118
MN 5	3.3	3.08235	0.21765
MN 6a	4.5	3.40083	1.09917
NJ 2	3.8	2.83911	0.96089
NJ 3-1	3.6	3.63516	0.03516
NJ 3-2	3.5	3.76978	0.26978
NY 1-1	4.0	3.92015	0.07985
NY 1-3	3.6	4.15360	0.55360
NY 1-4	3.4	3.85489	0.45489
NY 1-6	3.9	3.92557	0.02557
NY 1-8a	4.1	3.95757	0.14243
NY 1-8b	3.8	3.91852	0.11852
NY 2-3	4.2	3.99255	0.20745
NY 2-9	4.0	3.90905	0.09095
NY 2-11	4.1	3.93993	0.16007
NY 2-15	4.0	3.85947	0.14053
NC 1-1	3.4	3.85033	0.45033
NC 1-2	3.5	3.95012	0.45012
NC 1-3	3.6	4.04896	0.44896
NC 1-4	3.4	4.06291	0.66291
NC 1-5	3.2	4.00337	0.80337
NC 1-6	3.8	3.87389	0.07389
NC 1-7	3.4	1.50838	1.89162
NC 1-8	3.7	4.04642	0.34642
NC 2	4.2	4.19451	0.00549
OH 1-1	4.2	3.93890	0.26110
OH 1-3	4.2	4.00366	0.19634
OH 1-4	4.1	3.97630	0.12370
OH 1-6	4.2	4.12911	0.07089
OH 1-7	4.2	4.11390	0.08610
OH 1-9	4.2	4.12747	0.07253
OH 1-10	4.2	4.14088	0.05912
OH 2-33a	3.4	4.34672	0.94672
OH 2-33b	3.5	4.34672	0.84672
PA 1-1	4.2	4.38611	0.18611
PA 1-2	3.8	4.42772	0.62772
PA 1-3	3.7	4.37257	0.67257
PA 1-4	4.1	4.39782	0.29782
PA 1-5	4.1	4.36865	0.26865
ONT 1-1a	3.8	4.09728	0.29728
ONT 1-1b	3.8	4.09728	0.29728
ONT 1-2a	3.8	3.79059	0.00941
ONT 1-2b	3.7	3.79059	0.09059
ONT 1-3a	3.8	3.79059	0.00941
ONT 1-3b	3.8	3.79059	0.00941

Table 138. Actual PSR as determined by a panel of users versus PSR as predicted by the COPES PSR models for all Phase I sections (continued).

Section ID	Actual PSR	Predicted PSR	Difference
ONT 1-4a	3.7	3.71173	0.01173
ONT 1-4b	3.8	3.71173	0.08827
ONT 2	3.9	4.13088	0.23088

Analysis Variable : DIFPSR

N Obs	Mean	Std Error	T	Prob>|T|
99	0.4636004	0.0438740	10.5666278	0.0001

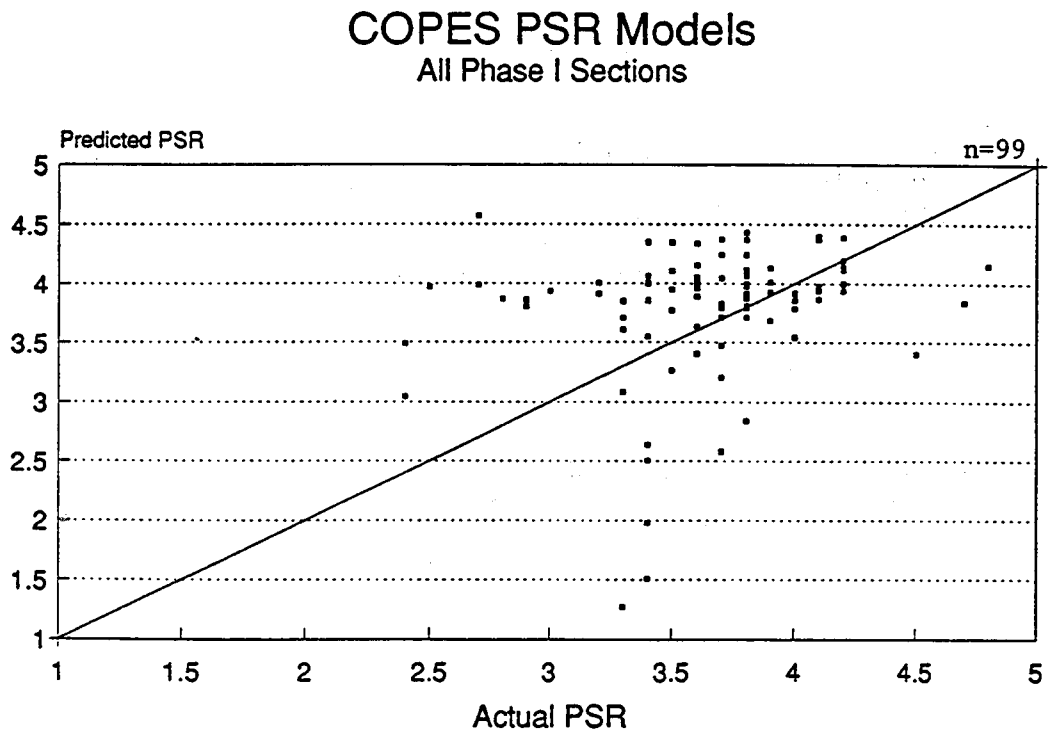

Figure 89. Actual PSR as determined by a panel of users versus PSR as predicted by the COPES PSR models for all Phase I sections.

Table 139. Actual PSR as determined by a panel of users versus PSR as predicted by the COPES PSR models for the dry-freeze region.

Section ID	Actual PSR	Predicted PSR	Difference
MN 1-1	3.7	3.20581	0.49419
MN 1-2	3.3	3.60511	0.30511
MN 1-3	3.4	2.50188	0.89812
MN 1-4	3.3	1.27563	2.02437
MN 1-5	3.4	2.63738	0.76262
MN 1-6	3.4	1.98083	1.41917
MN 1-7	3.6	3.40512	0.19488
MN 1-8	3.4	3.54900	0.14900
MN 1-9	3.7	3.47246	0.22754
MN 1-10	3.3	3.70563	0.40563
MN 1-11	3.7	2.58123	1.11877
MN 1-12	3.5	3.26538	0.23462
MN 2-1	3.8	3.81557	0.01557
MN 2-2	3.9	3.68496	0.21504
MN 2-3	4.0	3.78901	0.21099
MN 2-4	4.0	3.54447	0.45553
MN 3	3.8	3.80362	0.00362
MN 4b	4.7	3.83882	0.86118
MN 5	3.3	3.08235	0.21765
MN 6a	4.5	3.40083	1.09917

Analysis Variable : DIFPSR

N Obs	Mean	Std Error	T	Prob>|T|
20	0.5656383	0.1182948	4.7816008	0.0001

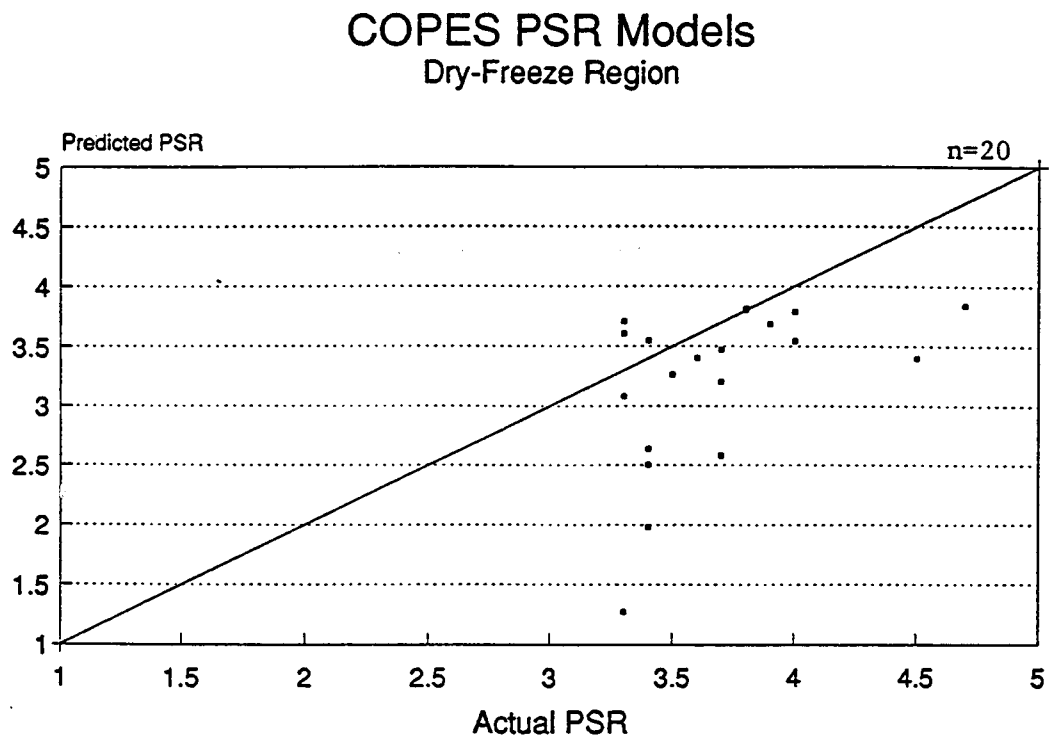

Figure 90. Actual PSR as determined by a panel of users versus PSR as predicted by the COPES PSR models for the dry-freeze region.

Table 140. Actual PSR as determined by a panel of users versus PSR as predicted by the COPES JPCP PSR model for the dry-freeze region.

Section ID	Actual PSR	Predicted PSR	Difference
MN 2-1	3.8	3.81557	0.01557
MN 2-2	3.9	3.68496	0.21504
MN 4b	4.7	3.83882	0.86118

Analysis Variable : DIFPSR

N Obs	Mean	Std Error	T	Prob>|T|
3	0.3639283	0.2552074	4.4260099	0.0043

Table 141. Actual PSR as determined by a panel of users versus PSR as predicted by the COPES JRCP PSR model for the dry-freeze region.

Section ID	Actual PSR	Predicted PSR	Difference
MN 1-1	3.7	3.20581	0.49419
MN 1-2	3.3	3.60511	0.30511
MN 1-3	3.4	2.50188	0.89812
MN 1-4	3.3	1.27563	2.02437
MN 1-5	3.4	2.63738	0.76262
MN 1-6	3.4	1.98083	1.41917
MN 1-7	3.6	3.40512	0.19488
MN 1-8	3.4	3.54900	0.14900
MN 1-9	3.7	3.47246	0.22754
MN 1-10	3.3	3.70563	0.40563
MN 1-11	3.7	2.58123	1.11877
MN 1-12	3.5	3.26538	0.23462
MN 2-3	4.0	3.78901	0.21099
MN 2-4	4.0	3.54447	0.45553
MN 3	3.8	3.80362	0.00362
MN 5	3.3	3.08235	0.21765
MN 6a	4.5	3.40083	1.09917

Analysis Variable : DIFPSR

N Obs	Mean	Std Error	T	Prob>|T|
17	0.6012342	0.1326096	4.5338673	0.0003

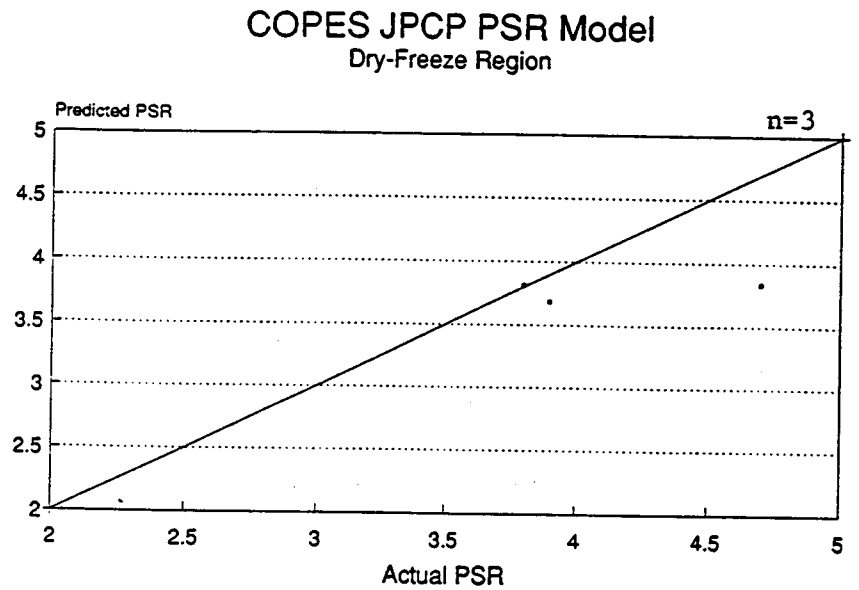

Figure 91. Actual PSR as determined by a panel of users versus PSR as predicted by the COPES JPCP PSR model for the dry-freeze region.

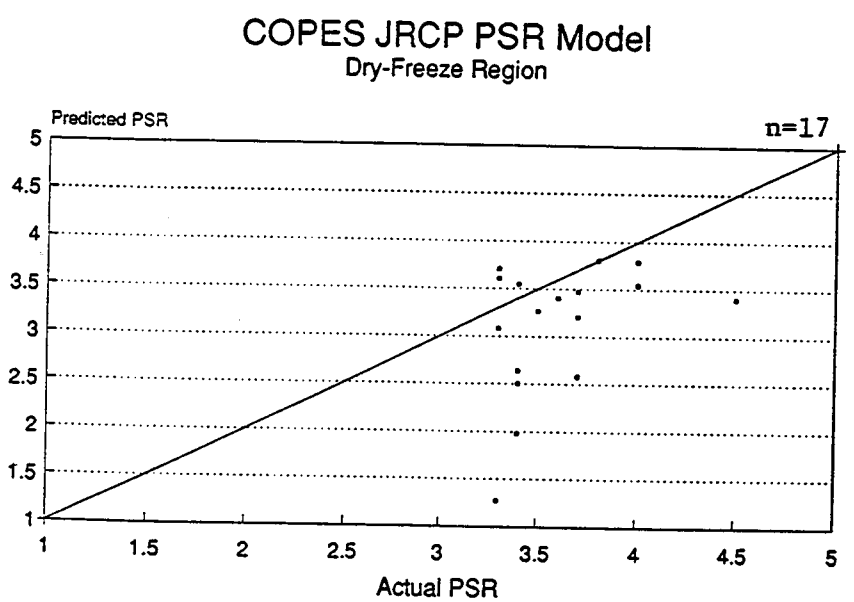

Figure 92. Actual PSR as determined by a panel of users versus PSR as predicted by the COPES JRCP PSR model for the dry-freeze region.

Table 142. Actual PSR as determined by a panel of users versus PSR as predicted by the COPES PSR models for the dry-nonfreeze region.

Section ID	Actual PSR	Predicted PSR	Difference
AZ 1-1	3.4	4.00695	0.60695
AZ 1-2	3.8	4.36878	0.56878
AZ 1-4	3.6	4.33839	0.73839
AZ 1-5	3.8	4.24284	0.44284
AZ 1-6	3.5	4.10210	0.60210
AZ 1-7	3.8	4.07014	0.27014
AZ 2	3.6	3.96170	0.36170
CA 1-1	2.9	3.80456	0.90456
CA 1-3	3.0	3.93104	0.93104
CA 1-5	2.7	4.57064	1.87064
CA 1-7	2.7	3.98799	1.28799
CA 1-9	2.5	3.96736	1.46736
CA 2-2	3.8	3.99735	0.19735
CA 2-3	4.1	3.86599	0.23401
CA 6	3.4	3.99465	0.59465
CA 7	3.8	3.97484	0.17484
CA 8	3.8	4.11389	0.31389

Analysis Variable : DIFPSR

N Obs	Mean	Std Error	T	Prob>|T|
17	0.6804251	0.1166592	5.8325908	0.0001

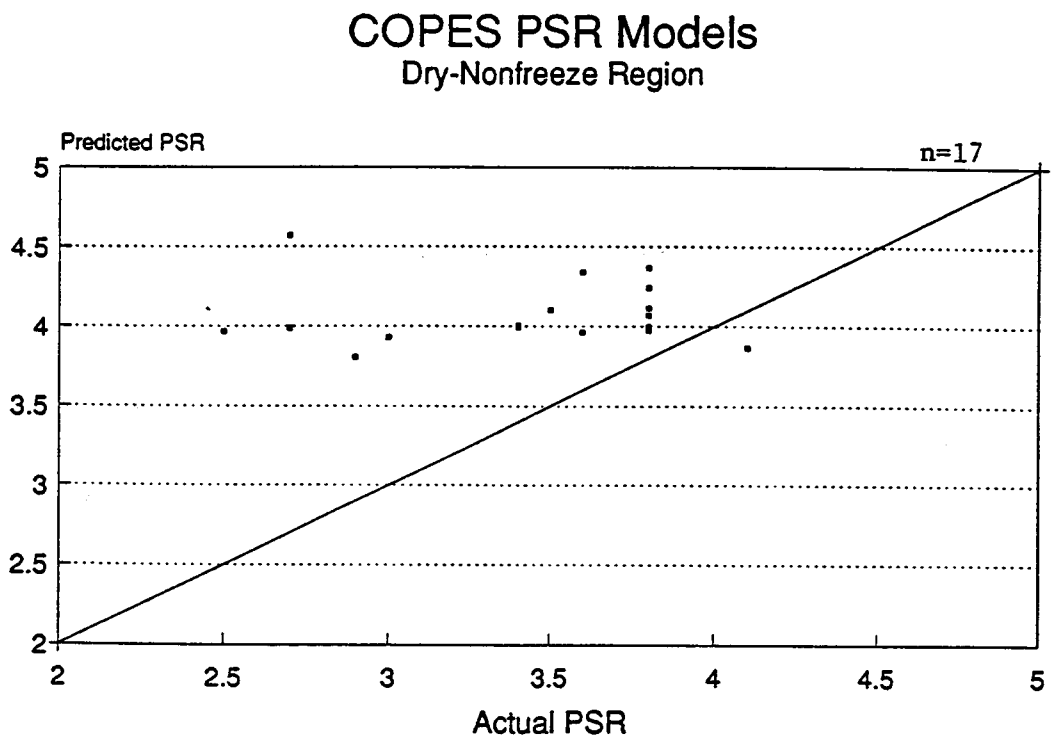

Figure 93. Actual PSR as determined by a panel of users versus PSR as predicted by the COPES PSR models for the dry-nonfreeze region.

Table 143. Actual PSR as determined by a panel of users versus PSR as predicted by the COPES PSR models for the wet-freeze region.

Section ID	Actual PSR	Predicted PSR	Difference
MI 1-1a	3.6	4.00076	0.40076
MI 1-1b	3.3	3.84963	0.54963
MI 1-4a	3.9	3.92404	0.02404
MI 1-7a	3.6	3.88818	0.28818
MI 1-7b	3.7	3.83044	0.13044
MI 1-10a	2.9	3.85272	0.95272
MI 1-10b	2.8	3.86863	1.06863
MI 1-25	2.9	3.86506	0.96506
MI 3	4.8	4.15033	0.64967
MI 4-1	2.4	3.04593	0.64593
MI 4-2	2.4	3.48948	1.08948
MI 5	4.2	4.00151	0.19849
NJ 2	3.8	2.83911	0.96089
NJ 3-1	3.6	3.63516	0.03516
NJ 3-2	3.5	3.76978	0.26978
NY 1-1	4.0	3.92015	0.07985
NY 1-3	3.6	4.15360	0.55360
NY 1-4	3.4	3.85489	0.45489
NY 1-6	3.9	3.92557	0.02557
NY 1-8a	4.1	3.95757	0.14243
NY 1-8b	3.8	3.91852	0.11852
NY 2-3	4.2	3.99255	0.20745
NY 2-9	4.0	3.90905	0.09095
NY 2-11	4.1	3.93993	0.16007
NY 2-15	4.0	3.85947	0.14053
OH 1-1	4.2	3.93890	0.26110
OH 1-3	4.2	4.00366	0.19634
OH 1-4	4.1	3.97630	0.12370
OH 1-6	4.2	4.12911	0.07089
OH 1-7	4.2	4.11390	0.08610
OH 1-9	4.2	4.12747	0.07253
OH 1-10	4.2	4.14088	0.05912
OH 2-33a	3.4	4.34672	0.94672
OH 2-33b	3.5	4.34672	0.84672
PA 1-1	4.2	4.38611	0.18611
PA 1-2	3.8	4.42772	0.62772
PA 1-3	3.7	4.37257	0.67257
PA 1-4	4.1	4.39782	0.29782
PA 1-5	4.1	4.36865	0.26865
ONT 1-1a	3.8	4.09728	0.29728
ONT 1-1b	3.8	4.09728	0.29728
ONT 1-2a	3.8	3.79059	0.00941
ONT 1-2b	3.7	3.79059	0.09059
ONT 1-3a	3.8	3.79059	0.00941
ONT 1-3b	3.8	3.79059	0.00941

Table 143. Actual PSR as determined by a panel of users versus PSR as predicted by the COPES PSR models for the wet-freeze region (continued).

Section ID	Actual PSR	Predicted PSR	Difference
ONT 1-4a	3.7	3.71173	0.01173
ONT 1-4b	3.8	3.71173	0.08827
ONT 2	3.9	4.13088	0.23088

Analysis Variable : DIFPSR

N Obs	Mean	Std Error	T	Prob>|T|
48	0.3325639	0.0470533	7.0678133	0.0001

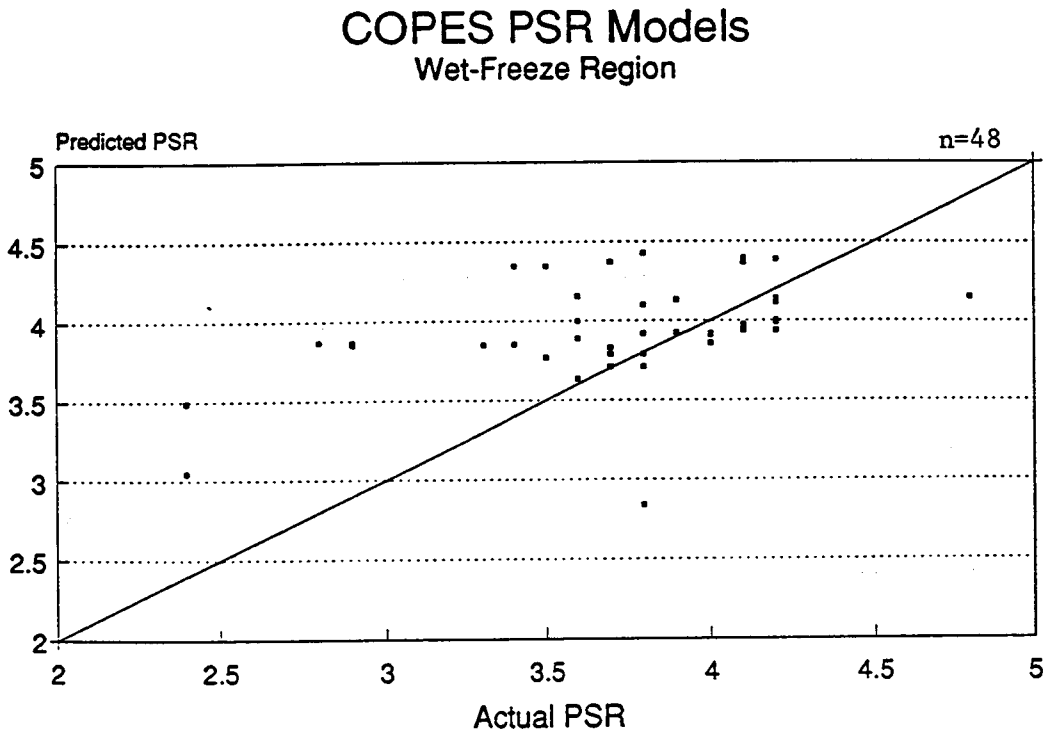

Figure 94. Actual PSR as determined by a panel of users versus PSR as predicted by the COPES PSR models for the wet-freeze region.

Table 144. Actual PSR as determined by a panel of users versus PSR as predicted by the COPES JPCP PSR model for the wet-freeze region.

Section ID	Actual PSR	Predicted PSR	Difference
MI 1-4a	3.9	3.92404	0.02404
MI 1-7a	3.6	3.88818	0.28818
MI 1-7b	3.7	3.83044	0.13044
MI 1-10a	2.9	3.85272	0.95272
MI 1-10b	2.8	3.86863	1.06863
MI 1-25	2.9	3.86506	0.96506
NY 1-1	4.0	3.92015	0.07985
NY 1-6	3.9	3.92557	0.02557
NY 1-8a	4.1	3.95757	0.14243
NY 1-8b	3.8	3.91852	0.11852
NY 2-3	4.2	3.99255	0.20745
NY 2-9	4.0	3.90905	0.09095
NY 2-11	4.1	3.93993	0.16007
ONT 1-1a	3.8	4.09728	0.29728
ONT 1-1b	3.8	4.09728	0.29728
ONT 1-2a	3.8	3.79059	0.00941
ONT 1-2b	3.7	3.79059	0.09059
ONT 1-3a	3.8	3.79059	0.00941
ONT 1-3b	3.8	3.79059	0.00941
ONT 1-4a	3.7	3.71173	0.01173
ONT 1-4b	3.8	3.71173	0.08827
ONT 2	3.9	4.13088	0.23088

Analysis Variable : DIFPSR

N Obs	Mean	Std Error	T	Prob>|T|
22	0.2408262	0.0685414	3.5135887	0.0021

Table 145. Actual PSR as determined by a panel of users versus PSR as predicted by the COPES JRCP PSR model for the wet-freeze region.

Section ID	Actual PSR	Predicted PSR	Difference
MI 1-1a	3.6	4.00076	0.40076
MI 1-1b	3.3	3.84963	0.54963
MI 3	4.8	4.15033	0.64967
MI 4-1	2.4	3.04593	0.64593
MI 4-2	2.4	3.48948	1.08948
MI 5	4.2	4.00151	0.19849
NJ 2	3.8	2.83911	0.96089
NJ 3-1	3.6	3.63516	0.03516
NJ 3-2	3.5	3.76978	0.26978
NY 1-3	3.6	4.15360	0.55360
NY 1-4	3.4	3.85489	0.45489
NY 2-15	4.0	3.85947	0.14053
OH 1-1	4.2	3.93890	0.26110
OH 1-3	4.2	4.00366	0.19634
OH 1-4	4.1	3.97630	0.12370
OH 1-6	4.2	4.12911	0.07089
OH 1-7	4.2	4.11390	0.08610
OH 1-9	4.2	4.12747	0.07253
OH 1-10	4.2	4.14088	0.05912
OH 2-33a	3.4	4.34672	0.94672
OH 2-33b	3.5	4.34672	0.84672
PA 1-1	4.2	4.38611	0.18611
PA 1-2	3.8	4.42772	0.62772
PA 1-3	3.7	4.37257	0.67257
PA 1-4	4.1	4.39782	0.29782
PA 1-5	4.1	4.36865	0.26865

Analysis Variable : DIFPSR

N Obs	Mean	Std Error	T	Prob>|T|
26	0.4101881	0.0618007	6.6372732	0.0001

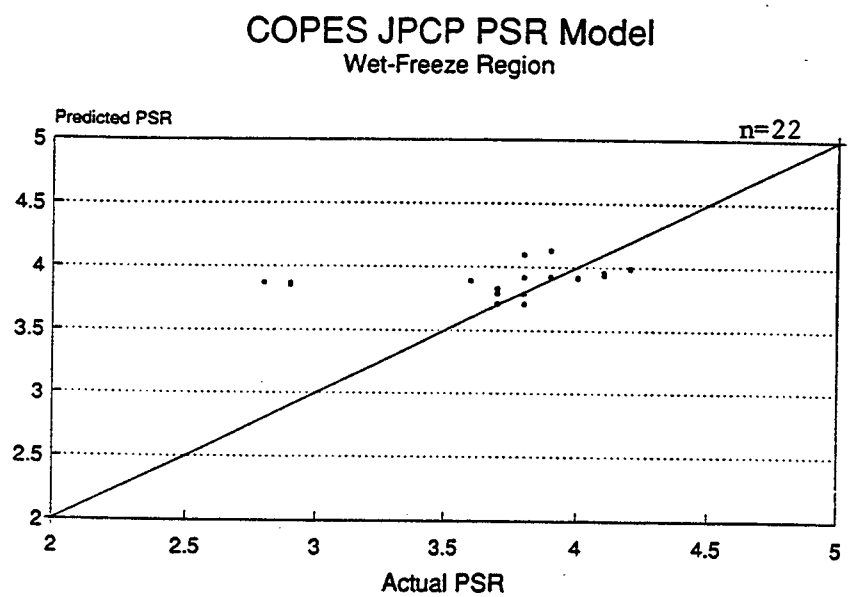

Figure 95. Actual PSR as determined by a panel of users versus PSR as predicted by the COPES JPCP PSR model for the wet-freeze region.

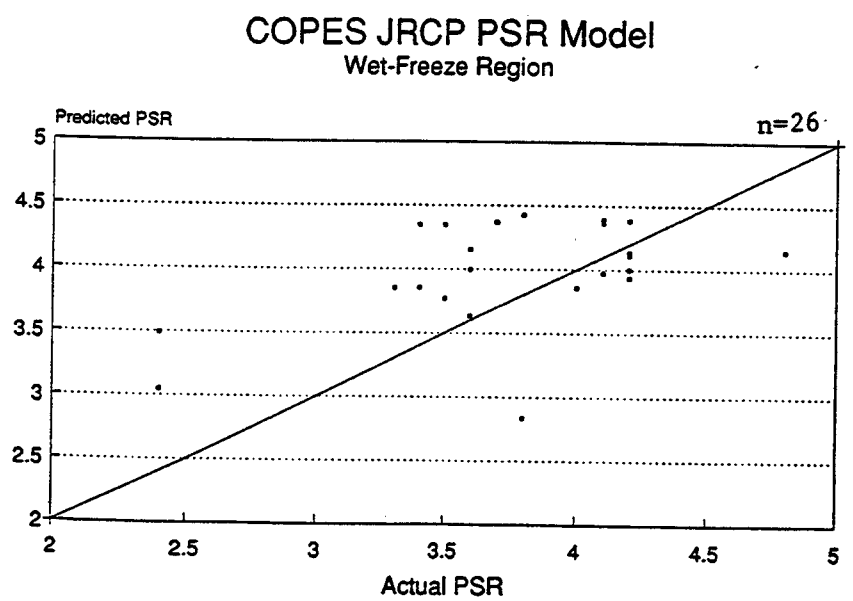

Figure 96. Actual PSR as determined by a panel of users versus PSR as predicted by the COPES JRCP PSR model for the wet-freeze region.

Table 146. Actual PSR as determined by a panel of users versus PSR as predicted by the COPES PSR models for the wet-nonfreeze region.

Section ID	Actual PSR	Predicted PSR	Difference
CA 3-1	3.6	3.89058	0.29058
CA 3-2	3.9	4.01175	0.11175
CA 3-5	3.8	4.06597	0.26597
FL 2	3.7	4.24266	0.54266
FL 3	3.2	3.90931	0.70931
NC 1-1	3.4	3.85033	0.45033
NC 1-2	3.5	3.95012	0.45012
NC 1-3	3.6	4.04896	0.44896
NC 1-4	3.4	4.06291	0.66291
NC 1-5	3.2	4.00337	0.80337
NC 1-6	3.8	3.87389	0.07389
NC 1-7	3.4	1.50838	1.89162
NC 1-8	3.7	4.04642	0.34642
NC 2	4.2	4.19451	0.00549

Analysis Variable : DIFPSR

N Obs	Mean	Std Error	T	Prob>|T|
14	0.5038130	0.1241950	4.0566287	0.0014

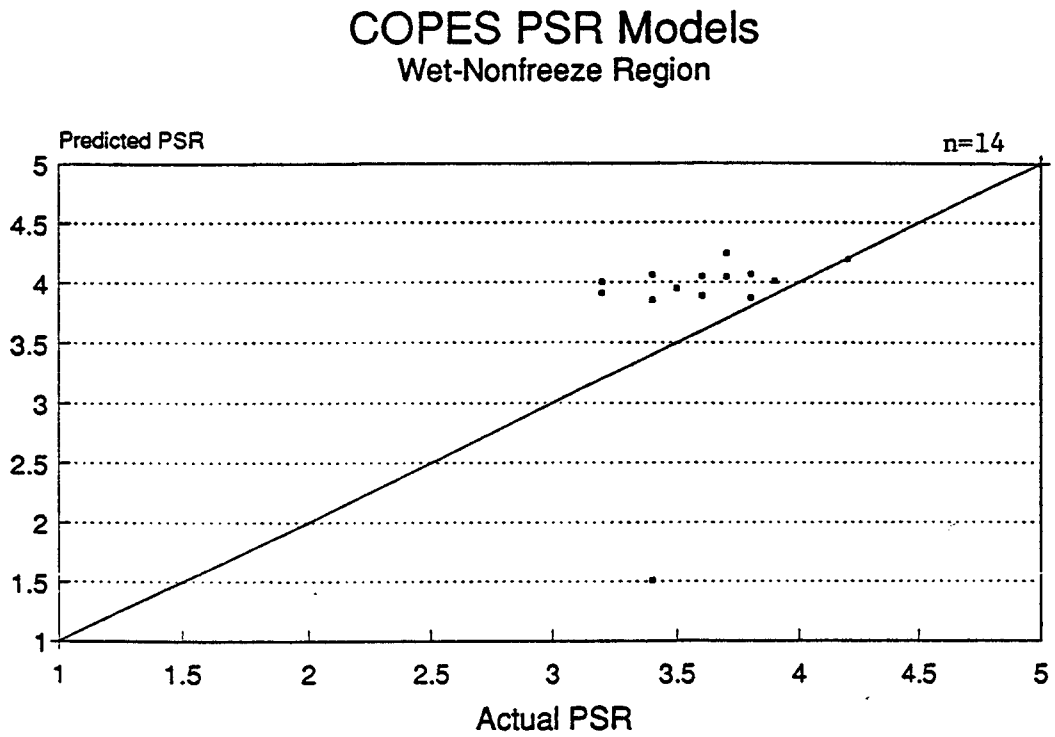

Figure 97. Actual PSR as determined by a panel of users versus PSR as predicted by the COPES PSR models for the wet-nonfreeze region.

Table 147. Actual field measured faulting versus faulting as predicted using the PFAULT models for all Phase I sections.

Section ID	Measured Faulting	Predicted Faulting	Difference
AZ 1-1	0.08	0.077858	0.00214
AZ 1-2	0.01	0.039557	0.02956
AZ 1-4	0.01	0.036415	0.02642
AZ 1-5	0.03	0.039118	0.00912
AZ 1-6	0.01	0.014583	0.00458
AZ 1-7	0.02	0.002306	0.01769
AZ 2	0.01	0.040206	0.03021
CA 1-1	0.06	0.060613	0.00061
CA 1-3	0.10	0.096556	0.00344
CA 1-5	0.11	0.093071	0.01693
CA 1-7	0.06	0.090313	0.03031
CA 1-9	0.13	0.096163	0.03384
CA 2-2	0.11	0.068054	0.04195
CA 2-3	0.11	0.065343	0.04466
CA 3-1	0.08	0.010149	0.06985
CA 3-2	0.11	0.009315	0.10068
CA 3-5	0.10	0.00829	0.09171
CA 6	0.15	0.03002	0.11998
CA 7	0.06	0.06532	0.00532
CA 8	0.04	0.01994	0.02006
FL 2	0.01	0.01149	0.00149
FL 3	0.08	0.09018	0.01018
MI 1-1a	0.05	0.04537	0.00463
MI 1-1b	0.08	0.04772	0.03228
MI 1-4a	0.03	0.09088	0.06088
MI 1-7a	0.04	0.01970	0.02030
MI 1-7b	0.04	0.02160	0.01840
MI 1-10a	0.14	0.09093	0.04907
MI 1-10b	0.19	0.10004	0.08996
MI 1-25	0.20	0.06617	0.13383
MI 3	0.02	0.11024	0.09024
MI 4-1	0.12	0.11917	0.00083
MI 4-2	0.06	0.13845	0.07845
MI 5	0.05	0.06584	0.01584
MN 1-1	0.31	0.21750	0.09250
MN 1-2	0.06	0.11171	0.05171
MN 1-3	0.31	0.21835	0.09165
MN 1-4	0.06	0.11029	0.05029
MN 1-5	0.37	0.25213	0.11787
MN 1-6	0.00	0.08991	0.08991
MN 1-7	0.31	0.25152	0.05848
MN 1-8	0.06	0.09094	0.03094
MN 1-9	0.37	0.19451	0.17549
MN 1-10	0.13	0.09306	0.03694

Table 147. Actual field measured faulting versus faulting as predicted using the PFAULT models for all Phase I sections. (Continued).

Section ID	Measured Faulting	Predicted Faulting	Difference
MN 1-11	0.50	0.19566	0.30434
MN 1-12	0.06	0.10421	0.04421
MN 2-1	0.06	0.09858	0.03858
MN 2-2	0.06	0.10269	0.04269
MN 2-3	0.05	0.09975	0.04975
MN 2-4	0.06	0.09808	0.03808
MN 3	0.02	0.05786	0.03786
MN 4b	0.01	0.02316	0.01316
MN 5	0.09	0.14776	0.05776
MN 6a	0.01	0.05233	0.04233
NJ 2	0.06	0.37709	0.31709
NJ 3-1	0.05	0.11055	0.06055
NJ 3-2	0.06	0.13366	0.07366
NY 1-1	0.02	0.14375	0.12375
NY 1-3	0.14	0.14400	0.00400
NY 1-4	0.09	0.16615	0.07615
NY 1-6	0.03	0.16553	0.13553
NY 1-8a	0.01	0.14301	0.13301
NY 1-8b	0.03	0.14371	0.11371
NY 2-3	0.01	0.05198	0.04198
NY 2-9	0.02	0.04403	0.02403
NY 2-11	0.01	0.05667	0.04667
NY 2-15	0.02	0.08424	0.06424
NC 1-1	0.12	0.15677	0.03677
NC 1-2	0.16	0.15502	0.00498
NC 1-3	0.13	0.13531	0.00531
NC 1-4	0.13	0.12856	0.00144
NC 1-5	0.16	0.14528	0.01472
NC 1-6	0.05	0.12805	0.07805
NC 1-7	0.15	0.28287	0.13287
NC 1-8	0.22	0.15738	0.06262
NC 2	0.02	0.03211	0.01211
OH 1-1	0.13	0.05389	0.07611
OH 1-3	0.06	0.03317	0.02683
OH 1-4	0.07	0.04383	0.02617
OH 1-6	0.03	0.03782	0.00782
OH 1-7	0.07	0.06654	0.003464
OH 1-9	0.14	0.06841	0.071586
OH 1-10	0.10	0.03924	0.060759
OH 2-33a	0.11	0.09452	0.015476
OH 2-33b	0.11	0.14710	0.037099
PA 1-1	0.03	0.01362	0.016381
PA 1-2	0.02	0.00606	0.013941
PA 1-3	0.03	0.01347	0.016533

Table 147. Actual field measured faulting versus faulting as predicted using the PFAULT models for all Phase I sections. (Continued)

Section ID	Measured Faulting	Predicted Faulting	Difference
PA 1-4	0.03	0.00854	0.021463
PA 1-5	0.03	0.01301	0.016988
ONT 1-1a	0.05	0.11157	0.061569
ONT 1-1b	0.07	0.11157	0.041569
ONT 1-2a	0.05	0.10397	0.053972
ONT 1-2b	0.06	0.10397	0.043972
ONT 1-3a	0.04	0.06076	0.020761
ONT 1-3b	0.09	0.06076	0.029239
ONT 1-4a	0.04	0.06158	0.02158
ONT 1-4b	0.07	0.06158	0.00842
ONT 2	0.01	0.26306	0.25306

Analysis Variable : DIFPFLT

N Obs	Mean	Std Error	T	Prob>|T|
99	0.0533128	0.0057157	9.3273860	0.0001

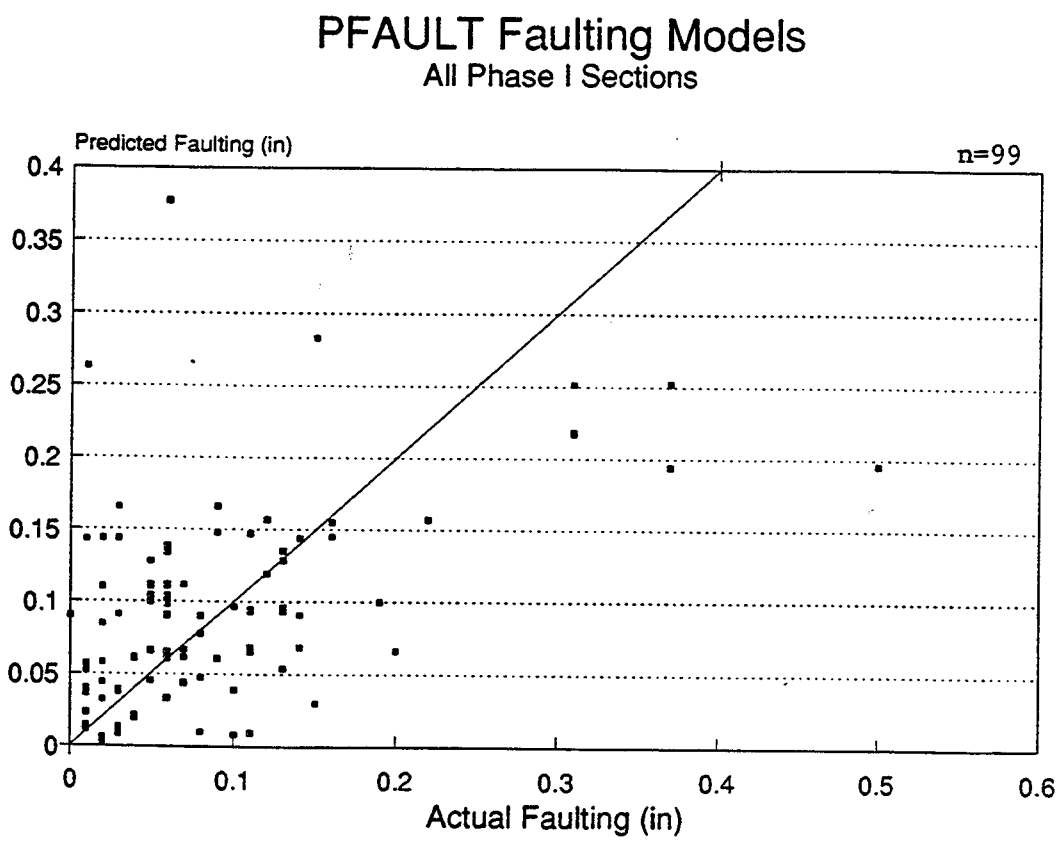

Figure 98. Actual field measured faulting versus faulting as predicted using the PFAULT models for all Phase I sections.

Table 148. Actual field measured faulting versus faulting as predicted using the PFAULT models for the dry-freeze region.

Section ID	Measured Faulting	Predicted Faulting	Difference
MN 1-1	0.31	0.21750	0.09250
MN 1-2	0.06	0.11171	0.05171
MN 1-3	0.31	0.21835	0.09165
MN 1-4	0.06	0.11029	0.05029
MN 1-5	0.37	0.25213	0.11787
MN 1-6	0.00	0.08991	0.08991
MN 1-7	0.31	0.25152	0.05848
MN 1-8	0.06	0.09094	0.03094
MN 1-9	0.37	0.19451	0.17549
MN 1-10	0.13	0.09306	0.03694
MN 1-11	0.50	0.19566	0.30434
MN 1-12	0.06	0.10421	0.04421
MN 2-1	0.06	0.09858	0.03858
MN 2-2	0.06	0.10269	0.04269
MN 2-3	0.05	0.09975	0.04975
MN 2-4	0.06	0.09808	0.03808
MN 3	0.02	0.05786	0.037857
MN 4b	0.01	0.02316	0.013162
MN 5	0.09	0.14776	0.057756
MN 6a	0.01	0.05233	0.042330

Analysis Variable : DIFPFLT

N Obs	Mean	Std Error	T	Prob>|T|
20	0.0732275	0.0146878	4.9855921	0.0001

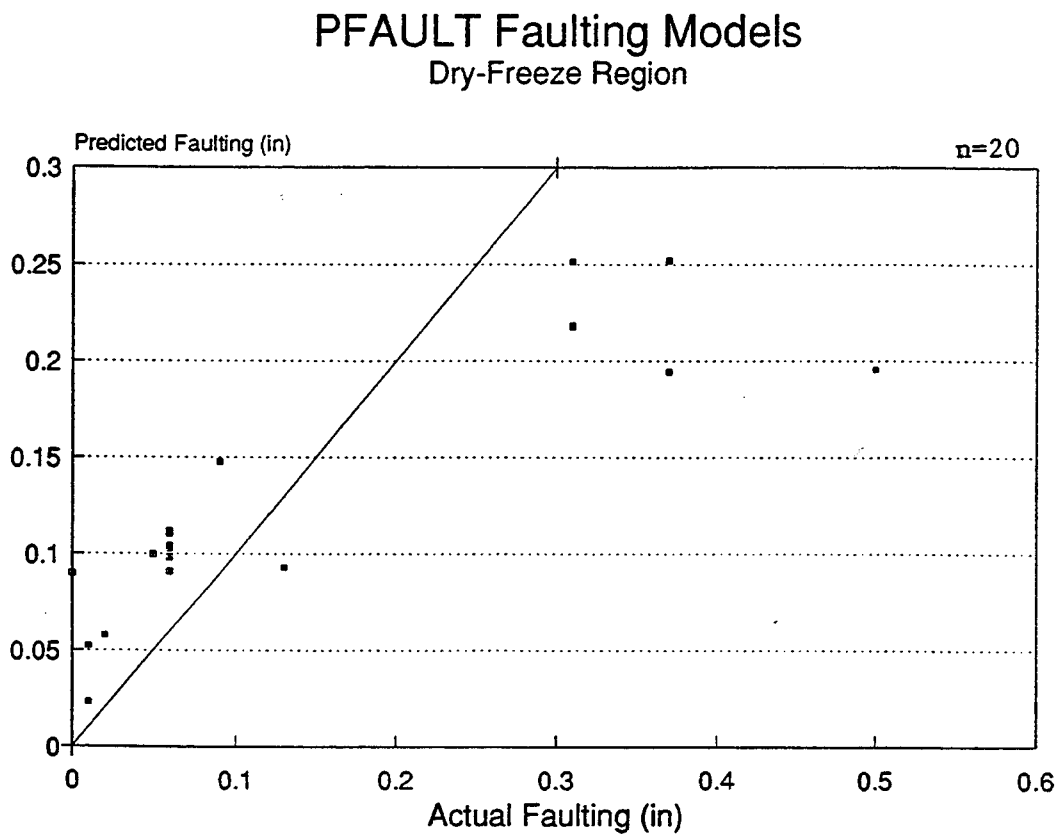

Figure 99. Actual field measured faulting versus faulting as predicted using the PFAULT models for the dry-freeze region.

Table 149. Actual field measured faulting versus faulting as predicted using the PFAULT models for dowled pavements for the dry-freeze region.

Section ID	Measured Faulting	Predicted Faulting	Difference
MN 1-2	0.06	0.11171	0.051714
MN 1-4	0.06	0.11029	0.050294
MN 1-6	0.00	0.08991	0.089915
MN 1-8	0.06	0.09094	0.030940
MN 1-10	0.13	0.09306	0.036943
MN 1-12	0.06	0.10421	0.044206
MN 2-1	0.06	0.09858	0.038584
MN 2-2	0.06	0.10269	0.042691
MN 2-3	0.05	0.09975	0.049751
MN 2-4	0.06	0.09808	0.038082
MN 3	0.02	0.05786	0.037857
MN 4b	0.01	0.02316	0.013162
MN 5	0.09	0.14776	0.057756
MN 6a	0.01	0.05233	0.042330

Analysis Variable : DIFPFLT

N Obs	Mean	Std Error	T	Prob>|T|
14	0.0445874	0.0045105	9.8852824	0.0001

Table 150. Actual field measured faulting versus faulting as predicted using the PFAULT models for nondoweled pavements for the dry-freeze region.

Section ID	Measured Faulting	Predicted Faulting	Difference
MN 1-1	0.31	0.21750	0.09250
MN 1-3	0.31	0.21835	0.09165
MN 1-5	0.37	0.25213	0.11787
MN 1-7	0.31	0.25152	0.05848
MN 1-9	0.37	0.19451	0.17549
MN 1-11	0.50	0.19566	0.30434

Analysis Variable : DIFPFLT

N Obs	Mean	Std Error	T	Prob>|T|
6	0.1400544	0.0365135	3.8356915	0.0122

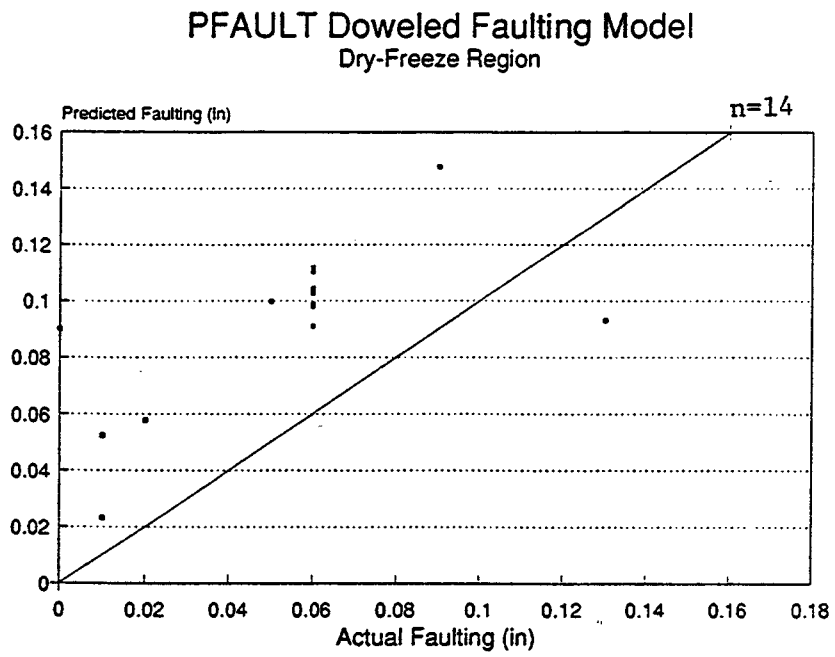

Figure 100. Actual field measured faulting versus faulting as predicted using the PFAULT models for doweled pavements for the dry-freeze region.

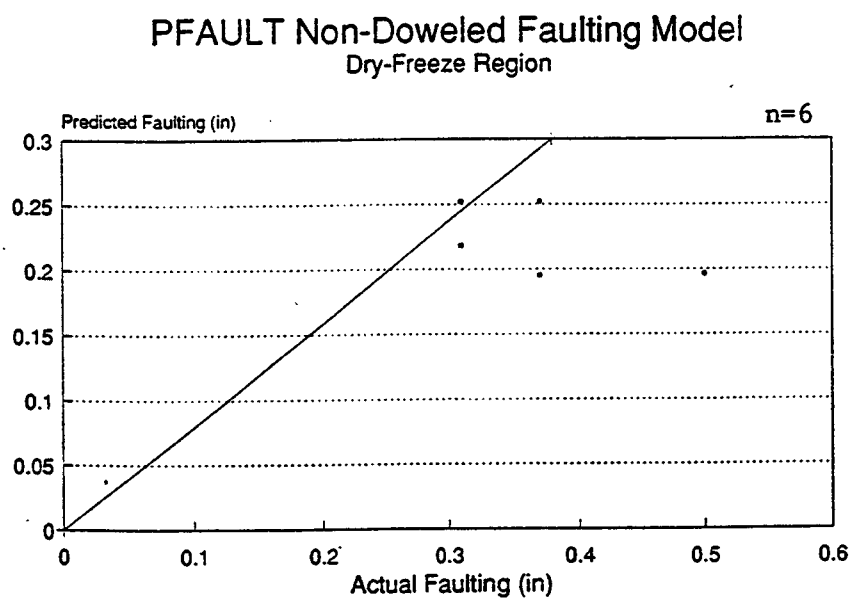

Figure 101. Actual field measured faulting versus faulting as predicted using the PFAULT models for nondoweled pavements for the dry-freeze region.

Table 151. Actual field measured faulting versus faulting as predicted using the PFAULT models for the dry-nonfreeze region.

Section ID	Measured Faulting	Predicted Faulting	Difference
AZ 1-1	0.08	0.077858	0.00214
AZ 1-2	0.01	0.039557	0.02956
AZ 1-4	0.01	0.036415	0.02642
AZ 1-5	0.03	0.039118	0.00912
AZ 1-6	0.01	0.014583	0.00458
AZ 1-7	0.02	0.002306	0.01769
AZ 2	0.01	0.000000	0.01000
CA 1-1	0.06	0.060613	0.00061
CA 1-3	0.10	0.096556	0.00344
CA 1-5	0.11	0.093071	0.01693
CA 1-7	0.06	0.090313	0.03031
CA 1-9	0.13	0.096163	0.03384
CA 2-2	0.11	0.068054	0.04195
CA 2-3	0.11	0.065343	0.04466
CA 6	0.15	0.030024	0.11998
CA 7	0.06	0.065317	0.00532
CA 8	0.04	0.019943	0.02006

Analysis Variable : DIFPFLT

N Obs	Mean	Std Error	T	Prob>|T|
17	0.0245058	0.0068667	3.5687939	0.0026

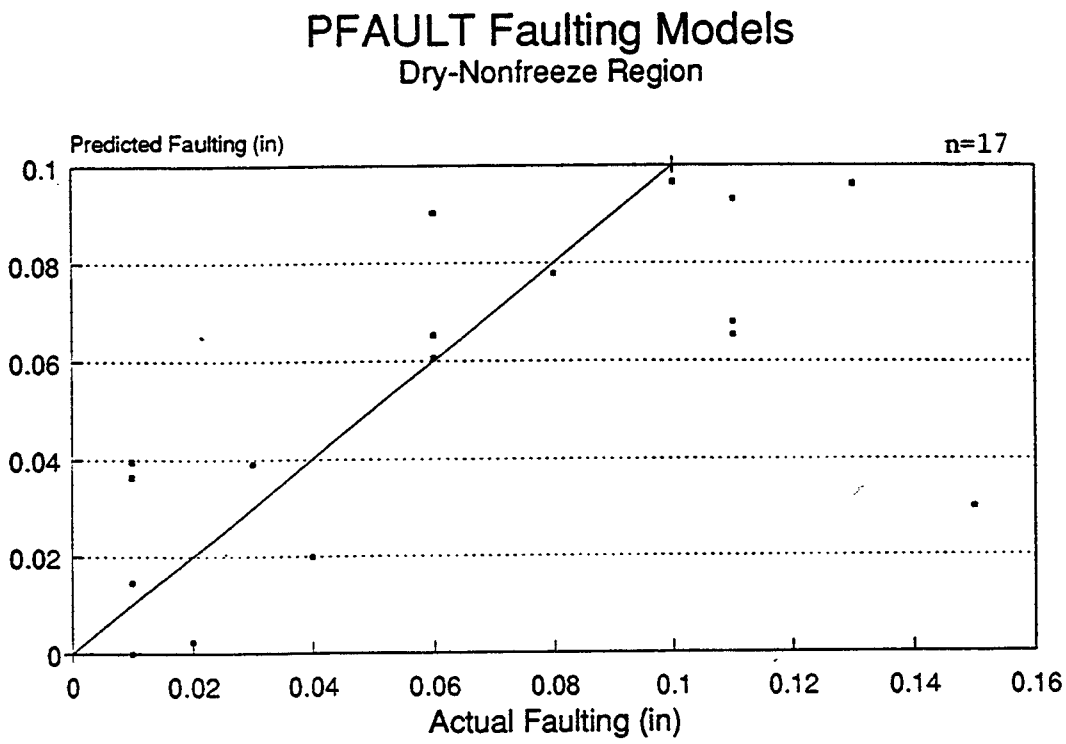

Figure 102. Actual field measured faulting versus faulting as predicted using the PFAULT models for the dry-nonfreeze region.

Table 152. Actual field measured faulting versus faulting as predicted using the PFAULT models for the wet-freeze region.

Section ID	Measured Faulting	Predicted Faulting	Difference
MI 1-1a	0.05	0.04537	0.00463
MI 1-1b	0.08	0.04772	0.03228
MI 1-4a	0.03	0.09088	0.06088
MI 1-7a	0.04	0.01970	0.02030
MI 1-7b	0.04	0.02160	0.01840
MI 1-10a	0.14	0.09093	0.04907
MI 1-10b	0.19	0.10004	0.08996
MI 1-25	0.20	0.06617	0.13383
MI 3	0.02	0.11024	0.09024
MI 4-1	0.12	0.11917	0.00083
MI 4-2	0.06	0.13845	0.07845
MI 5	0.05	0.06584	0.01584
NJ 2	0.06	0.37709	0.31709
NJ 3-1	0.05	0.11055	0.06055
NJ 3-2	0.06	0.13366	0.07366
NY 1-1	0.02	0.14375	0.12375
NY 1-3	0.14	0.14400	0.00400
NY 1-4	0.09	0.16615	0.07615
NY 1-6	0.03	0.16553	0.13553
NY 1-8a	0.01	0.14301	0.13301
NY 1-8b	0.03	0.14371	0.11371
NY 2-3	0.01	0.05198	0.04198
NY 2-9	0.02	0.04403	0.02403
NY 2-11	0.01	0.05667	0.04667
NY 2-15	0.02	0.08424	0.06424
OH 1-1	0.13	0.05389	0.07611
OH 1-3	0.06	0.03317	0.02683
OH 1-4	0.07	0.04383	0.02617
OH 1-6	0.03	0.03782	0.00782
OH 1-7	0.07	0.06654	0.00346
OH 1-9	0.14	0.06841	0.07159
OH 1-10	0.10	0.03924	0.06076
OH 2-33a	0.11	0.09452	0.01548
OH 2-33b	0.11	0.14710	0.03710
PA 1-1	0.03	0.01362	0.01638
PA 1-2	0.02	0.00606	0.01394
PA 1-3	0.03	0.01347	0.01653
PA 1-4	0.03	0.00854	0.02146
PA 1-5	0.03	0.01301	0.01699
ONT 1-1a	0.05	0.11157	0.06157
ONT 1-1b	0.07	0.11157	0.04157
ONT 1-2a	0.05	0.10397	0.05397
ONT 1-2b	0.06	0.10397	0.04397
ONT 1-3a	0.04	0.06076	0.02076

Table 152. Actual field measured faulting versus faulting as predicted using the PFAULT models for the wet-freeze region. (Continued)

Section ID	Measured Faulting	Predicted Faulting	Difference
ONT 1-3b	0.09	0.06076	0.02924
ONT 1-4a	0.04	0.06158	0.02158
ONT 1-4b	0.07	0.06158	0.00842
ONT 2	0.01	0.26306	0.25306

Analysis Variable : DIFPFLT

N Obs	Mean	Std Error	T	Prob>|T|
48	0.0573718	0.0087900	6.5269227	0.0001

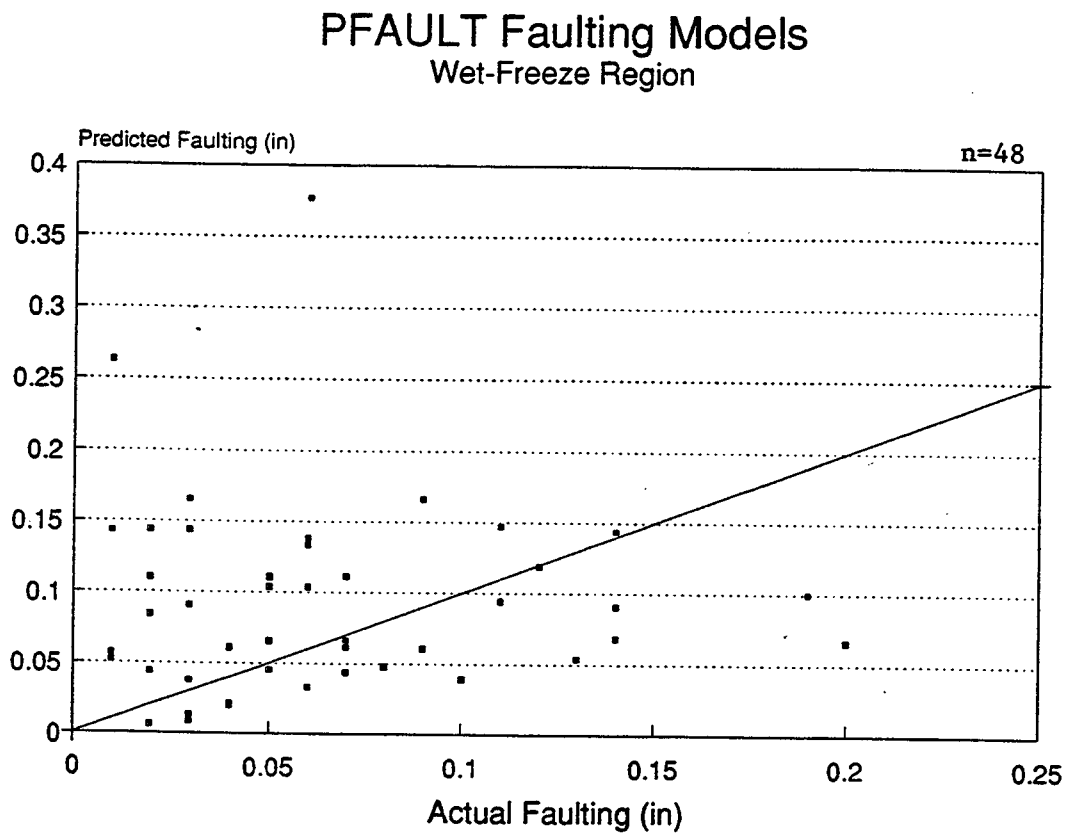

Figure 103. Actual field measured faulting versus faulting as predicted using the PFAULT models for the wet-freeze region.

Table 153. Actual field measured faulting versus faulting as predicted using the PFAULT models for doweled pavements for the wet-freeze region.

Section ID	Measured Faulting	Predicted Faulting	Difference
MI 1-1a	0.05	0.04537	0.00463
MI 1-1b	0.08	0.04772	0.03228
MI 1-7a	0.04	0.01970	0.02030
MI 1-7b	0.04	0.02160	0.01840
MI 3	0.02	0.11024	0.09024
MI 4-1	0.12	0.11917	0.00083
MI 4-2	0.06	0.13845	0.07845
MI 5	0.05	0.06584	0.01584
NJ 2	0.06	0.37709	0.31709
NJ 3-1	0.05	0.11055	0.06055
NJ 3-2	0.06	0.13366	0.07366
NY 2-3	0.01	0.05198	0.04198
NY 2-9	0.02	0.04403	0.02403
NY 2-11	0.01	0.05667	0.04667
NY 2-15	0.02	0.08424	0.06424
OH 1-1	0.13	0.05389	0.07611
OH 1-3	0.06	0.03317	0.02683
OH 1-4	0.07	0.04383	0.02617
OH 1-6	0.03	0.03782	0.00782
OH 1-7	0.07	0.06654	0.00346
OH 1-9	0.14	0.06841	0.07159
OH 1-10	0.10	0.03924	0.06076
PA 1-1	0.03	0.01362	0.01638
PA 1-2	0.02	0.00606	0.01394
PA 1-3	0.03	0.01347	0.01653
PA 1-4	0.03	0.00854	0.02146
PA 1-5	0.03	0.01301	0.01699
ONT 2	0.01	0.26306	0.25306

Analysis Variable : DIFPFLT

N Obs	Mean	Std Error	T	Prob>|T|
28	0.0535819	0.0134061	3.9968205	0.0004

Table 154. Actual field measured faulting versus faulting as predicted using the PFAULT models for nondoweled pavements for the wet-freeze region.

Section ID	Measured Faulting	Predicted Faulting	Difference
MI 1-4a	0.03	0.09088	0.06088
MI 1-10a	0.14	0.09093	0.04907
MI 1-10b	0.19	0.10004	0.08996
MI 1-25	0.20	0.06617	0.13383
NY 1-1	0.02	0.14375	0.12375
NY 1-3	0.14	0.14400	0.00400
NY 1-4	0.09	0.16615	0.07615
NY 1-6	0.03	0.16553	0.13553
NY 1-8a	0.01	0.14301	0.13301
NY 1-8b	0.03	0.14371	0.11371
OH 2-33a	0.11	0.09452	0.01548
OH 2-33b	0.11	0.14710	0.03710
ONT 1-1a	0.05	0.11157	0.06157
ONT 1-1b	0.07	0.11157	0.04157
ONT 1-2a	0.05	0.10397	0.05397
ONT 1-2b	0.06	0.10397	0.04397
ONT 1-3a	0.04	0.060761	0.020761
ONT 1-3b	0.09	0.060761	0.029239
ONT 1-4a	0.04	0.061576	0.021576
ONT 1-4b	0.07	0.061576	0.008424

Analysis Variable : DIFPFLT

N Obs	Mean	Std Error	T	Prob>|T|
20	0.0626776	0.0099302	6.3117859	0.0001

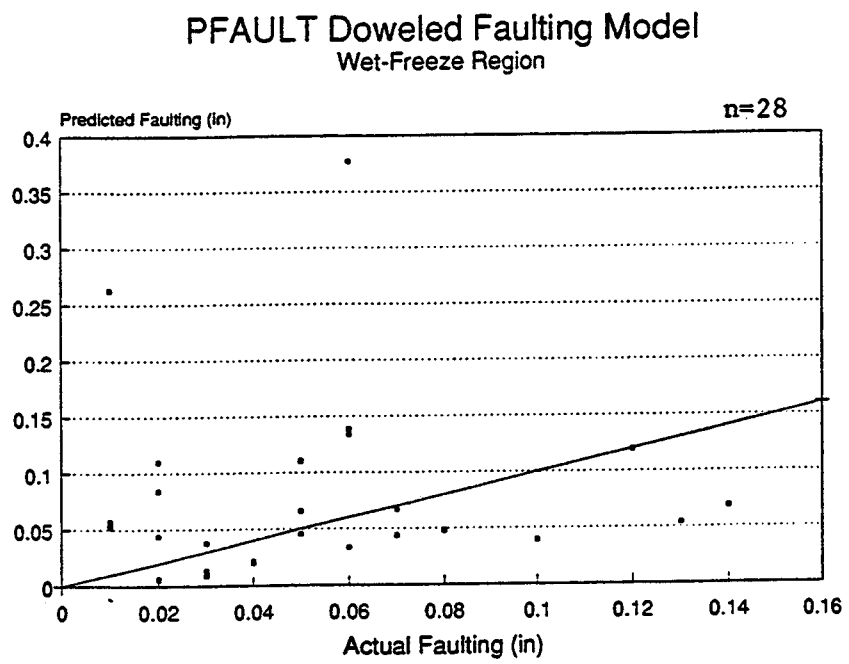

Figure 104. Actual field measured faulting versus faulting as predicted using the PFAULT models for doweled pavements for the wet-freeze region.

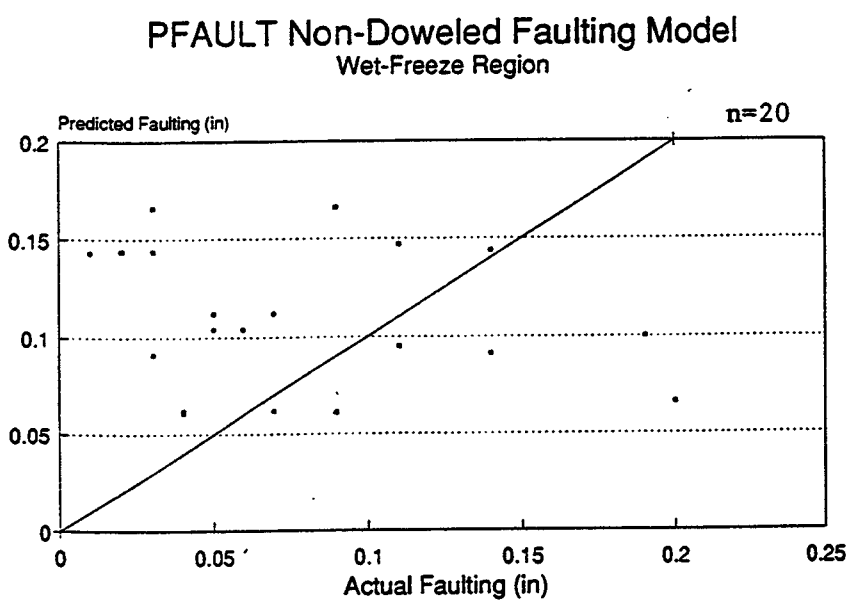

Figure 105. Actual field measured faulting versus faulting as predicted using the PFAULT models for nondoweled pavements for the wet-freeze region.

Table 155. Actual field measured faulting versus faulting as predicted using the PFAULT models for the wet-nonfreeze region.

Section ID	Measured Faulting	Predicted Faulting	Difference
CA 3-1	0.08	0.01015	0.06985
CA 3-2	0.11	0.00932	0.10068
CA 3-5	0.10	0.00829	0.09171
FL 2	0.01	0.01149	0.00149
FL 3	0.08	0.09018	0.01018
NC 1-1	0.12	0.15677	0.03677
NC 1-2	0.16	0.15502	0.00498
NC 1-3	0.13	0.13531	0.00531
NC 1-4	0.13	0.12856	0.00144
NC 1-5	0.16	0.14528	0.01472
NC 1-6	0.05	0.12805	0.07805
NC 1-7	0.15	0.28287	0.13287
NC 1-8	0.22	0.15738	0.06262
NC 2	0.02	0.03211	0.01211

Analysis Variable : DIFPFLT

N Obs	Mean	Std Error	T	Prob>|T|
14	0.0444837	0.0117831	3.7752242	0.0023

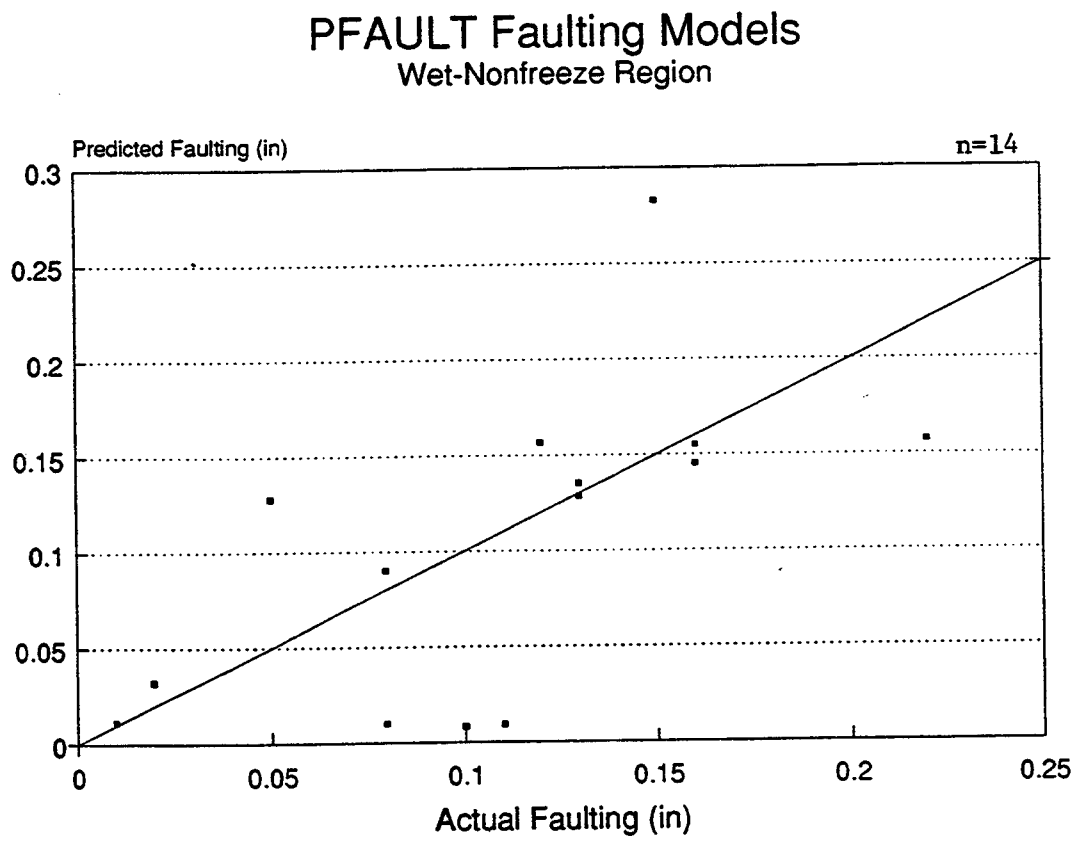

Figure 106. Actual field measured faulting versus faulting as predicted using the PFAULT models for the wet-nonfreeze region.

Table 156. Actual field measured faulting versus faulting as predicted using the PFAULT models for doweled pavements for the wet-nonfreeze region.

Section ID	Measured Faulting	Predicted Faulting	Difference
FL 2	0.01	0.01149	0.00149
FL 3	0.08	0.09018	0.01018
NC 1-2	0.16	0.15502	0.00498
NC 1-4	0.13	0.12856	0.00144
NC 1-7	0.15	0.28287	0.13287
NC 2	0.02	0.03211	0.01211

Analysis Variable : DIFPFLT

N Obs	Mean	Std Error	T	Prob>|T|
6	0.0271767	0.0212156	1.2809761	0.2564

Table 157. Actual field measured faulting versus faulting as predicted using the PFAULT models for nondoweled pavements for the wet-nonfreeze region.

Section ID	Measured Faulting	Predicted Faulting	Difference
CA 3-1	0.08	0.01015	0.06985
CA 3-2	0.11	0.00932	0.10068
CA 3-5	0.10	0.00829	0.09171
NC 1-1	0.12	0.15677	0.03677
NC 1-3	0.13	0.13531	0.00531
NC 1-5	0.16	0.14528	0.01472
NC 1-6	0.05	0.12805	0.07805
NC 1-8	0.22	0.15738	0.06262

Analysis Variable : DIFPFLT

N Obs	Mean	Std Error	T	Prob>|T|
8	0.0574640	0.0124074	4.6314298	0.0024

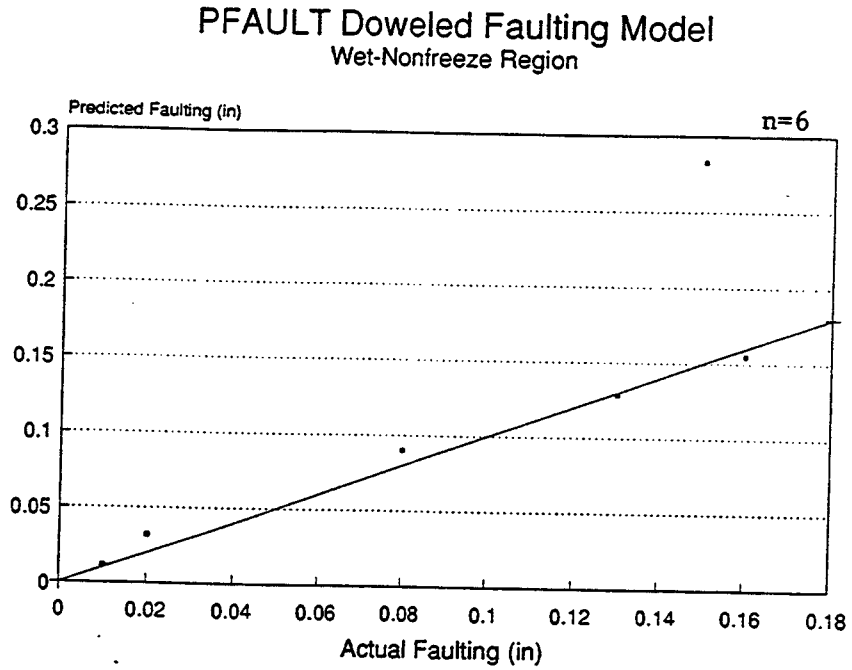

Figure 107. Actual field measured faulting versus faulting as predicted using the PFAULT models for doweled pavements for the wet-nonfreeze region.

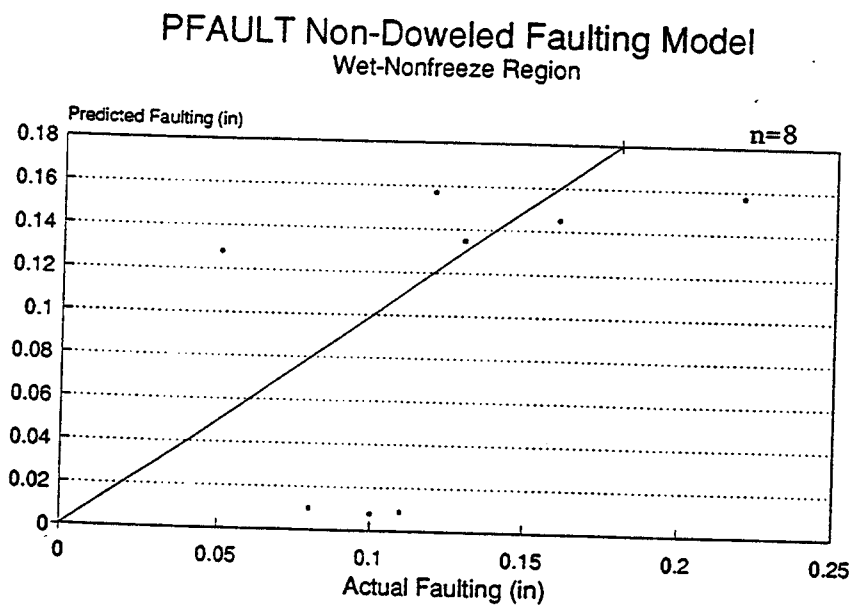

Figure 108. Actual field measured faulting versus faulting as predicted using the PFAULT models for nondoweled pavements for the wet-nonfreeze region.

Table 158. Data used for the analysis of the PEARDARP, COPES, and PFAULT predictive models.

Obs #	Section ID	Pvt. Type	Func. Class	Joint Space	Dowel Dia.	Epcc	MR	Cd	Envir. FI	ZONE	PSR
1	AZ 1-1	11	12	15.0	0.00	3140000	687	1.00	0	3	3.4
2	AZ 1-2	11	12	15.0	0.00	3440000	649	1.10	0	3	3.8
3	AZ 1-4	11	12	15.0	0.00	3490000	702	1.10	0	3	3.6
4	AZ 1-5	11	12	15.0	0.00	3290000	761	1.10	0	3	3.8
5	AZ 1-6	11	12	15.0	0.00	3090000	853	1.10	0	3	3.5
6	AZ 1-7	11	12	15.0	0.00	3690000	868	1.15	0	3	3.8
7	AZ 2	11	11	15.0	1.25	5560000	725	1.05	0	3	3.6
8	CA 1-1	11	1	7.8	0.00	6610000	650	1.10	0	3	2.9
9	CA 1-3	11	1	15.5	0.00	5240000	723	1.00	0	3	3.0
10	CA 1-5	11	1	15.5	0.00	5280000	918	1.10	0	3	2.7
11	CA 1-7	11	1	15.5	0.00	6480000	781	1.15	0	3	2.7
12	CA 1-9	11	1	15.5	0.00	6950000	802	1.10	0	3	2.5
13	CA 2-2	11	11	15.5	0.00	7040000	730	1.10	0	3	3.8
14	CA 2-3	11	11	15.5	0.00	4980000	644	0.90	0	3	4.1
15	CA 3-1	11	12	15.5	0.00	3530000	650	0.90	0	1	3.6
16	CA 3-2	11	12	15.5	0.00	4170000	796	1.00	0	1	3.9
17	CA 3-5	11	12	15.5	0.00	4380000	842	0.90	0	1	3.8
18	CA 6	11	12	13.5	0.00	6710000	791	1.10	0	3	3.4
19	CA 7	11	1	15.5	0.00	6260000	552	0.85	0	3	3.8
20	CA 8	11	12	13.5	0.00	6420000	727	0.95	0	3	3.8
21	FL 2	11	11	15.5	1.25	5550000	664	0.80	0	1	3.7
22	FL 3	11	1	19.5	1.00	4160000	599	0.75	0	1	3.2
23	MI 1-1a	12	2	71.2	1.25	5450000	744	1.00	875	2	3.6
24	MI 1-1b	12	2	71.2	1.25	5790000	650	0.90	875	2	3.3
25	MI 1-4a	11	2	15.5	0.00	5880000	756	1.10	875	2	3.9
26	MI 1-7a	11	2	14.5	1.25	6340000	744	0.90	875	2	3.6
27	MI 1-7b	11	2	14.4	1.25	6090000	650	0.80	875	2	3.7
28	MI 1-10a	11	2	15.5	0.00	6230000	650	0.85	875	2	2.9
29	MI 1-10b	11	2	15.5	0.00	5280000	650	0.85	875	2	2.8
30	MI 1-25	11	2	15.5	0.00	4500000	650	0.70	875	2	2.9
31	MI 3	12	1	41.0	1.00	4380000	810	1.12	563	2	4.8
32	MI 4-1	12	1	71.2	1.25	4830000	596	0.75	563	2	2.4
33	MI 4-2	12	1	71.2	1.25	4530000	756	0.70	563	2	2.4
34	MI 5	12	1	41.0	1.31	4490000	671	1.05	563	2	4.2
35	MN 1-1	12	1	27.0	0.00	7090000	650	1.05	2188	4	3.7
36	MN 1-2	12	1	27.0	1.00	7750000	801	1.05	2188	4	3.3
37	MN 1-3	12	1	27.0	0.00	6660000	650	1.05	2188	4	3.4
38	MN 1-4	12	1	27.0	1.00	6920000	552	1.05	2188	4	3.3
39	MN 1-5	12	1	27.0	0.00	9130000	650	0.85	2188	4	3.4
40	MN 1-6	12	1	27.0	1.00	9360000	587	0.85	2188	4	3.4
41	MN 1-7	12	1	27.0	0.00	8300000	650	0.85	2188	4	3.6
42	MN 1-8	12	1	27.0	1.00	7880000	689	0.85	2188	4	3.4
43	MN 1-9	12	1	27.0	0.00	6670000	650	0.80	2188	4	3.7
44	MN 1-10	12	1	27.0	1.00	6740000	735	0.80	2188	4	3.3
45	MN 1-11	12	1	27.0	0.00	8030000	650	0.80	2188	4	3.7
46	MN 1-12	12	1	27.0	1.00	7790000	763	0.80	2188	4	3.5
47	MN 2-1	11	1	15.5	1.00	6780000	682	0.85	1688	4	3.8
48	MN 2-2	11	1	15.5	1.00	8010000	650	0.75	1688	4	3.9
49	MN 2-3	12	1	27.0	1.00	7320000	744	0.80	1688	4	4.0

Table 158. Data used for the analysis of the PEARDARP, COPES, and PFAULT predictive models (continued).

Obs #	Section ID	Pvt. Type	Func. Class	Joint Space	Dowel Dia.	Epcc	MR	Cd	Envir. FI	ZONE	PSR
50	MN 2-4	12	1	27.0	1.00	6620000	650	0.95	1688	4	4.0
51	MN 3	12	11	27.0	1.00	8810000	650	0.80	1250	4	3.8
52	MN 4b	11	6	15.0	1.00	6300000	832	0.90	1800	4	4.7
53	MN 5	12	1	27.0	1.00	7560000	650	0.95	2188	4	3.3
54	MN 6a	12	6	27.0	1.00	6570000	616	1.05	1800	4	4.5
55	NJ 2	12	12	78.5	1.25	6720000	700	1.05	0	2	3.8
56	NJ 3-1	12	11	78.5	1.25	5400000	681	1.10	0	2	3.6
57	NJ 3-2	12	11	78.5	1.25	5330000	726	1.10	0	2	3.5
58	NY 1-1	11	7	20.0	0.00	3810000	650	0.90	500	2	4.0
59	NY 1-3	12	7	60.8	0.00	3890000	809	0.90	500	2	3.6
60	NY 1-4	12	7	60.8	0.00	3892000	658	0.80	500	2	3.4
61	NY 1-6	11	7	20.0	0.00	4020000	650	0.75	500	2	3.9
62	NY 1-8a	11	7	20.0	0.00	4100000	684	1.00	500	2	4.1
63	NY 1-8b	11	7	20.0	0.00	3880000	650	1.05	500	2	3.8
64	NY 2-3	11	1	20.0	1.00	5100000	864	1.00	500	2	4.2
65	NY 2-9	11	1	20.0	1.00	5090000	705	0.85	500	2	4.0
66	NY 2-11	11	1	26.7	1.00	6120000	812	0.80	500	2	4.1
67	NY 2-15	12	1	63.5	1.00	5520000	650	0.85	500	2	4.0
68	NC 1-1	1	1	30.0	0.00	4630000	736	0.75	0	1	3.4
69	NC 1-2	11	1	30.0	1.00	5190000	674	0.80	0	1	3.5
70	NC 1-3	11	1	30.0	0.00	3970000	705	0.80	0	1	3.6
71	NC 1-4	11	1	30.0	1.00	4210000	709	0.75	0	1	3.4
72	NC 1-5	11	1	30.0	0.00	5500000	674	0.75	0	1	3.2
73	NC 1-6	11	1	30.0	0.00	5140000	559	0.90	0	1	3.8
74	NC 1-7	12	1	60.0	1.00	5090000	644	0.90	0	1	3.4
75	NC 1-8	11	1	30.0	0.00	4220000	705	0.80	0	1	3.7
76	NC 2	11	1	21.2	1.38	5890000	712	1.00	0	1	4.2
77	OH 1-1	12	14	40.0	1.25	4430000	686	0.95	25	2	4.2
78	OH 1-3	12	14	21.0	1.25	5310000	650	0.90	25	2	4.2
79	OH 1-4	12	14	40.0	1.25	5230000	650	0.90	25	2	4.1
80	OH 1-6	12	14	21.0	1.25	4060000	761	0.85	25	2	4.2
81	OH 1-7	12	14	40.0	1.25	4430000	848	1.07	25	2	4.2
82	OH 1-9	12	14	40.0	1.25	3400000	833	0.90	25	2	4.2
83	OH 1-10	12	14	21.0	1.25	4510000	788	1.05	25	2	4.2
84	OH 2-33a	12	6	20.0	0.00	4500000	650	0.90	380	2	3.4
85	OH 2-33b	12	6	20.0	0.00	4500000	650	0.95	380	2	3.5
86	PA 1-1	12	16	46.5	1.25	4210000	731	0.80	300	2	4.2
87	PA 1-2	12	16	46.5	1.25	3390000	720	1.05	300	2	3.8
88	PA 1-3	12	16	46.5	1.25	3230000	709	1.05	300	2	3.7
89	PA 1-4	12	16	46.5	1.25	4530000	870	1.00	300	2	4.1
90	PA 1-5	12	16	46.5	1.25	3620000	704	1.00	300	2	4.1
91	ONT 1-1a	11	6	15.5	0.00	4500000	650	0.95	1000	2	3.8
92	ONT 1-1b	11	6	15.5	0.00	4500000	650	0.95	1000	2	3.8
93	ONT 1-2a	11	6	15.5	0.00	4500000	650	1.00	1000	2	3.8
94	ONT 1-2b	11	6	15.5	0.00	4500000	650	1.00	1000	2	3.7
95	ONT 1-3a	11	6	15.5	0.00	4500000	650	1.00	1000	2	3.8
96	ONT 1-3b	11	6	15.5	0.00	4500000	650	1.00	1000	2	3.8
97	ONT 1-4a	11	6	15.5	0.00	4500000	650	1.00	1000	2	3.7
98	ONT 1-4b	11	6	15.5	0.00	4500000	650	1.00	1000	2	3.8
99	ONT 2	11	12	15.5	1.00	4500000	650	0.80	1000	2	3.9

Table 158. Data used for the analysis of the PEARDARP, COPES, and PFAULT predictive models (continued).

Obs. #	Mays	Spalls	Pump	2-way ADT0	2-way Cum. ADT	Pt	Joint Open	Kstat	ESAL	AAPREC
1	114	22	N	15160	968080	3	0.05	273.0	3968618	3.3071
2	65	1	N	15500	837370	3	0.06	246.0	3414954	3.3071
3	102	0	N	28000	519540	3	0.06	172.0	2387085	3.3071
4	85	0	N	34000	627660	3	0.06	219.5	2801246	3.3071
5	97	1	N	23000	368150	3	0.05	310.5	2012173	3.3071
6	91	0	N	20000	269560	3	0.05	292.0	1522951	3.3071
7	71	0	N	37000	87000	3	0.05	87.0	1622817	2.8346
8	102	2	M	4600	141100	3	0.03	116.0	7621830	3.7795
9	94	0	N	4600	141100	3	0.05	174.5	7621830	3.7795
10	122	3	L	4600	141100	3	0.05	167.5	7621830	3.7795
11	102	9	H	4600	141100	3	0.05	216.5	7621830	3.7795
12	116	3	L	4600	141100	3	0.05	149.0	7621830	3.7795
13	107	0	N	30000	317000	3	0.04	711.5	4423827	6.1417
14	98	0	N	30000	317000	3	0.04	286.0	4423827	6.1417
15	134	2	N	10000	174300	3	0.04	143.0	3641197	17.0079
16	104	3	N	10000	174300	3	0.04	156.0	3641197	17.4803
17	102	6	N	10000	174300	3	0.04	198.5	3641197	17.4803
18	158	3	N	45500	355500	3	0.04	147.0	4434338	2.8346
19	87	0	N	12000	156100	3	0.04	163.0	10524966	6.6142
20	92	0	N	116000	628000	3	0.02	169.5	5263439	5.6693
21	64	0	N	25000	53700	3	0.04	189.0	2005755	18.4252
22	84	2	M	18850	158070	3	0.03	264.5	5967175	21.7323
23	96	0	N	6500	65600	3	0.27	176.5	885249	12.7559
24	91	0	N	6500	65600	3	0.27	150.0	885249	12.7559
25	48	9	N	6500	65600	3	0.06	234.0	885249	12.7559
26	58	12	N	6500	65600	3	0.07	146.0	885249	12.7559
27	36	11	N	6500	65600	3	0.07	134.5	885249	12.7559
28	98	41	L	6500	65600	3	0.06	218.0	885249	12.7559
29	104	63	L	6500	65600	3	0.06	251.0	885249	12.7559
30	159	75	L	6500	65600	3	0.06	200.0	885249	12.7559
31	37	0	N	31300	62600	3	0.15	93.0	2768818	13.2283
32	132	0	N	8500	178550	3	0.27	141.5	4367392	12.7559
33	112	6	N	8500	178550	3	0.27	94.5	4367392	12.7559
34	36	0	N	19500	79700	3	0.15	116.5	3123694	15.1181
35	53	4	L	3350	100130	3	0.12	95.5	5518188	9.4488
36	104	14	N	3350	100130	3	0.12	86.0	5518188	9.4488
37	44	8	L	3350	100130	3	0.12	108.5	5518188	9.4488
38	110	15	L	3350	100130	3	0.12	111.0	5518188	9.4488
39	46	24	L	3350	100130	3	0.10	152.0	5518188	9.4488
40	107	31	N	3350	100130	3	0.10	157.0	5518188	9.4488
41	32	15	M	3350	100130	3	0.10	143.5	5518188	9.4488
42	93	69	N	3350	100130	3	0.10	139.0	5518188	9.4488
43	50	4	L	3350	100130	3	0.10	145.5	5518188	9.4488
44	108	6	L	3350	100130	3	0.10	142.5	5518188	9.4488
45	50	37	L	3350	100130	3	0.10	122.5	5518188	9.4488
46	111	29	M	3350	100130	3	0.10	119.5	5518188	9.4488
47	72	3	N	4740	54860	3	0.08	64.0	2785505	11.8110
48	82	9	N	4740	54860	3	0.08	63.5	2785505	11.8110
49	76	3	N	4740	54860	3	0.11	81.0	2785505	11.8110
50	96	8	N	4740	54860	3	0.11	89.0	2785505	11.8110

Table 158. Data used for the analysis of the PEARDARP, COPES, and PFAULT predictive models (continued).

Obs. #	Mays	Spalls	Pump	2-way ADT0	2-way Cum. ADT	Pt	Joint Open	Kstat	ESAL	AAPREC
51	44	0	N	11000	43000	3	0.12	128.0	1495624	12.2835
52	37	0	N	2900	5800	2.5	0.08	111.0	218813	10.8661
53	100	36	L	3350	100130	3.0	0.18	78.0	5518188	9.4488
54	51	0	N	3800	19325	2.5	0.09	99.5	845032	11.8110
55	63	20	N	17340	575000	3.0	0.25	117.0	34813131	16.5354
56	134	0	N	60500	63450	3.0	0.21	178.0	4181394	17.4803
57	153	43	N	60500	63450	3.0	0.21	105.0	4181394	17.4803
58	56	6	N	5000	148478	2.5	0.06	274.5	3136345	15.1181
59	78	73	M	5000	148478	2.5	0.06	251.5	3136345	15.1181
60	90	9	N	5000	148478	2.5	0.08	267.0	3136345	15.1181
61	82	13	N	5000	148478	2.5	0.08	309.5	3136345	15.1181
62	64	0	N	5000	148478	2.5	0.06	319.0	3136345	15.1181
63	65	0	N	5000	148478	2.5	0.06	274.0	3136345	15.1181
64	61	0	N	3000	63650	3.0	0.07	170.5	1428074	16.0630
65	66	0	N	3000	63650	3.0	0.07	235.5	1428074	16.0630
66	76	0	N	3000	63650	3.0	0.10	148.0	1428074	16.0630
67	63	0	N	3000	63650	3.0	0.23	136.5	1428074	16.0630
68	83	0	N	9300	288750	3.0	0.10	269.0	9137389	18.4252
69	79	0	N	9300	288750	3.0	0.08	173.5	9137389	18.4252
70	77	0	N	9300	288750	3.0	0.08	247.0	9137389	18.4252
71	85	0	N	9300	288750	3.0	0.10	285.0	9137389	18.4252
72	105	0	N	9300	288750	3.0	0.08	314.0	9137389	18.4252
73	69	0	N	9300	288750	3.0	0.08	336.0	9137389	18.4252
74	85	0	N	9300	288750	3.0	0.19	64.0	9137389	18.4252
75	95	0	N	9300	288750	3.0	0.10	256.5	9137389	18.4252
76	64	0	H	21800	145400	3.0	0.06	146.5	5755336	16.5354
77	109	0	N	9420	159660	3.0	0.14	224.5	3424613	16.0630
78	106	13	N	9420	159660	3.0	0.06	220.0	3424613	16.0630
79	123	0	N	9420	159660	3.0	0.11	262.5	3424613	16.0630
80	104	0	N	9420	159660	3.0	0.07	215.5	3424613	16.0630
81	115	0	N	9420	159660	3.0	0.14	170.0	3424613	16.0630
82	109	0	N	9420	159660	3.0	0.14	175.5	3424613	16.0630
83	122	0	N	9420	159660	3.0	0.07	202.5	3424613	16.0630
84	90	15	L	8000	142425	2.5	0.07	200.0	3295668	13.2283
85	85	23	M	8000	142425	2.5	0.07	200.0	3295668	13.2283
86	75	0	N	3500	53775	2.5	0.14	365.5	603407	16.0630
87	91	0	N	3500	42125	2.5	0.14	520.0	270228	16.0630
88	113	0	N	3500	42125	2.5	0.17	269.0	270228	16.0630
89	109	0	N	3500	42125	2.5	0.17	373.5	270228	16.0630
90	82	0	N	3500	42125	2.5	0.17	270.0	270228	16.0630
91	90	0	L	5750	29750	2.5	0.06	200.0	1011133	12.7559
92	62	0	L	5750	29750	2.5	0.06	200.0	1011133	12.7559
93	78	0	M	5750	29750	2.5	0.05	200.0	1011133	12.7559
94	70	0	M	5750	29750	2.5	0.05	200.0	1011133	12.7559
95	57	0	L	5750	29750	2.5	0.05	200.0	1011133	12.7559
96	66	0	L	5750	29750	2.5	0.05	200.0	1011133	12.7559
97	65	0	N	5750	29750	2.5	0.05	200.0	1011133	12.7559
98	72	0	N	5750	29750	2.5	0.05	200.0	1011133	12.7559
99	104	0	N	70800	2628390	3.0	0.05	200.0	35649275	11.8110

Table 158. Data used for the analysis of the PEARDARP, COPES, and PFAULT predictive models (continued).

Obs #	Thick	Area Steel	Fault	Stress Ratio	Crack	Defl	Beta	X
1	9.0	.	0.08	0.28934	47.35	0.035923	7.8690	1.40776
2	13.0	.	0.01	0.17326	0.00	0.021947	11.3255	1.20568
3	13.0	.	0.01	0.16719	0.00	0.026366	11.3255	1.28860
4	11.0	.	0.03	0.19590	0.00	0.030060	10.0217	1.58363
5	9.0	.	0.01	0.22835	0.00	0.033712	7.8690	2.13221
6	9.0	.	0.02	0.23200	0.00	0.032186	7.8690	2.08936
7	10.0	.	0.01	0.28470	0.00	0.043984	9.0668	1.10963
8	8.4	.	0.06	0.41896	18.94	0.044528	7.0167	0.93372
9	8.4	.	0.10	0.34859	385.10	0.039858	7.0167	1.27172
10	11.4	.	0.11	0.16713	0.00	0.026488	10.3431	1.91263
11	8.4	.	0.06	0.32257	356.69	0.032174	7.0167	1.45922
12	8.4	.	0.13	0.33165	861.74	0.038061	7.0167	1.40619
13	8.4	.	0.11	0.29708	0.00	0.016182	7.0167	1.62761
14	8.4	.	0.11	0.36455	946.97	0.031211	7.0167	1.15503
15	9.0	.	0.08	0.33824	94.70	0.048391	7.8690	1.09157
16	9.0	.	0.11	0.27896	18.94	0.042758	7.8690	1.53966
17	9.0	.	0.10	0.25743	426.14	0.036710	7.8690	1.76622
18	9.0	.	0.15	0.29939	186.24	0.035382	7.8690	1.37641
19	10.2	.	0.06	0.34190	645.52	0.029018	9.2761	0.74924
20	10.2	.	0.04	0.25919	0.00	0.028088	9.2761	1.22430
21	13.0	.	0.01	0.18413	0.00	0.020156	11.3255	1.08918
22	9.0	.	0.08	0.34627	1275.25	0.032170	7.8690	1.03373
23	9.0	0.15	0.05	0.30380	37.88	0.035351	7.8690	1.32836
24	9.0	0.15	0.08	0.35721	75.76	0.037497	7.8690	1.00220
25	9.0	.	0.03	0.29146	0.00	0.029331	7.8690	1.42211
26	9.0	.	0.04	0.31645	0.00	0.036465	7.8690	1.24605
27	9.0	.	0.04	0.36399	0.00	0.038817	7.8690	0.97305
28	9.0	.	0.14	0.34445	0.00	0.029666	7.8690	1.06097
29	9.0	.	0.19	0.33144	37.88	0.029676	7.8690	1.12661
30	9.0	.	0.20	0.33430	37.88	0.036109	7.8690	1.11166
31	10.0	0.14	0.02	0.24640	18.94	0.047519	9.0668	1.42588
32	9.0	0.15	0.12	0.38389	1319.44	0.042090	7.8690	0.87935
33	9.0	0.15	0.06	0.31504	1325.76	0.053793	7.8690	1.25890
34	10.0	0.14	0.05	0.29077	1136.36	0.041679	9.0668	1.05892
35	9.0	0.08	0.31	0.38498	18.94	0.043341	7.8690	0.89065
36	9.0	0.08	0.06	0.31908	113.64	0.043919	7.8690	1.24765
37	8.0	0.09	0.31	0.45804	190.97	0.049235	6.3863	0.92146
38	8.0	0.09	0.06	0.54034	170.45	0.047778	6.3863	0.68762
39	8.0	0.09	0.37	0.45687	647.10	0.035502	6.3863	0.92510
40	8.0	0.09	0.00	0.50546	569.76	0.034492	6.3863	0.77310
41	9.0	0.08	0.31	0.37438	550.82	0.032440	7.8690	0.93083
42	9.0	0.08	0.06	0.35239	882.26	0.033807	7.8690	1.03591
43	9.0	0.08	0.37	0.36451	0.00	0.035676	7.8690	0.97084
44	9.0	0.08	0.13	0.32353	246.21	0.035898	7.8690	1.20047
45	8.0	0.09	0.50	0.46157	276.20	0.042289	6.3863	0.91057
46	8.0	0.09	0.06	0.39296	299.87	0.043464	6.3863	1.21126
47	9.0	.	0.06	0.38130	0.00	0.054663	7.8690	0.91252
48	8.0	.	0.06	0.49674	47.35	0.059962	6.3863	0.81220
49	9.0	0.09	0.05	0.34363	0.00	0.046568	7.8690	1.09398
50	9.0	0.09	0.06	0.38506	18.94	0.046465	7.8690	0.89036

Table 158. Data used for the analysis of the PEARDARP, COPES, and PFAULT predictive models (continued).

Obs #	Thick	Area Steel	Fault	Stress Ratio	Crack	Defl	Beta	X
51	9.0	0.05	0.02	0.38177	0.00	0.033511	7.8690	0.90254
52	7.5	.	0.01	0.39416	0.000	0.054623	5.5216	1.44909
53	9.0	0.04	0.09	0.39630	718.119	0.046783	7.8690	0.85067
54	8.0	.	0.01	0.48746	0.000	0.051888	6.3863	0.82670
55	10.0	0.14	0.06	0.29146	230.429	0.034399	9.0668	1.06238
56	9.0	0.16	0.05	0.33119	0.000	0.035341	7.8690	1.13925
57	9.0	0.16	0.06	0.33023	0.000	0.047133	7.8690	1.15951
58	9.0	.	0.02	0.31379	0.000	0.032812	7.8690	1.22638
59	9.0	0.20	0.14	0.25581	18.939	0.034091	7.8690	1.76787
60	9.0	0.20	0.09	0.31203	0.000	0.032991	7.8690	1.24055
61	9.0	.	0.03	0.31098	75.758	0.029991	7.8690	1.24358
62	9.0	.	0.01	0.29509	18.939	0.029237	7.8690	1.36432
63	9.0	.	0.03	0.31464	0.000	0.032574	7.8690	1.22126
64	9.0	.	0.01	0.26059	511.364	0.037138	7.8690	1.74246
65	9.0	.	0.02	0.30665	266.730	0.031238	7.8690	1.29423
66	9.0	.	0.01	0.28829	75.758	0.036803	7.8690	1.46839
67	9.0	0.02	0.02	0.35919	23.674	0.040321	7.8690	0.99356
68	9.0	.	0.12	0.28519	0.000	0.030357	7.8690	1.46241
69	9.0	.	0.16	0.33406	495.581	0.036495	7.8690	1.12157
70	9.0	.	0.13	0.29505	991.162	0.034110	7.8690	1.37404
71	9.0	.	0.13	0.29010	0.000	0.030721	7.8690	1.41231
72	9.0	.	0.16	0.31214	56.818	0.025799	7.8690	1.24658
73	9.0	.	0.05	0.36968	0.000	0.025646	7.8690	0.91970
74	8.0	0.17	0.15	0.47635	96.275	0.073936	6.3863	0.86530
75	9.0	.	0.22	0.29597	246.212	0.032499	7.8690	1.36748
76	11.0	.	0.02	0.23498	37.879	0.028404	10.0217	1.16606
77	9.0	0.09	0.13	0.31148	303.030	0.034168	7.8690	1.25562
78	9.0	0.09	0.06	0.33728	0.000	0.031782	7.8690	1.09639
79	9.0	0.09	0.07	0.32914	189.394	0.029092	7.8690	1.13891
80	9.0	0.09	0.03	0.27910	132.576	0.036358	7.8690	1.52350
81	9.0	0.09	0.07	0.26102	435.606	0.039701	7.8690	1.73113
82	9.0	0.09	0.14	0.25590	568.182	0.044077	7.8690	1.77848
83	9.0	0.09	0.10	0.27540	170.455	0.035831	7.8690	1.56740
84	15.0	.	0.11	0.14377	20.518	0.017633	11.9707	1.10077
85	15.0	.	0.11	0.14377	41.035	0.017633	11.9707	1.10077
86	10.0	0.09	0.03	0.22997	151.515	0.023232	9.0668	1.56228
87	10.0	0.09	0.02	0.21581	0.000	0.021119	9.0668	1.72106
88	10.0	0.09	0.03	0.23842	0.000	0.030973	9.0668	1.46702
89	10.0	0.09	0.03	0.19455	0.000	0.022205	9.0668	2.10468
90	10.0	0.09	0.03	0.24361	0.000	0.029341	9.0668	1.41593
91	12.0	.	0.05	0.20865	0.000	0.024178	10.7659	1.10354
92	12.0	.	0.07	0.20865	12.626	0.024178	10.7659	1.10354
93	8.0	.	0.05	0.40411	0.000	0.042453	6.3863	1.11687
94	8.0	.	0.06	0.40411	0.000	0.042453	6.3863	1.11687
95	8.0	.	0.04	0.40411	113.636	0.042453	6.3863	1.11687
96	8.0	.	0.09	0.40411	258.838	0.042453	6.3863	1.11687
97	7.0	.	0.04	0.49971	197.285	0.050903	4.5634	1.12436
98	7.0	.	0.07	0.49971	287.247	0.050903	4.5634	1.12436
99	9.0	.	0.01	0.33430	18.939	0.036109	7.8690	1.11166

Table 158. Data used for the analysis of the PEARDARP, COPES, and PFAULT predictive models (continued).

Obs #	Bearing Stress	Base Type	ERODF	SHLD	SUB	DR	DCRACK	RAGG	UNI	AGE	TJSD	INCOMP
1	0.00	1	1.0	0	0	0	0	0	0	15	0	0
2	0.00	0	2.5	1	0	0	0	0	0	12	0	0
3	0.00	0	2.5	1	0	0	0	0	0	8	0	0
4	0.00	0	2.5	1	0	0	0	0	0	8	1	1
5	0.00	1	0.5	1	0	0	0	0	0	6	0	0
6	0.00	1	0.5	1	0	1	0	0	0	6	1	1
7	292.15	1	0.5	1	0	0	0	0	0	1	0	0
8	0.00	1	1.0	0	0	0	0	1	0	16	1	1
9	0.00	1	1.0	0	0	0	0	1	0	16	1	1
10	0.00	1	1.0	0	0	0	0	1	0	16	1	1
11	0.00	1	0.5	0	0	0	0	1	0	16	1	1
12	0.00	1	1.0	0	0	0	0	1	0	16	1	1
13	0.00	1	2.0	0	0	0	0	0	0	7	1	1
14	0.00	1	1.0	0	0	0	0	1	0	7	1	1
15	0.00	1	1.0	1	0	0	0	1	0	12	0	0
16	0.00	1	1.0	1	0	0	0	1	0	12	1	1
17	0.00	1	1.0	1	0	0	0	1	0	12	1	1
18	0.00	1	0.5	0	1	1	0	1	0	7	1	1
19	0.00	1	1.0	0	0	1	0	0	0	8	1	1
20	0.00	1	2.0	0	0	1	0	0	0	4	1	1
21	52.80	0	2.5	1	1	0	0	0	0	1	0	0
22	48.19	1	0.5	1	1	0	0	0	0	5	0	0
23	1032.02	0	2.5	0	1	1	1	0	0	12	0	0
24	349.88	0	2.5	0	1	0	1	0	0	12	0	0
25	0.00	1	2.0	0	1	1	1	0	0	12	0	0
26	991.54	0	2.5	0	1	1	1	0	0	12	0	0
27	983.37	0	2.5	0	1	0	1	0	0	12	0	0
28	0.00	1	2.0	0	1	1	1	0	0	12	0	0
29	0.00	1	2.0	0	1	0	1	0	0	12	1	1
30	0.00	1	2.0	1	1	0	1	0	0	12	0	0
31	588.83	0	2.5	1	0	0	0	0	0	1	0	0
32	156.12	0	2.5	1	0	0	1	0	0	15	1	1
33	274.68	0	2.5	0	0	0	1	0	0	15	1	1
34	773.94	0	2.5	1	1	0	0	0	0	3	0	0
35	0.00	0	2.5	1	1	0	1	0	0	17	0	0
36	113.10	0	2.5	0	1	0	1	0	0	17	0	0
37	0.00	0	2.5	1	1	0	1	0	0	17	0	0
38	176.72	0	2.5	0	1	0	1	0	0	17	0	0
39	0.00	1	2.0	0	1	0	1	0	0	17	0	0
40	164.21	1	2.0	0	1	0	1	0	0	17	0	0
41	0.00	1	2.0	0	1	0	1	0	0	17	0	0
42	574.55	1	2.0	0	1	0	1	0	0	17	0	0
43	0.00	1	1.5	1	1	0	1	0	0	17	0	0
44	248.08	1	1.5	0	1	0	1	0	0	17	1	1
45	0.00	1	1.5	1	1	0	1	0	0	17	1	1
46	371.30	1	1.5	0	1	0	1	0	0	17	1	1
47	370.56	0	2.5	1	1	0	0	0	0	11	1	1
48	510.26	0	2.5	1	1	0	0	0	0	11	1	1
49	854.57	0	2.5	0	1	0	0	0	0	11	0	0
50	528.36	0	2.5	0	1	0	0	0	0	11	0	0

Table 158. Data used for the analysis of the PEARDARP, COPES, and PFAULT predictive models (continued).

Obs #	Bearing Stress	Base Type	ERODF	SHLD	SUB	DR	DCRACK	RAGG	UNI	AGE	TJSD	INCOMP
51	707.44	0	2.5	0	1	0	0	0	0	3	0	0
52	614.38	0	2.5	0	1	1	0	0	0	1	0	0
53	195.48	0	2.5	0	1	0	0	0	0	17	0	0
54	451.02	1	2.0	0	1	0	0	0	0	4	0	0
55	359.40	0	2.5	0	0	0	0	0	0	36	1	1
56	152.81	0	2.5	0	1	0	0	0	0	8	0	0
57	181.10	1	2.0	0	1	0	0	0	0	8	0	0
58	0.00	1	2.0	0	0	0	0	0	0	21	0	0
59	0.00	1	2.0	0	0	0	0	0	0	21	0	0
60	0.00	0	2.5	0	0	0	0	0	0	21	0	0
61	0.00	0	2.5	0	0	0	0	0	0	21	0	0
62	0.00	1	2.0	0	0	0	0	0	0	21	0	0
63	0.00	1	2.0	0	0	0	0	0	0	21	0	0
64	1075.46	0	2.5	1	1	0	0	0	0	12	0	0
65	1023.95	0	2.5	1	1	0	0	0	0	12	0	0
66	480.83	0	2.5	1	1	0	0	0	0	12	0	0
67	1006.10	0	2.5	0	0	0	0	0	0	12	0	0
68	0.00	0	2.5	0	1	0	0	0	0	19	0	0
69	1077.06	1	2.5	0	1	0	0	0	0	19	0	0
70	0.00	1	2.5	0	1	0	0	0	0	19	0	0
71	240.64	0	2.5	0	1	0	0	0	0	19	0	0
72	0.00	1	1.5	0	0	0	0	0	0	19	0	0
73	0.00	1	2.0	0	1	0	0	0	0	19	0	0
74	392.53	0	2.5	0	1	0	0	0	0	19	1	1
75	0.00	0	2.5	0	1	0	0	0	0	19	0	0
76	901.48	1	0.5	1	0	0	0	0	0	5	0	0
77	967.85	0	2.5	0	0	0	0	0	0	14	1	1
78	493.08	1	2.0	0	0	0	0	0	0	14	0	0
79	356.68	1	2.0	0	0	0	0	0	0	14	0	0
80	1157.01	0	2.5	0	0	0	0	0	0	14	0	0
81	1119.08	0	2.5	0	0	0	0	0	0	14	0	0
82	678.86	0	2.5	0	0	0	0	0	0	14	0	0
83	363.31	0	2.5	0	0	0	0	0	0	14	0	0
84	0.00	0	2.5	1	0	0	0	0	0	12	1	1
85	0.00	0	2.5	0	0	0	0	0	0	12	1	1
86	646.24	1	1.0	0	1	1	0	0	0	7	0	0
87	1324.96	1	2.0	0	0	1	0	0	0	7	0	0
88	1124.41	0	2.5	0	0	1	0	0	0	7	0	0
89	107.92	0	2.5	0	1	1	0	0	0	7	0	0
90	1106.18	0	2.5	0	0	1	0	0	0	7	0	0
91	0.00	0	2.5	0	0	1	0	0	0	5	0	0
92	0.00	0	2.5	0	0	1	0	0	0	5	0	0
93	0.00	1	2.0	0	0	1	0	0	0	5	0	0
94	0.00	1	2.0	0	0	1	0	0	0	5	0	0
95	0.00	1	0.5	1	0	1	0	0	0	5	0	0
96	0.00	1	0.5	1	0	1	0	0	0	5	0	0
97	0.00	1	0.5	1	0	1	0	0	0	5	0	0
98	0.00	1	0.5	1	0	1	0	0	0	5	0	0
99	22.03	1	1.5	0	0	1	0	0	0	17	0	0

Table 158. Data used for the analysis of the PEARDARP, COPES, and PFAULT predictive models (continued).

Obs #	AVGMT	TRANGE	K1	K2	VOL0	VOL	I	Fsd	Sdr	Pk1	T
1	69	69	.	.	1.5217	97.1710	0.06	1.4	2	0.014400	23346.30
2	69	69	.	.	1.5275	82.5228	0.06	1.0	2	0.003728	30946.06
3	69	69	.	.	2.8105	52.1488	0.06	1.0	2	0.003728	29333.72
4	69	69	.	.	3.3507	61.8559	0.06	1.0	2	0.007151	34793.94
5	69	69	.	.	2.8543	45.6874	0.06	1.0	2	0.014400	34265.56
6	69	69	.	.	2.5550	34.4363	0.06	0.6	1	0.009435	20684.15
7	71	66	.	.	4.1190	9.6853	0.06	1.0	2	0.009548	14574.86
8	61	57	.	.	0.7052	21.6306	0.04	1.0	2	0.000000	3408.49
9	61	57	.	.	0.7052	21.6306	0.04	1.4	2	0.019047	3690.13
10	61	57	.	.	0.7052	21.6306	0.04	1.0	2	0.005789	3995.05
11	61	57	.	.	0.7052	21.6306	0.04	0.6	1	0.012480	3839.56
12	61	57	.	.	0.7052	21.6306	0.04	1.0	2	0.019047	3546.51
13	64	48	.	.	3.3945	35.8686	0.06	1.0	2	0.019047	658.00
14	64	48	.	.	3.3945	35.8686	0.06	1.4	2	0.019047	940.56
15	60	54	.	.	1.4965	26.0840	0.06	1.4	2	0.014554	4318.82
16	60	54	.	.	1.4965	26.0840	0.06	1.4	2	0.014554	5702.24
17	60	54	.	.	1.4965	26.0840	0.06	1.4	2	0.014554	5267.02
18	62	66	.	.	5.0653	39.5760	0.06	1.0	2	0.000000	11233.29
19	61	55	.	.	1.7520	22.7906	0.04	1.4	2	0.008933	986.91
20	60	32	.	.	11.0084	59.5972	0.06	1.4	2	0.000000	49597.34
21	72	40	.	.	2.9656	6.3702	0.06	1.4	2	0.003995	1739.09
22	72	41	.	.	2.2017	18.4626	0.04	1.4	2	0.015157	677.79
23	45	72	0	1	1.0914	11.0142	0.04	1.4	2	0.037695	3877.09
24	45	72	0	1	1.0914	11.0142	0.04	1.4	2	0.037695	1381.23
25	45	72	.	.	1.0914	11.0142	0.04	1.0	2	0.014554	168.48
26	45	72	.	.	1.0914	11.0142	0.04	1.4	2	0.014185	4130.34
27	45	72	.	.	1.0914	11.0142	0.04	1.4	2	0.013830	4130.34
28	45	72	.	.	1.0914	11.0142	0.04	1.4	2	0.014554	403.48
29	45	72	.	.	1.0914	11.0142	0.04	1.4	2	0.014554	419.82
30	45	72	.	.	1.0914	11.0142	0.04	1.4	2	0.014554	80.84
31	48	68	0	1	4.3984	8.7969	0.04	0.6	2	0.020905	24983.91
32	47	71	0	1	1.3031	27.3717	0.04	1.4	2	0.037695	1193.06
33	47	71	0	1	1.3031	27.3717	0.04	1.4	2	0.037695	2251.66
34	50	66	0	1	2.8826	11.7817	0.04	1.0	2	0.020905	14153.29
35	42	87	1	0	0.5625	14.1456	0.04	1.0	2	0.026561	265.11
36	42	87	1	0	0.5625	14.1456	0.04	1.0	2	0.026561	586.44
37	42	87	1	0	0.5625	14.1456	0.04	1.0	2	0.042048	563.62
38	42	87	1	0	0.5625	14.1456	0.04	1.0	2	0.042048	805.65
39	42	87	1	0	0.5625	14.1456	0.04	1.4	2	0.024726	660.61
40	42	87	1	0	0.5625	14.1456	0.04	1.4	2	0.024726	744.16
41	42	87	1	0	0.5625	14.1456	0.04	1.4	2	0.015619	462.15
42	42	87	1	0	0.5625	14.1456	0.04	1.4	2	0.015619	2757.94
43	42	87	1	0	0.5625	14.1456	0.04	1.4	2	0.015619	520.60
44	42	87	1	0	0.5625	14.1456	0.04	1.4	2	0.015619	1151.61
45	42	87	1	0	0.5625	14.1456	0.04	1.4	2	0.024726	1022.32
46	42	87	1	0	0.5625	14.1456	0.04	1.4	2	0.024726	1712.79
47	45	81	.	.	0.8131	9.4112	0.04	1.4	2	0.016764	1699.91
48	45	81	.	.	0.8131	9.4112	0.04	1.4	2	0.026539	2244.43
49	45	81	1	0	0.8131	9.4112	0.04	1.4	2	0.026561	3760.33

Table 158. Data used for the analysis of the PEARDARP, COPES, and PFAULT predictive models (continued).

Obs #	AVGMT	TRANGE	K1	K2	VOL0	VOL	I	Fsd	Sdr	Pk1	T
50	45	81	1	0	0.8131	9.4112	0.04	1.4	2	0.026561	2244.43
51	45	81	1	0	1.7265	6.7488	0.06	1.4	2	0.026561	7791.86
52	46	84	.	.	0.52925	1.058	0.04	1.4	2	0.031848	2776.79
53	42	87	1	0	0.56247	16.812	0.04	1.4	2	0.026561	1000.60
54	44	82	1	0	0.69350	3.527	0.04	1.0	2	0.024726	1822.78
55	54	60	0	1	2.49999	82.901	0.06	1.0	2	0.025721	4061.70
56	53	63	0	1	6.29351	6.600	0.06	1.0	2	0.038792	518.43
57	53	63	0	1	6.29351	6.600	0.06	1.0	2	0.016554	684.50
58	46	72	.	.	0.81213	24.117	0.04	1.4	2	0.015202	5167.83
59	46	82	0	1	0.81213	24.117	0.04	1.4	2	0.016361	640.60
60	46	72	0	1	0.81213	24.117	0.04	1.4	2	0.035932	4138.74
61	46	82	.	.	0.81213	24.117	0.04	1.4	2	0.022271	5167.83
62	46	72	.	.	0.81213	24.117	0.04	1.4	2	0.015202	5167.83
63	46	72	.	.	0.81213	24.117	0.04	1.0	2	0.015202	5167.83
64	47	70	.	.	0.48180	10.222	0.04	1.4	2	0.022271	3833.32
65	47	70	.	.	0.48180	10.222	0.04	1.4	2	0.022271	3458.24
66	47	70	.	.	0.48180	10.222	0.04	1.4	2	0.026418	1832.38
67	47	70	0	1	0.48180	10.222	0.04	1.4	2	0.036416	3743.99
68	60	60	0	0	1.37477	42.684	0.06	1.4	2	0.027877	1411.66
69	60	60	.	.	1.37477	42.684	0.04	1.4	2	0.015736	10109.48
70	60	60	.	.	1.37477	42.684	0.04	1.4	2	0.015736	10109.48
71	60	60	.	.	1.37477	42.684	0.04	1.4	2	0.027877	2017.85
72	60	60	.	.	1.37477	42.684	0.04	1.4	2	0.015736	7478.40
73	60	60	.	.	1.37477	42.684	0.04	1.4	2	0.015736	1939.32
74	60	60	0	1	1.37477	42.684	0.04	1.4	2	0.056648	4122.96
75	60	60	.	.	1.37477	42.684	0.04	1.4	2	0.027877	366.07
76	60	60	.	.	2.62581	17.513	0.04	1.4	2	0.006994	15762.09
77	53	66	0	1	1.44409	24.476	0.06	1.4	2	0.031249	6555.76
78	53	66	0	0	1.44409	24.476	0.06	1.4	2	0.015283	3473.62
79	53	66	0	1	1.44409	24.476	0.06	1.4	2	0.016014	2430.09
80	53	86	0	0	1.44409	24.476	0.06	1.4	2	0.023053	7867.25
81	53	66	0	1	1.44409	24.476	0.06	1.0	2	0.031249	7867.25
82	53	66	0	1	1.44409	24.476	0.06	1.4	2	0.031249	4586.30
83	53	66	0	0	1.44409	24.476	0.06	1.0	2	0.023053	2528.50
84	51	64	0	0	1.22640	21.834	0.04	1.4	2	0.003038	160.24
85	51	64	0	0	1.22640	21.834	0.04	1.4	2	0.003038	160.24
86	49	67	0	1	0.54932	8.440	0.06	1.4	2	0.010704	2921.57
87	4	67	0	1	0.54932	6.612	0.06	1.0	2	0.010704	4250.26
88	4	67	0	1	0.54932	6.612	0.06	1.0	2	0.021845	3989.66
89	4	67	0	1	0.54932	6.612	0.06	1.4	2	0.021845	383.51
90	4	67	0	1	0.54932	6.612	0.06	1.4	2	0.021845	3989.66
91	49	61	.	.	1.04937	5.429	0.04	1.4	2	0.005459	95.63
92	49	61	.	.	1.04937	5.429	0.04	1.4	2	0.005459	95.63
93	49	61	.	.	1.04937	5.429	0.04	1.4	2	0.023039	95.63
94	49	61	.	.	1.04937	5.429	0.04	1.4	2	0.023039	95.63
95	49	61	.	.	1.04937	5.429	0.04	1.4	2	0.023039	95.63
96	49	61	.	.	1.04937	5.429	0.04	1.4	2	0.023039	95.63
97	49	61	.	.	1.04937	5.429	0.04	1.4	2	0.038783	95.63
98	49	61	.	.	1.04937	5.429	0.04	1.4	2	0.038783	95.63
99	48	66	.	.	6.20208	230.247	0.06	1.4	2	0.014554	1192.83

Table 158. Data used for the analysis of the PEARDARP, COPES, and PFAULT predictive models (continued).

Obs #	Fd	fsbl	fg	flt	fprec	Fsg	Fsb2	Fe	F
1	0.25000	0.75776	1.00000	0.87507	0.41565	1.00000	0.730	0.00020	4.48720
2	0.27735	1.00000	0.58401	0.51870	0.11868	1.00000	1.000	-0.00360	5.35157
3	0.33333	1.00000	0.56534	0.41295	0.07825	1.00000	1.000	-0.00313	5.35157
4	0.33333	1.00000	0.63368	0.61620	0.23631	1.00000	1.000	-0.00134	4.88597
5	0.37796	0.70466	0.67644	0.67449	0.33895	1.00000	0.730	0.00109	4.48720
6	0.37796	0.68288	0.34740	0.59223	0.30750	1.00000	0.730	0.00145	4.48720
7	0.70711	0.68785	0.63523	1.00000	0.24467	1.00000	0.710	0.00037	4.67629
8	0.24254	0.80877	0.76385	1.11460	0.53134	1.00000	0.742	-0.00005	4.38584
9	0.24254	0.80877	1.00000	1.11460	0.53134	1.00000	0.742	-0.00005	4.38584
10	0.24254	0.80877	0.67385	0.88060	0.32134	1.00000	0.682	-0.00305	4.97465
11	0.24254	0.80877	0.47631	1.11460	0.53134	1.00000	0.742	-0.00005	4.38584
12	0.24254	0.80877	0.76385	1.11460	0.53134	1.00000	0.742	-0.00005	4.38584
13	0.35355	0.76624	0.73550	0.95394	0.46991	1.00000	0.742	0.00066	4.38584
14	0.35355	0.76624	1.00000	0.95394	0.46991	1.00000	0.742	0.00066	4.38584
15	0.27735	0.75102	1.00000	0.84965	1.10633	1.00000	0.730	0.88316	4.48720
16	0.27735	0.75102	1.00000	0.84965	1.10633	1.00000	0.730	0.88316	4.48720
17	0.27735	0.75102	1.00000	0.84965	1.10633	1.00000	0.730	0.88316	4.48720
18	0.35355	0.76643	0.71762	0.90784	0.42818	0.70583	0.730	0.00006	4.48720
19	0.33333	0.83400	1.00000	1.06951	0.44178	1.00000	0.706	-0.00227	4.71672
20	0.44721	0.77983	1.00000	0.86486	0.36353	1.00000	0.706	-0.00136	4.71672
21	0.70711	1.00000	1.00000	1.00000	1.20186	0.63348	1.000	0.65093	5.35157
22	0.40825	0.78964	1.00000	1.00000	1.09345	0.73291	0.730	0.87673	4.48720
23	0.27735	1.00000	1.00000	1.00000	1.14318	0.55888	1.000	2.29499	4.48720
24	0.27735	1.00000	1.00000	1.00000	1.14318	0.55888	1.000	2.29499	4.48720
25	0.27735	0.64047	0.63365	0.43200	1.14318	0.55888	0.730	2.29499	4.48720
26	0.27735	1.00000	1.00000	1.00000	1.14318	0.55888	1.000	2.29499	4.48720
27	0.27735	1.00000	1.00000	1.00000	1.14318	0.55888	1.000	2.29499	4.48720
28	0.27735	0.64047	1.00000	0.43200	1.14318	0.55888	0.730	2.29499	4.48720
29	0.27735	0.64047	1.00000	0.43200	1.14318	0.55888	0.730	2.29499	4.48720
30	0.27735	0.64047	1.00000	0.43200	1.14318	0.55888	0.730	2.29499	4.48720
31	0.70711	1.00000	0.34634	1.00000	1.13346	1.00000	1.000	2.06405	4.67629
32	0.25000	1.00000	1.00000	1.00000	1.10159	1.00000	1.000	1.70581	4.48720
33	0.25000	1.00000	1.00000	1.00000	1.10159	1.00000	1.000	1.70581	4.48720
34	0.50000	1.00000	0.66936	1.00000	1.13032	0.67388	1.000	2.01953	4.67629
35	0.25820	1.00000	0.72902	0.97242	0.45287	0.72578	1.000	0.08263	4.48720
36	0.25820	1.00000	0.72902	1.00000	0.45287	0.72578	1.000	0.08263	4.48720
37	0.25820	1.00000	0.75902	1.05042	0.52287	0.72578	1.000	0.16263	4.32420
38	0.25820	1.00000	0.75902	1.00000	0.52287	0.72578	1.000	0.16263	4.32420
39	0.25820	0.78352	1.00000	1.05042	0.52287	0.72578	0.750	0.16263	4.32420
40	0.25820	0.78352	1.00000	1.00000	0.52287	0.72578	0.750	0.16263	4.32420
41	0.25820	0.78352	1.00000	0.97242	0.45287	0.72578	0.730	0.08263	4.48720
42	0.25820	0.78352	1.00000	1.00000	0.45287	0.72578	0.730	0.08263	4.48720
43	0.25820	0.78352	1.00000	0.97242	0.45287	0.72578	0.730	0.08263	4.48720
44	0.25820	0.78352	1.00000	1.00000	0.45287	0.72578	0.730	0.08263	4.48720
45	0.25820	0.78352	1.00000	1.05042	0.52287	0.72578	0.750	0.16263	4.32420
46	0.25820	0.78352	1.00000	1.00000	0.52287	0.72578	0.750	0.16263	4.32420
47	0.28868	1.00000	1.00000	1.00000	0.37568	0.66343	1.000	0.17763	4.48720
48	0.28868	1.00000	1.00000	1.00000	0.44568	0.66343	1.000	0.25763	4.32420
49	0.28868	1.00000	1.00000	1.00000	0.37568	0.66343	1.000	0.17763	4.48720

Table 158. Data used for the analysis of the PEARDARP, COPES, and PFAULT predictive models (continued).

Obs #	Fd	fsbl	fg	flt	fprec	Fsg	Fsb2	Fe	F
50	0.28868	1.00000	1.00000	1.00000	0.37568	0.66343	1.000	0.17763	4.48720
51	0.50000	1.00000	1.00000	1.00000	0.30545	0.60671	1.000	0.26406	4.48720
52	0.70711	1.00000	1.00000	1.00000	0.19342	0.43142	1.00	0.65118	4.25469
53	0.23570	1.00000	1.00000	1.00000	0.45287	0.72578	1.00	0.08263	4.48720
54	0.44721	0.63684	0.66122	1.00000	0.31099	0.55464	0.75	0.42340	4.32420
55	0.16440	1.00000	0.79501	1.00000	1.06750	1.00000	1.00	1.12952	4.67629
56	0.33333	1.00000	0.71456	1.00000	1.10272	0.70048	1.00	1.72188	4.48720
57	0.33333	0.76184	0.71456	1.00000	1.10272	0.70048	0.73	1.72188	4.48720
58	0.21320	0.73936	1.00000	0.80557	1.11021	1.00000	0.73	1.82804	4.48720
59	0.21320	0.73936	1.00000	0.80557	1.11021	1.00000	0.73	1.82804	4.48720
60	0.21320	1.00000	1.00000	0.80557	1.11021	1.00000	1.00	1.82804	4.48720
61	0.21320	1.00000	1.00000	0.80557	1.11021	1.00000	1.00	1.82804	4.48720
62	0.21320	0.73936	1.00000	0.80557	1.11021	1.00000	0.73	1.82804	4.48720
63	0.21320	0.73936	0.69957	0.80557	1.11021	1.00000	0.73	1.82804	4.48720
64	0.27735	1.00000	1.00000	1.00000	1.13071	0.60250	1.00	2.11846	4.48720
65	0.27735	1.00000	1.00000	1.00000	1.13071	0.60250	1.00	2.11846	4.48720
66	0.27735	1.00000	1.00000	1.00000	1.13071	0.60250	1.00	2.11846	4.48720
67	0.27735	1.00000	1.00000	1.00000	1.13071	1.00000	1.00	2.11846	4.48720
68	0.22361	1.00000	1.00000	1.12136	1.08235	0.77177	1.00	0.87118	4.48720
69	0.22361	0.82295	1.00000	1.00000	1.08235	0.77177	0.73	0.87118	4.48720
70	0.22361	0.82295	1.00000	1.12136	1.08235	0.77177	0.73	0.87118	4.48720
71	0.22361	1.00000	1.00000	1.00000	1.08235	0.77177	1.00	0.87118	4.48720
72	0.22361	0.82295	1.00000	1.12136	1.08235	1.00000	0.73	0.87118	4.48720
73	0.22361	0.82295	1.00000	1.12136	1.08235	0.77177	0.73	0.87118	4.48720
74	0.22361	1.00000	1.00000	1.00000	1.06235	0.77177	1.00	0.93118	4.32420
75	0.22361	1.00000	1.00000	1.12136	1.08235	0.77177	1.00	0.87118	4.48720
76	0.40825	0.78681	1.00000	1.00000	1.13440	1.00000	0.69	0.75720	4.88597
77	0.25820	1.00000	1.00000	1.00000	1.10792	1.00000	1.00	1.79558	4.48720
78	0.25820	0.74623	1.00000	1.00000	1.10792	1.00000	0.73	1.79558	4.48720
79	0.25820	0.74623	1.00000	1.00000	1.10792	1.00000	0.73	1.79558	4.48720
80	0.25820	1.00000	1.00000	1.00000	1.10792	1.00000	1.00	1.79558	4.48720
81	0.25820	1.00000	0.70415	1.00000	1.10792	1.00000	1.00	1.79558	4.48720
82	0.25820	1.00000	1.00000	1.00000	1.10792	1.00000	1.00	1.79558	4.48720
83	0.25820	1.00000	0.70415	1.00000	1.10792	1.00000	1.00	1.79558	4.48720
84	0.27735	1.00000	1.00000	0.35220	1.22892	1.00000	1.00	2.94975	5.86124
85	0.27735	1.00000	1.00000	0.35220	1.22892	1.00000	1.00	2.94975	5.86124
86	0.35355	0.61051	1.00000	1.00000	1.17316	0.52393	0.71	2.62648	4.67629
87	0.35355	0.54771	0.54181	1.00000	1.19410	1.00000	0.71	2.92303	4.67629
88	0.35355	1.00000	0.54181	1.00000	1.19410	1.00000	1.00	2.92303	4.67629
89	0.35355	1.00000	1.00000	1.00000	1.19410	0.45066	1.00	2.92303	4.67629
90	0.35355	1.00000	1.00000	1.00000	1.19410	1.00000	1.00	2.92303	4.67629
91	0.40825	1.00000	1.00000	0.23727	1.19971	1.00000	1.00	2.81591	5.11212
92	0.40825	1.00000	1.00000	0.23727	1.19971	1.00000	1.00	2.81591	5.11212
93	0.40825	0.65087	1.00000	0.54927	1.11971	1.00000	0.75	2.05591	4.32420
94	0.40825	0.65087	1.00000	0.54927	1.11971	1.00000	0.75	2.05591	4.32420
95	0.40825	0.65087	1.00000	0.54927	1.11971	1.00000	0.75	2.05591	4.32420
96	0.40825	0.65087	1.00000	0.54927	1.11971	1.00000	0.75	2.05591	4.32420
97	0.40825	0.65087	1.00000	0.62727	1.09971	1.00000	0.77	1.86591	4.19464
98	0.40825	0.65087	1.00000	0.62727	1.09971	1.00000	0.77	1.86591	4.19464
99	0.23570	0.92937	1.00000	1.00000	1.04688	1.00000	0.73	0.93076	4.48720

Table 158. Data used for the analysis of the PEARDARP, COPES, and PFAULT predictive models (continued).

Obs #	DE	kc	kr	DA	Rho	Z	Y	Alpha
1	3.84326	1072.00	1072.00	9396.39	4.5620	11501.83	0.08373	0.06801
2	0.18009	1432.21	2434.76	0.01	16.7940	13983.74	0.04579	0.03420
3	0.18009	1069.42	1818.01	21.92	16.7940	20290.70	0.06207	0.00981
4	0.83196	1231.20	2093.05	6198.50	10.1220	14988.61	0.11254	0.00981
5	3.84326	1176.95	1176.95	9199.84	4.5620	9951.69	0.18536	0.00404
6	3.84326	1125.64	1125.64	9159.65	4.5620	12636.99	0.18039	0.00404
7	1.78813	505.49	505.49	8847.42	7.2030	63908.05	0.02547	0.00002
8	6.08247	547.39	547.39	9948.24	3.1108	56982.76	-0.01679	0.08297
9	6.08247	736.17	736.17	9892.68	3.1108	30028.65	0.05885	0.08297
10	0.61260	895.95	895.95	7787.43	11.3674	31522.39	0.15875	0.08297
11	6.08247	860.87	860.87	9854.58	3.1108	29930.72	0.09251	0.08297
12	6.08247	656.44	656.44	9916.45	3.1108	46644.30	0.08345	0.08297
13	6.08247	2041.11	2041.11	9313.83	3.1108	9894.59	0.11925	0.00650
14	6.08247	1053.58	1053.58	9706.47	3.1108	17412.59	0.03528	0.00650
15	3.84326	670.55	670.55	9544.28	4.5620	24685.31	0.02145	0.03420
16	3.84326	714.25	714.25	9527.13	4.5620	26730.77	0.10565	0.03420
17	3.84326	850.69	850.69	9472.24	4.5620	22065.49	0.13926	0.03420
18	3.84326	684.10	684.10	9575.20	4.5620	45646.26	0.07821	0.00650
19	1.53440	808.97	808.97	9041.91	7.7646	38404.91	-0.07068	0.00981
20	1.53440	832.25	832.25	8840.74	7.7646	37876.11	0.04954	0.00116
21	0.18009	1154.95	1963.41	0.22	16.7940	29365.08	0.02091	0.00002
22	3.84326	1047.68	1047.68	9487.68	4.5620	15727.79	0.00812	0.00231
23	3.84326	960.90	1633.54	8724.44	4.5620	30878.19	0.06951	0.03420
24	3.84326	841.41	1430.39	8850.78	4.5620	38600.00	0.00054	0.03420
25	3.84326	958.56	958.56	9113.44	4.5620	25128.21	0.08621	0.03420
26	3.84326	823.05	1399.18	8869.43	4.5620	43424.66	0.05385	0.03420
27	3.84326	769.73	1308.54	8922.51	4.5620	45278.81	-0.00669	0.03420
28	3.84326	910.54	910.54	9138.02	4.5620	28577.98	0.01449	0.03420
29	3.84326	1008.60	1008.60	9087.42	4.5620	21035.86	0.02919	0.03420
30	3.84326	855.35	855.35	9165.84	4.5620	22500.00	0.02592	0.03420
31	1.78813	590.84	1004.43	8693.69	7.2030	47096.77	0.08686	0.00002
32	3.84326	802.28	1363.87	9286.26	4.5620	34134.28	-0.03148	0.06801
33	3.84326	577.04	980.97	9454.17	4.5620	47936.51	0.05637	0.06801
34	1.78813	710.14	1207.23	8596.01	7.2030	38540.77	0.01402	0.00048
35	3.84326	582.02	989.44	9496.19	4.5620	74240.84	-0.02835	0.10001
36	3.84326	534.31	908.33	9528.54	4.5620	90116.28	0.05417	0.10001
37	8.26038	619.97	1053.94	9897.52	2.1990	61382.49	-0.02002	0.10001
38	8.26038	631.60	1073.72	9891.58	2.1990	62342.34	-0.09169	0.10001
39	8.26038	642.37	642.37	10015.12	2.1990	60065.79	-0.01906	0.10001
40	8.26038	657.63	657.63	10010.96	2.1990	59617.83	-0.06300	0.10001
41	3.84326	672.25	672.25	9618.74	4.5620	57839.72	-0.01755	0.10001
42	3.84326	656.88	656.88	9624.41	4.5620	56690.65	0.00864	0.10001
43	3.84326	679.03	679.03	9616.22	4.5620	45841.92	-0.00724	0.10001
44	3.84326	668.84	668.84	9619.99	4.5620	47298.25	0.04473	0.10001
45	8.26038	549.27	549.27	10040.21	2.1990	65551.02	-0.02294	0.10001
46	8.26038	539.48	539.48	10042.81	2.1990	65188.28	0.04692	0.10001
47	3.84326	419.80	713.67	9476.20	4.5620	105937.50	-0.02241	0.02616
48	8.26038	400.36	680.61	9911.92	2.1990	126141.73	-0.05092	0.02616
49	3.84326	508.81	864.98	9413.00	4.5620	90370.37	0.02199	0.02616

Table 158. Data used for the analysis of the PEARDARP, COPES, and PFAULT predictive models (continued).

Obs #	DE	kc	kr	DA	Rho	Z	Y	Alpha
50	3.84326	549.48	934.11	9383.22	4.5620	74382.02	-0.02843	0.02616
51	3.84326	739.23	1256.69	9088.08	4.5620	68828.13	-0.02510	0.00048
52	12.1102	617.56	1049.86	9587.23	1.1218	56756.76	0.09081	0.00002
53	3.8433	493.38	838.74	9555.73	4.5620	96923.08	-0.03959	0.10001
54	8.2604	472.34	472.34	9800.84	2.1990	66030.15	-0.04659	0.00116
55	1.7881	712.62	1211.46	9249.09	7.2030	57435.90	0.01481	1.00893
56	3.8433	967.57	1644.86	9139.96	4.5620	30337.08	0.03192	0.00981
57	3.8433	535.91	535.91	9620.38	4.5620	50761.90	0.03623	0.00981
58	3.8433	1076.27	1076.27	9345.44	4.5620	13879.78	0.04996	0.19175
59	3.8433	1010.06	1010.06	9374.69	4.5620	15467.20	0.13949	0.19175
60	3.8433	1347.17	2290.20	8688.52	4.5620	14576.78	0.05277	0.19175
61	3.8433	1519.81	2583.67	8485.51	4.5620	12988.69	0.05337	0.19175
62	3.8433	1200.24	1200.24	9289.14	4.5620	12852.66	0.07605	0.19175
63	3.8433	1074.85	1074.85	9346.08	4.5620	14160.58	0.04893	0.19175
64	3.8433	934.16	1588.06	8892.15	4.5620	29912.02	0.13594	0.03420
65	3.8433	1215.96	2067.13	8586.75	4.5620	21613.59	0.06314	0.03420
66	3.8433	832.24	1414.80	8991.01	4.5620	41351.35	0.09405	0.03420
67	3.8433	779.06	1324.40	9040.43	4.5620	40439.56	-0.00158	0.03420
68	3.8433	1355.41	2304.19	8987.15	4.5620	17211.90	0.09305	0.14088
69	3.8433	771.53	771.53	9669.78	4.5620	29913.54	0.02809	0.14088
70	3.8433	996.91	996.91	9586.96	4.5620	16072.87	0.07779	0.14088
71	3.8433	1420.86	2415.47	8924.16	4.5620	14771.93	0.08451	0.14088
72	3.8433	1186.56	1186.56	9513.29	4.5620	17515.92	0.05396	0.14088
73	3.8433	1246.32	1246.32	9489.28	4.5620	15297.62	-0.02049	0.14088
74	8.2604	402.93	684.98	10067.63	2.1990	79531.25	-0.03542	0.14088
75	3.8433	1303.77	2216.41	9035.26	4.5620	16452.24	0.07662	0.14088
76	0.8320	791.74	791.74	8207.28	10.1220	40204.78	0.03761	0.00231
77	3.8433	1169.39	1987.97	8901.49	4.5620	19732.74	0.05573	0.05499
78	3.8433	916.60	916.60	9432.75	4.5620	24136.36	0.02253	0.05499
79	3.8433	1041.93	1041.93	9379.04	4.5620	19923.81	0.03184	0.05499
80	3.8433	1130.98	1922.67	8939.20	4.5620	18839.91	0.10307	0.05499
81	3.8433	931.92	1584.26	9122.44	4.5620	26058.82	0.13435	0.05499
82	3.8433	956.46	1625.98	9100.90	4.5620	19373.22	0.14095	0.05499
83	3.8433	1074.97	1827.45	8992.78	4.5620	22271.60	0.11002	0.05499
84	0.0390	1271.34	2161.29	0.00	24.5780	22500.00	0.02350	0.03420
85	0.0390	1271.34	2161.29	0.00	24.5780	22500.00	0.02350	0.03420
86	1.7881	1432.29	1432.29	7750.86	7.2030	11518.47	0.10922	0.00650
87	1.7881	1849.83	1849.83	6766.49	7.2030	6519.23	0.13292	0.00650
88	1.7881	1406.07	2390.32	5841.93	7.2030	12007.43	0.09382	0.00650
89	1.7881	1838.06	3124.71	4042.07	7.2030	12128.51	0.18218	0.00650
90	1.7881	1410.33	2397.57	5827.60	7.2030	13407.41	0.08514	0.00650
91	0.3871	1176.28	1999.67	1612.53	13.3190	22500.00	0.02412	0.00231
92	0.3871	1176.28	1999.67	1612.53	13.3190	22500.00	0.02412	0.00231
93	8.2604	783.91	783.91	9725.57	2.1990	22500.00	0.02706	0.00231
94	8.2604	783.91	783.91	9725.57	2.1990	22500.00	0.02706	0.00231
95	8.2604	783.91	783.91	9725.57	2.1990	22500.00	0.02706	0.00231
96	8.2604	783.91	783.91	9725.57	2.1990	22500.00	0.02706	0.00231
97	17.7542	710.10	710.10	10105.28	0.1140	22500.00	0.02870	0.00231
98	17.7542	710.10	710.10	10105.28	0.1140	22500.00	0.02870	0.00231
99	3.8433	855.35	855.35	9857.00	4.5620	22500.00	0.02592	0.10001

Table 158. Data used for the analysis of the PEARDARP, COPES, and PFAULT predictive models (continued).

Obs #	SVR	SVF	SV	Patch	Jfactor	R	Zr	DPSI	So
1	6.3050	122.873	129.178	0.006	4.2	0.95	1.645	1.1	0.3
2	1.7762	5.052	6.828	0.000	3.8	0.95	1.645	0.7	0.3
3	4.9064	1.140	6.046	0.000	3.8	0.95	1.645	0.9	0.3
4	3.2524	4.698	7.950	0.000	3.8	0.95	1.645	0.7	0.3
5	4.3806	5.670	10.051	0.000	3.8	0.95	1.645	1.0	0.3
6	3.7932	0.476	4.269	0.000	3.8	0.95	1.645	0.7	0.3
7	2.1675	0.001	2.168	0.000	2.8	0.95	1.645	0.9	0.3
8	4.9064	0.000	4.906	0.001	4.2	0.95	1.645	1.6	0.3
9	4.0810	10.018	14.099	0.000	4.2	0.95	1.645	1.5	0.3
10	7.3470	0.827	8.174	0.000	4.2	0.95	1.645	1.8	0.3
11	4.9064	1.203	6.109	0.000	4.2	0.95	1.645	1.8	0.3
12	6.5572	5.240	11.797	0.000	4.2	0.95	1.645	2.0	0.3
13	5.4655	0.017	5.482	0.000	4.2	0.95	1.645	0.7	0.3
14	4.4831	0.055	4.538	0.000	4.2	0.95	1.645	0.4	0.3
15	9.0780	3.067	12.145	0.864	3.8	0.95	1.645	0.9	0.3
16	5.1260	4.950	10.076	0.000	3.8	0.95	1.645	0.6	0.3
17	4.9064	4.317	9.223	0.003	3.8	0.95	1.645	0.7	0.3
18	13.1625	0.000	13.163	0.000	4.2	0.95	1.645	1.1	0.3
19	3.4276	0.026	3.453	0.000	4.2	0.95	1.645	0.7	0.3
20	3.8879	0.000	3.888	0.000	4.2	0.95	1.645	0.7	0.3
21	1.7152	0.000	1.715	0.000	2.8	0.95	1.645	0.8	0.3
22	3.1668	0.001	3.168	0.000	2.8	0.95	1.645	1.3	0.3
23	4.2795	0.313	4.593	0.000	3.2	0.95	1.645	0.9	0.3
24	3.7932	0.053	3.846	0.000	3.2	0.95	1.645	1.2	0.3
25	0.8965	0.006	0.903	0.000	4.2	0.95	1.645	0.6	0.3
26	1.3737	0.319	1.692	0.000	3.2	0.95	1.645	0.9	0.3
27	0.4686	0.307	0.776	0.000	3.2	0.95	1.645	0.8	0.3
28	4.4831	0.052	4.535	0.000	4.2	0.95	1.645	1.6	0.3
29	5.1260	0.055	5.181	0.000	4.2	0.95	1.645	1.7	0.3
30	13.3511	0.003	13.354	0.000	3.8	0.95	1.645	1.6	0.3
31	0.4985	0.001	0.500	0.000	2.8	0.95	1.645	0.1	0.3
32	8.7753	0.074	8.850	0.000	2.8	0.95	1.645	2.1	0.3
33	6.0584	0.222	6.280	0.000	3.2	0.95	1.645	2.1	0.3
34	0.4686	0.024	0.493	0.004	2.8	0.95	1.645	0.3	0.3
35	1.1210	0.039	1.160	0.002	3.8	0.95	1.645	0.8	0.3
36	5.1260	0.015	5.141	0.003	3.2	0.95	1.645	1.2	0.3
37	0.7368	0.313	1.049	0.004	3.8	0.95	1.645	1.1	0.3
38	5.8171	0.056	5.873	0.007	3.2	0.95	1.645	1.2	0.3
39	0.8145	0.294	1.108	0.141	4.2	0.95	1.645	1.1	0.3
40	5.4655	0.035	5.500	0.012	3.2	0.95	1.645	1.1	0.3
41	0.3593	0.072	0.431	0.008	4.2	0.95	1.645	0.9	0.3
42	3.9838	0.152	4.135	0.049	3.2	0.95	1.645	1.1	0.3
43	0.9830	0.088	1.071	0.000	3.8	0.95	1.645	0.8	0.3
44	5.5813	0.034	5.615	0.050	3.2	0.95	1.645	1.2	0.3
45	0.9830	0.623	1.606	0.036	3.8	0.95	1.645	0.8	0.3
46	5.9371	0.147	6.084	0.014	3.2	0.95	1.645	1.0	0.3
47	2.2369	0.068	2.305	0.000	2.8	0.95	1.645	0.7	0.3
48	2.9993	0.244	3.243	0.000	2.8	0.95	1.645	0.6	0.3

Table 158. Data used for the analysis of the PEARDARP, COPES, and PFAULT predictive models (continued).

Obs #	SVR	SVF	SV	Patch	Jfactor	R	Zr	DPSI	So
49	2.5270	0.341	2.868	0.000	3.2	0.95	1.645	0.5	0.3
50	4.2795	0.140	4.419	0.000	3.2	0.95	1.645	0.5	0.3
51	0.7368	0.035	0.772	0.000	3.2	0.95	1.645	0.7	0.3
52	0.4985	0.0006	0.4991	0.000	3.2	0.85	1.036	0.2	0.3
53	4.6921	0.1100	4.8021	0.010	3.2	0.95	1.645	1.2	0.3
54	1.0279	0.0032	1.0310	0.000	3.2	0.85	1.036	0.4	0.3
55	1.6553	1.5982	3.2535	0.007	3.2	0.95	1.645	0.7	0.3
56	9.0780	0.0018	9.0798	0.000	3.2	0.95	1.645	0.9	0.3
57	12.2419	0.0007	12.2425	0.000	3.2	0.95	1.645	1.0	0.3
58	1.2692	24.0053	25.2746	0.000	4.2	0.80	0.842	0.5	0.3
59	2.6794	0.2457	2.9251	0.104	4.2	0.80	0.842	0.9	0.3
60	3.6999	23.7073	27.4071	0.024	4.2	0.80	0.842	1.1	0.3
61	2.9993	46.3466	49.3459	0.000	4.2	0.80	0.842	0.6	0.3
62	1.7152	24.0053	25.7205	0.000	4.2	0.80	0.842	0.4	0.3
63	1.7762	13.4447	15.2209	0.000	4.2	0.80	0.842	0.7	0.3
64	1.5392	0.4421	1.9812	0.000	2.8	0.95	1.645	0.3	0.3
65	1.8384	0.3702	2.2086	0.014	2.8	0.95	1.645	0.5	0.3
66	2.5270	0.1246	2.6516	0.002	2.8	0.95	1.645	0.4	0.3
67	1.6553	0.3119	1.9672	0.000	3.2	0.95	1.645	0.5	0.3
68	3.0824	3.4449	6.5273	0.000	4.2	0.95	1.645	1.1	0.3
69	2.7575	2.8943	5.6518	0.000	3.2	0.95	1.645	1.0	0.3
70	2.6026	38.2220	40.8246	0.000	4.2	0.95	1.645	0.9	0.3
71	3.2524	0.4827	3.7352	0.000	3.2	0.95	1.645	1.1	0.3
72	5.2378	22.7382	27.9760	0.000	4.2	0.95	1.645	1.3	0.3
73	2.0322	2.2228	4.2551	0.000	4.2	0.95	1.645	0.7	0.3
74	3.2524	2.8045	6.0570	0.000	3.2	0.95	1.645	1.1	0.3
75	4.1796	0.3368	4.5164	0.000	4.2	0.95	1.645	0.8	0.3
76	1.7152	0.0618	1.7769	0.000	2.8	0.95	1.645	0.3	0.3
77	5.6986	1.5014	7.1999	0.000	3.2	0.95	1.645	0.3	0.3
78	5.3510	0.2792	5.6302	0.000	3.2	0.95	1.645	0.3	0.3
79	7.4835	0.0859	7.5693	0.000	3.2	0.95	1.645	0.4	0.3
80	5.1260	2.3183	7.4443	0.000	3.2	0.95	1.645	0.3	0.3
81	6.4305	1.1513	7.5817	0.000	3.2	0.95	1.645	0.3	0.3
82	5.6986	0.8113	6.5098	0.000	3.2	0.95	1.645	0.3	0.3
83	7.3470	0.1837	7.5307	0.000	3.2	0.95	1.645	0.3	0.3
84	3.6999	0.0006	3.7004	0.000	3.8	0.85	1.036	1.1	0.3
85	3.2524	0.0006	3.2530	0.000	4.2	0.85	1.036	1.0	0.3
86	2.4526	0.0080	2.4606	0.000	3.2	0.85	1.036	0.3	0.3
87	3.7932	0.0085	3.8018	0.000	3.2	0.85	1.036	0.7	0.3
88	6.1810	0.0262	6.2072	0.000	3.2	0.85	1.036	0.8	0.3
89	5.6986	0.0008	5.6994	0.000	3.2	0.85	1.036	0.4	0.3
90	2.9993	0.0467	3.0460	0.000	3.2	0.85	1.036	0.4	0.3
91	3.6999	0.0000	3.6999	0.000	4.2	0.85	1.036	0.7	0.3
92	1.5967	0.0000	1.5967	0.000	4.2	0.85	1.036	0.7	0.3
93	2.6794	0.0005	2.6799	0.000	4.2	0.85	1.036	0.7	0.3
94	2.0992	0.0005	2.0997	0.000	4.2	0.85	1.036	0.8	0.3
95	1.3209	0.0005	1.3214	0.000	3.8	0.85	1.036	0.7	0.3
96	1.8384	0.0005	1.8389	0.000	3.8	0.85	1.036	0.7	0.3
97	1.7762	0.0012	1.7773	0.000	3.8	0.85	1.036	0.8	0.3
98	2.2369	0.0012	2.2381	0.000	3.8	0.85	1.036	0.7	0.3
99	5.1260	0.0920	5.2180	0.000	3.2	0.95	1.645	0.6	0.3

REFERENCES

1. Tabatabaie, A. M., E. J. Barenberg, and R. E. Smith, "Longitudinal Joint Systems in Slip-Formed Rigid Pavements, Volume II Analysis of Load Transfer Systems for Concrete Pavements," U.S. Department of Transportation, Report No. FAA-RD-79-4, II, November, 1979.

2. Ioannides, A. M., "Analysis of Slab-on-Grade for a Variety of Loading and Support Conditions," Ph.D. Thesis, University of Illinois, Urbana, 1984.

3. Ioannides, A. M., E. J. Barenberg, and M. R. Thompson, "Finite Element Model with Stress Dependent Support," Transportation Research Record 954, Transportation Research Board, 1984.

4. Tayabji, S. D., and B. E. Colley, "Analysis of Jointed Concrete Pavements," Federal Highway Administration, FHWA/RD-86/041, February 1986.

5. Heinrichs, K. W., M. J. Lui, M. I. Darter, S. H. Carpenter, and A. M. Ioannides, "Rigid Pavement Analysis and Design," Federal Highway Administration, FHWA-RD-88-068, July 1989.

6. Chou, Y. T., "Structural Analysis Computer Programs for Rigid Multicomponent Pavement Structures with Discontinuities-WESLIQID and WESLAYER; Report 1: Program Development and Numerical Presentations; Report 2: Manual for the WESLIQID Finite Element Program; Report 3: Manual for the WESLAYER Finite Element Program," Technical Report GL-81-6, U. S. Army Engineer Waterways Experiment Station, May 1981.

7. Larralde, J., "PMARP User's Manual," Federal Highway Administration, FHWA Contract DTFH6l-85-C-00051, 1985.

8. Kopperman, S., G. Tiller, M. Tseng, "Purdue Pumping Model: PMARP and PEARDARP Interactive Microcomputer Version," Federal Highway Administration, FHWA Contract DTFH61-85-C-00051, 1986.

9. Majidzadeh, K., G. J. Ilves, and H. Sklyut, "Mechanistic Design of Rigid Pavements; Volume I: Development of the Design Procedure; Volume II: Design and Implementation Manual," Federal Highway Administration, FHWA Contract DTFH-11-9568, June 1984.

10. Kreger, W. C., "Computerized Aircraft Ground Flotation Analysis-Edge Loaded Rigid Pavement," Research Report No. ERR-FW-572, General Dynamics Corp., Fort Worth, Texas, January, 1967.

11. Pickett, G., and G. K. Ray, "Influence Charts for Concrete Pavements," Transactions, American Society of Civil Engineers, Vol. 116, 1951.

12. Dempsey, B. J., W. A. Herlache, and A. J. Patel, "The Climatic-Materials-Structural Pavement Analysis Program User's Manual," Federal Highway Administration, FHWA/RD-86/085, 1986.

13. Dempsey, B. J., W. A. Herlache, and A. J. Patel, "Environmental Effects on Pavements - Vol. III, Theory Manual," Federal Highway Administration, FHWA/RD-84/115, 1986.

14. Liu, S. J., and R. L. Lytton, "Environmental Effects on Pavements - Vol. IV, Drainage Manual," Federal Highway Administration, FHWA/RD-84/116, 1986.

15. Darter, M. I., J. M. Becker and M. B. Snyder, "Development of a Concrete Pavement Evaluation System (COPES), Vol. I - Research Report," Final Report, NCHRP Project 1-19, University of Illinois, 1984.

16. Darter, M. I., J. M. Becker and M. B. Snyder, "Development of a Concrete Pavement Evaluation System (COPES), Vol. II - User's Manual," Final Report, NCHRP Project 1-19, University of Illinois, 1984.

17. Darter, M. I., Program "PREDICT" written in Micro-Soft Basic language for the IBM Personal Computer, 1985.

18. van Wijk, A. J., "Purdue Economic Analysis of Rehabilitation and Design Alternatives in Rigid Pavements: A User's Manual for PEARDARP," FHWA Contract No. DTFH61-85-C-00051, 1985.

19. Darter, M. I. "Design of Zero-Maintenance Plain Jointed Pavement, Vol. I - Development of Design Procedures," Federal Highway Administration, FHWA-RD-77-111, April 1977.

20. Darter, M. I. and E. J. Barenberg, "Design of Zero-Maintenance Plain Jointed Pavement, Vol. II - Design Manual," Federal Highway Administration, FHWA-RD-77-112, April 1977.

21. "AASHTO Guide for Design of Pavement Structures," American Association of State, Highway, and Transportation Officials, Washington, D. C., 1986.

22. Kher, R. K., W. R. Hudson and B. F. McCullough, "A Systems Analysis of Rigid Pavement Design," Research Report 123-5, University of Texas at Austin, November 1970.

23. Carmichael, R. F. and B. F. McCullough, "Modification and Implementation of Rigid Pavement Design System," Research Report 123-26, University of Texas at Austin, January 1975.

24. "Thickness Design for Concrete Highway and Street Pavements," Portland Cement Association, 1984.

25. "Highway Design Manual," California Department of Transportation, 1975.

26. Sawan, J. S., M. I. Darter, and B. J. Dempsey, "Structural Analysis and Design of Portland Cement Concrete Highway Shoulders," Federal Highway Administration, FHWA/RD-81/122, 1982.

27. Robertson, N. F., "Report on a Study of a Computer Program for Cracking Analysis of Jointed Reinforced Concrete Pavements," Technical Memorandum 472-4, University of Texas at Austin, 1985.

HNR-20/8-90(700)QE